



# Functional Profiling of PIF3 Regulated Genes In The Dark

## Análisis funcional de los genes regulados por PIF3 en oscuridad

Maria Sentandreu Benavent

**ADVERTIMENT.** La consulta d'aquesta tesi queda condicionada a l'acceptació de les següents condicions d'ús: La difusió d'aquesta tesi per mitjà del servei TDX ([www.tdx.cat](http://www.tdx.cat)) i a través del Dipòsit Digital de la UB ([diposit.ub.edu](http://diposit.ub.edu)) ha estat autoritzada pels titulars dels drets de propietat intel·lectual únicament per a usos privats emmarcats en activitats d'investigació i docència. No s'autoritza la seva reproducció amb finalitats de lucre ni la seva difusió i posada a disposició des d'un lloc aliè al servei TDX ni al Dipòsit Digital de la UB. No s'autoritza la presentació del seu contingut en una finestra o marc aliè a TDX o al Dipòsit Digital de la UB (framing). Aquesta reserva de drets afecta tant al resum de presentació de la tesi com als seus continguts. En la utilització o cita de parts de la tesi és obligat indicar el nom de la persona autora.

**ADVERTENCIA.** La consulta de esta tesis queda condicionada a la aceptación de las siguientes condiciones de uso: La difusión de esta tesis por medio del servicio TDR ([www.tdx.cat](http://www.tdx.cat)) y a través del Repositorio Digital de la UB ([diposit.ub.edu](http://diposit.ub.edu)) ha sido autorizada por los titulares de los derechos de propiedad intelectual únicamente para usos privados enmarcados en actividades de investigación y docencia. No se autoriza su reproducción con finalidades de lucro ni su difusión y puesta a disposición desde un sitio ajeno al servicio TDR o al Repositorio Digital de la UB. No se autoriza la presentación de su contenido en una ventana o marco ajeno a TDR o al Repositorio Digital de la UB (framing). Esta reserva de derechos afecta tanto al resumen de presentación de la tesis como a sus contenidos. En la utilización o cita de partes de la tesis es obligado indicar el nombre de la persona autora.

**WARNING.** On having consulted this thesis you're accepting the following use conditions: Spreading this thesis by the TDX ([www.tdx.cat](http://www.tdx.cat)) service and by the UB Digital Repository ([diposit.ub.edu](http://diposit.ub.edu)) has been authorized by the titular of the intellectual property rights only for private uses placed in investigation and teaching activities. Reproduction with lucrative aims is not authorized nor its spreading and availability from a site foreign to the TDX service or to the UB Digital Repository. Introducing its content in a window or frame foreign to the TDX service or to the UB Digital Repository is not authorized (framing). Those rights affect to the presentation summary of the thesis as well as to its contents. In the using or citation of parts of the thesis it's obliged to indicate the name of the author.



**Universitat de Barcelona**

Genetics Department; Genetics program

Molecular Genetics Department

Centre for Research in Agrigenomics (CRAG)

Doctoral Thesis

**Functional Profiling of PIF3 Regulated  
Genes In The Dark**

**Análisis funcional de los genes regulados por PIF3  
en oscuridad**

Memory presented by Maria Sentandreu Benavent performed under the Dr. Elena Monte Collado supervision in the Department of Molecular Genetics at "Center for Research in Agricultural Genomics (CRAG)" and tutored by Dr. Marc Valls i Matheu, to obtain the title of Ph. Doctor from the University of Barcelona.

Supervisor,

Author,

Tutor,

Dr. Elena Monte  
Collado

Maria Sentandreu  
Benavent

Dr. Marc Valls  
i Matheu

Barcelona, September 2012





...I el que compta és l'esforç de cada dia compartit  
tenaçment amb els qui creuen que cada gest eixampla  
l'esperança, que cap dia no es perd per als qui lluiten...

Miquel Martí i Pol



Done gràcies en aquesta memòria de tesis, a tots aquells que han caminat al meu costat durant aquests cinc anys, perquè d'ells he après indubtablement sobre ciència però, també sobre la importància de l'amor i l'amistat.

Dedique l'esforç invertit especialment als meus avis que són els qui m'ensenyaren a lluitar...

... i ho faig en valencià, doncs valenciana és la naturalesa del meu cor.



**Maria Sentandreu  
PhD Thesis**



## Index

▪ Acronyms list.....	5
▪ General introduction.....	9
1. What is Skotomorphogenesis? And why plants need it?.....	11
2. Light Photoreceptors in Arabidopsis Thaliana.....	11
3. How is Skotomorphogenesis achieved? And how the deetiolation occurs?.....	13
4. PIFs roles along plant development .....	18
5. Previous expression profile studies performed in PIFs .....	22
▪ Objectives.....	27
▪ Publication's Impact Factor report .....	31
▪ General Discussion.....	33
▪ Main Conclusions.....	47
▪ Spanish Resume.....	51
▪ Bibliography.....	59
▪ Publications .....	75
o Student's Contribution in each article report.....	77
o Functional Profiling Identifies Genes Involved In Organ-Specific Branches of The PIF3 Regulatory Network in Arabidopsis.....	81
o Supplemental Analysis 1.....	99
o Supplemental Figures.....	107
o Resume 1st article .....	125
o Branching of the PIF3 Regulatory Network in Arabidopsis.....	129
o Resume. 2nd article.....	133
o Phytochrome-imposed oscillations in PIF3 protein abundance regulate hypocotyl growth under diurnal light/dark conditions in Arabidopsis.....	137
o Supplemental Figures.....	149
Resume. 3rd article.....	155
Appendix.....	157



## Acronyms List

phyA: phytochrome A

phyB: phytochrome B

phyC: phytochrome C

phyD: phytochrome D

phyE: phytochrome E

Rc : continuous red light

FRc : continuous far red light

Pr : inactive phytochrome conformation

Pfr : active phytochrome conformation

WT : wild type

COP: constitutive photomorphogenic

DET : deetiolated

FUS : fusca

LAF1: long after far red 1

HY5 : elongated Hypocotyl 5

cry1 : cryptochrome 1

cry2 : cryptochrome 2

PIF : phytochrome interacting factor

PIF3 : phytochrome interacting factor 3

PIF1 : phytochrome interacting factor 1

PIF4 : phytochrome interacting factor 4

PIF5 : phytochrome interacting factor 5

PIF6 : phytochrome interacting factor 6

PIF7 : phytochrome interacting factor 7

FHY1: far red elongated hypocotyl-like 1

NLS : nuclear localization signal domain

*pifq* : *pif1 pif3 pif4 pif5* (*pif* quadruple mutant)

HMR : hemera

GA : gibberellin

ABA : abscisic acid

GAI : gibberellin insensitive

RGA : repressor of GA3 1  
SOM: somnus (nucleus-localized CCCH-type zinc finger protein)  
DAG1: dof affecting germination 1  
SD: short day  
POR: protochlorophyllide oxidoreductase  
FeChII: ferro-chelatase  
HO3: heme oxygenase  
AUX/IAA: auxin resistant / indole-3-acetic acid inducible.  
SSTF: statistically significant two fold  
SS1.5F: statistically significant 1.5 fold  
SAS: shade avoidance syndrome  
MIDA: misregulated in the dark  
MIDA1-OX: misregulated in the dark 1 overexpressor line  
MIDA9: misregulated in the dark 9  
MIDA10: misregulated in the dark 10  
MIDA11: misregulated in the dark 11  
HSD1: hydroxysteroid dehydrogenase (MIDA1)  
BR : brassinosteroids  
BRI1 : brassinosteroids insensitive 1  
PP2C : type-2C phosphatase  
ABI1 : ABA insensitive 1  
ABI2 : ABA insensitive 2  
STH6 : salt tolerance homolog 6  
STH2 : salt tolerance homolog 2  
STH3 : salt tolerance homolog 3  
BBX23: B-Box 23  
MPK12: MAP kinase 12  
IBR5 : indole-3-butyric acid response 5  
MIDA7 : misregulated in the dark 7  
CIPK17: CBL-interacting protein kinase 17  
MIDA8 : misregulated in the dark 8  
MIDA13: misregulated in the dark 1





# **General Introduction**



## General introduction

### 1. What is skotomorphogenesis? And why plants need it?

Plants acquire energy solely from light, and plant survival depends on its availability. Therefore, light is a relevant environmental cue that affects development throughout the whole life cycle of the plant and with a particular significance at seedling stage ([Neff et al. 1999](#)) ([Franklin and Quail 2010](#)) ([Kami et al. 2010](#)).

Upon germination, newly emerging seedlings monitor their environment and, depending on the absence or presence of light, they undergo one of two developmental programs: skoto- or photo- morphogenesis, respectively ([Deng et al. 1991b](#)). After germination in the dark, etiolated seedlings grow heterotrophically on seed reserves and follow a skotomorphogenic strategy of development, characterized by fast hypocotyl elongation and the formation and maintenance of an apical hook with appressed cotyledons ([Quail 2002b](#)) assuring a rapid emergence of the seedling to the sunlight, by minimizing deleterious effects of pushing through the soil. Once in the surface, light is perceived by the photoreceptors that will trigger photomorphogenesis by a massive rearrangement of gene expression ([Nagy and Schafer 2002](#)) ([Rockwell et al. 2006](#)).

### 2. Light Photoreceptors in *Arabidopsis thaliana*

To adapt on local light conditions, plants are equipped with a high repertory of photoreceptors. The phytochrome (phy) family of photoreceptors (phyA through phyE) is mainly involved in detection of red (R) and far-red (FR) light wavelengths of the spectrum, and plays a central role in the regulation of germination, seedling deetiolation, growth and flowering ([Quail 2002b](#)), ([Rockwell et al. 2006](#)) 2006; ([Nagy and Schafer 2002](#)) ([Tepperman et al. 2006](#)) (Fig.1). Besides the R and FR, deetiolation can also be promoted by blue light through the phyA-signaling pathway ([Castillon et al. 2009](#)).

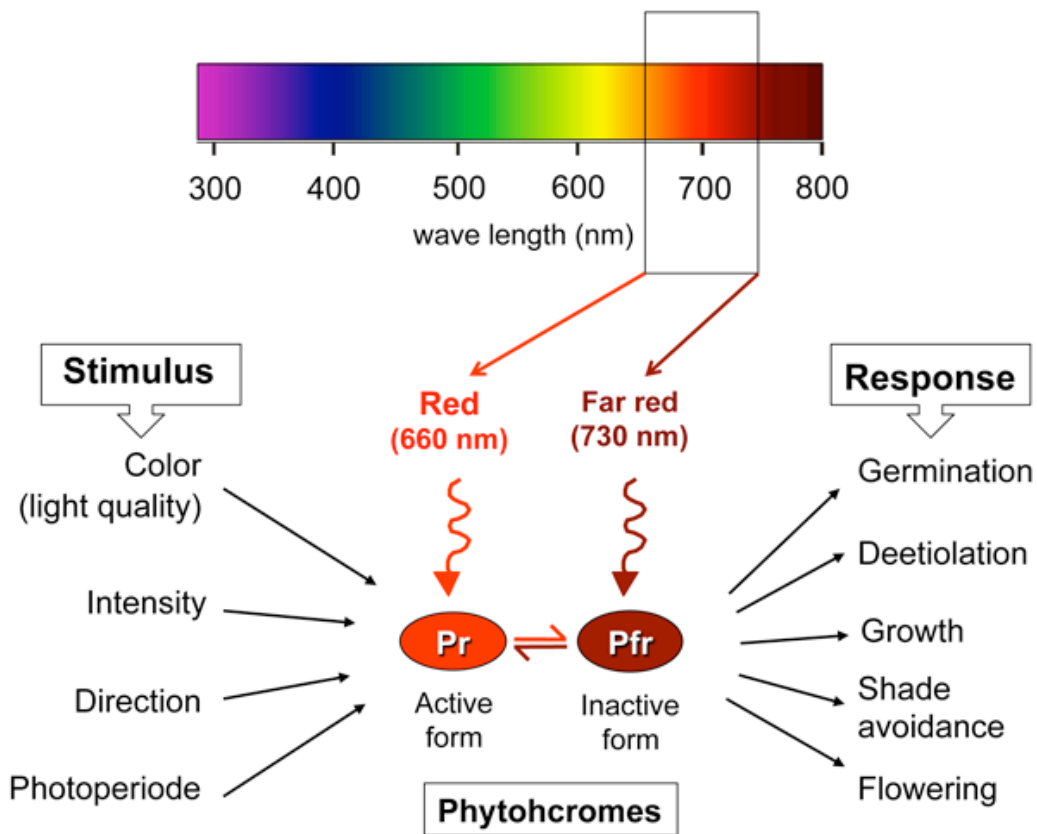


**Figure 1: Phytochromes photoreceptors.** Phytochromes percept mainly R and FR light and detect variations in the light quality, intensity, direction, and diurnal cycles. Once activated, phytochromes regulate diverse development processes as germination, deetiolation, growth, shade avoidance and flowering.

Arabidopsis' phytochromes are dimeric proteins typically consisting of two identical apoproteins covalently linked with a phytochromobilin, a linear tetrapyrrole bilin compound that acts as a chromophore ([Lagarias and Villarejo 1985](#)). The ability of phytochromes to absorb red and far-red light depends on its bound phytochromobilin conformation, which undergoes a reversible photoisomerization at the C15-C16 double bond in response to red light (666 nm) and far-red light (730 nm) ([Chen et al. 2004](#)).

After initial assembly of the phytochrome, the phytochromobilin assumes the C15-Z, *anti* conformation and is ready to absorb R light. This form of phytochrome is called the Pr form and localizes in the cytosol, and is considered biologically inactive. Upon the absorption of R light, the C15-Z,*anti* conformation is converted to the C15-E,*anti* conformation and the phytochrome becomes photoactivated (Pfr form). The Pfr interacts with other

proteins either in the cytosol or inside the nucleus (after translocation into the nucleus) and regulates their functions to induce light responses ([Sakamoto and Nagatani 1996](#)); ([Ni et al. 1998](#)); ([Fankhauser and Chory 1999](#)). The conversion between Pr and Pfr by R is reverted after FR exposure, allowing the phytochrome to act as a switch that is turned on by red light and turned off by far-red light ([Borthwick et al. 1952](#)).

Based on their relative stability upon light treatment, phytochrome family members are classified into two groups. The labile phytochrome, type I, contains only one family member, phyA, which is rapidly degraded during seedling deetiolation ([Neff et al. 2000](#)); ([Bae and Choi 2008](#)). In contrast, the type II phytochromes, phyB, C, D, and E, are relatively stable and slowly degraded upon irradiation with R light ([Sharrock and Quail 1989](#)), ([Sharrock and Quail 1989](#)).

In *Arabidopsis*, both phyA and phyB promote seed germination and de-etiolation in response to FR and R light but interestingly, phyA dominates in regulating the transcription of early responding genes during the dark to light transition ([Reed et al. 1994](#)) ([Neff et al. 2000](#)) ([Tepperman et al. 2001](#)) ([Bae and Choi 2008](#)). One explanation is that, although phyB dominates the long-term red light suppression of hypocotyl cell elongation, phyA and other phytochromes have a significant role in the apical-zone responses of hook opening, cotyledon expansion and chloroplast biogenesis ([Chen and Chory 2011](#)); ([Monte et al. 2004](#))

### **3. How is skotomorphogenesis achieved? And how the deetiolation occurs?**

Skotomorphogenesis is achieved mainly through a repression of the photomorphogenesis ([Ma et al. 2002](#)) ([Tepperman et al. 2006](#)) ([Hu et al. 2009](#)); ([Leivar et al. 2009](#)), the default development program after germination in angiosperms, and transcriptional regulation and controlled proteolysis, play pivotal role in this process.

The CONSTITUTIVE PHOTOMORPHOGENIC / DEETIOLATED / FUSCA (COP/DET/FUS) proteins act in a proteolytic pathway aimed at degrading photomorphogenesis promoting factors in the absence of light ([Osterlund et al. 2000](#)) ([Holm et al. 2002](#)) ([Seo et al. 2003](#)) ([Yang et al. 2005](#)). COP1 was also found to interact with several photoreceptors, such as LAF1, HY5, phyA, cry1, and cry2 ([Ballesteros et al. 2001](#)) ([Duek and Fankhauser 2003](#)) ([Oyama et al. 1997](#)) ([Yang et al. 2001](#)) ([Shalitin et al. 2002](#)) ([Seo et al. 2004](#)), for its degradation, as in the case of phyA ([Seo et al. 2004](#)), or to regulate its abundance, as in cry2 ([Shalitin et al. 2002](#)). Through molecular genetic approaches, there have been identified several transcription factors acting downstream of the photoreceptors that positively regulate photomorphogenesis and that are targets for the COP1 degradation ([Datta et al. 2008](#)). These transcription factors act downstream to a single or a combination of photoreceptors allowing a light-regulated transcriptional network. Accordingly, dark-grown mutant seedlings that are defective in COP1 activity resemble wildtype seedlings grown in the light ([Deng et al. 1991a](#)).

Phytochrome interacting factors (PIFs) are nuclear basic helix-loop-helix (bHLH) transcription factors that negatively regulate photomorphogenesis both in the dark (Figure 2 A) and in the light in Arabidopsis. PIFs belong to a subset of basic helix-loop-helix transcription factors (PIF1, PIF3, PIF4, PIF5, PIF6, and PIF7 in Arabidopsis) ([Ni et al. 1998](#)) ([Toledo-Ortiz et al. 2003](#)) that accumulate in the nucleus in the dark ([Quail 2000](#)) where act regulating gene expression by directly binding to the DNA in specific promoter-regions of the target genes called G-Boxes (CACGTG) ([Martinez-Garcia et al. 2000](#)).

PIFs play a central role in phytochrome-mediated signal transduction ([Toledo-Ortiz et al. 2003](#)), ([Duek and Fankhauser 2005](#)) by conformer-specifically and photoreversibly interacting with the phy-Pfr molecules in the light ([Toledo-Ortiz et al. 2003](#)); ([Duek and Fankhauser 2005](#)); ([Castillon et al. 2007](#)); ([Monte et al. 2007](#)). Recent studies with Arabidopsis seedlings deficient in one or multiple PIF proteins have established that progressive genetic removal of PIFs results in additive or synergistic effects in the dark that culminate in a partial constitutively photomorphogenic (*cop*)-like phenotype

exhibited by *pif3 pif4 pif5 (pifq)*, which is deficient in *PIF1*, *PIF3*, *PIF4*, and *PIF5* ([Bae and Choi 2008](#)); ([Josse and Halliday 2008](#)); ([Leivar et al. 2008a](#)) (Figure 2 B). These results provide evidence that the PIF proteins function in the dark in a partially redundant manner, independently of phy action, to repress photomorphogenesis and promote skotomorphogenesis unless the precise mechanism through which PIFs maintain the etiolated state remains still unclear.

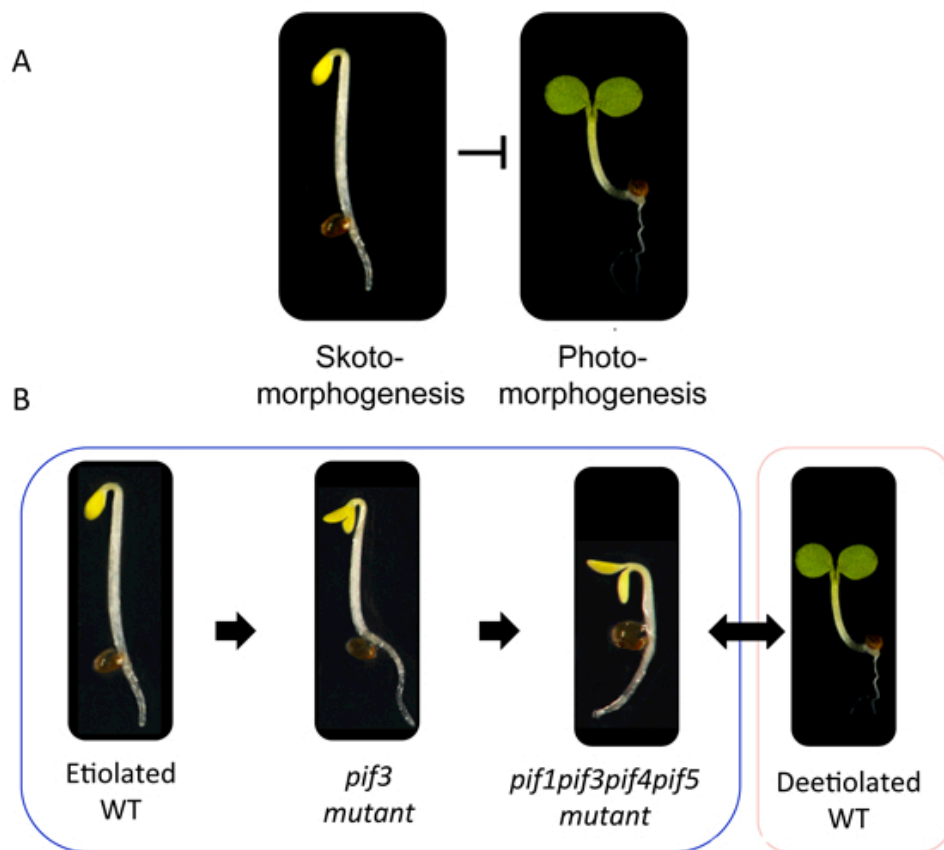


**Figure 2: Phytochrome Interacting Factors (PIFs) repress photomorphogenesis.** (A) Skotomorphogenesis is achieved by the repression of the photomorphogenic development program. (B) PIF1, PIF3, PIF4 and PIF5 contribute additively in repressing deetiolation.

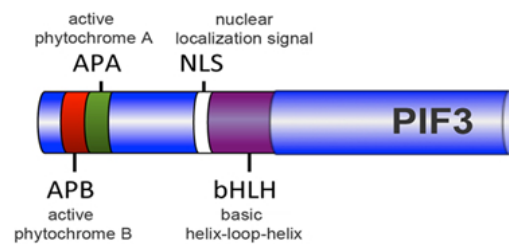
Upon light exposure, active phy translocate to the nucleus where reverse the PIFs action by interacting with and inducing a rapid phosphorylation and degradation of them in the photobodies (Fig. 3) ([Quail 2002a](#)) ([Huq et al. 2003](#)) ([Bae and Choi 2008](#)) ([Bauer et al. 2004](#)) ([Park et al.](#)

[2004b](#)) ([Shen et al. 2005](#)) ([Al-Sady et al. 2006](#)) ([Khanna et al. 2006a](#)) ([Nozue et al. 2007](#)); ([Shen et al. 2007](#)) ([Lorrain et al. 2008](#)) ([Shen et al. 2008a](#)). PIFs interact with the active form of phyB (PIF1, PIF3–5 and PIF7) or with phyA (PIF1 and PIF3) through a domain located in the N-terminal part of the protein called APB (active phytochrome B) or APA (active phytochrome A), respectively (Fig.3 A) ([Khanna et al. 2004](#)) ([Al-Sady et al. 2006](#)) ([Leivar et al. 2008a](#)) ([Shen et al. 2008b](#)). All the PIFs described so far are stable in the dark. After light exposure, PIF1 and PIF3 are degraded in both Rc and FRC ([Al-Sady et al. 2006](#)); ([Leivar et al. 2008b](#)), while PIF4 and PIF5 are degraded only in Rc remaining in stable levels when exposed to long FR periods ([Lorrain et al. 2009](#)). Upon phyA and PIFs interaction, PIFs are phosphorylated and subsequently ubiquitinated for its degradation in the 26S proteasome in approximately one hour in Rc (Fig 3 B-C)([Al-Sady et al. 2006](#)). However, in striking contrast, unless PIF7 also migrates to the speckles where binds with phyB upon light exposure, the seventh PIF is not degraded ([Leivar et al. 2008b](#)). All together, those data suggest that the consequences of interaction with photoactivated phytochromes differ among PIFs.

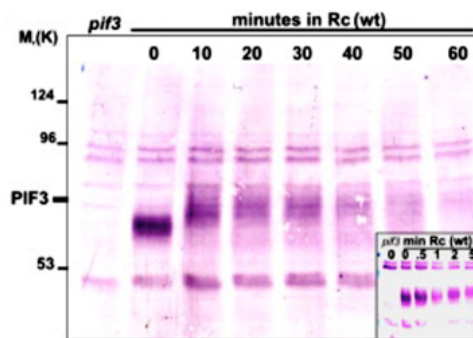
Multiple advances had been unveiled recently about the deetiolation process. Regarding to the phytochromes translocation into the nucleus after its photoactivation ([Ma et al. 2001](#)) ([Tepperman et al. 2001](#)) ([Fankhauser and Chen 2008](#)), it was prior described that Pfr-phyA cannot translocate into the nucleus *per se*. Instead, phyA requires two paralogous proteins FAR RED ELONGATED HYPOCOTYL 1 (FHY1) and the FHY1-like (FHL) ([Hiltbrunner et al. 2005](#)) ([Zhou et al. 2005](#)). Both proteins interact in a light-dependent manner with phyA and uncover a functional nuclear localization signal (NLS) allowing a “piggy-back” mechanism as basis of the phyA transport to the nucleus ([Hiltbrunner et al. 2006](#)); ([Genoud et al. 2008](#)). Similar situation has been recently described for phyB. Pfeiffer and colleagues demonstrate *in vitro* the Pfr-phyB dependency on PIF1 and PIF3 for its translocation into the nucleus during the deetiolation and propose the same role, as phyB transport facilitators, for other PIF members given the decreased nuclear phyB levels exhibited in the *pifq* in *in vivo* assays ([Pfeiffer et al. 2012](#)). Nevertheless, how PIFs perform this action is still unknown.

Another recent discovering shows how phys/PIFs binding is bridged by a third one protein called HEMERA (HMR), prior the speckles formation. It is still unclear which is the photobodies function, ranging from providing a place for PIFs phosphorylation, ubiquitylation, and posterior degradation or just giving a proper environment for the phosphorylation ([Galvao et al. 2012](#)).

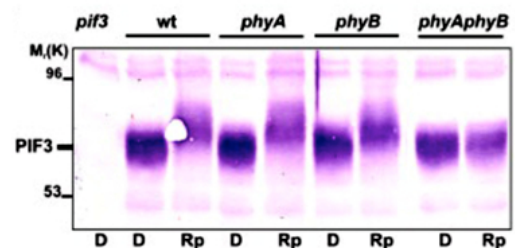
A



B



C



D

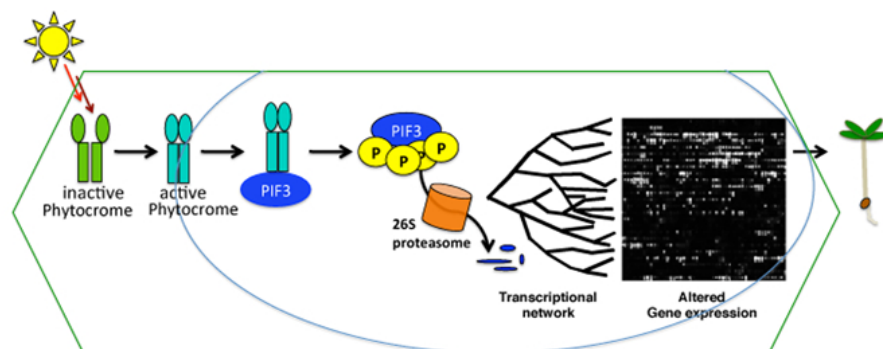


**Figure 3: Photoactivated phytochromes induce PIF3 degradation.** (Adapted from Al-Sady et al.2006) (A) PIF3 scheme depicting the N-terminal APB and APA do-mains and the NLS and the bHLH domains. (B) Protein-Blot analysis showing PIF3 accumulation in darkness and a subsequent degradation after Rc exposure. (C) PIF3 degradation depends on phyA and phyB action. (D) Diagram representing the phytochrome activation and translocation to the nucleus where binds with PIF3 promoting its phosphorylation and degradation in the 26S proteasome. PIF3 degradation promotes transcriptional changes that allow photomorphogenesis to proceed.

The results published by Jang and colleagues are especially interesting. The authors demonstrate a new mechanism underlying the phyB levels regulation (and other light-stable phy levels) during deetiolation through a direct interaction with the COP1 E3 ligase in a PIF dependent manner. In such case, PIFs act promoting the interaction and the polyubiquitination of phyB by COP1. That new role of PIFs seems to be directly related with the recently discovered action of phyB in preventing the PIF binding to the promoters of its downstream-regulated genes ([Park et al. 2012](#)). Thus, the activity of the N-terminal domain of phyB (NG-GUS-NLS; NGB) ([Matsushita et al. 2003](#)) is not to target the degradation of PIF3 in response to red light. Instead, the N-terminal phyB domain inhibits the binding of PIF3 to its target promoters in a red light-dependent manner *in vivo* ([Matsushita et al. 2003](#)). Moreover, they also show that the full-length phyB also inhibits the binding of PIFs to their target promoters under red light *in vivo*. Based on these new findings, phyB inhibits negatively acting PIFs by two different modes of action: by releasing them from their target promoters and by mediating their degradation.

In darkness, photobiological experiments demonstrate that photoactivated phytochrome in the ungerminated seeds is stably retained and acts in the Pfr form to promote partial photomorphogenic responses assuring subsequent growth of the postgerminative seedling in the dark ([Leivar et al. 2008b](#)). So it would be not surprising if PIFs were not only promoting phyB ubiquitylation by COP1 during the deetiolation but also during the etiolated state in order to assure the seedling survival through a proper transcriptional regulation in dark conditions.

#### 4. PIF roles during plant development

PIF3 was first described as Phytochrome B interactor through a yeast-two-hybrid analysis ([Ni et al. 1998](#)) ([Shimizu-Sato et al. 2002](#)) performed light conditions. It was rapidly demonstrated its ability to bind conformer-specifically, in photoreversible fashion, to the Pfr form of both phyA and phyB. Posterior analysis of PIF3 homologous proteins revealed five more PIF family

members, PIF1, PIF4, PIF5, PIF6, and PIF7 ([Quail 2000](#)). Because homologous proteins tend to have similar roles, there was expected that the new PIF members might also play roles in Phy-mediated light signaling.

In darkness, PIFs constitutively act in a light-independent manner as transcription factors ([Leivar et al. 2008b](#)). In addition, PIFs implement phy-transduced signals coming from a broad light conditions as R light, FR light, blue light or shade and participate in seedling growth under different diurnal cycles ([Al-Sady et al. 2008](#); [Leivar et al. 2012b](#); [Leivar et al. 2009](#); [Lorrain et al. 2008](#); [Monte et al. 2003](#); [Moon et al. 2008](#); [Oh et al. 2009](#); [Shin et al. 2009](#)). Their relative contribution during the seedling development differs or overlaps depending on the light nature, the temperature, or the growth stage of the seedling.

PIF1 is the main PIF regulating seed germination ([Oh et al. 2004a](#)). In the dark, PIF1 represses germination through reducing GA responsiveness and regulating GA and ABA levels ([Oh et al. 2006](#)) ([Finch-Savage and Leubner-Metzger 2006](#)) where GA is an inductor and ABA a repressor of germination. First, PIF1 directly activates transcription of two *DELLA* genes, *GAI* and *RGA*, which are negative regulators in GA signaling. Second, low GA and high ABA levels in darkness are at least achieved through two proteins, SOM and DAG1 ([Kim et al. 2008](#)) ([Gabriele et al. 2010](#)), which regulate the expression of GA and ABA metabolic genes. PIF1 activates *SOM* and *DAG1*, directly and indirectly, respectively regulating at the end GA and ABA levels. When light-activated phytochromes interact with PIF1, promote its degradation, negating the PIF1-repressive effects and thus promoting germination ([Shen et al. 2005](#)) ([Lau and Deng 2010b](#)).

During deetiolation in Rc, PIF1 contributes in a partial redundant manner with PIF3 and PIF4 to the hypocotyl elongation ([Shin et al. 2009](#)) ([Leivar et al. 2012b](#)) and shares leading role with PIF3 in the inhibitory action on chlorophyll biosynthesis and gravitropism regulation ([Monte et al. 2004](#)) ([Huq et al. 2004](#)) ([Oh et al. 2004b](#)) ([Moon et al. 2008](#)). Besides the PIF1 role in Rc, the transcription factor also negatively regulates photomorphogenesis at the seedling stage under blue light conditions. *pif1* seedlings displayed more open

cotyledons and slightly reduced hypocotyl length compared to wild type under diurnal (12 hr. light/12 hr. dark) blue light conditions ([Castillon et al. 2009](#)). In contrast, PIF5 role in hypocotyl elongation under Rc is not very relevant.

FRc light mimics a growth environment under a dense canopy. Deetiolation in such conditions is mainly regulated by PIF3 and PIF1, but also by PIF4 and PIF5 which remain stable after long periods of FR exposure regulating growth-related genes in the Dark, some of them related to hormone pathways as hormones ([Lorrain et al. 2009](#)), evidencing again the close relation between PIFs and hormones regulation.

During the deetiolation, photoactivated phytochromes trigger the degradation of PIF protein levels to a new steady state levels that represent 10% of their dark levels ([Monte et al. 2004](#)) ([Shen et al. 2005](#)) ([Nozue et al. 2007](#)). In Rc grown seedlings, the reminiscent levels of PIFs induce phyB proteolytic degradation through the proteasome system using COP1 as an E3 ligase ([Khanna et al. 2007](#)) ([Al-Sady et al. 2008](#)) ([Leivar et al. 2008a](#)) ([Jang et al. 2010](#)). That fact suggests the existence of a mutually negative feedback loop between the phyB and PIF proteins in Rc conditions ([Leivar and Quail 2011](#)). Progressive genetic removal of multiple PIFs results in an additive effect that correlates with increasing hypersensitivity of the seedling to Rc ([Leivar et al. 2008a](#)) demonstrating an active role of PIFs in regulating phyB levels in Rc light. Similar situation occurs in short day conditions. The light-induced phyB degradation contributes to the progressive decrease in Pfr levels during the dark period under diurnal conditions (light/dark cycles). In addition, the PIFs re-accumulate in light-grown seedlings upon exposure to darkness (such as under diurnal conditions) ([Monte et al. 2004](#)) ([Shen et al. 2005](#)) ([Nozue et al. 2007](#)) or far-red light-enriched environments (such as vegetational shade) ([Lorrain et al. 2008](#)) through a process that depends on the activation state (or Pfr/Pr ratio) of the phytochromes.

Hypocotyl elongation is a well-established light-regulated response that is maximal in seedlings grown in continuous dark. In post-germinative darkness, the PIF proteins promote hypocotyl elongation through their intrinsic

transcription factor capacity, regulating a transcriptional network that sustains etiolated growth ([Leivar et al. 2009](#)) ([Shin et al. 2009](#)). This conclusion is supported by the observation that a quadruple mutant deficient in PIF1, 3, 4 and 5 (*pifq*) exhibits a partial constitutively photomorphogenic phenotype in the dark, characterized by a short-hypocotyl phenotype ([Leivar et al. 2008b](#)). In continuous light, under which PIFs induce phyB degradation, PIF-deficient mutants display a hypersensitive short-hypocotyl phenotype that is interpreted to be, at least partially, the result of enhanced photosensitivity of the seedling due to elevated photoreceptor levels ([Khanna et al. 2007](#)) ([Al-Sady et al. 2008](#)) ([Leivar et al. 2008a](#)).

Under diurnal conditions, with an alternating light/dark cycle, the extent of hypocotyl elongation depends on the duration of the dark period ([Niwa et al. 2009](#)). During dark hours, the hypocotyl elongation rate is maximal at the end of the night in seedlings grown under short-day (SD) photoperiods ([Nozue et al. 2007](#)). Studies have indicated that PIF4 and PIF5 are positive regulators of this response ([Nozue et al. 2007](#)) ([Niwa et al. 2009](#)). The precise regulation of their time of action at the end of the dark period has been proposed to involve a coincidence mechanism that combines regulation of PIF4 and PIF5 transcript levels by the circadian clock, superimposed on the control of PIF protein accumulation by light ([Nozue et al. 2007](#)) ([Nusinow et al. 2011](#)). In addition to PIF4 and PIF5, the current model predicts additional, yet to be identified, factors are involved in the regulation of seedling growth under SD conditions.

Upon unveiled the main roles of PIF proteins in seedling development through genetic analyses with single or high order mutants, it becomes necessary to unveil which are downstream genes implementing the PIFs signal to completely understand the phy-PIFs-development system. Multiple studies in recent years have been carried out with this purpose. Microarray transcriptional analysis, Chip-seq and Chip-on-Chip, have been the best techniques to elucidate the transcriptional network regulated by the PIF, family and have documented the pleiotropic function of these factors in coordinating the seedling development ([Monte et al. 2004](#)) ([Moon et al. 2008](#)) ([Lorrain et al.](#)

[2008](#)) ([Oh et al. 2009](#)) ([Leivar et al. 2009](#)) ([Lorrain et al. 2009](#)) ([Shin et al. 2009](#)) ([Toledo-Ortiz et al. 2010](#)) ([Hao et al. 2012](#)).

## 5. Previous expression profile studies performed in PIFs.

The first expression profile study of PIF network regulation was to define the primary events in phy signaling and transcriptional regulation, focusing on the potential role of PIF3 in this process during the initial period of seedling deetiolation after exposure to Rc light ([Monte et al. 2004](#)). Phenotypic experiments with *pif3*, demonstrate that PIF3 is necessary for normal greening and chloroplast development during the early hours of deetiolation. The genome-wide microarray analysis identified rapidly Rc-responsive induced and repressed genes in the *pif3*, suggesting that PIF3 regulates deetiolation by inducing and repressing genes in Rc. The 70% of the genes with highest significant difference with the WT were encoding for chloroplast components, suggesting that PIF3 may have a primary function in regulating phy-induced expression of a key subset of nuclear-encoded chloroplast proteins.

Sequent studies performed in darkness identified the chlorophyll biosynthetic genes PROTOCHLOROPHYLLIDE OXIDOREDUCTASE (*POR*), FERRO-CHELATASE (*FeChII*), and HEME OXIGENASE (*HO3*), as PIF1 negatively regulated genes in darkness, adding information to the preceding study on the PIFs role in regulating chlorophyll related genes ([Moon et al. 2008](#)). ChIP and DNA gel-shift assays completed the study demonstrating the direct binding of PIF1 to the PORC promoter suggesting that PIF1 directly and indirectly regulates chlorophyll biosynthesis involved genes to optimize the greening process in Arabidopsis. Deetiolation studies in FRc ([Lorrain et al. 2008](#)) revealed PIF4 and PIF5 as repressors of gene expression during this process. Both PIFs act mainly in repressing transcriptionally photosynthesis related genes, lipid transport and tetrapyrrole synthesis after prolonged periods (24h) in FRc. Contrary, a minor percentage of the PIF4 and PIF5 regulated genes are repressed in the *pif4 pif5* mutant. Those genes are mainly involved in metabolic processes as well as auxin stimulus, specifically in inducing the AUX/IAA transcription factor genes.

Two independent expression profile studies performed on the *pif1 pif3 pif4 pif5* quadruple mutant ([Shin et al. 2009](#)) ([Leivar et al. 2009](#)), resulted in similar results.

The first group demonstrated the PIF3 role in negatively regulating chlorophyll biosynthesis by repressing biosynthetic genes in the dark, consistent with the previous published results about the same PIF3 role in Rc or the PIF1 role in darkness, demonstrating once more, the overlapping or redundant roles of PIF family members. When four phytochrome-interacting protein genes were mutated, the resulting quadruple mutant seedlings displayed constitutive photomorphogenic phenotypes, including short hypocotyls, open cotyledons, and disrupted hypocotyl gravitropism in the dark. Microarray analysis further confirmed that the dark-grown quadruple mutant has a gene expression pattern similar to that of red light-grown WT. Together, the data indicated that the four PIF1, PIF3, PIF4 and PIF5 proteins are required for skotomorphogenesis and phytochromes activate photomorphogenesis by inhibiting these factors. The second study ([Leivar et al. 2009](#)) provided a more detailed analysis of the transcriptional changes regulating skotomorphogenesis and de-etiolation. Results of Leivar and colleagues agree with the Shin's group in the deetiolated phenotype of the *pifq* mutant in dark conditions and add information describing also the hypersensitive phenotype of the *pifq* mutant in Rc. As PIFs regulate phyB levels in continuous Rc, it is not surprising the two fold more levels of phyB in the *pifq* in continuous Rc when compared with the WT explaining the hypersensitive phenotype of the *pifq*. Contrary, phyB levels are not affected in darkness in the mutant when compared with the WT suggesting that PIFs role in darkness is light independent. Cellular phenotypic studies using light and electronic microscopes, revealed altered cell organization in the *pifq* grown in darkness phenocopying a WT grown in Rc instead of a WT grown in darkness with exaggerated cell expansion and intracellular air spaces. Looking at the subcellular level, the *pifq* displays large vacuoles and low oil bodies' amount when compared with a dark grown WT, again, resembling more to a Rc grown WT. By comparing the rapidly light-responsive genes in wild-type seedlings with those responding in darkness in the *pifq* mutant, the authors identified a subset, enriched in transcription factor–encoding genes, that are potential

primary targets of PIF transcriptional regulation because of having in most cases G-boxes in their promoters. Chip-seq analysis might be performed to test the possibility of those genes for being direct PIF-target genes.

Collectively, those data suggest that the transcriptional response elicited by light-induced PIF proteolysis is a key component of the mechanism by which the phytochromes pleiotropically regulate deetiolation and that at least some of the rapidly light-responsive genes may comprise a transcriptional network directly regulated by the PIF proteins.

Finalizing a recently published work ([Leivar et al. 2012b](#)) defends the idea of an overlapping on the early shade-induced genes with the light-repressed ones during the deetiolation. Through a transcriptomic analysis, the authors identify 123 statistically significant two fold (SSTF) PIF-dependent shade early responsive genes from which 103 are induced in the *pifq* and 20 repressed. Among the induced, they find ATHB2, XTR7 or HFR1, suggesting that PIFs promote shade avoidance syndrome (SAS) by inhibiting photomorphogenesis inductor genes. Between those 103 genes, the subsets most differentially expressed when compared with the WT are highly enriched in g-box containing genes in their promoters suggesting the possibility of being primary direct targets of PIFs. Those g-box containing genes, are themselves highly enriched in transcription factors genes. Expanding the signal transduction received by the phys and transduced downstream by the PIFs. Among the non G-box containing genes, it is remarkably the enrichment in hormone related genes, especially in auxin responsive genes.

The parallelism Dark-Shade presented in this work, results in a 64% of overlapping in statistically significant differently expressed genes in both conditions but remains without functionally characterizing the genes regulated downstream the PIFs signalling. Additionally, that work leads to think in other parallelisms as the deetiolation and the periodical dark to light transition in diurnal conditions. We talk about similar situations controlled by similar factors, so it wouldn't be strange to find overlapping genes exerting its function in both situations. More investigation should be done to address that question in the future.

Here in this thesis, we identify a set of genes called MIDA genes from MISREGULATED IN THE DARK, acting downstream of PIF3 during the etiolation and deetiolation processes. Different MIDA genes regulate different organ morphogenesis evidencing a branching in the PIF3 signal. We also propose a new phy-PIFs-MIDA explanatory model of the deetiolation process, suggesting one early and strong response, which allows the swift from skotomorphogenesis to photomorphogenesis, and a late response which modulates the first one in order to avoid over-responses to light.

Additionally, through a collaboration in the Judit Soy's research project, we unveiled the PIF3 role in the hypocotyl elongation at the end of the night together with PIF4 and PIF5 in short day conditions.



## **Objectives**

## Objectives

The main objective of this thesis was to elucidate the mechanism by which the transcription factor PIF3 regulates seedling development in the dark, through functional profiling of the PIF3-regulated gene network in *Arabidopsis*.

The specific objectives were:

1. Identification of downstream components that might be mediating PIF3 function as a repressor of photomorphogenesis in the dark.
  - 1.1. Analysis of the PIF3-regulated transcriptome in dark conditions.
  - 1.2. Selection of PIF3-regulated MIDA (MISREGULATED IN DARK) genes as potential regulators of the skotomorphogenesis.
  - 1.3. Functional characterization of *Arabidopsis mida* mutants in darkness.
  - 1.4. Characterization of MIDAs expression profiles during the dark to light response.
  - 1.5. Phenotypic characterization of *midas* during the dark to light transition.
  - 1.6. Phenotypic characterization of *pif3* and *pif3pif4pif5* during the dark to light transition.
  
2. Phenotypic characterization of PIF3 role in *Arabidopsis thaliana* seedlings grown in short-day conditions.





To Whom It May Concern:

Maria Sentandreu has participated in 3 publications during his PhD thesis, 2 of them with high Impact Factor:

1-Author(s): **Sentandreu, Maria**; Martin, Guiomar; Gonzalez-Schain, Nahuel; Leivar, Pablo; Soy, Judit; Tepperman, James M.; Quail, Peter H.; Monte, Elena  
Title: Functional Profiling Identifies Genes Involved in Organ-Specific Branches of the PIF3 Regulatory Network in Arabidopsis  
Source: **PLANT CELL**, 2011. 23: 3974  
Impact Factor in the Year of Publication: 8.987  
Quartile within the Area and the Year: Q1

2-Author(s): **Sentandreu, Maria**; Leivar, Pablo; Martin, Guiomar; Monte, Elena  
Title: Branching of the PIF3 regulatory network in Arabidopsis: Roles of PIF3-regulated MIDAs in seedling development in the dark and in response to light.  
Source: **PLANT SIGNALING BEHAVIOUR**, 2012. 7: 510  
Impact Factor in the Year of Publication: -  
Quartile within the Area and the Year: -

3-Author(s): Soy, Judit; Leivar, Pablo; Gonzalez-Schain, Nahuel; **Sentandreu, Maria**; Prat, Salome; Quail, Peter H.; Monte, Elena  
Title: Phytochrome-imposed oscillations in PIF3 protein abundance regulate hypocotyl growth under diurnal light/dark conditions in Arabidopsis  
Journal: **PLANT JOURNAL**, 2012. 71: 390  
Impact Factor in the Year of Publication: 6.160 in 2011  
Quartile within the Area and the Year: Q1 in 2011

Plant Cell as well as Plant Journal belong to the first quartile within their research area of Plant Biology and the corresponding impact factors are 8,987 and 6.16 respectively. Plant Signaling Behavior is a new magazine that does not have assessment of impact factor.

Plant Cell is the magazine with the highest Impact Factor in Plant Biology.

Elena Monte Collado

## **General Discussion**



## **General Discussion.**

### **1. Identification of downstream components that might be mediating PIF3 function as a repressor of photomorphogenesis in the dark**

Although significant progress has been made in elucidating the role of PIF proteins during the plant development, it remains uncompleted and unclear how PIFs implement signalling cues coming from light variations, temperature, circadian clock and hormones to regulate it. The knowledge about PIFs action is more extended in some fields but maybe, because PIF3 was first described as a phytochrome interacting factor acting in light conditions, there is little known in the skotomorphogenesis one. Several works published in recent years demonstrate that multiple PIFs assure the etiolation by repressing photomorphogenesis nevertheless any gene acting downstream was functionally described previously to the publication of our work. From here, our interest in elucidating how PIF3 promotes skotomorphogenesis through the transcriptional regulation of other genes. Trough a transcriptional profile comparing expression in wild type seedlings with *pif3* mutant ones, there were identified several genes acting downstream the transcription factor which implement the signal received by PIF3 in order to maintain the etiolation and to assure a proper deetiolation process. This new genes were called MIDAs from MISREGULATED IN DARK. Now, at that time point and achieved the objective, our work reports valuable information to better understand the etiolation process and an innovating model which provides new insights about the PIFs role during the deetiolation.

#### **1.1 Analysis of the PIF3-regulated transcriptome in dark conditions.**

Through a transcriptional profiling and after applying some cut-offs and statistics we obtained 82 SS1.5FC misregulated genes in the *pif3* when compared with the WT. From them, we saw that 42 were induced and 40 were repressed, so we could affirm that PIF3, out of the PIFs group, acts regulating gene expression positively and negatively regarding to the photomorphogenesis repression.

## **1.2 Selection of PIF3-regulated MIDA (MISREGULATED IN DARK) genes as potential regulators of the skotomorphogenesis.**

Later on, analyzing the inferred function of those 82 genes in databases as TAIR, we could observe how PIF3 exerts its action on genes involved in a broad field of processes as growth and development, metabolism, signaling, hormones, photosynthesis, stress or defense responses and transcriptional regulation, providing strong evidence about the broad spectrum of action of PIF3 during the etiolation. Between those genes, there were some yet described as for example the *cab* genes, which are involved positively in the photosynthesis and repressed by PIF3 in the dark. The fact to find those genes strengthened to our results.

From those 82 genes, we chose 10 with a related function in transcriptional activity, signaling, growth, development, stress and defense, or hormone-related activity, to be analyzed in detail because of the importance of those processes during the etiolation.

Transcriptional data derived from the microarray was validated through qPCR expression analysis, expanding the analysis from 2 to 4 days and from expression in *pif3* to expression in the multiple mutant *pifq*. Here we observed different patterns of transcriptional regulation for the *MIDAs* along the development suggesting a precise fine-tuning in the time of action of those genes. In addition, expression studies in the *pifq* revealed that PIFs regulate synergistically *MIDA* genes, what might evidence again an accurate modulation in their activity. PIFs contribution varies depending on the different processes of the etiolation; for example, PIF5 is the only one PIF described as involved in the hook development and PIF1 regulates mainly the hypocotyl elongation ([Khanna et al. 2007](#)); ([Leivar et al. 2012a](#)) so different PIFs might regulate *MIDAs* depending on the moment. Another possibility is that PIFs might be heterodimerizing at that stage providing one more level of regulation

so different combinations of PIFs may adjust temporally or spatially the MIDA genes expression.

### **1.3 Functional characterization of *Arabidopsis mida* mutants in darkness.**

As this study is the first to systematically characterize the role of PIF3-regulated genes in the dark and after having the gene expression data for all of them, we thought specially interesting to determine whether *mida* mutants would be affected phenotypically along the days and/or if we would be able to detect organ-specificity in its action during the etiolation.

Based on the *mida* phenotypes, and after applying strong cut-offs to strengthening the analysis we got four genes MIDA1, MIDA9, MIDA10 and MIDA11, as potential regulators of skotomorphogenesis downstream PIF3.

*MIDA1-OX* exerts its action along all the skotomorphogenesis while *MIDA9*, *MIDA10*, and *MIDA11* have prominent roles at 2 and 3 days, suggesting modulation in the MIDAs activity during the etiolation. Moreover and very interesting is the fact that different MIDAs regulate morphogenesis in diverse organs, in a way where, *MIDA1* regulates cotyledon aperture, *MIDA9* and *MIDA10* regulate hook aperture and *MIDA11* is involved in the hypocotyl elongation. All the results together, propose a branching in the PIF3 signal where PIF3 regulates the expression of multiple genes involved independently in the development of different organs during the etiolation. Different environmental cues perceived by PIFs in each organ or the different stages of development might promote the dissection in the PIF3 signal. Branching is a new point of view of the etiolation process where it was always thought that hook aperture, cotyledon unfolding and hypocotyl elongation were such dependent processes occurring together.

Remarkable are the diverse roles of MIDAs. MIDA1 is a hydroxysteroid dehydrogenase (HSD1) with a related role in hormone signaling which participates in the brassinosteroids (BR) biosynthesis ([Li et al. 2007](#)). It was

described that adult plants constitutively overexpressing HSD1 display phenotypes similar to those displayed by plants overproducing BR or the BR receptor BRI1, it is, bigger plants with increased branching and longer roots and also expressing in a constitutively way BR responding genes. Based on the phenotype of BR-deficient mutants, BRs have also been shown to participate in seedling deetiolation ([Szekeres et al. 1996](#)). Even more investigation should be done, MIDA1 could be participating in the interplay between light and hormone signaling pathways, a essential integration for the coordination of seedling development ([Halliday 2004](#)); ([Alabadi and Blazquez 2009](#)) ([Lau and Deng 2010a](#)) ([Lau and Deng 2010a](#)), ([Shen et al. 2012](#)).

Independently MIDA9 is a type-2C phosphatase positively regulating hook maintenance in darkness. So far, some type-2C phosphatases have been described as involved in the abscisic acid (ABA) pathway as ABI1 and ABI2, controlling the full range of ABA responses, including the regulation of transpiration, vegetative growth and seed germination ([Meyer et al. 1994](#)) ([Meyer et al. 1994](#)) ([Rodriguez 1998](#)). Those PP2Cs belong to the A clade, the first of the 10 clades in which are divided the 80 PP2C members in Arabidopsis. Contrary to ABIs, MIDA9 belongs to the D clade of predicted nuclear phosphatases with a transmembrane domain ([Schweighofer et al. 2004](#)). MIDA9 is the first phosphatase described in its clade and is to our knowledge, the first type-2C phosphatase described with a role during the etiolation and deetiolation processes.

The second MIDA gene with a phenotype involved in the hook maintaining is MIDA10. MIDA10 encodes for a BBX23, a previous uncharacterized member of the Arabidopsis B-BOX family of transcription factors. Within this family, MIDA10/BBX23 forms part of a clade of 8 members with four of them (BBX21, BBX22, BBX24 and BBX25), previously implicated in light signaling ([Khanna et al. 2006b](#)) ([Indorf et al. 2007](#)) ([Datta et al. 2007](#)) ([Datta et al. 2008](#)) well as negative regulators STO and STH1 or well as positively regulators of light signaling as STH2 or STH3. Those B-BOX members have been described as components of a large complex formed with COP1 where STH3 and STH2 would be ubiquitylated by COP1 in darkness for

its degradation. MIDA10/BBX23 could also be interacting directly or indirectly with COP1 but further analysis beyond the scope of this study should be done to address that question.

The last gene found contributing to the etiolated development is MIDA11. MIDA11 acts positively regulating hypocotyl elongation during the etiolation and encodes for a MAP-kinase. It was recently reported as a substrate of IBR5, a MPK phosphatase and as a novel negative regulator of auxin signaling in Arabidopsis ([Lee et al. 2009](#)). MPK12 will be inhibiting auxin signaling and its dephosphorilation by IBR5 will release the inhibition allowing the signal to be transduced. Interestingly, etiolated seedlings treated with exogenous auxins display short hypocotyls and roots ([Jensen et al. 1998](#)) ([Zhao et al. 2003](#)) ([Lee et al. 2009](#)) so deficient seedlings in MPK12 could be hypersensitive to auxins displaying an arrest in the hypocotyl elongation.

Resuming, even more investigation is required, so far, our data indicate that PIF3 signaling branches downstream in a way that the action of MIDA1, MIDA9, MIDA10 and MIDA11 regulate development in different organs through independent specific pathways which might be involving COP1 and hormone biosynthesis and/or signaling to coordinate the etiolation. Branching of the signal that PIF3 relays downstream could be achieved through differential spatial expression patterns of these MIDA factors in specific tissues or organs. More analyses need to be done in order to asses this possibility.

Some possible explanations support the case of the other eight MIDA genes which mutants did not display any interesting phenotype. The first one is that even transcriptional changes in the expression were detected in the *pif3*, those changes could not be relevant at the functional level therefore not contributing to the *pif3* phenotype. The second option is based on the functional redundancy with other factors. For example, *MIDA7* is a CIPK17 belonging to a big family of kinases and *MIDA8* is part of the hydroxysteroid dehydrogenases family, which operates activating steroid hormones as brassinosteroids. It is common the functional redundancy between members of a same family ensuring that disruption of a single gene will not have any

phenotypic relevance for the organism; PIFs themselves are a good example of that ([Leivar et al. 2008b](#)) ([Shin et al. 2009](#)). Another possibility would be that the displayed phenotypes are not strong enough to achieve our cut-off requirements for bona-fide phenotypes, it is to say, maybe the phenotype is just maintained during one day instead of the two days required or maybe the difference with the WT don't achieve the levels we asked for. Finally, another simple explanation would be that perturbations in those *mida* mutants could be promoting functional defects we are not considering in our study.

To address whether functionally relevant MIDAs are directly regulated by PIF3 we investigated for the presence of the G-box motif CACGTG in the 3kb region of the promoter upstream of the initial transcriptional site as PIF3 binds specifically to G-box motifs to regulate gene expression. As a result, we found that among the four MIDA genes with relevant functionality during the skotomorphogenesis, only MIDA9 has a G-box while out of the other eight MIDAs with no relevant roles, just MIDA6, MIDA8 and MIDA13 had G-box in their promoter sequences. This means that there is not correlation between the presence of G-box in the MIDA's promoters and the fact of being functionally relevant during the etiolation. Additional analysis should be done to asses the possibility that PIF3 regulates the MIDA9, MIDA6, MIDA8, and MIDA13 expression by directly binding to their promoters.

As PIF3 regulates negatively photomorphogenesis, we wrongly assumed that this regulation would be achieved through the repression of genes, which promote photomorphogenesis in coordination with the induction of genes that repress the same. Surprisingly, the picture that our previously discussed results drawn, was far away from the one expected. The branching of the PIF3 signal unravel a different level of regulation where PIF3 induces either inductors or repressors of photomorphogenesis, and might repress both, repressors and inductors of photomorphogenesis.

This finding, prompted us to hypothesize whether this apparent contradiction might be reflecting the scenario played out once the wild-type etiolated seedling is exposed to light and PIF3 is degraded, rather than being a dark-specific phenomenon.

#### **1.4 Characterization of MIDAs expression profiles during the dark to light response.**

The new hypothesis took us forward to study the *MIDAs* role during the deetiolation. We rescue the available Rc data complementing our dark expression analysis, together with the data published for the pifq transcriptome ([Monte et al. 2004](#)) ([Leivar et al. 2009](#)). 3 out of the 4 *MIDA* genes, *MIDA1*, *MIDA9* and *MIDA11* displayed increased gene expression in pifq and after Rc light exposure suggesting an interesting new role of those genes during deetiolation.

*MIDA10*, a PIF3 induced negative regulator of hook aperture was rapidly degraded after one hour of Rc exposure relieving this inhibition and allowing the hook aperture to proceed accordingly to the deetiolation process. Contrary, *MIDA9*, the second *MIDA* acting as a negative regulator of hook unfolding which expression is repressed not only by PIF3 but also by other PIFs in the dark, displayed a decrease in its expression during the first hour to increase it gradually again during the sequent hours, arriving to a maximal point after 6h of Rc exposure. Similarly occurred with the inductor of hypocotyl elongation *MIDA11*, which expression, is repressed by PIFs in darkness. After 12h of Rc exposure, *MIDA11* expression increases three times the dark levels suggesting together with *MIDA9* the possibility that those genes could be acting both in dark and during the dark to light transition. Finally, *MIDA1*, which induces cotyledon aperture, experiments a big increase in its expression during the first hours of deetiolation accordingly with the necessity of the seedling for opening them and begin to realize the photosynthesis to become autotrophic.

*MIDAs* expression pattern during deetiolation suggested two kinds of responses after the deetiolation. An early response were the seedling would be performing strong and fast changes to attain the dark to light shift, it is to say, to arrest the skotomorphogenic development and begin with the photomorphogenic one. And a second step where the seedling would need to modulate this previous response in order to optimize it according to the

environmental conditions all around assuring in this way, its own survival.

Given this third hypothesis, we focused our efforts in unveil this new role for the MIDAs and subsequently for the PIFs.

### **1.5 Phenotypic characterization of *mida* during the dark to light**

*mida* phenotypes during deetiolation are weak but robust. Cotyledons open faster compared with its WT sibling in the case of *mida1-OX* line and short hypocotyls are displayed in the case of *mida11* when transferred to Rc light. Differences between WT and mutants increase along time suggesting in both cases that the mutants are defective in modulating their response to light giving rise to an over-responding phenotype. In the case of MIDA9 and MIDA10, the differences are subtler maybe because the hook aperture is a process regulated by multiple factors. Small differences where found in the *mida9* mutant even appreciable ones are distinguishable when the seedlings are transferred to FRc instead of Rc. In the MIDA10 case, increasing differences were appreciable during the first hours coinciding in time with the expression arrest of the gene and probably the degradation of the protein while responses became equivalent with the WT later on reflecting that MIDA10 was no exerting its action any more and suggesting therefore that the degradation of MIDA10 is an early response during the deetiolation.

### **1.6 Phenotypic characterization of *pif3* and *pif3pif4pif5* during the dark to light transition.**

The same experiments where performed in parallel with the *pif3* and the *pif3pif4pif5* mutants. The triple *pif3pif4pif5* mutant was chosen instead of the *pifq* to avoid big differences coming from the etiolated state and thus strengthening the light responses displayed by the seedlings.

The results were more obvious in the case of PIFs. Our data revealed that *pif3* and in greater magnitude *pif3pif4pif5* also fail in moderating the trigger of light responses exhibiting exaggerated cotyledon separation and inhibition of hypocotyl elongation, effects that are apparent after 1-2days in Rc

for cotyledon separation or only a few hours for hypocotyl elongation. These data suggest that PIF3, together with other PIFs, such as PIF4 and PIF5, continue signaling beyond the initial light trigger and exert a late repressive action to avoid excessive cotyledon separation and hypocotyl elongation inhibition. This late action is in apparent discrepancy with the rapid degradation of PIF3 in the light ([Bauer et al. 2004](#)); ([Monte et al. 2004](#)) ([Park et al. 2004a](#)) ([Al-Sady et al. 2008](#)). The late action of PIF3 could occur indirectly through secondary downstream targets and/or be exerted by the remaining light-stable pool of PIF3 (10% of the levels in the dark) after the initial degradation ([Monte et al. 2004](#)). This late PIF modulation of the light response seems likely to be fundamental for the seedling survival during the initial exposure to light. For example, it ensures that the cotyledons will separate rapidly and will be maintained at an angle parallel to the soil, optimal for the light perception. The existence of mechanisms that prevent over responsiveness to the initial stimulus is an emerging theme in the regulation of responses to light, as has been described in the shade avoidance syndrome ([Sessa et al. 2005](#)) and, more recently, in responses to FR light ([Li et al. 2010](#)).

In conclusion, this study identifies downstream branching of the PIF3 signal as a means to optimize seedling deetiolation. We show that regulation of novel MIDA factors by the phy/PIF system enables the seedling to repress photomorphogenesis in the dark and respond optimally to light by regulating the abundance of positive and negative regulators of specific facets of photomorphogenesis, such as hypocotyl elongation, hook unfolding, and cotyledon separation. Major challenge for the future will be to determine how this regulation is achieved in the seedling by identifying additional PIF3-regulated components and the direct targets of PIF3 that orchestrate these organ-specific responses.

## **2. Phenotypic characterization of PIF3 role in *Arabidopsis thaliana* seedlings grown in short-day conditions.**

Relative contribution of each PIF in the hypocotyl elongation varies in diurnal respect other light conditions. For example in darkness is PIF1, the main actor regulating this process while in shade is PIF3 the main regulator if the seedling was grown in diurnal cycles. In the other hand, PIF4 regulates hypocotyl elongation as a response of high temperatures. Manifesting in this way, that PIFs contribution on hypocotyl growth depends on the environmental conditions in which the seedling is growing.

Short day (SD) is one of the options in which seedling may grow after deetiolation. Under diurnal conditions, with an alternating light/dark cycle, the extent of hypocotyl elongation depends on the duration of the dark period ([Niwa et al. 2009](#)). Previous studies indicated the PIF4 and PIF5 are positive regulators of hypocotyl elongation in SD. The circadian and the light coordinate the process in part by regulating PIF4 and PIF5 gene expression and protein accumulation ([Nozue et al. 2007](#)) ([Niwa et al. 2009](#)) ([Nusinow et al. 2011](#)). Nevertheless, the current models predict additional factors involved in the regulation of seedling growth under SD conditions and here demonstrate with our studies, the PIF3 additional and important role in that system.

*pif3* mutants lines displayed shorter hypocotyls when compared with WT ones after being grown for two days in short day conditions plus a third one, where the growth was monitored every 30 minutes. The growth kinetics demonstrates acceleration in the velocity which is initiated around 6-8 hours after dark exposure (figure 5 a), coinciding with the PIF3 re-accumulation pattern (Figure 1 b-c) (Figure 1 experiments were realized by another author in the article) and in a way where as much PIF3 accumulates the seedling, major is the acceleration in the growth velocity. In contrast, the growth velocity of the *pif3* mutant is maintained as in light conditions and only displays an increase after 13h of dark treatment probably coinciding with the circadian clock inhibition release on the *PIF4* and *PIF5* transcriptional expression and

subsequent protein accumulation and action. Indeed, PIF3 lack in the seedling promotes a decrease of approximately two fold in the growth velocity at 23h, suggesting that the PIF3 role is similar in importance to the PIF4 and PIF5 together.



## **Main Conclusions**

## Main Conclusions

1. Identification of downstream components that might be mediating PIF3 function as a repressor of photomorphogenesis in the dark

1.1 Analysis of the PIF3-regulated transcriptome in dark conditions.

- **PIF3 functions to repress photomorphogenesis from 2 days onwards after germination, with a role in promoting hypocotyl elongation and maintaining of the hook and the cotyledons closed.**
- **PIF3 fixes skotomorphogenesis by inducing and repressing gene expression in a similar level.**

1.2 Selection of MIDA genes as potential regulators of skotomorphogenesis.

- **PIF3 signal is implemented by genes related to a broad range of functions as for example, transcription factors, signaling, growth and hormones.**
- **PIF3 signal branches downstream through out the MIDAs to regulate specific aspects of the deetiolation response.**

1.3 Functional characterization of Arabidopsis mida mutants in darkness

- **MID1 is a PIF3-induced inducer of photomorphogenesis in the dark with a specific role in cotyledon opening.**
- **MID9 is a PIF3-repressed repressor of photomorphogenesis in the dark with a specific role in hook unfolding.**
- **MID10 is a PIF3-induced repressor of photomorphogenesis in the dark with a specific role in hook unfolding.**

- **MID11 is a PIF3-repressed repressor of photomorphogenesis in the dark with a specific role in hypocotyl elongation.**

#### 1.4 Characterization of MIDAs expression profiles during the dark to light transition

- **All four MIDA genes expression is light regulated during the de-etiolation. *MIDA10* is light repressed while *MID9*, *MID11*, and *MID1* are light induced.**
- **PIF3 degradation triggers an early light response in *MID10* and *MID1*, and a late light response in *MID9* and *MID11*.**

#### 1.5 Characterization of MIDAs expression profiles during the dark to light transition

- **MID10 might act as a repressor of hook opening during the initial deetiolation response.**
- **MID1 has a role as inducer of cotyledon separation during early deetiolation.**
- **MID9 may act a repressor of hook unfolding during the deetiolation in R and FRc.**
- **MID11 is a repressor of hypocotyl elongation inhibition in the dark-to-light transition, with a more prominent role after 3 h of light exposure.**

1.6 Phenotypic characterization of PIF3, PIF4 and PIF5 roles during the deetiolation.

- **PIF3 prevent over separation of the cotyledons during the seedling establishment in a partially redundant manner with PIF4 and PIF5.**
- **PIF3 prevents light over response in the hypocotyl elongation during the deetiolation together with PIF4 and PIF5.**

2. Phenotypic characterization of the PIF3 role in *Arabidopsis thaliana* seedlings grown in short-day conditions.

- **PIF3 induces hypocotyl elongation at the end of the night in Arabidopsis seedlings grown in short day conditions in a partially redundant manner with PIF4 and PIF5.**

## Resumen



## **Análisis funcional de los genes regulados por PIF3 en oscuridad.**

Como organismos autótrofos, la supervivencia de las plantas depende drásticamente de la energía solar recibida. No obstante, tras la germinación de en oscuridad, la plántula sigue un sistema de desarrollo heterótrofo, llamado etiolación o escotomorfogénesis. ([Neff et al. 1999](#)) ([Franklin and Quail 2010](#)) ([Kami et al. 2010](#)) ([Deng et al. 1991b](#)). Este sistema, aún siendo perecedero, permitirá a la plántula elongar su hipocotilo manteniendo el meristema protegido mediante la formación de un gancho apical y el mantenimiento de los cotiledones cerrados para atravesar el suelo sin deteriorar ninguna de sus estructuras ([Quail 2002b](#)). La exposición a la luz, una vez alcanzada la superficie, promoverá una reorganización transcripcional permitiendo a la plántula desetiolarse y poner en marcha el sistema fotosintético asegurando así su supervivencia ([Nagy and Schafer 2002](#)) ([Rockwell et al. 2006](#)).

Las proteínas interactoras de fitocromo, PIF (del inglés PHYTOCHROME INTERACTING FACTOR), son claves en este proceso. Se trata de factores de transcripción de tipo bHLH caracterizados por su capacidad para unirse directamente al DNA en regiones específicas del promotor de los genes diana, llamadas Cajas-G ([Ni et al. 1998](#))([Toledo-Ortiz et al. 2003](#)) ([Martinez-Garcia et al. 2000](#)). Se han descrito hasta cinco miembros de la familia PIF, *PIF1*, *PIF3*, *PIF4*, *PIF5* y *PIF7*. Al remover gradualmente los PIF de una plántula crecida en oscuridad, se observa como esta se desetiola parcialmente, hasta llegar al punto de que el cuádruple mutante *pifq* (*pif1pif3pif4pif5*) presenta un fenotipo en oscuridad similar al de una plántula salvaje crecida en condiciones de luz *PIF5* ([Bae and Choi 2008](#)); ([Josse and Halliday 2008](#)); ([Leivar et al. 2008a](#)). Las proteínas PIF se acumulan en el núcleo celular de las plántulas, pero son fosforiladas, ubiquitinadas y posteriormente degradadas en el proteosoma tras la exposición a la luz

debido a la acción de los fitocromos, los receptores de luz roja y roja lejana que se traslocan al núcleo una vez activados donde regulan negativamente la acumulación de los PIFs ([Quail 2002a](#)) ([Huq et al. 2003](#)) ([Bae and Choi 2008](#)) ([Bauer et al. 2004](#)) ([Park et al. 2004b](#)) ([Shen et al. 2005](#)) ([Al-Sady et al. 2006](#)) ([Khanna et al. 2006a](#)) ([Nozue et al. 2007](#)); ([Shen et al. 2007](#)) ([Lorrain et al. 2008](#)) ([Shen et al. 2008a](#)).

El objetivo de esta tesis ha sido detallar el papel de la proteína PIF3 durante la etiolación y desetiolación, identificando y describiendo funcionalmente los genes que implementan aguas abajo su señal.

Mediante un análisis transcripcional donde se compararon líneas salvajes (WT) y líneas mutantes defectivas en la proteína PIF3 (*pif3*) crecidas en oscuridad durante 4 días, se identificaron un total de 82 genes expresados significativamente de manera diferente a nivel estadístico. Entre ellos, se escogieron en función de su rol potencial en la especie *Arabidopsis thaliana* diez de ellos para estudiarlos a nivel funcional. Se eligieron con preferencia genes involucrados en funciones relacionadas con el crecimiento y el desarrollo, la regulación transcripcional, la señalización, la regulación hormonal, y el metabolismo. Además se escogieron tres genes que aún no cumpliendo con la totalidad de los parámetros estadísticos aplicados, la elevada diferencia en la expresión génica cuando comparados con el WT les hicieron atractivos o potencialmente interesantes para nuestro estudio. Entre los genes escogidos se hallaban algunos sin función conocida. Se denominó a los 13 genes seleccionados genes *MIDA*, del inglés MISREGULATED IN THE DARK.

Tras una aproximación de genética reversa dónde se estudiaron los fenotipos de líneas mutantes defectivas en estos genes, a dos, tres y cuatro días de desarrollo en oscuridad, sólo cuatro líneas presentaron diferencias significativas con las líneas salvajes. Las líneas mutantes correspondían a los genes *MIDA1*, *MIDA9*, *MIDA10* y *MIDA11*. *MIDA1* es una deshidroxi hidrogenasa que participa durante la activación de hormonas esteroideas como los brasinosteroides ([Li et al. 2007](#)). *MIDA9* es una fosfatasa de tipo 2C, con una localización predicha nuclear ([Schweighofer et al. 2004](#)). Ninguna

fosfatasa del grupo de las fosfatasas tipo 2C nucleares se ha descrito con anterioridad así como ninguna fosfatasa de tipo 2C ha sido involucrada en procesos de etiolación o desetiolación. *MIDA10* es un factor de transcripción de tipo B-BOX también llamado *B-BOX23* o *STH6* sin función descrita con anterioridad ([Khanna et al. 2006b](#)) ([Indorf et al. 2007](#)) ([Datta et al. 2007](#)). Finalmente, *MIDA11* es una quinasa ya descrita en condiciones lumínicas como inhibidora en las cascadas de señalización por auxinas.

Líneas sobreexpresoras de *MIDA1* se caracterizaron por sus cotiledones abiertos en oscuridad durante los tres días estudiados, sugiriendo que una sobreexpresión de *MIDA1* induciría fotomorfogénesis en oscuridad. Las plántulas defectivas tanto en *MIDA9* (*mida9*) como en *MIDA10* (*mida10*), presentaron ganchos apicales abiertos lo cual infiere una función para estos genes involucrada en el mantenimiento del gancho apical durante la etiolación. En último lugar, los mutantes *mida11* se distinguían de los salvajes por sus cortos hipocotilos, fenotipo del cual se deduce una función inductora en cuanto a la elongación del hipocotilo para este gen. Conjuntamente, nuestros resultados indicaban que la señal que PIF3 trasnduce mediante la regulación transcripcional se ramifica de manera que la expresión de diferentes genes se regula distintamente según el órgano sobre el cual ejercen su acción, así como que el desarrollo de los diferentes órganos de la plántula acontece de manera independiente de los unos con los otros.

Contrariamente a lo esperado, la represión de la fotomorfogénesis mediada por PIF3 se basa en una inducción y represión génica ejercidas ambas tanto sobre inductores como represores de la fotomorfogénesis, lo cual presentaba un esquema difícil de entender y más parecido al de una plántula desarrollada en luz que al de una plántula crecida en oscuridad. Tal razonamiento nos hizo pensar en la posibilidad de que los genes *MIDA* tuviesen una función relevante durante la transición a la luz.

Con la intención de probar tal posibilidad se re-analizaron estudios transcripcionales hechos en condiciones lumínicas, tras 1 y 18 horas de exposición a luz roja así como estudios del mismo género realizados en el cuádruple mutante *pifq* (*pif1pif3pif4pif5*). Los resultados indicaron un potencial rol de los genes *MIDA* durante la desetiolación por lo que se realizaron estudios de expresión más detallados durante periodos de 12h. A partir de los

patrones de expresión génica durante la desetiación presentados por los *MIDA*, se planteó la posibilidad de que la plántula respondiese a la exposición lumínica en dos etapas. La primera etapa se caracterizaría por un cambio rápido y fuerte a nivel transcripcional y post-traducciona que permitiría a la plántula cambiar desde un patrón de desarrollo adaptado a la oscuridad, etiolado, al patrón de desarrollo opuesto, desetiado, que permitiría a la plántula crecer en condiciones de luz. La segunda etapa se caracterizaría por la regulación de la primera, esto es, tras iniciar toda la maquinaria fotomorfogénica, la plántula modularía el proceso de desetiación con el objetivo de adaptarse de manera óptima a las condiciones ambientales que la rodearían evitando así una sobre respuesta fotomorfogénica tras la exposición a la luz.

Se planteaba así una tercera hipótesis que nos ayudaría a elucidar el papel de la proteína PIF3 así como de los genes que esta regula, durante la etiolación y la desetiación.

Paso seguido, se realizaron estudios fenotípicos que detallaron las cinética de desetiación de las líneas WT y mutantes defectivas en los genes *MIDA* así como en los genes *PIF*. Tales cinéticas demostraron sutilmente en los *mida* y robustamente en los *pif3* y *pif3pif4pif5* el papel modulador que estos factores ejercen durante la desetiación puesto que las líneas mutantes presentaron, exceptuando el caso de *MIDA10*, una hipersensibilidad o sobre-respuesta tras la exposición a la luz caracterizada por hipocotilos cortos, y cotiledones abiertos hasta 180° respecto a la vertical del hipocotilo. Tales fenotipos incrementaron o se exageraron con el paso del tiempo, sugiriendo la necesidad de una acción moduladora de la respuesta inexistente en el caso de los mutantes *mida*, *pif3* y *pif3 pif4 pif5*.

Una vez desetiadas, las plántulas crecen modulando o adaptando su desarrollo a las condiciones ambientales de su alrededor. Crecer en condiciones de día corto es una de las alternativas caracterizada principalmente por la alternancia periódica de 8h de luz seguidas por 16h horas de oscuridad.

Estudios anteriores realizados por otros grupos en plántulas crecidas en día corto describen una aceleración en la elongación del hipocotilo concentrado al

final de la noche justo antes del amanecer (Niwa et al., 2009) (Nozue et al., 2007) donde PIF4 y PIF5 actuarían como reguladores transcripcionales promoviendo la elongación de este. La expresión génica de PIF4 y PIF5 viene regulada principalmente por el reloj circadiano y de manera secundaria por la acción de la luz (Nozue et al., 2007; Nusinow et al., 2011). Aún así, los modelos actuales que describen la acción de PIF4 y PIF5 en la elongación del hipocotilo al final de la noche, contemplan la acción más factores implicados en el proceso. Dada la relativa redundancia funcional ya descrita para los PIFs en otras condiciones como el desarrollo en oscuridad o el proceso de desetiación, en nuestro estudio quisimos analizar la potencial acción reguladora de PIF3 en la elongación del hipocotilo al final de la noche.

Para ello se monitorizó el crecimiento de plántulas salvajes y *pif3* mutantes crecidas durante dos días en condiciones de día corto, cada 30 minutos durante 24h. Las plántulas deficientes en la proteína PIF3 presentaron hipocotilos más cortos al final de la noche cuando comparadas con el WT debido a una no aceleración en la velocidad de crecimiento o elongación de éste durante el que sería el periodo de máximo crecimiento en el WT. Los resultados sugieren, de este modo, que PIF3 participa junto con PIF4 y PIF5 en la elongación del hipocotilo en condiciones de día corto.

Resumiendo, el trabajo realizado durante esta tesis, demuestra una vez más la importancia de las proteínas PIF en el desarrollo de *Arabidopsis thaliana*, durante la etiolación, la desetiación y el crecimiento en condiciones diurnas. De manera concreta, desvelamos que PIF3 regula de manera positiva y negativa transcripción génica con el objetivo de preservar la etiolación pero también permitiendo un proceso de desetiación rápido y controlado junto con PIF1, PIF4 y PIF5.

Identificamos a los genes MIDA como efectores de la señalización de PIF3 y como reguladores de la morfogénesis y desarrollo de diferentes órganos de la plántula, evidenciando de este modo una ramificación en la señal de PIF3. Detallamos funcionalmente el papel de los genes MIDA, entre los cuales, MIDA1 actúa como inductor de la apertura de los cotiledones, MIDA9 y

MIDA10 regulan negativamente la apertura del gancho apical y MIDA11 induce positivamente la elongación del hipocotilo.

Adicionalmente y como resultado de una colaboración en el proyecto de otro miembro de nuestro grupo. Presentamos en esta tesis a PIF3 como regulador de la elongación del hipocotilo junto con PIF4 y PIF5.

De manera global, el trabajo aquí presentado, suma información al complejo sistema de regulación y de acción de los PIFs dónde se incluyen cada vez más variables tales como alteraciones en la composición de la luz (sombra, luz roja, luz roja lejana, luz azul) hormonas, temperatura y reloj circadiano. Recientes publicaciones (Leivar et al. 2012) asemejan la respuesta de huida de la sombra a lo que vendría a ser un proceso de reetiolación. Cambios transcripcionales promovidos tras la exposición a la luz, son revertidos en condiciones de sombra por un enriquecimiento en luz roja lejana en la composición lumínica total. Estudios de este tipo, dan pie, en cierto modo a pensar en un posible paralelismo entre el proceso de desetiolación tras un crecimiento post-germinativo etiolado, y la transición oscuridad-luz que se repite periódicamente en plantas crecidas en condiciones diurnas. Al fin y al cabo, se trataría de situaciones similares reguladas por proteínas similares por lo que no sería de extrañar encontrar genes regulados directa o indirectamente por los PIFs participando en ambos procesos. Estudios adicionales deberían llevarse a cabo para resolver esta posibilidad.

## **Bibliography**

## Bibliography

- Al-Sady B, Kikis EA, Monte E, Quail PH (2008) Mechanistic duality of transcription factor function in phytochrome signaling. *Proceedings of the National Academy of Sciences of the United States of America* 105: 2232-2237
- Al-Sady B, Ni W, Kircher S, Schafer E, Quail PH (2006) Photoactivated phytochrome induces rapid PIF3 phosphorylation prior to proteasome-mediated degradation. *Molecular cell* 23: 439-446
- Alabadi D, Blazquez MA (2009) Molecular interactions between light and hormone signaling to control plant growth. *Plant molecular biology* 69: 409-417
- Bae G, Choi G (2008) Decoding of light signals by plant phytochromes and their interacting proteins. *Annual review of plant biology* 59: 281-311
- Ballesteros ML, Bolle C, Lois LM, Moore JM, Vielle-Calzada JP, Grossniklaus U, Chua NH (2001) LAF1, a MYB transcription activator for phytochrome A signaling. *Genes & development* 15: 2613-2625
- Bauer D, Viczian A, Kircher S, Nobis T, Nitschke R, Kunkel T, Panigrahi KCS, Adam E, Fejes E, Schafer E, Nagy F (2004) Constitutive photomorphogenesis 1 and multiple photoreceptors control degradation of phytochrome interacting factor 3, a transcription factor required for light signaling in Arabidopsis. *The Plant cell* 16: 1433-1445
- Borthwick HA, Hendricks SB, Parker MW, Toole EH, Toole VK (1952) A Reversible Photoreaction Controlling Seed Germination. *Proceedings of the National Academy of Sciences of the United States of America* 38: 662-666

- Castillon A, Shen H, Huq E (2007) Phytochrome Interacting Factors: central players in phytochrome-mediated light signaling networks. *Trends in plant science* 12: 514-521
- Castillon A, Shen H, Huq E (2009) Blue light induces degradation of the negative regulator phytochrome interacting factor 1 to promote photomorphogenic development of *Arabidopsis* seedlings. *Genetics* 182: 161-171
- Chen M, Chory J (2011) Phytochrome signaling mechanisms and the control of plant development. *Trends in cell biology* 21: 664-671
- Chen M, Chory J, Fankhauser C (2004) Light signal transduction in higher plants. *Annual review of genetics* 38: 87-117
- Datta S, Hettiarachchi C, Johansson H, Holm M (2007) SALT TOLERANCE HOMOLOG2, a B-box protein in *Arabidopsis* that activates transcription and positively regulates light-mediated development. *The Plant cell* 19: 3242-3255
- Datta S, Johansson H, Hettiarachchi C, Irigoyen ML, Desai M, Rubio V, Holm M (2008) LZFI/SALT TOLERANCE HOMOLOG3, an *Arabidopsis* B-box protein involved in light-dependent development and gene expression, undergoes COP1-mediated ubiquitination. *The Plant cell* 20: 2324-2338
- Deng XW, Caspar T, Quail PH (1991a) Cop1 - a Regulatory Locus Involved in Light-Controlled Development and Gene-Expression in *Arabidopsis*. *Genes & development* 5: 1172-1182
- Deng XW, Caspar T, Quail PH (1991b) cop1: a regulatory locus involved in light-controlled development and gene expression in *Arabidopsis*. *Genes & development* 5: 1172-1182
- Duek PD, Fankhauser C (2003) HFR1, a putative bHLH transcription factor, mediates both phytochrome A and cryptochrome signalling. *The Plant journal : for cell and molecular biology* 34: 827-836

- Duek PD, Fankhauser C (2005) bHLH class transcription factors take centre stage in phytochrome signalling. *Trends in plant science* 10: 51-54
- Fankhauser C, Chen M (2008) Transposing phytochrome into the nucleus. *Trends in plant science* 13: 596-601
- Fankhauser C, Chory J (1999) Light receptor kinases in plants! *Current biology* : CB 9: R123-126
- Finch-Savage WE, Leubner-Metzger G (2006) Seed dormancy and the control of germination. *The New phytologist* 171: 501-523
- Franklin KA, Quail PH (2010) Phytochrome functions in Arabidopsis development. *Journal of experimental botany* 61: 11-24
- Gabriele S, Rizza A, Martone J, Circelli P, Costantino P, Vittorioso P (2010) The Dof protein DAG1 mediates PIL5 activity on seed germination by negatively regulating GA biosynthetic gene AtGA3ox1. *The Plant journal : for cell and molecular biology* 61: 312-323
- Galvao RM, Li M, Kothadia SM, Haskel JD, Decker PV, Van Buskirk EK, Chen M (2012) Photoactivated phytochromes interact with HEMERA and promote its accumulation to establish photomorphogenesis in Arabidopsis. *Genes & development* 26: 1851-1863
- Genoud T, Schweizer F, Tscheuschler A, Debrieux D, Casal JJ, Schafer E, Hiltbrunner A, Fankhauser C (2008) FHY1 Mediates Nuclear Import of the Light-Activated Phytochrome A Photoreceptor. *PLoS genetics* 4
- Halliday KJ (2004) Plant hormones: the interplay of brassinosteroids and auxin. *Current biology* : CB 14: R1008-1010
- Hao Y, Oh E, Choi G, Liang Z, Wang ZY (2012) Interactions between HLH and bHLH factors modulate light-regulated plant development. *Molecular plant* 5: 688-697

- Hiltbrunner A, Tscheuschler A, Viczian A, Kunkel T, Kircher S, Schafer E (2006) FHY1 and FHL act together to mediate nuclear accumulation of the phytochrome A photoreceptor. *Plant & cell physiology* 47: 1023-1034
- Hiltbrunner A, Viczian A, Bury E, Tscheuschler A, Kircher S, Toth R, Honsberger A, Nagy F, Fankhauser C, Schafer E (2005) Nuclear accumulation of the phytochrome A photoreceptor requires FHY1. *Current biology : CB* 15: 2125-2130
- Holm M, Ma LG, Qu LJ, Deng XW (2002) Two interacting bZIP proteins are direct targets of COP1-mediated control of light-dependent gene expression in *Arabidopsis*. *Genes & development* 16: 1247-1259
- Hu W, Su YS, Lagarias JC (2009) A light-independent allele of phytochrome B faithfully recapitulates photomorphogenic transcriptional networks. *Molecular plant* 2: 166-182
- Huq E, Al-Sady B, Hudson M, Kim C, Apel K, Quail PH (2004) Phytochrome-interacting factor 1 is a critical bHLH regulator of chlorophyll biosynthesis. *Science* 305: 1937-1941
- Huq E, Al-Sady B, Quail PH (2003) Nuclear translocation of the photoreceptor phytochrome B is necessary for its biological function in seedling photomorphogenesis. *The Plant journal : for cell and molecular biology* 35: 660-664
- Indorf M, Cordero J, Neuhaus G, Rodriguez-Franco M (2007) Salt tolerance (STO), a stress-related protein, has a major role in light signalling. *The Plant journal : for cell and molecular biology* 51: 563-574
- Jang IC, Henriques R, Seo HS, Nagatani A, Chua NH (2010) *Arabidopsis* PHYTOCHROME INTERACTING FACTOR proteins promote phytochrome B polyubiquitination by COP1 E3 ligase in the nucleus. *The Plant cell* 22: 2370-2383

- Jensen PJ, Hangarter RP, Estelle M (1998) Auxin transport is required for hypocotyl elongation in light-grown but not dark-grown Arabidopsis. *Plant Physiol* 116: 455-462
- Josse EM, Halliday KJ (2008) Skotomorphogenesis: the dark side of light signalling. *Current biology* : CB 18: R1144-1146
- Kami C, Lorrain S, Hornitschek P, Fankhauser C (2010) Light-regulated plant growth and development. *Current topics in developmental biology* 91: 29-66
- Khanna R, Huq E, Kikis EA, Al-Sady B, Lanzatella C, Quail PH (2004) A novel molecular recognition motif necessary for targeting photoactivated phytochrome signaling to specific basic helix-loop-helix transcription factors. *The Plant cell* 16: 3033-3044
- Khanna R, Shen Y, Marion CM, Tsuchisaka A, Theologis A, Schafer E, Quail PH (2007) The basic helix-loop-helix transcription factor PIF5 acts on ethylene biosynthesis and phytochrome signaling by distinct mechanisms. *The Plant cell* 19: 3915-3929
- Khanna R, Shen Y, Toledo-Ortiz G, Kikis EA, Johannesson H, Hwang YS, Quail PH (2006a) Functional profiling reveals that only a small number of phytochrome-regulated early-response genes in Arabidopsis are necessary for optimal deetiolation. *The Plant cell* 18: 2157-2171
- Khanna R, Shen Y, Toledo-Ortiz G, Kikis EA, Johannesson H, Hwang YS, Quail PH (2006b) Functional profiling reveals that only a small number of phytochrome-regulated early-response genes in Arabidopsis are necessary for optimal deetiolation. *The Plant cell* 18: 2157-2171
- Kim DH, Yamaguchi S, Lim S, Oh E, Park J, Hanada A, Kamiya Y, Choi G (2008) SOMNUS, a CCCH-type zinc finger protein in Arabidopsis, negatively regulates light-dependent seed germination downstream of PIL5. *The Plant cell* 20: 1260-1277

- Lagarias DM, Villarejo M (1985) Coordinate expression of a small polypeptide with the lactose carrier of *Escherichia coli*. *The Journal of biological chemistry* 260: 14235-14241
- Lau OS, Deng XW (2010a) Plant hormone signaling lightens up: integrators of light and hormones. *Current opinion in plant biology* 13: 571-577
- Lau OS, Deng XW (2010b) Plant hormone signaling lightens up: integrators of light and hormones. *Current opinion in plant biology* 13: 571-577
- Lee JS, Wang S, Sritubtim S, Chen JG, Ellis BE (2009) *Arabidopsis* mitogen-activated protein kinase MPK12 interacts with the MAPK phosphatase IBR5 and regulates auxin signaling. *The Plant journal : for cell and molecular biology* 57: 975-985
- Leivar P, Monte E, Al-Sady B, Carle C, Storer A, Alonso JM, Ecker JR, Quail PH (2008a) The *Arabidopsis* phytochrome-interacting factor PIF7, together with PIF3 and PIF4, regulates responses to prolonged red light by modulating phyB levels. *The Plant cell* 20: 337-352
- Leivar P, Monte E, Cohn MM, Quail PH (2012a) Phytochrome signaling in green *Arabidopsis* seedlings: impact assessment of a mutually negative phyB-PIF feedback loop. *Molecular plant* 5: 734-749
- Leivar P, Monte E, Oka Y, Liu T, Carle C, Castillon A, Huq E, Quail PH (2008b) Multiple phytochrome-interacting bHLH transcription factors repress premature seedling photomorphogenesis in darkness. *Current biology : CB* 18: 1815-1823
- Leivar P, Quail PH (2011) PIFs: pivotal components in a cellular signaling hub. *Trends in plant science* 16: 19-28
- Leivar P, Tepperman JM, Cohn MM, Monte E, Al-Sady B, Erickson E, Quail PH (2012b) Dynamic antagonism between phytochromes and PIF family basic helix-loop-helix factors induces selective reciprocal responses to

light and shade in a rapidly responsive transcriptional network in Arabidopsis. *The Plant cell* 24: 1398-1419

Leivar P, Tepperman JM, Monte E, Calderon RH, Liu TL, Quail PH (2009) Definition of early transcriptional circuitry involved in light-induced reversal of PIF-imposed repression of photomorphogenesis in young Arabidopsis seedlings. *The Plant cell* 21: 3535-3553

Li F, Asami T, Wu X, Tsang EW, Cutler AJ (2007) A putative hydroxysteroid dehydrogenase involved in regulating plant growth and development. *Plant Physiol* 145: 87-97

Li J, Li G, Gao S, Martinez C, He G, Zhou Z, Huang X, Lee JH, Zhang H, Shen Y, Wang H, Deng XW (2010) Arabidopsis transcription factor ELONGATED HYPOCOTYL5 plays a role in the feedback regulation of phytochrome A signaling. *The Plant cell* 22: 3634-3649

Lorrain S, Allen T, Duek PD, Whitelam GC, Fankhauser C (2008) Phytochrome-mediated inhibition of shade avoidance involves degradation of growth-promoting bHLH transcription factors. *The Plant journal : for cell and molecular biology* 53: 312-323

Lorrain S, Trevisan M, Pradervand S, Fankhauser C (2009) Phytochrome interacting factors 4 and 5 redundantly limit seedling de-etiolation in continuous far-red light. *The Plant journal : for cell and molecular biology* 60: 449-461

Ma L, Gao Y, Qu L, Chen Z, Li J, Zhao H, Deng XW (2002) Genomic evidence for COP1 as a repressor of light-regulated gene expression and development in Arabidopsis. *The Plant cell* 14: 2383-2398

Ma L, Li J, Qu L, Hager J, Chen Z, Zhao H, Deng XW (2001) Light control of Arabidopsis development entails coordinated regulation of genome expression and cellular pathways. *The Plant cell* 13: 2589-2607

- Martinez-Garcia JF, Huq E, Quail PH (2000) Direct targeting of light signals to a promoter element-bound transcription factor. *Science* 288: 859-863
- Matsushita T, Mochizuki N, Nagatani A (2003) Dimers of the N-terminal domain of phytochrome B are functional in the nucleus. *Nature* 424: 571-574
- Meyer K, Leube MP, Grill E (1994) A protein phosphatase 2C involved in ABA signal transduction in *Arabidopsis thaliana*. *Science* 264: 1452-1455
- Monte E, Al-Sady B, Leivar P, Quail PH (2007) Out of the dark: how the PIFs are unmasking a dual temporal mechanism of phytochrome signalling. *Journal of experimental botany* 58: 3125-3133
- Monte E, Alonso JM, Ecker JR, Zhang Y, Li X, Young J, Austin-Phillips S, Quail PH (2003) Isolation and characterization of phyC mutants in *Arabidopsis* reveals complex crosstalk between phytochrome signaling pathways. *The Plant cell* 15: 1962-1980
- Monte E, Tepperman JM, Al-Sady B, Kaczorowski KA, Alonso JM, Ecker JR, Li X, Zhang Y, Quail PH (2004) The phytochrome-interacting transcription factor, PIF3, acts early, selectively, and positively in light-induced chloroplast development. *Proceedings of the National Academy of Sciences of the United States of America* 101: 16091-16098
- Moon J, Zhu L, Shen H, Huq E (2008) PIF1 directly and indirectly regulates chlorophyll biosynthesis to optimize the greening process in *Arabidopsis*. *Proceedings of the National Academy of Sciences of the United States of America* 105: 9433-9438
- Nagy F, Schafer E (2002) Phytochromes control photomorphogenesis by differentially regulated, interacting signaling pathways in higher plants. *Annual review of plant biology* 53: 329-355
- Neff MM, Fankhauser C, Chory J (2000) Light: an indicator of time and place. *Genes & development* 14: 257-271

- Neff MM, Nguyen SM, Malancharuvil EJ, Fujioka S, Noguchi T, Seto H, Tsubuki M, Honda T, Takatsuto S, Yoshida S, Chory J (1999) BAS1: A gene regulating brassinosteroid levels and light responsiveness in Arabidopsis. *Proceedings of the National Academy of Sciences of the United States of America* 96: 15316-15323
- Ni M, Tepperman JM, Quail PH (1998) PIF3, a phytochrome-interacting factor necessary for normal photoinduced signal transduction, is a novel basic helix-loop-helix protein. *Cell* 95: 657-667
- Niwa Y, Yamashino T, Mizuno T (2009) The circadian clock regulates the photoperiodic response of hypocotyl elongation through a coincidence mechanism in Arabidopsis thaliana. *Plant & cell physiology* 50: 838-854
- Nozue K, Covington MF, Duek PD, Lorrain S, Fankhauser C, Harmer SL, Maloof JN (2007) Rhythmic growth explained by coincidence between internal and external cues. *Nature* 448: 358-361
- Nusinow DA, Helfer A, Hamilton EE, King JJ, Imaizumi T, Schultz TF, Farre EM, Kay SA (2011) The ELF4-ELF3-LUX complex links the circadian clock to diurnal control of hypocotyl growth. *Nature* 475: 398-U161
- Oh E, Kang H, Yamaguchi S, Park J, Lee D, Kamiya Y, Choi G (2009) Genome-wide analysis of genes targeted by PHYTOCHROME INTERACTING FACTOR 3-LIKE5 during seed germination in Arabidopsis. *The Plant cell* 21: 403-419
- Oh E, Kim J, Park E, Kim JI, Kang C, Choi G (2004a) PIL5, a phytochrome-interacting basic helix-loop-helix protein, is a key negative regulator of seed germination in Arabidopsis thaliana. *The Plant cell* 16: 3045-3058
- Oh E, Kim J, Park E, Kim JI, Kang C, Choi G (2004b) PIL5, a phytochrome-interacting basic helix-loop-helix protein, is a key negative regulator of seed germination in Arabidopsis thaliana. *The Plant cell* 16: 3045-3058

- Oh E, Yamaguchi S, Kamiya Y, Bae G, Chung WI, Choi G (2006) Light activates the degradation of PIL5 protein to promote seed germination through gibberellin in Arabidopsis. *The Plant journal : for cell and molecular biology* 47: 124-139
- Osterlund MT, Hardtke CS, Wei N, Deng XW (2000) Targeted destabilization of HY5 during light-regulated development of Arabidopsis. *Nature* 405: 462-466
- Oyama T, Shimura Y, Okada K (1997) The Arabidopsis HY5 gene encodes a bZIP protein that regulates stimulus-induced development of root and hypocotyl. *Genes & development* 11: 2983-2995
- Park E, Kim J, Lee Y, Shin J, Oh E, Chung WI, Liu JR, Choi G (2004a) Degradation of phytochrome interacting factor 3 in phytochrome-mediated light signaling. *Plant & cell physiology* 45: 968-975
- Park E, Kim J, Lee Y, Shin J, Oh E, Chung WI, Liu JR, Choi G (2004b) Degradation of phytochrome interacting factor 3 in phytochrome-mediated light signaling. *Plant and Cell Physiology* 45: 968-975
- Park E, Park J, Kim J, Nagatani A, Lagarias JC, Choi G (2012) Phytochrome B inhibits binding of Phytochrome-Interacting Factors to their target promoters. *The Plant journal : for cell and molecular biology*
- Pfeiffer A, Nagel MK, Popp C, Wust F, Bindics J, Viczian A, Hiltbrunner A, Nagy F, Kunkel T, Schafer E (2012) Interaction with plant transcription factors can mediate nuclear import of phytochrome B. *Proceedings of the National Academy of Sciences of the United States of America* 109: 5892-5897
- Quail PH (2000) Phytochrome-interacting factors. *Seminars in cell & developmental biology* 11: 457-466

- Quail PH (2002a) Photosensory perception and signalling in plant cells: new paradigms? *Current opinion in cell biology* 14: 180-188
- Quail PH (2002b) Phytochrome photosensory signalling networks. *Nature reviews. Molecular cell biology* 3: 85-93
- Reed JW, Nagatani A, Elich TD, Fagan M, Chory J (1994) Phytochrome A and Phytochrome B Have Overlapping but Distinct Functions in Arabidopsis Development. *Plant Physiol* 104: 1139-1149
- Rockwell NC, Su YS, Lagarias JC (2006) Phytochrome structure and signaling mechanisms. *Annual review of plant biology* 57: 837-858
- Rodriguez PL (1998) Protein phosphatase 2C (PP2C) function in higher plants. *Plant molecular biology* 38: 919-927
- Sakamoto K, Nagatani A (1996) Nuclear localization activity of phytochrome B. *The Plant journal : for cell and molecular biology* 10: 859-868
- Schweighofer A, Hirt H, Meskiene I (2004) Plant PP2C phosphatases: emerging functions in stress signaling. *Trends in plant science* 9: 236-243
- Seo HS, Watanabe E, Tokutomi S, Nagatani A, Chua NH (2004) Photoreceptor ubiquitination by COP1 E3 ligase desensitizes phytochrome A signaling. *Genes & development* 18: 617-622
- Seo HS, Yang JY, Ishikawa M, Bolle C, Ballesteros ML, Chua NH (2003) LAF1 ubiquitination by COP1 controls photomorphogenesis and is stimulated by SPA1. *Nature* 423: 995-999
- Sessa G, Carabelli M, Sassi M, Ciolfi A, Possenti M, Mitterpergher F, Becker J, Morelli G, Ruberti I (2005) A dynamic balance between gene activation and repression regulates the shade avoidance response in Arabidopsis. *Genes & development* 19: 2811-2815

- Shalitin D, Yang H, Mockler TC, Maymon M, Guo H, Whitelam GC, Lin C (2002) Regulation of Arabidopsis cryptochrome 2 by blue-light-dependent phosphorylation. *Nature* 417: 763-767
- Sharrock RA, Quail PH (1989) Novel phytochrome sequences in Arabidopsis thaliana: structure, evolution, and differential expression of a plant regulatory photoreceptor family. *Genes & development* 3: 1745-1757
- Shen H, Moon J, Huq E (2005) PIF1 is regulated by light-mediated degradation through the ubiquitin-26S proteasome pathway to optimize photomorphogenesis of seedlings in Arabidopsis. *The Plant journal : for cell and molecular biology* 44: 1023-1035
- Shen H, Zhu L, Bu QY, Huq E (2012) MAX2 affects multiple hormones to promote photomorphogenesis. *Molecular plant* 5: 750-762
- Shen H, Zhu L, Castillon A, Majee M, Downie B, Huq E (2008a) Light-induced phosphorylation and degradation of the negative regulator PHYTOCHROME-INTERACTING FACTOR1 from Arabidopsis depend upon its direct physical interactions with photoactivated phytochromes. *The Plant cell* 20: 1586-1602
- Shen Y, Han YJ, Kim JI, Song PS (2008b) Arabidopsis nucleoside diphosphate kinase-2 as a plant GTPase activating protein. *BMB reports* 41: 645-650
- Shen Y, Khanna R, Carle CM, Quail PH (2007) Phytochrome induces rapid PIF5 phosphorylation and degradation in response to red-light activation. *Plant Physiol* 145: 1043-1051
- Shimizu-Sato S, Huq E, Tepperman JM, Quail PH (2002) A light-switchable gene promoter system. *Nature biotechnology* 20: 1041-1044
- Shin J, Kim K, Kang H, Zulfugarov IS, Bae G, Lee CH, Lee D, Choi G (2009) Phytochromes promote seedling light responses by inhibiting four negatively-acting phytochrome-interacting factors. *Proceedings of the*

National Academy of Sciences of the United States of America 106:  
7660-7665

Szekeres M, Nemeth K, Koncz-Kalman Z, Mathur J, Kauschmann A, Altmann T, Redei GP, Nagy F, Schell J, Koncz C (1996) Brassinosteroids rescue the deficiency of CYP90, a cytochrome P450, controlling cell elongation and de-etiolation in Arabidopsis. *Cell* 85: 171-182

Tepperman JM, Hwang YS, Quail PH (2006) phyA dominates in transduction of red-light signals to rapidly responding genes at the initiation of Arabidopsis seedling de-etiolation. *The Plant journal : for cell and molecular biology* 48: 728-742

Tepperman JM, Zhu T, Chang HS, Wang X, Quail PH (2001) Multiple transcription-factor genes are early targets of phytochrome A signaling. *Proceedings of the National Academy of Sciences of the United States of America* 98: 9437-9442

Toledo-Ortiz G, Huq E, Quail PH (2003) The Arabidopsis basic/helix-loop-helix transcription factor family. *The Plant cell* 15: 1749-1770

Toledo-Ortiz G, Huq E, Rodriguez-Concepcion M (2010) Direct regulation of phytoene synthase gene expression and carotenoid biosynthesis by phytochrome-interacting factors. *Proceedings of the National Academy of Sciences of the United States of America* 107: 11626-11631

Yang HQ, Tang RH, Cashmore AR (2001) The signaling mechanism of Arabidopsis CRY1 involves direct interaction with COP1. *The Plant cell* 13: 2573-2587

Yang J, Lin R, Sullivan J, Hoecker U, Liu B, Xu L, Deng XW, Wang H (2005) Light regulates COP1-mediated degradation of HFR1, a transcription factor essential for light signaling in Arabidopsis. *The Plant cell* 17: 804-821

Zhao Y, Dai X, Blackwell HE, Schreiber SL, Chory J (2003) SIR1, an upstream component in auxin signaling identified by chemical genetics. *Science* 301: 1107-1110

Zhou Q, Hare PD, Yang SW, Zeidler M, Huang LF, Chua NH (2005) FHL is required for full phytochrome A signaling and shares overlapping functions with FHY1. *The Plant journal : for cell and molecular biology* 43: 356-370



## **Publications**



## Informe del Director de tesis de la participación del Doctorando en los artículos.

La participación de la Doctoranda Maria Sentandreu en los artículos presentados en su Tesis Doctoral ha sido (por artículo):

1- Functional Profiling Identifies Genes Involved in Organ-Specific Branches of the PIF3 Regulatory Network in Arabidopsis

**Sentandreu, Maria;** Martin, Guiomar; Gonzalez-Schain, Nahuel; Leivar, Pablo; Soy, Judit; Tepperman, James M.; Quail, Peter H.; Monte, Elena  
**PLANT CELL**, 2011. 23: 3974

En este artículo, Maria Sentandreu ha realizado la práctica totalidad de los experimentos presentados en las Figuras, con la excepción del trabajo de análisis de los experimentos de microarray (Figuras 1C y 1D). Asimismo, Maria ha preparado las Figuras para su publicación y ha participado en la redacción del artículo.

Las co-autoras Judit Soy y Guiomar Martín son asimismo Doctorandas del Departamento de Genética de la Universidad de Barcelona, y han participado en la identificación inicial y caracterización de los mutantes respectivamente, trabajo que se presenta en la Figura 2. Judit Soy y Guiomar Martín no han presentado aún sus respectivas Tesis Doctorales.

2- Branching of the PIF3 regulatory network in Arabidopsis: Roles of PIF3-regulated MIDAs in seedling development in the dark and in response to light.

**Sentandreu, Maria;** Leivar, Pablo; Martin, Guiomar; Monte, Elena  
Source: **PLANT SIGNALING BEHAVIOUR**, 2012. 7: 510

En este artículo, Maria Sentandreu ha realizado los experimentos presentados en todas las Figuras. Asimismo, Maria ha preparado las Figuras para su publicación y ha participado en la redacción del artículo.

La co-autora Guiomar Martín, Doctoranda del Departamento de Genética de la Universidad de Barcelona, ha participado en la caracterización de los mutantes que se presenta en la Figura 1. Guiomar Martín no ha presentado aún su Tesis Doctoral.

3- Phytochrome-imposed oscillations in PIF3 protein abundance regulate hypocotyl growth under diurnal light/dark conditions in Arabidopsis

Soy, Judit; Leivar, Pablo; Gonzalez-Schain, Nahuel; **Sentandreu, Maria**; Prat, Salome; Quail, Peter H.; Monte, Elena

Journal: **PLANT JOURNAL**, 2012. 71: 390

Este artículo forma parte del trabajo de Tesis Doctoral de la Doctoranda Judit Soy, su autora principal. La Doctoranda Maria Sentandreu ha participado de forma decisiva produciendo los datos que se muestran en la Figura 5A. Para ello, Maria puso a punto un método de fotografía y medición de plántulas en oscuridad que ha permitido establecer que el crecimiento rítmico de las plántulas en día corto está afectado en nuestros mutantes deficientes en PIF3.

Elena Monte Collado

## **1<sup>st</sup> Article**



# Functional Profiling Identifies Genes Involved in Organ-Specific Branches of the PIF3 Regulatory Network in *Arabidopsis*

Maria Sentandreu,<sup>a</sup> Guiomar Martín,<sup>a</sup> Nahuel González-Schain,<sup>a</sup> Pablo Leivar,<sup>a</sup> Judit Soy,<sup>a</sup> James M. Tepperman,<sup>b,c</sup> Peter H. Quail,<sup>b,c</sup> and Elena Monte<sup>a,1</sup>

<sup>a</sup>Departament de Genètica Molecular, Center for Research in Agricultural Genomics, Centro Superior de Investigaciones Científicas-Institut de Recerca i Tecnologia Agroalimentàries-Universitat Autònoma de Barcelona-Universitat de Barcelona, Campus Universitat Autònoma de Barcelona, Bellaterra, 08193 Barcelona, Spain

<sup>b</sup>Department of Plant and Microbial Biology, University of California, Berkeley, California 94720

<sup>c</sup>United States Department of Agriculture, Plant Gene Expression Center, Albany, California 94710

**The phytochrome (phy)-interacting basic helix-loop-helix transcription factors (PIFs) constitutively sustain the etiolated state of dark-germinated seedlings by actively repressing deetiolation in darkness. This action is rapidly reversed upon light exposure by phy-induced proteolytic degradation of the PIFs. Here, we combined a microarray-based approach with a functional profiling strategy and identified four PIF3-regulated genes misexpressed in the dark (MIDAs) that are novel regulators of seedling deetiolation. We provide evidence that each one of these four MIDA genes regulates a specific facet of etiolation (hook maintenance, cotyledon appression, or hypocotyl elongation), indicating that there is branching in the signaling that PIF3 relays. Furthermore, combining inferred MIDA gene function from mutant analyses with their expression profiles in response to light-induced degradation of PIF3 provides evidence consistent with a model where the action of the PIF3/MIDA regulatory network enables an initial fast response to the light and subsequently prevents an overresponse to the initial light trigger, thus optimizing the seedling deetiolation process. Collectively, the data suggest that at least part of the phy/PIF system acts through these four MIDAs to initiate and optimize seedling deetiolation, and that this mechanism might allow the implementation of spatial (i.e., organ-specific) and temporal responses during the photomorphogenic program.**

## INTRODUCTION

The phytochrome (phy) family of photoreceptors (phyA through phyE in *Arabidopsis thaliana*) plays a central role in the regulation of seedling deetiolation, the developmental transition from skotomorphogenesis to photomorphogenesis that dark-germinated seedlings undergo upon exposure to light (Rockwell et al., 2006; Schäfer and Nagy, 2006; Quail, 2010). After germination in the dark, etiolated seedlings grow heterotrophically on seed reserves and follow a skotomorphogenic strategy of development, characterized by fast hypocotyl elongation and maintenance of an apical hook and appressed cotyledons, to rapidly reach for sunlight at the soil surface. Upon reaching the surface, light triggers seedling deetiolation, the developmental switch to photomorphogenesis, which involves the coordinated inhibition of hypocotyl elongation, unfolding of the apical hook, separation and expansion of the cotyledons, and activation of functional

chloroplast and pigment biosynthesis to initiate photosynthesis. Photoactivation of the Pr form of the phy molecule during deetiolation results in rapid translocation of the Pfr form from the cytoplasm into the nucleus (Yamaguchi et al., 1999; Nagatani, 2004). Nuclear photoactivated phy molecules associate with phy-interacting factors (PIFs). The PIFs are a subset of basic helix-loop-helix transcription factors (PIF1, PIF3, PIF4, PIF5, PIF6, and PIF7 in *Arabidopsis*) that accumulate in the nucleus in the dark and interact conformer-specifically and photoreversibly with the phy-Pfr molecules in the light (Toledo-Ortiz et al., 2003; Duek and Fankhauser, 2005; Castillon et al., 2007; Monte et al., 2007). This phy-Pfr/PIF interaction initiates the gene expression changes that orchestrate the deetiolation response (Quail, 2002; Jiao et al., 2007; Bae and Choi, 2008). Nuclear interaction between active phyA and/or phyB and several of these transcription factors (including PIF1, PIF3, PIF4, and PIF5) has also been shown to induce rapid phosphorylation and degradation (within minutes) of the PIF proteins (Bauer et al., 2004; Park et al., 2004; Shen et al., 2005; Al-Sady et al., 2006; Oh et al., 2006; Nozue et al., 2007; Shen et al., 2007; Lorrain et al., 2008; Shen et al., 2008).

Recent studies with *Arabidopsis* seedlings deficient in one or multiple PIF proteins have established that progressive genetic removal of PIFs results in additive or synergistic effects in the dark that culminate in a partial *constitutively photomorphogenic (cop)*-like phenotype exhibited by the *pif* quadruple mutant *pif1*

<sup>1</sup> Address correspondence to elena.monte@cragenomica.es

The author responsible for distribution of materials integral to the findings presented in this article in accordance with the policy described in the Instructions for Authors (www.plantcell.org) is: Elena Monte (elena.monte@cragenomica.es).

 Some figures in this article are displayed in color online but in black and white in the print edition.

 Online version contains Web-only data.

www.plantcell.org/cgi/doi/10.1105/tpc.111.088161

*pif3 pif4 pif5 (pifq)*, which is deficient in PIF1, PIF3, PIF4, and PIF5 (Bae and Choi, 2008; Josse and Halliday, 2008; Leivar et al., 2008b). These results provide evidence that the PIF proteins function in the dark in a partially redundant manner, independently of phy action, to repress photomorphogenesis and promote skotomorphogenesis. Upon light exposure, active phy reverse this action by interacting with and inducing rapid degradation of the PIF proteins, allowing deetiolation to proceed.

The phy-mediated degradation of PIFs in dark-grown seedlings first exposed to light triggers the reduction of PIF protein levels to new steady state levels that represent ~10% of their dark levels (Monte et al., 2004; Shen et al., 2005; Nozue et al., 2007). *pif* mutant seedlings growing in continuous red light (Rc) display a hypersensitive phenotype that was initially interpreted as indicative of the PIFs having a negative role in phyB signaling in Rc (Huq and Quail, 2002; Kim et al., 2003; Fujimori et al., 2004; Monte et al., 2004; Khanna et al., 2007; de Lucas et al., 2008; Leivar et al., 2008a). However, more recent studies have shown that this phenotype is the result of elevated phyB levels in the absence of PIF proteins, an additive effect that correlates with increasing hypersensitivity to Rc with progressive genetic removal of multiple PIFs (Leivar et al., 2008a). Recently, Jang et al. (2010) have shown that the mechanism underlying the regulation of phyB levels (and other light-stable phys) during deetiolation involves direct interaction with the COP1 E3 ligase and that PIFs promote this interaction and the polyubiquitination of phyB by COP1.

Genome-wide expression analyses have started to provide some insight into the transcriptional network regulated by the PIFs. In dark-grown seedlings, transcriptomic profiling of single and double *pif1* (Moon et al., 2008), *pif3* (Leivar et al., 2009), and *pif4 pif5* (Lorrain et al., 2009) mutants have identified a small number of genes that are statistically and significantly deregulated in the mutants compared with their respective wild-type controls by at least twofold (Statistically Significantly and Two Fold [SSTF] genes). By contrast, microarray analysis of the *pifq* mutant compared with the wild type has resulted in the identification of a large subset of SSTF genes (~1000) that depend on PIF1, PIF3, PIF4, and PIF5 for their expression in the dark (Leivar et al., 2009; Shin et al., 2009). These results suggest redundancy at the molecular level between different members of the PIF family, similarly to their redundant contribution in establishing the *cop*-like visible phenotype of dark-grown *pifq* seedlings as explained above. The PIFq-regulated genes represent ~5% of the total genome and largely overlap with the transcriptome of wild-type seedlings grown under prolonged light, in accordance with the partial photomorphogenic phenotype of the *pifq* mutant in the dark (Leivar et al., 2009; Shin et al., 2009).

Some of these PIF-regulated genes are key regulators of pigment biosynthesis. PIF involvement in the regulation of chlorophyll biosynthesis became apparent upon transfer of 2-d-old or older dark-grown *pif* mutant seedlings to light, which failed to green (Huq et al., 2004; Stephenson et al., 2009). Microarray analysis identified the chlorophyll-biosynthesis-related genes *GLUTAMYL-tRNA REDUCTASE 1 (HEMA1)*, *Mg-CHELATASE H SUBUNIT (CHLH)*, *GENOMES UNCOUPLED 4 (GUN4)*, and *PROTOCHLOROPHYLLIDE OXIDOREDUCTASE C (PORC)* to present altered levels in *pif* mutants (Moon et al., 2008; Stephenson et al., 2009).

Misregulation of these genes in the dark results in exaggerated accumulation of the photooxidizing chlorophyll precursor protochlorophyllide in etiolated PIF-deficient seedlings, which causes photo bleaching upon transfer to light (Huq et al., 2004; Stephenson et al., 2009). PIFs also regulate the expression of the *PSY* gene encoding for the key carotenoid biosynthesis enzyme, which is upregulated during deetiolation to induce carotenoid accumulation (Toledo-Ortiz et al., 2010). In addition, many photosynthetic genes and genes associated with chloroplast biogenesis and function, like *LIGHT HARVESTING COMPLEX (LHC)* and *CHLOROPHYLL A/B BINDING PROTEIN (CAB)* genes, are also regulated by the PIFs in the dark (Moon et al., 2008; Leivar et al., 2009; Lorrain et al., 2009; Shin et al., 2009). This molecular phenotype is consistent with the partial conversion of etioplasts into chloroplasts exhibited by *pifq* seedlings in the dark (Leivar et al., 2009).

With the exception of pigment biosynthesis and chloroplast function, detailed analysis of the functional relevance of identified PIF-regulated genes in implementing the deetiolation program is still largely lacking (Leivar and Quail, 2011). Here, we identified an expanded set of genes that are regulated by PIF3 in the dark and examined their role in implementing seedling deetiolation by functional profiling of mutants. Integration of this information with the light-responsiveness of these genes is consistent with a model whereby the rapid initial deetiolation response is branched through PIF3-regulated genes and is subsequently counteracted to prevent an overresponse to light that could be detrimental for the emerging seedling.

## RESULTS

### PIF3 Represses Seedling Photomorphogenesis in the Dark by Regulating Gene Expression Both Positively and Negatively

Previous results have shown a role for PIF3 as negative regulator of photomorphogenesis in seedlings grown at specific time points in the dark (Leivar et al., 2008b; Stephenson et al., 2009). To characterize the role of PIF3 in more detail during extended periods of skotomorphogenic growth, we examined the morphological phenotype of the null *pif3-3* mutant (Monte et al., 2004) compared with the wild-type control during dark development for 4 d after germination (Figures 1A and 1B). During this period of dark growth, the wild-type hypocotyl elongates to ~12 mm, the hook partially and progressively unfolds to ~80°, and the cotyledons remain appressed. Compared with the wild type, *pif3* mutants are indistinguishable during germination and initial dark growth in the first 1.5 d (Figure 1A). By contrast, 2 d after germination, *pif3* mutants start displaying a partial photomorphogenic phenotype with more open hooks and cotyledons and marginal differences in hypocotyl elongation. These differences are maintained with increasing dark growth time up to 4 d of dark development (Figures 1A and 1B), in accordance with and expanding upon previous results by Leivar et al. (2008b) and Stephenson et al. (2009). Altogether, these results indicate that in the wild-type seedling growing in the dark for 4 d, cotyledons remain appressed, whereas there is a progressive elongation of the hypocotyl and

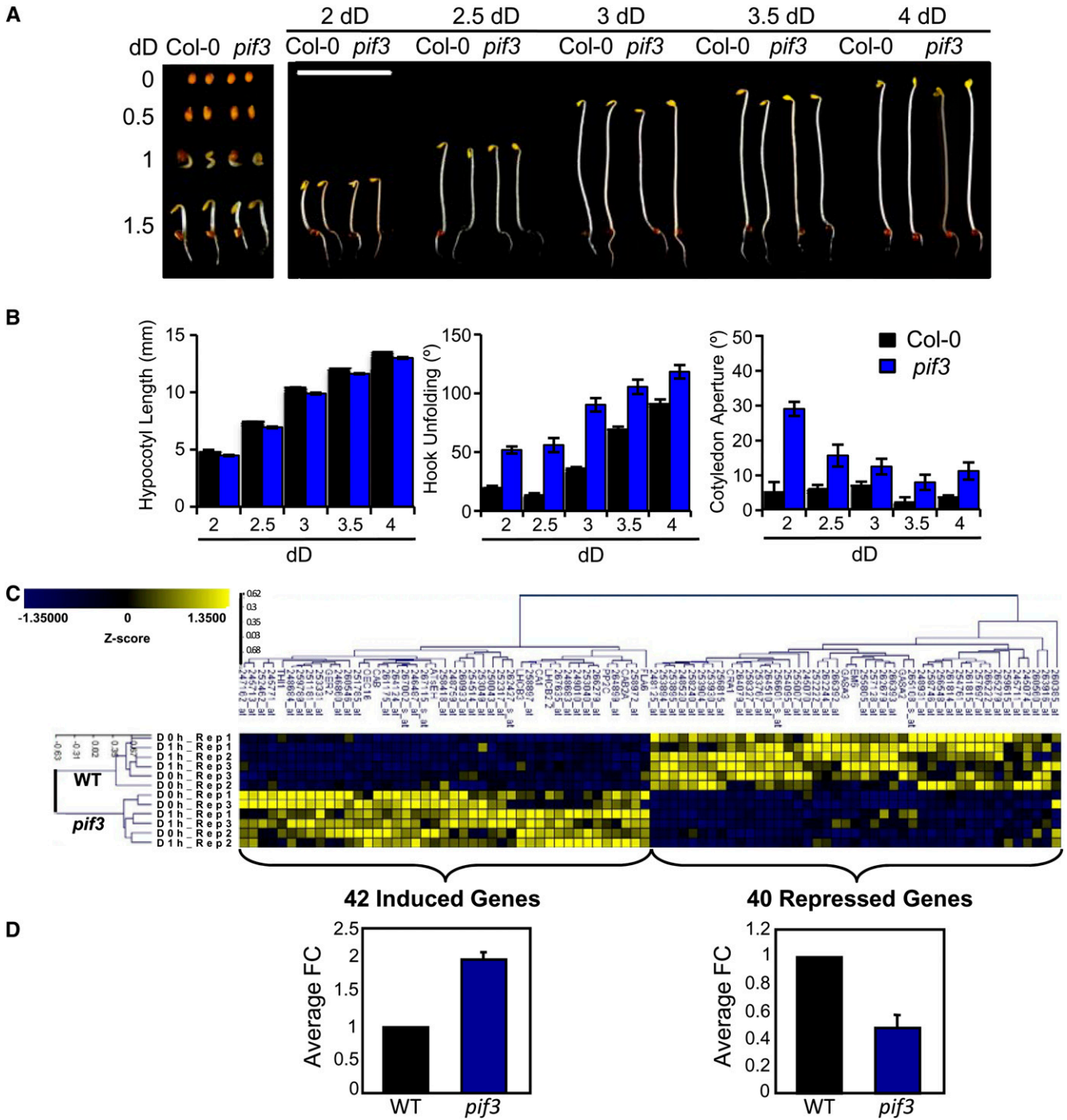


**Figure 1.** PIF3 Negatively Regulates Seedling Photomorphogenesis in the Dark from 2 d Onward after Germination.

(A) and (B) Characterization of the time of action of PIF3 during seedling etiolation in the dark. dD indicates days in the dark.

(A) Visual phenotype of representative seeds, embryos and seedlings for *Arabidopsis* wild-type Col-0 and *pif3-3* mutant seedlings in the dark at the indicated time points after germination.

(B) Quantification of hypocotyl length, hook unfolding, and cotyledon separation angle of *pif3-3* mutants compared with the wild-type Col-0 in the dark at the indicated time points after germination. Data represent the mean and SE of at least 30 seedlings.

(C) and (D) Regulation of gene expression in the dark by PIF3. Microarray expression profiling identified 82 HC target genes that are statistically significantly deregulated in the absence of PIF3 in the dark and by a FC greater than 1.5 (SS1.5F-HC).

(C) Two-dimensional-cluster diagram depicting the identified 82 SS1.5F-HC genes in 4-d-old dark-grown *pif3-3* seedlings compared with the wild-type

partial opening of the hook with increasing growth time in the dark. During this developmental process, PIF3 functions to repress photomorphogenesis from 2 d onward after germination and up to 4 d, with a role in promoting hypocotyl elongation and maintaining the hook and the cotyledons appressed, an effect that is sustained over time.

To identify downstream components that mediate PIF3 function as a repressor of photomorphogenesis in the dark, we first aimed to determine putative candidates by defining the PIF3-regulated transcriptome in the dark. To do so, we took advantage of a previous microarray study using Affymetrix ATH1 GeneChips, in which we analyzed the role of PIF3 in the regulation of phy-mediated gene expression in Rc (Monte et al., 2004). In that early work, our focus was to define the contribution of PIF3 in the regulation of the phy-mediated early transcriptional network in Rc. Here, given the current evidence that PIF3 and other PIF proteins act in the dark to sustain the skotomorphogenic state independently of phy activation (Bae and Choi, 2008; Leivar et al., 2008b), we analyzed the same raw microarray data (Monte et al., 2004), focusing now on the expression profiles in the dark (which were previously used exclusively to identify Rc responsive genes). In our current analysis, we took into consideration that, despite the obvious (although subtle) phenotypes observed for dark-grown *pif3* (Figures 1A and 1B) (Leivar et al., 2008b; Shin et al., 2009; Stephenson et al., 2009) and *pif1* (Leivar et al., 2008b; Shin et al., 2009; Stephenson et al., 2009) single mutant seedlings, previous microarray analysis of these mutants in the dark only identified 14 PIF3-regulated genes (Leivar et al., 2009) that were statistically and significantly expressed differently and by twofold (SSTF genes), and did not identify any SSTF genes regulated by PIF1 (Moon et al., 2008). Possible redundancy among PIFs in the regulation of gene expression (in accordance with their proposed redundant function as repressors of seedling deetiolation in the dark [Bae and Choi, 2008; Leivar et al., 2008b]) might translate into gene expression changes in single *pif* mutants smaller than SSTF. For this reason, we have decided to use a 1.5-fold cutoff in our new analysis presented here, a strategy that allowed Moon and colleagues to identify bona fide PIF1 targets (Moon et al., 2008).

Using the Rosetta Resolver platform (Rosetta Biosoftware), we analyzed two data sets of 4-d-old dark-grown seedlings (D0 h and D1 h) harvested 1 h apart and each including three biological replicates for wild type and three for *pif3-3* (Monte et al., 2004) (see Methods and Supplemental Figure 1A online). The complete analysis is presented in Supplemental Analysis 1 and associated Supplemental Figure 1 online; see also Supplemental References 1 online. This analysis identified a set of 121 PIF3-regulated genes (see Supplemental Figure 1A online) that are statistically and significantly expressed differently and by 1.5-fold in *pif3* compared

with the wild type (SS1.5F; see Supplemental Data Set 1 online), and a subset of 82 high-confidence (HC) PIF3 targets (SS1.5F-HC; see Supplemental Figure 1A and Supplemental Data Set 2 online). The gene list containing the 39 SS1.5F genes that did not make the HC cutoff is presented in Supplemental Data Set 3 online.

A two-dimensional cluster diagram representing the z-score-normalized signal intensities for the 82 SS1.5F-HC genes is shown in Figure 1C. The diagram contains the expression data for each of the six (three D0 h and three D1 h) wild-type and *pif3* biological replicates used in the analysis, and shows clustering of the 82 SS1.5F-HC genes in two subsets (induced and repressed) that have opposite expression patterns in their dependence on PIF3: approximately one-half of the 82 genes (40 genes) are repressed in *pif3* compared with the wild type, whereas the other one-half (42 genes) are induced (Figures 1C and 1D). The mean fold change (FC) for the up- and downregulated subset of genes is approximately twofold (Figure 1D). Further distribution of the 82 genes by FC is presented in Supplemental Analysis 1 and Supplemental Figure 1 online. It can be concluded that PIF3 represses photomorphogenesis in the dark, at least in part, by positively and negatively regulating the expression of the identified 40 and 42 genes, respectively (Figure 1D), and that, conversely, the misregulation of these genes in dark-grown *pif3* mutant seedlings might contribute to the observed phenotypes (Figures 1A and 1B). Functional classification of the 82 SS1.5F-HC genes is detailed in Supplemental Analysis 2 and the associated Supplemental Figure 2 online; see also Supplemental References 1 online. Notably, 25% of the annotated genes in the induced group in *pif3* relative to the wild type were photosynthesis-/chloroplast-related genes, indicating a degree of photomorphogenesis derepression in *pif3* consistent with its phenotype in the dark.

These expression patterns detected by microarray analysis were validated for selected genes by quantitative RT-PCR (qRT-PCR) analysis (see Supplemental Figure 3 online). Interestingly, the fold difference in expression between the wild type and the *pif3* mutant was more robust after 2 d of dark growth compared with 4 d for some of the tested genes (*AT5G16030*, *AT3G05730*, and *AT5G02760*) (see Supplemental Figure 3B online). These results suggest the existence of a developmentally regulated expression program during seedling growth in the dark. Similar observations were reported by Stephenson et al. (2009) for the behavior of three chlorophyll-biosynthesis genes (*HEMA1*, *GUN4*, and *CHLH*) in dark-grown *pif1*, *pif3*, and *pif1 pif3* mutants. In addition, seed batch variation could also account for some of the data variability, especially when differences are small, as previously reported (Leivar et al., 2008b).

To provide a broader molecular framework for the PIF3-regulated transcriptome in the dark defined here (Figures 1C and 1D; see Supplemental Figure 1 online), we compared it with

**Figure 1.** (continued).

(WT) Col-0. A total of 42 genes are upregulated (induced) in the absence of PIF3, whereas 40 correspond to genes that are downregulated (repressed), suggesting that PIF3 can act both as repressor and activator of gene expression in the dark.

(D) Mean FC for the 42 upregulated genes (left) and the 40 downregulated genes (right) in the *pif3-3* mutant in the dark relative to the wild-type dark value set at unity. Bars indicate SE for the genes averaged for each group.

Bar in (A) = 10 mm.

previous genome-wide studies on *pif4 pif5* (Lorrain et al., 2009) and *pifq* (Leivar et al., 2009). This comparative analysis is presented in Supplemental Analysis 3 online and is associated with Supplemental Figures 4 and 5 and Supplemental Data Set 4 online; see also Supplemental References 1 online. Consistent with the described phenotypic data (Leivar et al., 2008b, Shin et al., 2009; Stephenson et al., 2009), the comparative analysis suggests that PIF3 regulates gene expression in the dark in a partially redundant manner with other PIF factors, including PIF1, and that some specificity might exist among the genes targeted by PIF3 and PIF4/PIF5 in the presence of other PIFs.

### Selection of PIF3-Regulated *MISREGULATED IN DARK* Genes and Functional Characterization of *Arabidopsis mida* Mutants

The 82 PIF3-regulated genes identified by microarray analysis were considered good candidate genes to encode regulators of plant growth and development during the deetiolation process. To begin to determine whether some of them have functionally relevant roles in photomorphogenesis, we selected a subset of 10 genes functionally categorized as having potential transcription (*AT4G10240* and *AT5G04340*), signaling (*AT1G48260* and *AT5G02760*), growth and development (*AT4G37300*), stress and defense (*AT3G05730*), or hormone-related (*AT5G50600* and *AT4G10020*) activity, as well as two annotated as unknown (*AT3G47250* and *AT1G02470*), for systematic functional analysis using mutants. To this list, we have added three genes (*AT2G46070* encoding a MAPK kinase, and *AT1G05510* and *AT5G45690* of unknown function) from our SS1.5F gene set for their potential interest based on the predicted function (see Supplemental Analysis 2 online) and/or robust difference in expression in the *pifq* mutant (see Supplemental Analysis 3 online). Most of these genes show a response with respect to the wild type substantially more robust in the *pifq* mutant (Leivar et al. 2009) compared with *pif3* (see Supplemental Figure 6A online). Given that the two gene expression profile experiments were done using samples grown under different conditions (Monte et al., 2004; Leivar et al., 2009), we have validated these differences by qRT-PCR in *pif3* and *pifq* dark-grown seedlings grown at the same time and under the same conditions (see Supplemental Figure 6B online). These results suggest that these genes are targeted by PIF3 and possibly other PIFs during postgerminative growth in the dark.

These 13 genes were named *MISREGULATED IN DARK* (*MIDA*) genes. Table 1 contains a summary of these 13 *MIDA* genes, indicating for each one: *Arabidopsis* Gene Identification (AGI) number, previously ascribed name and reference (if published), FC in *pif3* with respect to the wild type, assigned functional group, our designated *MIDA* name, and the corresponding insertional mutant line isolated or the mutant line obtained if already available. The available mutants include one overexpressor line for *AT5G50600* (Li et al., 2007) and two RNA interference (RNAi) lines for *AT2G46070* (Lee et al., 2009). For *AT5G50600*, T-DNA insertional mutants were available; however, because the gene exists in two copies located in a large duplicated region, it is not possible to distinguish between homozygous and heterozygous lines, because the gene-specific

primers cross-hybridize with the intact copy of the duplicated gene (not carrying the T-DNA insertion) during the genotyping process, and thus prevent the identification of *AT5G50600* mutants that are suitable for characterization.

For the T-DNA insertional *mida* mutants, we identified homozygous mutant lines together with corresponding wild-type siblings for the phenotypic studies. For *mida6*, we were unable to find homozygous plants, even after analyzing the progeny of several heterozygous lines, indicating that the mutation might be lethal in homozygosity. All the *mida* mutant lines are in the ecotype Columbia (Col-0) background. Any phenotypes observed in the homozygous lines compared with their wild-type siblings were further confirmed by comparisons with Col-0 seedlings. The 12 mutated loci investigated over here were analyzed for statistically significant differences from the wild type in hypocotyl, cotyledon, and hook phenotypes in 2-, 3-, and 4-d-old dark-grown seedlings. Given the observed wild-type phenotypes during this period of dark development (Figures 1A and 1B), we reasoned that possible photomorphogenic phenotypes of the *mida* mutants might include deviations in both directions in hypocotyl growth (shorter or longer compared with the wild type) and/or in hook opening (decreased or increased angle with respect to the wild type), and deviations in cotyledon separation only in the direction of enhanced opening, because cotyledons remain essentially appressed in the wild type throughout dark development (Figures 1A and 1B). *mida* loss-of-function mutants showing a derepression of photomorphogenesis in the dark (i.e., displaying a shorter hypocotyl and/or a more open hook and cotyledons) would correspond to *MIDA* factors that potentially function as repressors of photomorphogenesis, whereas those showing enhanced skotomorphogenesis in the dark (i.e., displaying a longer hypocotyl and/or a closer hook) would correspond to *MIDA* factors with a potential role as inducers of photomorphogenesis.

Figure 2 and Supplemental Data Set 5 online show the functional characterization of *Arabidopsis mida* mutants in the dark, with the quantitative data and statistical analysis for hypocotyl length, hook unfolding, and cotyledon aperture. For comparison, data from multiple experiments are compiled in Figure 2, whereas the complete primary data and statistical analysis for each *mida* line are presented in Supplemental Data Set 5 online. For simplicity, data from each *mida* mutant line in Figure 2 are shown relative to their respective wild-type sibling set at unity, and a horizontal black dashed line set at 1 is included as the wild-type reference. An asterisk indicates the *mida* lines displaying statistically significant differences (see Methods) compared with their respective wild-type sibling in 2-, 3-, and 4-d-old dark-grown seedlings (see Supplemental Data Set 5 online for the associated P values). Even where statistically significant differences were detected (Figure 2; see Supplemental Data Set 5 online), the phenotypic differences between the wild type and *mida* lines ranged in magnitude from marginal to moderate. To define which lines display bona fide phenotypes, we applied a FC criterion, comparing the magnitude of the phenotype to their respective wild-type sibling (Figure 2; see Supplemental Data Set 5 online). Based on the phenotypes displayed by single and double PIF-deficient mutants (Leivar et al., 2008b), we set a FC cutoff at 40% for the hook, 80% for the cotyledon, and 20% for

**Table 1.** List of the 13 *MIDA* Genes Analyzed, Including the AGI Loci, the Designated Protein Names, the FC in Expression in *piF3* Mutant in the Dark Relative to the Wild Type, and Their Functional Category

<i>MIDA</i>	AGI No.	Protein Name	FC at D0 h <i>piF3</i> versus Wild Type	Functional Category	Reported Function	Mutant Line	<i>Mida Line</i>
<i>MIDA1</i>	AT5G50600	HSD1	-1.61226	H	Li et al. (2007)	AOHSD16 (Li et al., 2007)	<i>mida1-OX</i>
<i>MIDA2</i>	AT3G05730	DEFL	2.78217	S/D	ND	SALK_031670	<i>mida2</i>
<i>MIDA3</i>	AT4G37300	MEE59	1.54716	G/D	ND	SALK_040468	<i>mida3</i>
<i>MIDA4</i>	AT1G02470	UNKNOWN	2.33482	UNK	ND	SALK_123221	<i>mida4</i>
<i>MIDA5</i>	AT3G47250	UNKNOWN	1.568	UNK	ND	SALK_099356	<i>mida5</i>
<i>MIDA6</i>	AT5G04340	ZN FINGER	-2.04231	TXN	ND	SALK_140448	<i>mida6</i>
<i>MIDA7</i>	AT1G48260	CIPK17	-1.76389	S	ND	SALK_130764	<i>mida7</i>
<i>MIDA8</i>	AT4G10020	HSD5	-1.50981	H	ND	SAIL_129B11	<i>mida8</i>
<i>MIDA9</i>	AT5G02760	PP2C	1.76423	S	ND	SAIL_764H11	<i>mida9-1</i>
<i>MIDA9</i>	AT5G02760	PP2C	1.76423	S	ND	SALK_672093	<i>mida9-2</i>
<i>MIDA10</i>	AT4G10240	BBX23	-1.50432	TXN	ND	SALK_053389C	<i>mida10</i>
<i>MIDA11</i>	AT2G46070	MPK12	1.679	S	Lee et al. (2009)	MPK12RNAi-9 (Lee et al., 2009)	<i>mida11-1</i>
<i>MIDA11</i>	AT2G46070	MPK12	1.679	S	Lee et al. (2009)	MPK12RNAi-17 (Lee et al., 2009)	<i>mida11-2</i>
<i>MIDA12</i>	AT1G05510	UNKNOWN	-2.5	UNK	ND	SALK_117754	<i>mida12</i>
<i>MIDA13</i>	AT5G45690	UNKNOWN	-1.705	UNK	ND	SALK_145109	<i>mida13</i>

The corresponding mutant lines isolated from SALK or SAIL, and the previously identified mutants are indicated together with their *mida* nomenclature. Functional categories: G/D, growth/development; H, hormone; S, signaling; S/D, stress/defense; TXN, transcription; UNK, unknown. ND, not determined.

the hypocotyl (represented by horizontal red dashed dotted lines in Figure 2). In addition, given the variation in gene expression during dark development (see Supplemental Figures 3 and 4E online), which suggests that the action of PIF3-regulated genes might have variable relevance during the process of skotomorphogenesis, we required that the statistically significant differences and FC cutoffs had to be met in at least 2 d. Together, based on these three defined criteria (P value, FC, and time of action), mutations in four genes caused apparent photomorphogenic seedling phenotypes in the dark (Figure 2): *mida9* and *mida10* showed enhanced hook unfolding, whereas *mida11* displayed shorter hypocotyls, and *mida1-OX* had more separated cotyledons. These results suggest branching of the signal that PIF3 relays through the MIDAs to regulate specific aspects of the deetiolation response. Figures 3 and 4 show a more detailed characterization of these *mida* mutants (see below).

### MIDA9 and MIDA10 Are Novel Repressors of Hook Unfolding

Figure 3 shows the *mida9* and *mida10* phenotypes, together with a more detailed characterization of the *mida* mutants, a diagram of the *MIDA* gene that indicates the position of the T-DNA insertion, and an RNA gel blot that confirms the disruption of the transcript in the *mida* mutant. A bar graph showing the FC difference in expression in the *piF3* mutant compared with the wild type in the dark is also included.

For *MIDA9*, a PIF3-repressed gene (Figure 3C), we identified a T-DNA insertional allele, designated *mida9-1*, that carries a T-DNA insertion in the first exon, from the Syngenta Arabidopsis Insertion Library (SAIL) collection (Figure 3A, Table 1). The *mida9-1* allele produced no detectable *MIDA9* transcript and is therefore likely a null (Figure 3B). Hook unfolding phenotypes of two mutant siblings compared with a wild-type sibling and with Col-0 showed that the

*mida9* mutant exhibited enhanced hook unfolding after 2, 3, and 4 d in the dark (Figures 3D and 3E). Similar results were obtained for a second null mutant allele of *MIDA9* (*mida9-2*) (Table 1; see Supplemental Figure 7 online). *MIDA9* encodes a previously uncharacterized type 2C phosphatase, predicted to be nuclear, belonging to the D clade of type 2C phosphatases in *Arabidopsis* (Schweighofer et al., 2004). Based on these results, we conclude that *MIDA9* is a PIF3-repressed repressor of photomorphogenesis in the dark with a specific role in hook unfolding.

For *MIDA10*, a PIF3-induced gene (Figure 3H), we identified a T-DNA insertional allele designated *mida10-1* from the SALK collection (Alonso et al., 2003; <http://signal.salk.edu>) that carries a T-DNA insertion in the second exon (Figure 3F, Table 1). The *mida10-1* allele produced no detectable *MIDA10* transcript and is therefore likely a null (Figure 3G). Hook unfolding phenotypes of a wild-type sibling and two mutant siblings compared with Col-0 show the enhanced hook unfolding of the *mida10* mutant after 3 and 4 d in the dark (Figures 3I and 3J). *MIDA10* encodes B-BOX CONTAINING PROTEIN 23 (BBX23) (Datta et al., 2008; Khanna et al., 2009). *BBX23/MIDA10* belongs to a clade among the B-Box family of proteins that consists of eight genes, with several of its related members previously implicated in light-dependent development (Datta et al., 2008 and references therein; Khanna et al., 2009). Based on these results, we conclude that *BBX23/MIDA10* is a PIF3-induced repressor of photomorphogenesis in the dark with a specific role in hook unfolding. For simplicity, we refer to *BBX23/MIDA10* as *MIDA10* hereafter.

### MIDA11 Is a Novel Regulator of Hypocotyl Elongation

*mida11* is a previously published dexamethasone (DEX)-inducible RNAi line (Table 1) (Lee et al., 2009). It was originally shown to have a phenotype in root elongation under continuous

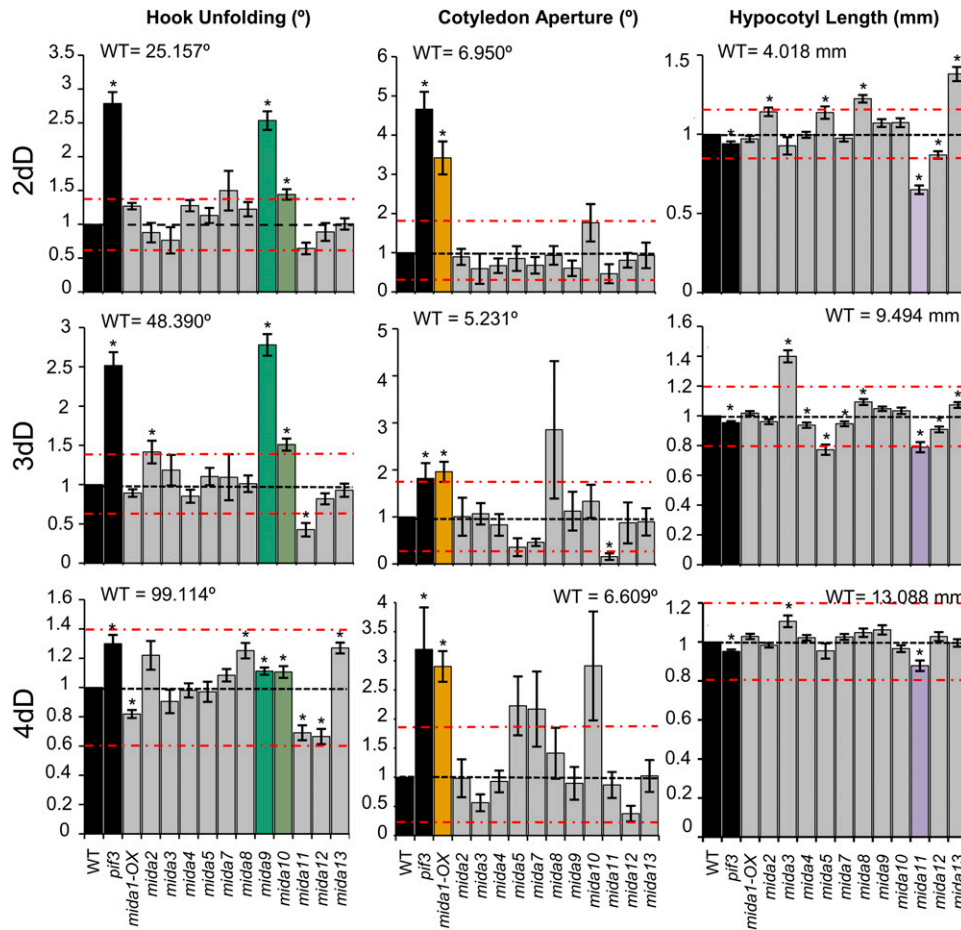


**Figure 2.** Functional Characterization of *Arabidopsis mida* Mutants Defective in PIF3 Target Genes Identifies Four Novel Regulators of Seedling Deetiolation.

Hook unfolding angle (left), cotyledon separation angle (middle), and hypocotyl length (right), displayed by 2- (top), 3- (middle), and 4-d-old (bottom) *mida* mutant lines. A total of 30 seedlings were used for measurements, and values were normalized to the corresponding wild-type (WT) sibling (see Supplemental Data Set 5 online for primary data and statistical analysis). For each *mida* line, a corresponding wild-type sibling was used as control to calculate the P value and FC difference (see Methods and Supplemental Data Set 5 online for further details). In the bar graph, measurements for *mida* mutant lines are expressed as a FC with respect to their wild-type sibling, whereas error bars represent the variation (SE) of this FC response of at least 30 seedlings (see Supplemental Data Set 5 online). For comparison purposes, a wild type set at unity is shown as reference (shown as horizontal dashed line). The *pif3* mutant is also included as reference. Based on statistical difference (P value < 0.05) (marked with an asterisk in the graph) together with a FC relative to the corresponding wild type greater than 40% for hook, and/or 80% for cotyledon, and/or 20% for hypocotyl (these cutoff percentage values are indicated by a dashed dotted line) in at least two of the 3 d assayed, four *mida* lines were determined to display a partial photomorphogenic phenotype in the dark: *mida9* and *mida10* display partially open hooks, *mida11* displays short hypocotyls, and *mida1-OX* displays partially separated cotyledons. The actual degrees of aperture or the length of the hypocotyl of an average wild-type response from the multiple experiments is indicated as reference on the top of each graph (see Supplemental Data Set 5 online for the calculation). The *mida9* and *mida11* mutant alleles used were *mida9-1* and *mida11-2*, respectively. [See online article for color version of this figure.]

white light (WLc) (Lee et al., 2009). Figure 4B shows the effect of DEX on the amount of *MIDA11* transcript in the wild type and two independent *mida11* (*mida11-1* and *mida11-2*) dark-grown seedlings, indicating that *mida11* has reduced levels in the dark (a 60 to 80% reduction compared with the wild type) in the presence of DEX. DEX application induced a hypocotyl phenotype in both *mida11* RNAi lines compared with the control Col-0 treated with DEX (Figures 4C and 4D). *MIDA11*, a PIF3-repressed gene (Figure 4A), encodes a MAP kinase (MPK12) that has been proposed to regulate auxin signaling (Lee et al., 2009).

Based on these results, we conclude that MPK12/MIDA11 is a PIF3-repressed repressor of photomorphogenesis in the dark with a specific role in hypocotyl elongation. For simplicity, we refer to MPK12/MIDA11 as MIDA11 hereafter.

#### MIDA1 Is a Novel Regulator of Cotyledon Separation

*mida1-OX* is a previously published *HYDROXYSTEROID DEHYDROGENASE 1 (HSD1)* overexpressor line (Table 1) (Li et al., 2007). It was originally shown to exhibit a growth phenotype in

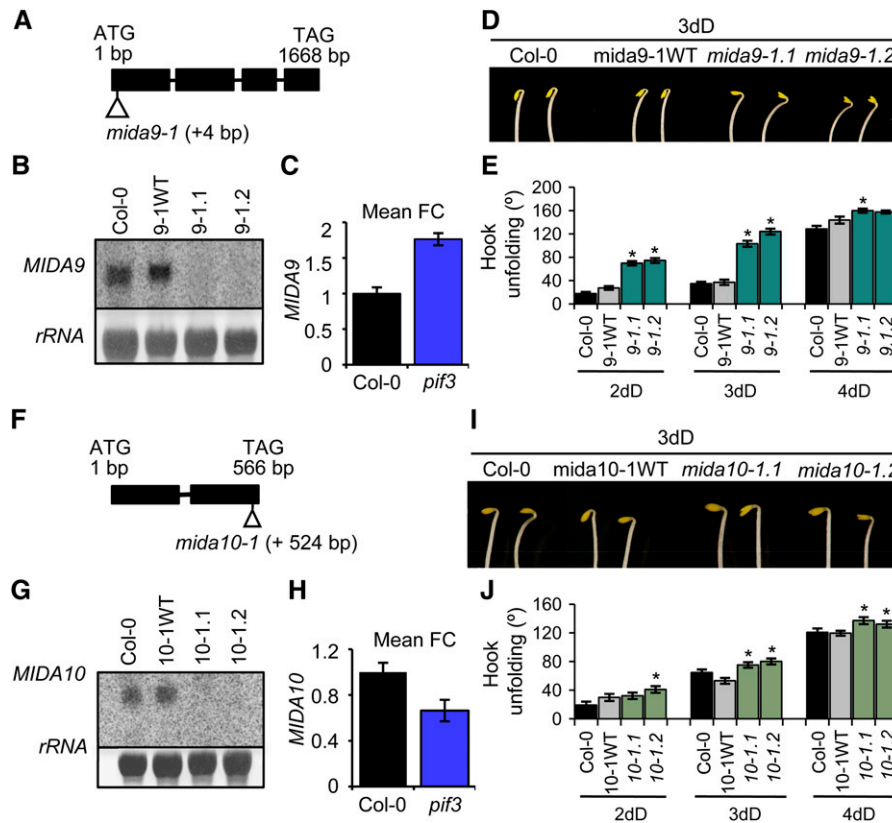


**Figure 3.** MIDA9 and MIDA10 Are Novel Repressors of Hook Unfolding in the Dark.

(A) The mutation identified in *Arabidopsis MIDA9*. The T-DNA insert in *mida9-1* is indicated at position +4 bp relative to the ATG.  
 (B) RNA gel blots of 2-d-old, dark-grown Col-0, *mida9-1.1*, and *mida9-1.2* mutant seedlings, and a corresponding *mida9-1* wild-type (WT) sibling. No *MIDA9* transcript was detected in *mida9-1*, indicating that it is likely a functional knockout mutant.  
 (C) Bar graph of microarray data showing the FC in *MIDA9* expression in *pif3* relative to the wild-type in the dark. Data correspond to biological triplicates, and bars indicate SE.  
 (D) Visual hook phenotype of 3-d-old, dark-grown Col-0, wild-type sibling, and *mida9-1* mutant seedlings.  
 (E) Quantification of hook angle in *mida9-1* compared with Col-0 and a wild-type sibling line after 2, 3, and 4 d of growth in the dark (dD) after germination. Data represent the mean and SE of at least 30 seedlings, and asterisks indicate statistically different mean values compared with their corresponding wild type.  
 (F) The mutation identified in *Arabidopsis MIDA10*. The T-DNA insert in *mida10-1* is indicated at position +524 bp relative to the ATG.  
 (G) RNA gel blot of 2-d-old, dark-grown Col-0, *mida10-1.1*, and *mida10-1.2* mutant seedlings, and a corresponding *mida10-1* wild-type sibling. No *MIDA10* transcript was detected in *mida10-1*, indicating that it is likely a functional knockout mutant.  
 (H) Bar graph of microarray data showing the FC in *MIDA10* expression in *pif3* relative to the wild type in the dark. Data correspond to biological triplicates and bars indicate SE.  
 (I) Visual hook phenotype of 3-d-old dark-grown Col-0, a wild-type sibling, and *mida10-1* seedlings.  
 (J) Quantification of hook angle in *mida10* compared with Col-0 and a wild-type sibling line after 2, 3, and 4 d of growth in the dark after germination. Data represent the mean and SE of at least 30 seedlings, and asterisks indicate statistically different mean values compared with their corresponding wild type. [See online article for color version of this figure.]

adult plants grown in WLC conditions (Li et al., 2007). Figure 4F shows the expression levels of *HSD1/MIDA1* in two overexpressor lines grown in the dark, indicating that *mida1-OX* exhibits increased levels of *HSD1/MIDA1* in the dark (between 1.5-fold to fourfold compared with the wild type). Enhanced cotyledon separation in these two overexpressor lines compared with Col-0 after 2, 3, and 4 d in the dark is shown in Figures 4G and 4H. *HSD1/MIDA1*, a PIF3-induced gene (Figure 4E), has been proposed to encode an enzyme involved in brassinosteroid (BR) synthesis (Li et al., 2007). Based on these results, we conclude

that *HSD1/MIDA1* is a PIF3-induced inducer of photomorphogenesis in the dark with a specific role in cotyledon separation. For simplicity, we refer to *HSD1/MIDA1* as *MIDA1* hereafter.

#### Light-Responsiveness of PIF3-Regulated Genes in the Dark

The above data are summarized in Supplemental Table 1 online and suggest that PIF3 action in the dark involves the induction of *MIDA10* and *MIDA1*, a negative and a positive regulator of photomorphogenesis, respectively, and the repression of *MIDA9*

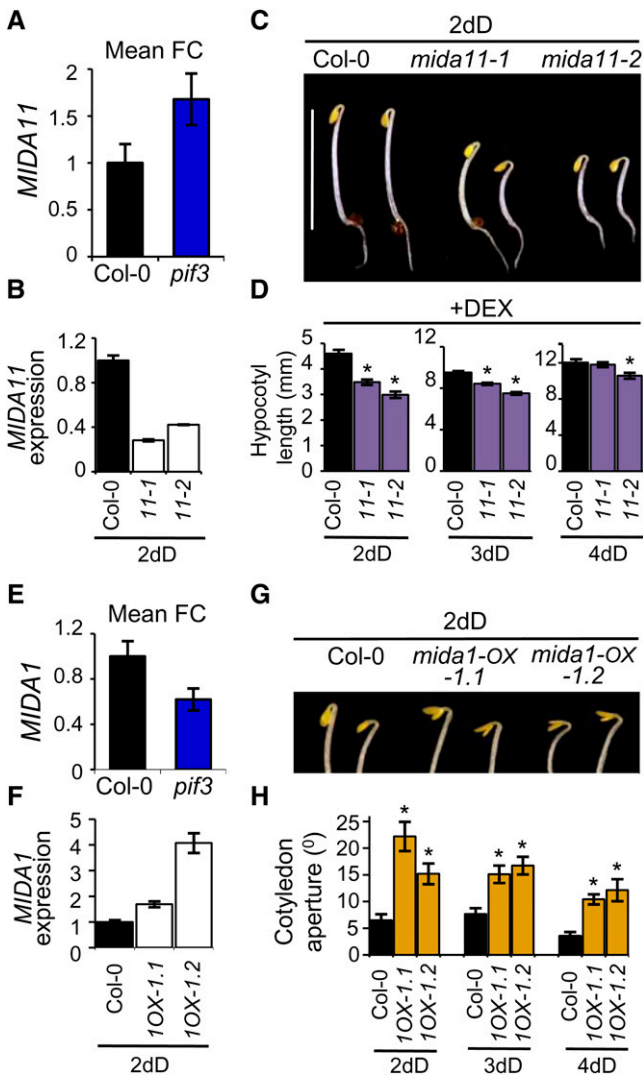


**Figure 4.** *MIDA11* Is a Novel Inducer of Hypocotyl Length and *MIDA1* Is a Novel Regulator of Cotyledon Separation in the Dark.

**(A)** Bar graph of microarray data showing the FC in *MIDA11* expression in *pif3* relative to the wild type in the dark. Data correspond to biological triplicates, and bars indicate SE.

**(B)** qRT-PCR analysis of 2-d-old, dark-grown Col-0 and *mida11-1* and *mida11-2* mutant seedlings grown in the presence of DEX. Expression levels were normalized to *PP2A* as described previously (Shin et al., 2007) and expressed relative to the wild-type value set at unity. *MIDA11* transcript levels were reduced ~80% in the two lines used, confirming that *MIDA11* expression is suppressed by the DEX-induced RNAi in dark conditions. *mida11-1* and *mida11-2*, two independent RNAi lines, were obtained from Lee et al. (2009) (Table 1). Error bars represent SE values of technical triplicates.

**(C)** Visual hypocotyl phenotype of 3-d-old dark-grown Col-0 and *mida11-1* and *mida11-2* seedlings in the presence of DEX.

**(D)** Quantification of hypocotyl length in *mida11* compared with Col-0 after 2, 3, and 4 d of growth in the dark (dD) after germination in the presence of DEX. Data represent the mean and SE of at least 30 seedlings, and asterisks indicate statistically different mean values compared with their corresponding wild type.

and *MIDA11*, both negative regulators of photomorphogenesis in the dark (Figures 2 to 4). These data provide a complex and somewhat contradictory picture of how PIF3 might exert its function as a repressor of photomorphogenesis. To further analyze how this complex regulatory network might participate during seedling deetiolation, we next addressed the question of how the rapid phy-induced degradation of PIF3 (and other PIFs) upon illumination of dark-grown seedlings might affect the expression of the four identified *MIDAs*.

To do this, we reanalyzed the light data from the same microarray experiment (wild type after 1 h of Rc [R1 h], included in Monte et al., 2004, and the previously unpublished wild type [E. Monte and P. Quail, unpublished data] after 18 h of Rc [R18 h]), using the Rosetta Resolver software for consistency (see Methods). We defined early (R1 h) and late (R18 h) red light-responsive genes as genes that display SSTF alterations when comparing the wild type after 1 h of Rc (R1 h) versus the wild type kept in darkness for 1 h (D1 h) and the wild type after 18 h of Rc (R18 h) versus the wild type kept in darkness for 18 h (D18 h), respectively. We identified 546 R1 h SSTF genes and 2764 R18 h SSTF genes in our experiment. Supplemental Data Sets 6 and 7 online show the gene lists containing R1 h SSTF and R18 h SSTF genes, respectively. We then compared the genes displaying SS1.5F-HC alterations in *pif3* after 4 d in darkness (*pif3*-D) with genes displaying SSTF alterations in the wild type after R1 h and after R18 h. This comparative analysis is presented in Supplemental Analysis 4, the associated Supplemental Figure 8, and Supplemental Data Set 8 online; see also Supplemental References 1 online. Notably, 67% of *pif3*-D genes were light-responsive at R1 h and/or R18 h, with 83.6% of these responding to Rc later than 1 h after illumination (see Supplemental Figure 8A and Supplemental Analysis 4 online).

To establish the light-responsive kinetics of the four *MIDA* genes identified to have a role in deetiolation (Figures 3 and 4), we combined the R1 h and R18 h microarray information for each gene (see Supplemental Figure 9 online) with a detailed time-

**(E)** Bar graph of microarray data showing the fold change in *MIDA1* expression in *pif3* relative to the wild type in the dark. Data correspond to biological triplicates and bars indicate SE.

**(F)** qRT-PCR analysis of 2-d-old, dark-grown wild type and *mida1-OX* mutant seedlings. Expression levels were normalized to *PP2A* as described previously (Shin et al., 2007) and expressed relative to the wild-type value set at unity. *MIDA1* transcript was overexpressed in *mida1-OX-1.1* and *mida1-OX-1.2*, confirming that the lines overexpress *MIDA1* in dark conditions. Overexpressor *mida1-OX-1.1* and *mida1-OX-1.2* lines (represented in the figure as 1OX-1.1 and 1OX-1.2, respectively) are two siblings from a transgenic line obtained from Li et al. (2007) (Table 1). Error bars represent SE values of technical triplicates.

**(G)** Visual cotyledon phenotype of 2-d-old, dark-grown Col-0 and *mida1-OX-1* seedlings.

**(H)** Quantification of cotyledon angle in *mida1-OX-1* (represented as 1OX-1 in the figure) compared with Col-0 after 2, 3, and 4 d of growth in the dark after germination. Data represent the mean and SE of at least 30 seedlings, and asterisks indicate statistically different mean values compared with their corresponding wild type.

Bar in **(C)** = 5 mm.

[See online article for color version of this figure.]

course qRT-PCR analysis of 2-d-old dark-grown wild-type seedlings exposed to Rc for increasing periods of time (Figure 5A). Our results show that light triggers an immediate early response of the *MIDA10* transcript, with a 10-fold light repression at 1 h compared with dark levels, and reaches almost nondetectable levels after 12 h of Rc exposure (Figure 5A). *MIDA1* also responds early with a sixfold induction after 2 h of Rc exposure in 2-d-old dark-grown seedlings (Figure 5A). This induction of *MIDA1* in light conditions is transient, and transcript levels return to dark levels after 6 h of irradiation (Figure 5A). Finally, Rc triggers a twofold induction of *MIDA9* and *MIDA11* transcripts relative to their dark control after 3 and 6 to 9 h, respectively (Figure 5A), an induction that decreases again after 18 h of Rc (see Supplemental Figure 9 online). For all four genes, expression levels in the *pif3* mutant kept in the dark during this time showed little variation (Figure 5A). These qRT-PCR results validate and expand on the microarray data at R1 h and R18 h for these genes (see Supplemental Figure 9 online), and together indicate that the rapid phy-induced degradation of PIF3 triggers a light response in all four *MIDA* genes in the wild type that is in the same direction as the alteration in expression caused by PIF3 deficiency in the dark: One is light-repressed (*MIDA10*), and three are light-induced (*MIDA9*, *MIDA11* and *MIDA1*). In addition, these results indicate that PIF3 degradation triggers an early light response in *MIDA10* and *MIDA1* and a late light response in *MIDA9* and *MIDA11* (Figure 5A). Altogether, these data suggest that the *MIDA* factors induced by light (*MIDA9*, *MIDA11*, and *MIDA1*) might not only

have a role during skotomorphogenesis in the dark but also function during deetiolation either early (after 1 to 3 h of Rc) and/or late (after more than 3 h of Rc) once the seedling has been exposed to light.

### Participation of the MIDAs in the Seedling Responses to Light

We examined the phenotypes of *mida9*, *mida10*, *mida11*, and *mida1-OX* in the dark-to-Rc transition. Figure 5B shows the results for each of the mutants. For *mida10*, 2-d-old etiolated seedlings show a weak unfolded hook phenotype in the dark (Figures 2, 3J, and 5B), and exposure to light accelerates the hook opening response compared with the corresponding wild type, resulting in an aperture of 40° after 3 h (Figure 5B). These results suggest that *MIDA10* acts as a repressor of hook opening during the initial deetiolation response, consistent with its role as a hook repressor in the dark (Figures 2, 3I, and 3J) and its rapid degradation upon exposure to light (Figure 5A). For *mida1-OX*, the differences in cotyledon separation between the mutant and the wild type in the dark (Figures 2, 4G, 4H, and 5B) are larger in response to Rc (Figure 5B): Cotyledons in 2-d-old wild-type seedlings are basically appressed in the dark (10° aperture) and start responding to light 12 h after Rc exposure, to reach an aperture of 80° after 24 h of illumination. By contrast, the cotyledons of *mida1-OX* are partially separated in the dark (30°, threefold the wild-type aperture), start responding to Rc

**Figure 5.** Light-Responsiveness of *MIDA* Gene Expression and Phenotypic Characterization of *mida* Mutants during the Dark-to-Light Transition.

**(A)** Light-responsiveness of selected PIF3-regulated *MIDA* genes in dark-grown wild-type (WT) seedlings exposed to Rc (8  $\mu\text{mol}/\text{m}^2/\text{s}$ ). Wild-type siblings were exposed to Rc for increasing periods from 0 (dark control) to 12 h, and expression levels were assayed by qRT-PCR, normalized to *PP2A* as described previously (Shin et al., 2007), and expressed relative to the Col-0 dark value set at unity. Expression levels in the *pif3* mutant in the dark are indicated with a dashed line for comparison. The expression level in Col-0 maintained in the dark for 12 h is indicated in the graph with an X. Error bars correspond to SE values of technical triplicates.

**(B)** Time-course quantification of hook opening (*mida9* and *mida10*), cotyledon separation (*mida1-OX*), and hypocotyl growth (*mida11*) (in the presence of DEX), of 2-d-old, dark-grown wild type (WT) (solid lines) and *mida* mutant seedlings (dashed lines) during the dark-to-red light transition. Data represent the mean and SE of at least 30 seedlings.

[See online article for color version of this figure.]

earlier than the wild type (after only 3 h of illumination), and reach an angle of 140° after 24 h of Rc. These results indicate that MIDA1 functions as an inducer of cotyledon separation during early deetiolation, consistent with the observed phenotype of *mida1-OX* in the dark (Figures 2, 4G, and 4H) and with the rapid MIDA1 induction in response to Rc (Figure 5A). For *mida9*, our results showed more open hooks in *mida9* mutants compared with the wild type over the time-course analysis in response to light (Figure 5B). This effect is difficult to attribute specifically to light, given that *mida9* hooks are already opened in the dark (Figures 2, 3D, 3E, and 5B), similar to the hook response of *pif* mutants in the dark and in the dark-to-light response (Leivar et al., 2008b). Alternative evidence of a role for MIDA9 in hook repression in the light was obtained by growing seedlings continuously in low far-red light (FR) (see Supplemental Figure 10 online). In these conditions, the wild-type hooks are only partially opened after 4 d (aperture of 120°), and the hooks of *mida9* seedlings are wider open (160°) (see Supplemental Figure 10 online). These data suggest a role for MIDA9 as a repressor of hook unfolding in the dark (Figures 2, 3D, and 3E) and in the light, consistent with the observed phenotype of *mida9* in the dark (Figures 2, 3D, and 3E) and with the MIDA9 induction in response to light (Figure 5A). Finally, for the DEX-inducible *mida11*, the differences in hypocotyl length between the mutant and the wild type in the dark (Figures 2, 4C, and 4D) increase in response to Rc in the presence of DEX (Figure 5B). Whereas the wild-type seedlings grow from 2.4 mm in the dark to 6.2 mm after 24 h of Rc, *mida11* seedlings grow from 1.9 mm in the dark (20% shorter than the wild type) to only 4.4 mm after 24 h of Rc (30% shorter than the wild type at the same time point) (Figure 5B). Hypocotyl elongation rate in *mida11* compared with the wild type seems to be progressively affected over time after the first 3 h of light exposure (Figure 5B). As a control, etiolated *mida11* seedlings grown in the absence of DEX showed no difference in hypocotyl length in the dark or in the transition to light compared with the control (see Supplemental Figure 11 online). These results indicate that MIDA11 functions as a repressor of hypocotyl elongation inhibition in the dark-to-light transition (Figure 5B), with a more prominent role after 3 h of light exposure, consistent with the observed phenotype of *mida11* in the dark (Figures 2, 4C, and 4D) and with the induction of MIDA11 in response to Rc (Figure 5A).

Altogether, our data suggest that the apparent contradiction of having PIF3 in the dark induce MIDA10 and MIDA1, a negative and a positive regulator of photomorphogenesis, respectively, and repress MIDA9 and MIDA11, both negative regulators, can be explained if one considers the early or late light responsiveness of these MIDA factors as well as their time of action in the dark-to-light transition. A summary of the above data regarding light responsiveness of the four MIDA genes and light phenotypes of their *mida* mutants, integrated with the results of our previous analysis of the expression of each gene in seedlings grown in the dark, is shown in Supplemental Table 1 online. For MIDA10, these data suggest a simple scenario, where early PIF3/phy-mediated light repression allows the rapid removal of a dark hook repressor, which facilitates the rapid hook unfolding that occurs during the initiation of deetiolation. Likewise, for MIDA1, the early PIF3/phy-mediated induction upon exposure of the

seedling to light allows for the rapid accumulation of a cotyledon separation inducer, which contributes to cotyledon separation during the initiation of deetiolation. Given that *mida1-OX* is an overexpressor mutant line (Figure 4F), the high levels of MIDA1 in this mutant in the dark compared with those of the wild type possibly mimic the levels reached in the wild type after light induction, and *mida1-OX* mutant seedlings display a phenotype of separated cotyledons in the absence of light. Also, the transient nature of its light induction suggests that after a few hours of illumination, the expression of MIDA1 is repressed to stop its cotyledon separation action. MIDA10 and MIDA1 might therefore participate in the dark and/or the early (1 to 3 h of Rc) steps of deetiolation induction of hook unfolding and cotyledon separation. By contrast, MIDA9 and MIDA11 are both repressors of photomorphogenesis (specifically of hook opening and of the inhibition of hypocotyl elongation, respectively) that are late light-induced (after 3 to 6 h of Rc) and seem to function not only in the dark but also during deetiolation, once the seedling has been exposed to light (Figure 5B).

Interestingly, our unexpected finding that the seedlings possess photomorphogenesis repressors (MIDA9 and MIDA11) that are late light-induced (after 3 to 6 h of Rc), is consistent with the existence of a PIF3/phy-mediated regulatory response in the deetiolation process that might function after deetiolation is initiated. This late (after 3 to 6 h of Rc) regulatory response could represent a mechanism for the seedling to moderate the rapid initial response.

### PIF3 Together with Other PIFs Prevent an Exaggerated Inhibition of Hypocotyl Elongation and Cotyledon Separation in Response to Light

PIFs have been previously reported to be negative regulators of hypocotyl elongation in Rc conditions, with PIF-deficient mutants showing hypersensitivity to Rc (Huq and Quail, 2002; Kim et al., 2003; Fujimori et al., 2004; Monte et al., 2004; Khanna et al., 2007; de Lucas et al., 2008; Leivar et al., 2008a). However, a possible role for the PIFs in the regulation of hypocotyl inhibition in the initial dark-to-light transition has not been explored. We examined the inhibition of hypocotyl elongation in *pif3* and *pif3 pif4 pif5* mutants. Figure 6A shows that dark-grown wild-type seedlings respond to the light trigger by inhibiting hypocotyl elongation and reducing the hypocotyl growth rate. Red light has been shown to induce inhibition of hypocotyl growth in dark-grown seedlings exposed to Rc during the first 3 h of illumination, effectively slowing down the hypocotyl growth rate (Parks and Spalding, 1999). This inhibition begins to decrease after 3 h of irradiation, and seedlings in red light keep growing at a reduced speed compared with seedlings maintained in darkness (Parks and Spalding, 1999). In accordance, our results show that the wild-type hypocotyls elongate from 3.8 mm to 8 mm 24 h after exposure to Rc, whereas seedlings kept in the dark maintain a more constant hypocotyl growth speed and reach 9.6 mm (Figure 6A). Strikingly, *pif3 pif4 pif5* seedlings almost completely stop elongating after exposure to light (Figure 6A). This phenotype suggests that there is an exaggerated inhibition of hypocotyl elongation during deetiolation in the absence of PIF3, PIF4, and PIF5. *pif3 pif4 pif5* mutants maintained in the dark during this

**Figure 6.** PIF-Regulated Transcriptional Network.

- (A) to (C)** Dark-grown PIF-deficient seedlings exhibit an exaggerated response to Rc ( $8 \mu\text{mol}/\text{m}^2/\text{s}$ ).
- (A)** Time-course quantification of hypocotyl length of 2-d-old dark-grown Col-0 and *pif3 pif4 pif5* seedlings kept in the dark (dashed lines) or during the dark-to-light transition (solid lines) for 24 h. Data represent the mean and SE of at least 30 seedlings.
- (B)** Visual phenotype of 2-d-old, dark-grown Col-0, *pif3*, and *pif3 pif4 pif5* seedlings exposed to 0, 1, or 5 d of Rc.
- (C)** Time-course quantification of cotyledon separation of 2-d-old, dark-grown Col-0, *pif3*, and *pif3 pif4 pif5* seedlings during the transition to Rc light for 5 d. Data represent the mean and SE of at least 30 seedlings.
- (D)** Simplified schematic model depicting the branching in the signaling that PIF3 relays to regulate specific aspects of deetiolation, like cotyledon separation, hook opening, and hypocotyl inhibition through the MIDAs.
- (E) and (F)** Simplified schematic model depicting the PIF3-dependent *MIDA* transcriptional network that regulates seedling deetiolation in response to phy-mediated light signals. PIF3 acts constitutively in darkness as either a transcriptional repressor or activator, resulting in the regulation of *MIDA* gene expression. Phy-mediated, light-induced degradation of PIF3 triggers reversal of PIF3 action on *MIDA* genes that are early **(E)** or late **(F)** light-responsive. Early (1 h) light-responsive genes rapidly initiate deetiolation in response to phy-mediated PIF degradation **(E)**, acting either as light-induced inducers (such as *MIDA1*) or light-repressed repressors (such as *MIDA10*) of deetiolation. By contrast, late (3 to 6 h) light-responsive genes **(F)** have the opposite function to slow down and fine-tune the initial response and optimize seedling deetiolation, as exemplified here by *MIDA9* and *MIDA11*.

period kept growing at the same rate (Figure 6A). Single *pif3* mutants exhibit only a marginal phenotype after exposure to Rc (see Supplemental Figure 12A online), suggesting that PIF3 might be redundant to other PIFs, including PIF4 and PIF5, in the regulation of hypocotyl elongation during the dark-to-light transition, as has previously been described for skotomorphogenesis in the dark (Bae and Choi, 2008; Leivar et al., 2008b).

PIF-deficient mutants have also been shown to have more separated cotyledons during the dark-to-light transition, a phenotype that is partially established in the dark, and reach a maximum angle of  $180^\circ$  during the first 24 h of illumination (Leivar et al., 2008b). Closer examination of *pif3 pif4 pif5* mutant seedlings during extended Rc exposure after 2 d of dark growth

reveals a striking cotyledon overseparation in response to light. The cotyledons of the wild-type seedlings separate to  $\sim 100^\circ$  after 24 h of exposure to Rc (Figures 6B and 6C). This fast response is followed by a slower response over the next 3 d of growth in Rc, when cotyledons reach a maximum angle of  $185^\circ$  (i.e., perpendicular to the hypocotyl), effectively maintaining an optimum angle for light perception (Figures 6B and 6C). The cotyledons of the wild-type seedlings kept in darkness for this time period remain appressed (see Supplemental Figure 12B online). Compared with the wild-type seedlings, *pif3 pif4 pif5* mutants exhibit partially separated cotyledons in the dark ( $60^\circ$ ), as previously described (Leivar et al., 2008b), and have a fast initial response during the first 24 h of light exposure that is similar

in magnitude to the wild-type response, reaching a cotyledon separation of 200° (Figures 6B and 6C). However, in contrast with the wild type, this fast response is maintained over the next 3 d of growth in Rc to reach a cotyledon separation of 310° (Figures 6B and 6C). The cotyledons of *pif3 pif4 pif5* mutants maintained in the dark during this time period open from 60° to 150° (see Supplemental Figure 12B online), a difference that was greatly amplified by light (Figures 6B and 6C). The response of *pif3* (which reaches a cotyledon angle of 240°) is also greater than the wild-type response (which reaches 185° of cotyledon aperture, as detailed above) (Figures 6B and 6C). These results indicate that, in the absence of PIF3, seedlings undergo exaggerated cotyledon separation in response to light, suggesting that PIF3 regulates the inhibition of cotyledon separation. A detailed examination of *pif3 pif4 pif5* also shows an overresponse during the first 24 h of exposure to light (see Supplemental Figure 12C online), as occurs to a lesser extent in *pif3* (see Supplemental Figure 12C online) (Leivar et al., 2008b). Together, our data indicate that the PIF proteins have an important role in preventing the overseparation of cotyledons during seedling establishment, with PIF3 acting in a partially redundant manner to PIF4 and PIF5.

## DISCUSSION

Despite much progress in recent years, our understanding of how PIFs function during seedling deetiolation is incomplete, partly because the role of PIF target genes remains largely unknown. In this study, we have expanded on the morphological and molecular characterization of the *pif3* mutant to identify bona fide target genes of PIF3 action in the dark. Functional profiling of the identified PIF3-target genes suggests branching of the signaling that PIF3 relays to regulate specific facets of deetiolation, such as hypocotyl elongation, cotyledon separation, and hook opening. The regulation of these downstream organ-specific targets by light is consistent with a model of PIF3/MIDA action that enables an initial fast response to the light and subsequently prevents overresponses to the light trigger.

### Branching of PIF3 Signaling through Four Novel PIF3-Regulated MIDA Factors to Regulate Different Facets of Seedling Development in the Dark

Our analysis of PIF3-regulated gene expression in etiolated seedlings shows that, in darkness, PIF3 regulates 82 genes (Figure 1; see Supplemental Figure 1 online). With the objective of determining to what extent these PIF3-regulated genes are necessary for transducing the PIF3 signal during seedling deetiolation, we selected 13 PIF3 target genes (*MIDA1* to *MIDA13*) based on their predicted function for systematic analysis of mutant phenotypes (Table 1). Our phenotypic data analysis determined that four of the *MIDA* genes mutagenized in this study (*MIDA9*, *MIDA10*, *MIDA11*, and *MIDA1*) exhibit significant perturbation of the etiolated phenotypes and represent novel regulators of seedling development in the dark (Figure 2). Expression analyses by qRT-PCR and microarray suggest that these *MIDA* factors are likely targeted by other PIFs in addition to PIF3 (see Supplemental Figure 6 and Sup-

plemental Analysis 3 online), because their response is more robust in *pifq* than in *pif3*.

Because this study systematically characterizes the role of PIF3-regulated genes in the dark, it was of interest to determine whether the *mida* mutants would be affected in the complete seedling etiolation development, and/or whether we would detect organ-specific actions. Based on the phenotypes of these four *mida* mutants, our data indicate that there is branching in the regulation of seedling deetiolation that PIF3 relays. Indeed, *MIDA9* and *MIDA10* are necessary for hook maintenance in the dark, whereas *MIDA11* regulates hypocotyl elongation, and *MIDA1* is involved in cotyledon separation (Figures 2, 3, and 4), indicating that these *MIDA* factors have organ-specific activity. One of these *MIDA* factors, *MIDA10*, is a negative regulator of hook unfolding (Figures 2 and 3). *MIDA10* encodes BBX23, a previously uncharacterized member of the *Arabidopsis* B-box family of transcription factors. Within this family, BBX23 forms part of a clade of eight members, four of which (BBX21, BBX22, BBX24, and BBX25) were previously implicated in light signaling (Khanna et al., 2006; Datta et al., 2007; Indorf et al., 2007) and possibly form a large complex with COP1 (Datta et al., 2008). BBX23 might also interact directly or indirectly with COP1. *MIDA9*, the second *MIDA* gene that participates in the regulation of hook maintenance as a negative regulator of hook unfolding, encodes a type 2C-phosphatase (PP2C) (Figures 2 and 3). Out of the 76 PP2Cs identified in *Arabidopsis* (Schweighofer et al., 2004), *MIDA9* is the only PP2C shown to be involved in seedling deetiolation. The third gene found to make a significant contribution to seedling deetiolation, specifically in the regulation of hypocotyl elongation, is *MIDA11* (Figures 2 and 4), a gene that encodes a MAP kinase. *MIDA11* has been recently reported to regulate auxin signaling in *Arabidopsis* roots (Lee et al., 2009). Interestingly, auxin participates in the induction of fast hypocotyl growth in dark-grown seedlings (De Grauwe et al., 2005). Also related to hormone signaling, the fourth gene, *MIDA1*, encodes HSD1, a hydroxysteroid dehydrogenase proposed to participate in the biosynthesis of BRs (Li et al., 2007). Adult *Arabidopsis* plants constitutively overexpressing HSD1 constitutively express BR response genes and display phenotypes similar to those of plants overproducing BR or the BR receptor, BRI1; that is, greater growth with increased branching and longer roots (Li et al., 2007). Based on the phenotype of BR-deficient mutants, BRs have also been shown to participate in seedling deetiolation (Li et al., 1996; Szekeres et al., 1996). Although more investigation is required, both *MIDA11* and *MIDA1* might contribute to the interplay between light and hormone signaling pathways, an integration that is essential for the coordination of seedling development (Halliday, 2004; Alabadi and Blázquez, 2009; Lau and Deng, 2010). Altogether, our data indicate that PIF3 signaling branches at a point where *MIDA9*, *MIDA10*, *MIDA11*, and *MIDA1* regulate different organ-specific pathways that might involve COP1 and hormone biosynthesis and/or signaling to coordinate the deetiolation response (see model in Figure 6D). Branching of the PIF3 signal might be achieved through differential spatial expression patterns of these *MIDA* factors in specific tissues or organs. More detailed analyses are required to assess this possibility (Bou-Torrent et al., 2008).

Eight out of the 12 tested loci seem not to have a significant role in regulating the hypocotyl, cotyledon, or hook responses downstream of PIF3 in the dark (Figure 2). Possible explanations for this lack of phenotype include: First, the expression changes detected in *pif3* for these *MIDA* genes might be functionally insignificant for the etiolated seedling, and thus irrelevant for the *pif3* phenotype in the dark. Although most of these genes are also targets of PIFq (see Supplemental Figures 4 and 6 online) and their expression is more robustly affected in *pifq*, correlating with the stronger phenotype, this remains a possibility. Second, some of these *MIDA* genes might cause a detectable phenotype when mutated, but this phenotype is not strong enough and/or sustained for long enough along dark development to meet our cutoff requirements for a bona fide phenotype and thus was not considered further (e.g., *mida11* and *mida12* in hook opening) (Figure 2; see Supplemental Data Set 5 online). Third, these genes might be relevant for PIF3-imposed seedling deetiolation, but functional redundancy with other factors ensures that disruption of a single gene does not have any phenotypic relevance. Functional redundancy is the most common explanation for lack of apparent phenotype, and the PIFs themselves exemplify this possibility (Leivar et al., 2008b; Shin et al., 2009). For the *MIDA* genes that lack an apparent phenotype, a search of the *Arabidopsis* databases reveals that two (*MIDA7* and *MIDA8*) belong to gene families (to the *CBL-INTERACTING PROTEIN KINASE [CIPK]* and the *HSD* gene families, respectively), and that *MIDA8* has another family member (*MIDA1*) that is also a PIF3 target (Gene Set 2) (Table 1). An assessment of possible functional redundancy in these cases would require the construction of higher-order combinations of the candidate genes. Finally, another possibility is that these *MIDA* factors might specifically affect deetiolation aspects that were not scored in our phenotypic analysis, such as chloroplast development or cotyledon expansion. More detailed analyses are needed to determine why mutation of each of these *MIDA* genes does not result in a dark seedling phenotype.

Given that PIF3 binds specifically to the G-box motif (Martínez-García et al., 2000; Shin et al., 2007), we inspected the 3-kb region upstream of the transcription start site of *MIDA* genes for the presence of the G-box motif CACGTG (See Methods) to determine whether functionally relevant *MIDAs* could potentially be directly regulated by PIF3. We found that of the four *MIDA* genes displaying a phenotype in the dark when mutated (*MIDA9*, *MIDA10*, *MIDA11*, and *MIDA1*) (Figures 3 and 4), only *MIDA9* had a G-box in its promoter sequence. Three other *MIDA* genes (*MIDA6*, *MIDA8*, and *MIDA13*) had G-boxes in their promoter sequences, but their mutants did not display a phenotype when examined in the dark (Figure 2), suggesting a lack of correlation in *MIDA* genes between the presence of a G-box in their promoters and the phenotypic effect in the dark when mutated.

### Light Regulation of PIF3 Signaling through the Organ-Specific *MIDA* Factors

Our data indicate that two of the *mida* mutants (*mida9* and *mida10*) exhibiting a similar phenotype in the dark (failure to maintain an apical hook) correspond to genes that are both negative regulators of hook opening and are regulated by PIF3 in

opposite directions in the dark: whereas *MIDA9* is repressed, *MIDA10* is induced by PIF3 (Figure 3, Table 1). This finding prompted us to hypothesize that this apparent contradiction might reflect the scenario played out once the wild-type etiolated seedling is exposed to light and PIF3 is degraded, rather than being a dark-specific phenomenon. A combination of Rc microarray data and detailed time courses analyzed by qRT-PCR (Figure 5; see Supplemental Figures 8 and 9 online) indicated that *MIDA10* is an early (1 h) light-repressed gene whose repression is maintained after 18 h of Rc, whereas *MIDA1* is early and transiently induced by light, and *MIDA9* and *MIDA11* show late light-induction after 3 to 6 h of Rc illumination (Figure 5; see Supplemental Figures 8 and 9 online). Our data show that these *MIDA* genes do not respond to light exposure simultaneously but rather in at least two temporally separated responses: one early (after 1 to 3 h of Rc) (*MIDA10* and *MIDA1*), and one late (after 3 to 6 h of Rc) (*MIDA9* and *MIDA11*). These data suggest that these *MIDA* factors that have a role in organ-specific seedling deetiolation might exert their function at different times, with those induced by light (*MIDA9*, *MIDA11*, and *MIDA1*) possibly extending their action beyond the dark period. Indeed, when we examined these *mida* mutants phenotypically in dark-to-red time courses, we detected that they also have defects in the deetiolation response upon Rc exposure (Figure 5B). Our data indicate that *MIDA11* is a negative regulator of hypocotyl elongation inhibition both in the dark and upon illumination, *MIDA1* is a positive regulator of cotyledon separation in the dark and during the first hours of red light illumination, and *MIDA10* is a negative regulator of hook opening in the dark and in the early initiation of deetiolation. Furthermore, *MIDA9* is a negative regulator of hook opening in the dark and during deetiolation, with a role that might be more prominent after 6 h of irradiation.

PIFs have been described as repressors of photomorphogenesis in the dark (Bae and Choi, 2008; Leivar et al., 2008b). The current model proposes that PIF action in the dark is exerted through the regulation of the expression of hundreds of genes by inducing presumptive repressors and by repressing presumptive inducers of photomorphogenesis, a function that is reversed by phy-induced PIF-degradation in response to light (Leivar et al., 2009; Shin et al., 2009). The functional profiling of PIF3-induced and -repressed genes presented here suggests an additional layer of complexity by which the PIF-phy system regulates deetiolation. Our data indicate that, in the dark, PIF3 both up- and downregulates inducers as well as repressors of photomorphogenesis, inducing the repressor *MIDA10* and the inducer *MIDA1*, and repressing the repressors *MIDA9* and *MIDA11* (see Supplemental Table 1 online). A model for the phy/PIF/*MIDA* mode of action is shown in Figures 6E and 6F. Given the partially deetiolated phenotype of *pif3*- in the dark, these findings suggest that the PIF system maintains a balance of inducer and repressor factors in the dark, with a preponderance of photomorphogenesis repressor activity, to maintain the etiolated state of the seedling in darkness. This action would be rapidly reversed upon light-induced degradation of the PIFs, shifting this balance to a dominance of photomorphogenesis inducer activity to initiate deetiolation. Accordingly, during this early and rapid initiation of seedling deetiolation (after 1 to 3 h of Rc), our data show that the repressor *MIDA10* is repressed in response to light, whereas the

inducer MIDA1 is induced by light. Furthermore, some of these MIDA regulators (MIDA9 and MIDA11) are late light-induced (after 3 to 6 h of Rc) (Figure 5A), suggesting that they act beyond the dark state and beyond the initial deetiolation trigger. Given that MIDA9 and MIDA11 correspond to repressors of photomorphogenesis (Figures 2, 3, and 5B) and that their induction takes place simultaneously with the late light repression of early inducers, such as MIDA1 (Figure 5A), our findings suggest that, after a few hours of illumination, once deetiolation is underway, the seedling again accumulates repressors of photomorphogenesis. These results are consistent with a scenario in which PIF3 regulates not only the rapid initial deetiolation trigger but also a subsequent counteractive response to prevent overresponses to light. In accordance, our data reveal that *pif3* and, to a greater extent, *pif3 pif4 pif5* are affected in the moderation of the initial light trigger and exhibit exaggerated cotyledon separation and inhibition of hypocotyl elongation, effects that are apparent after 1 to 2 d of Rc for cotyledon separation or after a few hours of illumination for hypocotyl response (Figures 6A to 6C). These data suggest that PIF3, together with other PIFs, such as PIF4 and PIF5, signal beyond the initial light trigger and exert a late repressive action to avoid excessive cotyledon separation and hypocotyl elongation inhibition. This late action is in apparent discrepancy with the rapid degradation of PIF3 in the light (Bauer et al., 2004; Monte et al., 2004; Park et al., 2004; Al-Sady et al., 2006). The late action of PIF3 could occur indirectly through secondary downstream targets and/or be exerted by the remaining light-stable pool of PIF3 (~10% of the levels in the dark) after the initial degradation (Monte et al., 2004). This late PIF-mediated process seems likely to be fundamental for seedling survival during the initial exposure to light. For example, it ensures that the cotyledons separate rapidly and are maintained at an angle parallel to the soil, optimal for light perception (Figures 6B and 6C). The existence of mechanisms that prevent overresponsiveness to the initial stimulus is an emerging theme in the regulation of responses to light, as has been described in the shade avoidance syndrome (Sessa et al., 2005) and, more recently, in responses to FR light (Li et al., 2010).

In conclusion, this study identifies downstream branching of PIF3 signaling as a means to optimize seedling deetiolation. We show that regulation of novel MIDA factors by the phy/PIF system enables the seedling to repress photomorphogenesis in the dark and respond optimally to light by regulating the abundance of positive and negative regulators of specific facets of photomorphogenesis, such as hypocotyl elongation, hook unfolding, and cotyledon separation. It will be of interest to determine how this regulation is achieved in the seedling by identifying additional PIF3-regulated components and the direct targets of PIF3 that orchestrate these organ-specific responses.

## METHODS

### Plant Material, Seedling Growth, and Measurements

T-DNA lines in the ecotype Col-0 background were identified by searching the Salk Institute Genomic Analysis Laboratory database (Alonso et al., 2003) (<http://signal.salk.edu/cgi-bin/tdnaexpress>). When possible, insertions within the promoter or in the 5'-region of the gene were favored

as specified in Table 1. Homozygous T-DNA insertion lines and wild-type siblings were identified using PCR with T-DNA- and gene-specific primers designed using the iSct Primers tool available in the Salk Institute Genomic Analysis Laboratory website. The primer sequences for each line can be found in Supplemental Table 2 online. For phenotypic analyses, two sibling mutant lines were compared with a wild-type sibling line and with the Col-0 controls. Wild-type and mutant seedlings were plated on GM medium without Suc as previously described (Monte et al., 2003). Seedlings were then stratified for 4 d at 4°C in darkness, induced to germinate with 3 h of WLC, and then placed in the dark for the indicated period of time. For hypocotyl, hook, and cotyledon measurements, seedlings grown for 2, 3, and 4 d were arranged horizontally on a plate and photographed using a digital camera (Nikon D80). Measurements were performed using NIH Image software (Image J, National Institutes of Health), as described before (Leivar et al., 2008b). Hook angle was measured as the angle between the hypocotyl and an imaginary line between the cotyledons, and cotyledon angle was measured as the angle between the central axes of the two cotyledons. Measurements of at least 30 seedlings for each mutant line were tested using Excel (Microsoft) for statistically significant differences with the wild-type sibling controls. P values were determined by Student's *t* test (equal variance, two-tailed distribution), and values below  $P = 0.05$  were considered statistically significant for differences in hypocotyl length, hook angle, or cotyledon angle between the wild-type and mutant lines. Mean values were used to calculate relative differences between the mutant and wild-type sibling, and phenotypes were expressed relative to the wild-type sibling value set at unity. Representative lines for each mutant were used in Figure 2 and Supplemental Data Set 5 online, whereas Figures 3 and 4 show all lines used in the analysis of the selected genes. For the red light treatments shown in Figure 5, seedlings were transferred after dark growth to Rc (8  $\mu\text{mol}/\text{m}^2/\text{s}$ ) for the time indicated. For the cotyledon separation experiment shown in Figure 6, cotyledon angle was calculated as specified above except for angles exceeding 180°, where outer angles were measured and corrections applied, because Image J only measures angles between 0° and 180°. For the FR treatments shown in Supplemental Figure 10 online, seedlings were transferred after 21 h of dark growth to continuous FR (0.01  $\mu\text{mol}/\text{m}^2/\text{s}$ ) at 21°C for 3 d. Control seedlings were kept in darkness. The DEX treatment shown in Figure 4 was performed using DEX (Sigma-Aldrich) diluted in HPLC-grade ethanol (minimum 98%) at a concentration of 5  $\mu\text{M}$ .

### Microarray-Based Expression Profiling: Samples and Data Analysis

Samples for microarray experiments in the dark correspond to samples in Monte et al. (2004), with the exception of R18 h and D18 h, which were part of the same experiment but were not included in the original analysis. Briefly, three biological replicates of wild-type and *pif3-3* seedlings were grown separately in GM medium without Suc for 4 d (96 h) in the dark (D0 h time point) as previously described (Monte et al., 2003). For dark treatments, D0 h (D96 h) and D1 h (D97 h) samples were harvested 1 h apart and were used in this work to identify PIF3-regulated genes in the dark. For red light treatments, 4-d-old wild-type seedlings were transferred to Rc (8  $\mu\text{mol}/\text{m}^2/\text{s}$ ) at D0 h, and samples were collected after 1 h (R1 h) and 18 h (R18 h), together with controls at D1 h and D18 h. These red light-treated samples and their dark controls were used in this work to identify early (R1 h) and late (R18 h) red light-responsive genes.

Dark data analysis was performed using the Rosetta Resolver Gene Expression Analysis System, version 7.0 (Rosetta Biosoftware). A gene list of transcripts whose expression is significantly altered by the *PIF3* mutation in 4-d-old, dark-grown seedlings was calculated by performing a two-group, two-way, error-weighted, Benjamini-Hochberg false discovery rate error-corrected analysis of variance comparing D0 h and D1 h samples for the wild type and *pif3*, with a *P*-value cutoff of 0.05, resulting

in 1402 significant transcripts. This statistical significance test was combined with experimental consistency by further reducing the statistically significant transcript list to only those transcripts exhibiting an absolute FC of greater than 1.5-fold in both D0 h and D1 h conditions. This resulted in a nonredundant list of 122 transcripts (statistically and significantly different by an absolute FC of 1.5, SS1.5F). Next, a ratio error model (Weng et al., 2006) that reduced the transcript list to 82 HC PIF3 target genes in the dark (SS1.5F-HC) was applied.

To identify early and late red light-responsive genes, wild-type red (R1 h and R18 h) and wild-type dark samples (D1 h and D18 h) were analyzed at each time point using the Rosetta Resolver Gene Expression Analysis System, version 7.0 (Rosetta Biosoftware). A list of Rc-responsive transcripts was calculated by performing a ratio analysis applying a ratio error model cutoff of 0.05 (Weng et al., 2006) and an absolute FC of greater than twofold. These analyses resulted in 546 significant transcripts (statistically and significantly different by an absolute FC of 2; SS2F) for R1 h, and 2764 SS2F genes for R18 h.

### Gene Expression Analysis

For the RNA gel blot analyses in Figure 3, total RNA was isolated from 2-d-old, dark-grown seedlings using the RNeasy Plant Mini Kit (Qiagen), according to a previously described procedure (Monte et al., 2003). Gene-specific probes were amplified by PCR and labeled by random priming (Roche). Primer sequences can be found in Supplemental Table 2 online. Hybridization signal was detected with a Storm 860 Phosphor-Imager (Molecular Dynamics).

For qRT-PCR analysis, seedlings were grown in the dark for the indicated times (for Figure 4; see Supplemental Figures 2 and 6 online) or subsequently treated with red light ( $8 \mu\text{mol}/\text{m}^2/\text{s}$ ) for up to 12 h for the analysis shown in Figure 5B. qRT-PCR analysis was performed as described previously (Khanna et al., 2007) with variations. Briefly,  $10 \mu\text{g}$  of total RNA extracted using the RNeasy Plant Mini Kit (Qiagen) were treated with DNase (Ambion) according to the manufacturer's instructions. First-strand cDNA synthesis was performed using the SuperScript III reverse transcriptase (Invitrogen) and oligo dT as a primer (dT30). cDNA was then treated with RNase Out (Invitrogen) before 1:20 dilution with water, and  $20 \mu\text{L}$  was used for real-time PCR (Light Cycler 480; Roche) using SYBR Premix Ex Taq (Takara) and primers at a 300 nM concentration. Each PCR was repeated at least two times, and the mean expression values from these technical replicates were used for further calculations. Gene expression was measured from at least two biological replicates, and *PP2A* was used as a normalization control as described previously (Shin et al., 2007). Normalized gene expression is represented relative to the dark-grown wild-type set at unity. Primer sequences for qRT-PCR can be found in Supplemental Table 2 online.

### Promoter Analysis for Presence of G-Box Motifs

Promoter analysis was performed using the "Motif Analysis" tool available at The Arabidopsis Information Resource (<http://Arabidopsis.org/tools/bulk/motiffinder/index.jsp>) to look for the CACGTG G-box motif in the 3-kb region upstream of the start codon of each of the *MIDA* genes.

### Accession Numbers

The microarray data reported in this publication have been deposited in the National Center for Biotechnology Information Gene Expression Omnibus (GEO; <http://www.ncbi.nlm.nih.gov/geo/>) under the GEO Series accession number GSE30030. Sequence data can be found in the *Arabidopsis* Genome Initiative database under accession numbers AT5G50600 (*MIDA1/HSD1*), AT3G05730 (*MIDA2*), AT4G37300 (*MIDA3*), AT1G02470 (*MIDA4*), AT3G47250 (*MIDA5*), AT5G04340 (*MIDA6*), AT1G48260 (*MIDA7/CIPK17*), AT4G10020 (*MIDA8/HSD5*), AT5G02760

(*MIDA9*), AT4G10240 (*MIDA10/BBX23*), AT2G46070 (*MIDA11/MPK12*), AT1G05510 (*MIDA12*), AT5G45690 (*MIDA13*), and *PP2A* (AT1G13320).

### Supplemental Data

The following materials are available in the online version of this article.

**Supplemental Figure 1.** PIF3 Regulation of Gene Expression in the Dark.

**Supplemental Figure 2.** Distribution of PIF3-Regulated Genes among Functional Categories.

**Supplemental Figure 3.** qRT-PCR Validation of Microarray Data.

**Supplemental Figure 4.** Comparative Expression Analysis of PIF3 Function with Other PIF Factors in the Dark.

**Supplemental Figure 5.** Comparison of *pif3*-D SSTF-HC Genes versus *pifq*-D and *pif4pif5*-D.

**Supplemental Figure 6.** Expression of *MIDA* Genes in *pif3* and *pifq*.

**Supplemental Figure 7.** Characterization of *mida9-2*.

**Supplemental Figure 8.** Light-Responsiveness of PIF3-Regulated Genes in the Dark.

**Supplemental Figure 9.** Microarray Data Displaying the Mean Expression Level of *MIDA10*, *MIDA9*, *MIDA11*, and *MIDA1* after 1 h and 18 h of Rc Treatment.

**Supplemental Figure 10.** Hook Angle Phenotype Displayed by *mida9-1* in Continuous FR.

**Supplemental Figure 11.** Quantification of Hypocotyl Length Displayed by *mida11* in the Dark-to-Light Transition in the Absence of DEX.

**Supplemental Figure 12.** Quantification of Hypocotyl Length in *pif3* and Cotyledon Separation Angle in *pif3* and *pif3 pif4 pif5* after Dark-to-Light Transition.

**Supplemental Table 1.** Summary of *MIDA9*, *MIDA10*, *MIDA11*, and *MIDA1* Gene Regulation by PIF3 and by Red Light, as well as the Phenotype of Their Respective *Arabidopsis* Mutants.

**Supplemental Table 2.** Primer Sequences Used for PCR Amplification.

**Supplemental Analysis 1.** Definition of the PIF3-Regulated Transcriptome in the Dark.

**Supplemental Analysis 2.** Functional Classification of PIF3-Regulated Genes in the Dark.

**Supplemental Analysis 3.** Comparative Analysis of PIF3-, PIF4PIF5-, and PIFq-regulated Transcriptomes in the Dark.

**Supplemental Analysis 4.** Comparative Analysis of PIF3-Regulated Transcriptome in the Dark with Genes Displaying SSTF Alterations in the Wild Type after 1 h and 18 h of Red Light Treatment.

**Supplemental References 1.** The Supplemental References for Supplemental Analyses 1 to 4.

**Supplemental Data Set 1.** Expression Data and Statistical Analysis for the SS1.5F Genes at D0 h and D1 h Reported in Figure 1 and Supplemental Figure 1 online.

**Supplemental Data Set 2.** Expression Data and Statistical Analysis for the SS1.5F-HC Genes at D0 h and D1 h Reported in Figure 1 and Supplemental Figure 1 online.

**Supplemental Data Set 3.** List of SS1.5F Genes That Do Not Meet the Requirements to be Designated as SS1.5F-HC Genes as Reported in Supplemental Figure 1 online.

**Supplemental Data Set 4.** List of Class P3, P3/PQ, P3/P4P5, and P4P5/PQ Genes Reported in Supplemental Figure 4 online.

**Supplemental Data Set 5.** Primary Data and Statistical Analysis for *mida* Mutant Phenotypic Characterization Shown in Figure 2.

**Supplemental Data Set 6.** List of Early Light-Responsive Genes in Dark-Grown Wild-Type Seedlings after 1 h of Red Light Treatment (8  $\mu\text{mol}/\text{m}^2/\text{s}$ ) Reported in Supplemental Figure 8 online.

**Supplemental Data Set 7.** List of Late Light-Responsive Genes in Dark-Grown Wild-Type Seedlings after 18 h of Red Light Treatment (8  $\mu\text{mol}/\text{m}^2/\text{s}$ ) Reported in Supplemental Figure 8 online.

**Supplemental Data Set 8.** List of Induced Class 1 to 3 Genes (Ind-Class) and Repressed Class 1 to 4 Genes (Rep-Class) as Defined in Supplemental Figure 8 online.

## ACKNOWLEDGMENTS

We thank Adrian J. Cutler for AOHSD seeds (*mida1-OX*) (Li et al., 2007) and Brian E. Ellis for MPK12RNAi seeds (*mida11*) (Lee et al., 2009). SALK (Alonso et al., 2003) and SAIL T-DNA lines were obtained from Nottingham Arabidopsis Stock Centre. We thank Josep M. Casacuberta for helpful comments on the manuscript. This work was supported by a Junta para la Ampliación de Estudios predoctoral fellowship from Consejo Superior de Investigaciones Científicas to J.S. (JaePre\_08\_01049), by a “Comissionat per a Universitats i Recerca del Departament d’Innovació, Universitats i Empresa” fellowship of the Generalitat de Catalunya (Beatriu de Pinós program) and Marie Curie IRG PIRG06-GA-2009-256420 grant to P.L., and by Marie Curie IRG-046568, Spanish “Ministerio de Ciencia e Innovación” BIO2006-09254 and BIO2009-07675, and Generalitat de Catalunya 2009-SGR-206 grants to E.M.

## AUTHOR CONTRIBUTIONS

M.S., P.L., P.Q., and E.M. designed the research; M.S., G.M., N.G., J.S., J.T., and E.M. performed research. M.S. and E.M. analyzed data; and M.S., P.L., P.Q., and E.M. wrote the article.

Received June 19, 2011; revised September 7, 2011; accepted November 3, 2011; published November 22, 2011.

## REFERENCES

- Alabadi, D., and Blázquez, M.A. (2009). Molecular interactions between light and hormone signaling to control plant growth. *Plant Mol. Biol.* **69**: 409–417.
- Alonso, J.M., et al. (2003). Genome-wide insertional mutagenesis of *Arabidopsis thaliana*. *Science* **301**: 653–657.
- Al-Sady, B., Ni, W., Kircher, S., Schäfer, E., and Quail, P.H. (2006). Photoactivated phytochrome induces rapid PIF3 phosphorylation prior to proteasome-mediated degradation. *Mol. Cell* **23**: 439–446.
- Bae, G., and Choi, G. (2008). Decoding of light signals by plant phytochromes and their interacting proteins. *Annu. Rev. Plant Biol.* **59**: 281–311.
- Bauer, D., Viczián, A., Kircher, S., Nobis, T., Nitschke, R., Kunkel, T., Panigrahi, K.C.S., Adám, E., Fejes, E., Schäfer, E., and Nagy, F. (2004). Constitutive photomorphogenesis 1 and multiple photoreceptors control degradation of phytochrome interacting factor 3, a transcription factor required for light signaling in *Arabidopsis*. *Plant Cell* **16**: 1433–1445.
- Bou-Torrent, J., Roig-Villanova, I., and Martínez-García, J.F. (2008). Light signaling: Back to space. *Trends Plant Sci.* **13**: 108–114.
- Castillon, A., Shen, H., and Huq, E. (2007). Phytochrome Interacting Factors: Central players in phytochrome-mediated light signaling networks. *Trends Plant Sci.* **12**: 514–521.
- Datta, S., Hettiarachchi, C., Johansson, H., and Holm, M. (2007). SALT TOLERANCE HOMOLOG2, a B-box protein in *Arabidopsis* that activates transcription and positively regulates light-mediated development. *Plant Cell* **19**: 3242–3255.
- Datta, S., Johansson, H., Hettiarachchi, C., Irigoyen, M.L., Desai, M., Rubio, V., and Holm, M. (2008). LZFI/SALT TOLERANCE HOMOLOG3, an *Arabidopsis* B-box protein involved in light-dependent development and gene expression, undergoes COP1-mediated ubiquitination. *Plant Cell* **20**: 2324–2338.
- De Grauwe, L., Vandenbussche, F., Tietz, O., Palme, K., and Van Der Straeten, D. (2005). Auxin, ethylene and brassinosteroids: Tripartite control of growth in the *Arabidopsis* hypocotyl. *Plant Cell Physiol.* **46**: 827–836.
- de Lucas, M., Davière, J.M., Rodríguez-Falcón, M., Pontin, M., Iglesias-Pedraz, J.M., Lorrain, S., Fankhauser, C., Blázquez, M.A., Titarenko, E., and Prat, S. (2008). A molecular framework for light and gibberellin control of cell elongation. *Nature* **451**: 480–484.
- Duek, P.D., and Fankhauser, C. (2005). bHLH class transcription factors take centre stage in phytochrome signalling. *Trends Plant Sci.* **10**: 51–54.
- Fujimori, T., Yamashino, T., Kato, T., and Mizuno, T. (2004). Circadian-controlled basic/helix-loop-helix factor, PIL6, implicated in light-signal transduction in *Arabidopsis thaliana*. *Plant Cell Physiol.* **45**: 10781086.
- Halliday, K.J. (2004). Plant hormones: The interplay of brassinosteroids and auxin. *Curr. Biol.* **14**: R1008–R1010.
- Huq, E., and Quail, P.H. (2002). PIF4, a phytochrome-interacting bHLH factor, functions as a negative regulator of phytochrome B signaling in *Arabidopsis*. *EMBO J.* **21**: 2441–2450.
- Huq, E., Al-Sady, B., Hudson, M., Kim, C., Apel, K., and Quail, P.H. (2004). Phytochrome-interacting factor 1 is a critical bHLH regulator of chlorophyll biosynthesis. *Science* **305**: 1937–1941.
- Indorf, M., Cordero, J., Neuhaus, G., and Rodríguez-Franco, M. (2007). Salt tolerance (STO), a stress-related protein, has a major role in light signalling. *Plant J.* **51**: 563–574.
- Jang, I.C., Henriques, R., Seo, H.S., Nagatani, A., and Chua, N.H. (2010). *Arabidopsis* PHYTOCHROME INTERACTING FACTOR proteins promote phytochrome B polyubiquitination by COP1 E3 ligase in the nucleus. *Plant Cell* **22**: 2370–2383.
- Jiao, Y., Lau, O.S., and Deng, X.W. (2007). Light-regulated transcriptional networks in higher plants. *Nat. Rev. Genet.* **8**: 217–230.
- Josse, E.M., and Halliday, K.J. (2008). Skotomorphogenesis: The dark side of light signalling. *Curr. Biol.* **18**: R1144–R1146.
- Khanna, R., Kronmiller, B., Maszle, D.R., Coupland, G., Holm, M., Mizuno, T., and Wu, S.H. (2009). The *Arabidopsis* B-box zinc finger family. *Plant Cell* **21**: 3416–3420.
- Khanna, R., Shen, Y., Marion, C.M., Tsuchisaka, A., Theologis, A., Schäfer, E., and Quail, P.H. (2007). The basic helix-loop-helix transcription factor PIF5 acts on ethylene biosynthesis and phytochrome signaling by distinct mechanisms. *Plant Cell* **19**: 3915–3929.
- Khanna, R., Shen, Y., Toledo-Ortiz, G., Kikis, E.A., Johannesson, H., Hwang, Y.S., and Quail, P.H. (2006). Functional profiling reveals that only a small number of phytochrome-regulated early-response genes in *Arabidopsis* are necessary for optimal deetiolation. *Plant Cell* **18**: 2157–2171.
- Kim, J.Y., Yi, H.K., Choi, G., Shin, B., Song, P.S., and Choi, G.S. (2003). Functional characterization of phytochrome interacting factor 3 in phytochrome-mediated light signal transduction. *Plant Cell* **15**: 2399–2407.
- Lau, O.S., and Deng, X.W. (2010). Plant hormone signaling lightens up: Integrators of light and hormones. *Curr. Opin. Plant Biol.* **13**: 571–577.
- Lee, J.S., Wang, S., Sritubtim, S., Chen, J.G., and Ellis, B.E. (2009). *Arabidopsis* mitogen-activated protein kinase MPK12 interacts with

- the MAPK phosphatase IBR5 and regulates auxin signaling. *Plant J.* **57**: 975–985.
- Leivar, P., and Quail, P.H.** (2011). PIFs: Pivotal components in a cellular signaling hub. *Trends Plant Sci.* **16**: 19–28.
- Leivar, P., Tepperman, J.M., Monte, E., Calderon, R.H., Liu, T.L., and Quail, P.H.** (2009). Definition of early transcriptional circuitry involved in light-induced reversal of PIF-imposed repression of photomorphogenesis in young *Arabidopsis* seedlings. *Plant Cell* **21**: 3535–3553.
- Leivar, P., Monte, E., Al-Sady, B., Carle, C., Storer, A., Alonso, J.M., Ecker, J.R., and Quail, P.H.** (2008a). The *Arabidopsis* phytochrome-interacting factor PIF7, together with PIF3 and PIF4, regulates responses to prolonged red light by modulating phyB levels. *Plant Cell* **20**: 337–352.
- Leivar, P., Monte, E., Oka, Y., Liu, T., Carle, C., Castillon, A., Huq, E., and Quail, P.H.** (2008b). Multiple phytochrome-interacting bHLH transcription factors repress premature seedling photomorphogenesis in darkness. *Curr. Biol.* **18**: 1815–1823.
- Li, F., Asami, T., Wu, X., Tsang, E.W., and Cutler, A.J.** (2007). A putative hydroxysteroid dehydrogenase involved in regulating plant growth and development. *Plant Physiol.* **145**: 87–97.
- Li, J., Nagpal, P., Vitart, V., McMorris, T.C., and Chory, J.** (1996). A role for brassinosteroids in light-dependent development of *Arabidopsis*. *Science* **272**: 398–401.
- Li, J., Li, G., Gao, S., Martinez, C., He, G., Zhou, Z., Huang, X., Lee, J.H., Zhang, H., Shen, Y., Wang, H., and Deng, X.W.** (2010). *Arabidopsis* transcription factor ELONGATED HYPOCOTYL5 plays a role in the feedback regulation of phytochrome A signaling. *Plant Cell* **22**: 3634–3649.
- Lorrain, S., Trevisan, M., Pradervand, S., and Fankhauser, C.** (2009). Phytochrome interacting factors 4 and 5 redundantly limit seedling de-etiolation in continuous far-red light. *Plant J.* **60**: 449–461.
- Lorrain, S., Allen, T., Duek, P.D., Whitelam, G.C., and Fankhauser, C.** (2008). Phytochrome-mediated inhibition of shade avoidance involves degradation of growth-promoting bHLH transcription factors. *Plant J.* **53**: 312–323.
- Martínez-García, J.F., Huq, E., and Quail, P.H.** (2000). Direct targeting of light signals to a promoter element-bound transcription factor. *Science* **288**: 859–863.
- Monte, E., Al-Sady, B., Leivar, P., and Quail, P.H.** (2007). Out of the dark: How the PIFs are unmasking a dual temporal mechanism of phytochrome signalling. *J. Exp. Bot.* **58**: 3125–3133.
- Monte, E., Alonso, J.M., Ecker, J.R., Zhang, Y., Li, X., Young, J., Austin-Phillips, S., and Quail, P.H.** (2003). Isolation and characterization of phyC mutants in *Arabidopsis* reveals complex crosstalk between phytochrome signaling pathways. *Plant Cell* **15**: 1962–1980.
- Monte, E., Tepperman, J.M., Al-Sady, B., Kaczorowski, K.A., Alonso, J.M., Ecker, J.R., Li, X., Zhang, Y.L., and Quail, P.H.** (2004). The phytochrome-interacting transcription factor, PIF3, acts early, selectively, and positively in light-induced chloroplast development. *Proc. Natl. Acad. Sci. USA* **101**: 16091–16098.
- Moon, J., Zhu, L., Shen, H., and Huq, E.** (2008). PIF1 directly and indirectly regulates chlorophyll biosynthesis to optimize the greening process in *Arabidopsis*. *Proc. Natl. Acad. Sci. USA* **105**: 9433–9438.
- Nagatani, A.** (2004). Light-regulated nuclear localization of phytochromes. *Curr. Opin. Plant Biol.* **7**: 708–711.
- Nozue, K., Covington, M.F., Duek, P.D., Lorrain, S., Fankhauser, C., Harmer, S.L., and Maloof, J.N.** (2007). Rhythmic growth explained by coincidence between internal and external cues. *Nature* **448**: 358–361.
- Oh, E., Yamaguchi, S., Kamiya, Y., Bae, G., Chung, W.I., and Choi, G.** (2006). Light activates the degradation of PIL5 protein to promote seed germination through gibberellin in *Arabidopsis*. *Plant J.* **47**: 124–139.
- Parks, B.M., and Spalding, E.P.** (1999). Sequential and coordinated action of phytochromes A and B during *Arabidopsis* stem growth revealed by kinetic analysis. *Proc. Natl. Acad. Sci. USA* **96**: 14142–14146.
- Park, E., Kim, J., Lee, Y., Shin, J., Oh, E., Chung, W.I., Liu, J.R., and Choi, G.** (2004). Degradation of phytochrome interacting factor 3 in phytochrome-mediated light signaling. *Plant Cell Physiol.* **45**: 968–975.
- Quail, P.H.** (2002). Phytochrome photosensory signalling networks. *Nat. Rev. Mol. Cell Biol.* **3**: 85–93.
- Quail, P.H.** (2010). Phytochromes. *Curr. Biol.* **20**: R504–R507.
- Rockwell, N.C., Su, Y.S., and Lagarias, J.C.** (2006). Phytochrome structure and signaling mechanisms. *Annu. Rev. Plant Biol.* **57**: 837–858.
- Schäfer, E., and Nagy, F.** (2006). Photomorphogenesis in Plants and Bacteria. (Dordrecht, The Netherlands: Springer).
- Schweighofer, A., Hirt, H., and Meskiene, I.** (2004). Plant PP2C phosphatases: Emerging functions in stress signaling. *Trends Plant Sci.* **9**: 236–243.
- Sessa, G., Carabelli, M., Sassi, M., Ciolfi, A., Possenti, M., Mitterpergher, F., Becker, J., Morelli, G., and Ruberti, I.** (2005). A dynamic balance between gene activation and repression regulates the shade avoidance response in *Arabidopsis*. *Genes Dev.* **19**: 2811–2815.
- Shen, H., Moon, J., and Huq, E.** (2005). PIF1 is regulated by light-mediated degradation through the ubiquitin-26S proteasome pathway to optimize photomorphogenesis of seedlings in *Arabidopsis*. *Plant J.* **44**: 1023–1035.
- Shen, Y., Khanna, R., Carle, C.M., and Quail, P.H.** (2007). Phytochrome induces rapid PIF5 phosphorylation and degradation in response to red-light activation. *Plant Physiol.* **145**: 1043–1051.
- Shen, H., Zhu, L., Castillon, A., Majee, M., Downie, B., and Huq, E.** (2008). Light-induced phosphorylation and degradation of the negative regulator PHYTOCHROME-INTERACTING FACTOR1 from *Arabidopsis* depend upon its direct physical interactions with photoactivated phytochromes. *Plant Cell* **20**: 1586–1602.
- Shin, J., Park, E., and Choi, G.** (2007). PIF3 regulates anthocyanin biosynthesis in an HY5-dependent manner with both factors directly binding anthocyanin biosynthetic gene promoters in *Arabidopsis*. *Plant J.* **49**: 981–994.
- Shin, J., Kim, K., Kang, H., Zulfugarov, I.S., Bae, G., Lee, C.H., Lee, D., and Choi, G.** (2009). Phytochromes promote seedling light responses by inhibiting four negatively-acting phytochrome-interacting factors. *Proc. Natl. Acad. Sci. USA* **106**: 7660–7665.
- Stephenson, P.G., Fankhauser, C., and Terry, M.J.** (2009). PIF3 is a repressor of chloroplast development. *Proc. Natl. Acad. Sci. USA* **106**: 7654–7659.
- Szekeres, M., Németh, K., Koncz-Kálmán, Z., Mathur, J., Kauschmann, A., Altmann, T., Rédei, G.P., Nagy, F., Schell, J., and Koncz, C.** (1996). Brassinosteroids rescue the deficiency of CYP90, a cytochrome P450, controlling cell elongation and de-etiolation in *Arabidopsis*. *Cell* **85**: 171–182.
- Toledo-Ortiz, G., Huq, E., and Quail, P.H.** (2003). The *Arabidopsis* basic/helix-loop-helix transcription factor family. *Plant Cell* **15**: 1749–1770.
- Toledo-Ortiz, G., Huq, E., and Rodríguez-Concepción, M.** (2010). Direct regulation of phytoene synthase gene expression and carotenoid biosynthesis by phytochrome-interacting factors. *Proc. Natl. Acad. Sci. USA* **107**: 11626–11631.
- Weng, L., Dai, H., Zhan, Y., He, Y., Stepaniants, S.B., and Bassett, D.E.** (2006). Rosetta error model for gene expression analysis. *Bioinformatics* **22**: 1111–1121.
- Yamaguchi, R., Nakamura, M., Mochizuki, N., Kay, S.A., and Nagatani, A.** (1999). Light-dependent translocation of a phytochrome B-GFP fusion protein to the nucleus in transgenic *Arabidopsis*. *J. Cell Biol.* **145**: 437–445.

### **SUPPLEMENTAL ANALYSIS 1. Definition of the PIF3-regulated transcriptome in the dark.**

We applied an ANOVA approach using the Rosetta Resolver platform to look for genes whose expression was statistically different between the *pif3* mutant and the wild type (WT) at D0h and D1h dark time points (Supplemental Figure 1A and Methods). Each data set (D0h and D1h) included three biological replicates for the WT and three for *pif3-3* of 4-day-old dark-grown seedlings harvested one hour apart (Monte et al., 2004) (Supplemental Figure 1A and Methods). This analysis identified 1402 genes with a false discovery rate (FDR) set at 5%. To this analysis, we next applied a 1.5 fold-change (FC) cutoff that had to be met independently at both D0h and D1h time points, and rendered a gene set of 122 genes (Supplemental Figure 1A). As expected and confirming the validity of the analysis, this gene set included *PIF3*, which was removed from the list. The remaining 121 PIF3-regulated genes are statistically and significantly expressed differently and by 1.5 fold in *pif3* compared to the wild type (SS1.5F, Gene Set 1). See Supplemental Dataset 1 for the gene list containing the 121 SS1.5F genes. To further increase the confidence in identifying relevant downstream targets, we next applied to the SS1.5F gene set a Ratio Error model available in the Rosetta software (Weng et al., 2006) that reduced the gene list to 82 genes (Supplemental Figure 1A). We consider that these 82 genes correspond to high confidence (HC) PIF3 targets (SS1.5F-HC, Gene Set 2). See Supplemental Dataset 2 for the gene list containing the 82 SS1.5F-HC genes, and Supplemental Dataset 3 for the gene list containing the 39 SS1.5F genes that did not make the HC cut-off.

A distribution of the FC for all 82 genes is shown in Supplemental Figure 1B. Further classification of these genes in two categories according to their FC value (between 1.5-1.9 or greater than 1.9), shows a distribution where approximately half of the genes fall into each fold-change category (Supplemental Figure 1C and 1D).

### **SUPPLEMENTAL ANALYSIS 2. Functional classification of PIF3-regulated genes in the dark**

We classified the induced and repressed genes (Figure 1D) into eight broad functional categories according to their predicted or established function as annotated in The Arabidopsis Information Resource database (TAIR, [www.arabidopsis.org](http://www.arabidopsis.org)). The data show that in the repressed group, 66% of the annotated genes are predicted to encode

proteins involved in cellular metabolism and growth/development (Supplemental Figure 2). The group of hormone-related genes is also well represented (16% of the genes), whereas signaling, stress/defense, transport and transcription are only represented by a small number of genes. In contrast, the induced subset has a high percent (25%) of photosynthesis/chloroplast-related genes (Supplemental Figure 2). This is mainly due to the presence of several *CAB* genes that are upregulated in the mutant (See Supplemental Dataset 2). These genes are normally induced during deetiolation (Gilmartin et al., 1990), which indicates a degree of photomorphogenesis de-repression in *pif3* in the dark at the transcriptional level. Together, these results are consistent with the partial photomorphogenic phenotype of the *pif3* mutant in the dark (Figures 1A and 1B; Leivar et al., 2008; Shin et al., 2009; Stephenson et al., 2009), and suggest a correlation of the gene expression profile of *pif3* in the dark with its morphological phenotype.

### **SUPPLEMENTAL ANALYSIS 3. Comparative analysis of PIF3-, PIF4 PIF5- and PIFq-regulated transcriptomes in the dark.**

To begin to gain some insight into whether the PIF3-regulated transcriptome in the dark defined here (Figures 1C and 1D, and Supplemental Figure 1) is also targeted by other PIFs, we took advantage of previous genome-wide studies of *pif4 pif5* (Lorrain et al., 2009) and *pif1 pif3 pif4 pif5 (pifq)* (Leivar et al., 2009). Although this comparison has the limitation that the seedlings are of different age (4-d-old for *pif3*, 3-d-old for *pif4 pif5* and 2d-old for *pifq*), and growth protocols (pseudo-dark for *pif3* and *pif4 pif5*, and true-dark for *pifq*), and that the genes have been selected in each case using different methods (Leivar et al., 2009; Lorrain et al., 2009), we reasoned that it could be informative as a first approach into a possible functional redundancy of the PIFs on gene expression regulation in the dark given the established partial redundancy of PIF function in promoting skotomorphogenesis (Leivar et al., 2008; Shin et al., 2009; Stephenson et al., 2009).

The Venn diagram in Supplemental Figure 4A compares the differential genes in each genotype grown in the dark: Eighty-two genes displaying SS1.5F-HC alterations in *pif3* (*pif3*-D), 1028 genes displaying alterations in *pifq* (*pifq*-D) (Leivar et al., 2009), and 113 genes in *pif4 pif5* (*pif4pif5*-D) (Lorrain et al., 2009). The data show that 50 out of the 82 *pif3*-D genes (60.9%) are shared with *pifq*-D (Supplemental Figure 4A). We have designated these 50 genes as P3/PQ Class genes. A scatter plot of the log2

fold of these 50 genes in *pif3* and *pifq* shows the correlation in responsiveness between *pif3* and *pifq* for each gene, with a  $R^2$  coefficient of 0.7075, indicating a moderately high correlation between the genotypes (Supplemental Figure 4B, top panel). The results are similar when comparing only *pif3* SSTF genes with *pifq* (32 of the 82 SS1.5F-HC genes, 16 of the 50 P3/PQ genes) (see Supplemental Figure 5A), which discards a possible effect of the lower FC cutoff value of the PIF3 experiment in the overall results of the comparison with *pifq*. The associated trendline slope indicates that the fold-change expression in *pifq-D* relative to WT-D is higher compared to that of *pif3-D* relative to WT-D (Supplemental Figure 4B). Comparison of the mean FC shows that class P3/PQ genes have an average mean FC in *pif3-D* of 2.08, whereas the average mean FC in *pifq-D* is 15.08 (Supplemental Figure 4C). Altogether, the data suggest that, for P3/PQ-Class genes, PIF3 is not the only PIF factor responsible for the regulation of the expression in the WT, and additional PIF factors might be involved. qRT-PCR analysis of the expression of some selected P3/PQ genes in 2-d-old dark-grown seedlings (*AT3G05730*, *AT4G10020*, *AT5G02760*, and *AT5G16030*), together with controls selected from Leivar et al., 2009 (*AT2G46830* and *AT2G46970*) shows that the response with respect to the WT is more robust in the *pifq* mutant compared to *pif3* (Supplemental Figure 4D), confirming that PIF factors other than PIF3 participate in the regulation of their expression in the dark.

Conversely, the 32 P3-Class genes are *pif3-D* genes that are not shared with *pifq*. This finding is surprising given that *pifq* contains the *pif3* mutation. A possibility to explain this apparent discrepancy is that these genes were not SSTF for *pifq*. In this case, these genes could represent potential PIF3-specific genes with a FC lower than two in the *pifq* experiment. Although possible, it seems unlikely given that almost half of the genes in this P3 Class (16 genes) have a FC in *pif3-D* greater than two compared to WT-D (Supplemental Figure 4C), with a mean FC of 2.3. Alternatively, these differences could be explained by the differences in seedling age between *pif3* and *pifq* microarrays, a possibility raised by our observations that expression levels in the WT seedlings and FC difference in *pif3* mutants varied along dark development (See Supplemental Figure 3). To test for this, we checked the expression of two P3-Class genes (*AT1G48260* and *AT5G04340*) in 2-d- and 4-d-old dark-grown seedlings by qRT-PCR. Supplemental Figure 4E shows that, indeed, no difference in expression was detected in *pif3* and *pifq* mutants relative to the WT after 2 days of dark growth,

whereas the same genes show clear differential expression in 4-d-old *pif* mutant seedlings compared to WT. Again, data show that the response relative to the WT is substantially more robust in the *pifq* mutant compared to *pif3* (Supplemental Figure 4E). These results discard the possibility that these genes might correspond to PIF3-specific targets and suggest that P3-Class genes might also represent *pif3* genes shared with *pifq* after 4 d of dark growth.

In contrast, comparison of *pif3*-D with *pif4pif5*-D showed that only nine genes are in common (10.9% of the 82 *pif3* SS1.5F-HC genes). These nine genes were designated as P3/P4P5 Class genes and are also shared with *pifq* (Supplemental Figure 4A). A scatter plot of the log<sub>2</sub> fold of these nine genes in *pif3* and *pif4 pif5* showed absence of linear correlation in responsiveness, with a R<sup>2</sup> coefficient of 0.016 (Supplemental Figure 4B, middle panel). Similar data were obtained when taking only SSTF genes for *pif3* for comparison with *pif4 pif5* (32 of the 82 SS1.5F-HC genes, four of the nine P3/P4P5 genes) (see Supplemental Figure 5B), which discards a possible effect of the cutoff value in the overall results of this comparison. Although further analysis needs to be done, these results suggest that, in the presence of the other PIFs, PIF3 and PIF4/PIF5 might regulate different target genes in etiolated seedlings.

To complete the analysis, we also compared *pifq*-D and *pif4 pif5*-D (Supplemental Figure 4A). The data show that 84 *pif4 pif5*-D genes are in common with *pifq*-D (75% of *pif4 pif5*-D genes), and were designated as P4P5/PQ Class genes (Supplemental Figure 4A). A scatter plot of the log<sub>2</sub> fold of these 84 genes in *pif4 pif5* and *pifq* showed a high correlation in responsiveness between the genotypes, with a R<sup>2</sup> coefficient of 0.7618 (Supplemental Figure 4B, bottom panel). The associated trendline slope indicates that the FC expression in *pifq*-D relative to WT-D is higher compared to that of *pif4 pif5*-D relative to WT-D (Supplemental Figure 4B). Comparison of the mean FC shows that class P4P5/PQ genes have an average mean FC in *pif4 pif5*-D of 1.82, whereas the average mean FC in *pifq*-D is 6.298 (Supplemental Figure 4C). These results are similar to those obtained when comparing *pif3* with *pifq*, and likewise suggest that for P4P5/PQ-Class genes, PIF4 and PIF5 are not the only PIF factors responsible for regulating the expression in the WT, and additional PIF factors might be involved.

See Supplemental Dataset 4 for lists of the P3, P3/PQ, P3/P4P5, and P4P5/PQ genes. Altogether, in spite of the limitations of this analysis due to the heterogeneity of the data used (see above), the comparison of the PIF3-, PIF4/PIF5- and PIFq-regulated

transcriptomes was informative in at least two ways. First, the above comparative data found extensive overlap of the PIF3-regulated transcriptome with PIF<sub>q</sub>, and small overlap with PIF4/PIF5 (Supplemental Figure 4). This analysis also found that the magnitude of the effect on gene expression in *pifq* is much greater than the magnitude in *pif3* or *pif4 pif5* (Supplemental Figure 4). These data suggest that there is redundancy in the PIF-transcriptional network, and are in agreement with the proposed redundant action of the PIFs as repressors of seedling deetiolation in the dark, based on the mild phenotypes of simple *pif1*, *pif3*, *pif4* and *pif5* mutants in the dark (Figures 1A and 1B; Leivar et al., 2008; Shin et al., 2009; Stephenson et al., 2009), and with the stronger phenotypes of higher order *pif* mutant combinations (Leivar et al., 2008; Shin et al., 2009; Stephenson et al., 2009). Our conclusions are also in agreement with the proposed prominent role of PIF1 in the repression of photomorphogenesis in the dark in the absence of other PIFs based on the relatively mild phenotype of the *pif3 pif4 pif5* mutant in the dark compared to the *pif1 pif3 pif4 pif5* mutant (Leivar et al., 2008). Second, in contrast to the suggested redundancy in PIF transcriptional function, the small overlap identified between the PIF3- and PIF4/PIF5-regulated transcriptomes (Supplemental Figure 4) also suggests that there is some specialization in the network of genes targeted by PIF3 and PIF4/PIF5 at least in the presence of other PIFs like PIF1. Although differences in experimental conditions might to some extent contribute to this lack of overlap, this finding might reflect different DNA binding specificities or intrinsic properties between PIF3 and PIF4/PIF5. Consistent with this idea, our data also show that PIF3 regulates gene expression both positively and negatively (Figures 1C and 1D), whereas PIF4/PIF5 have been reported to act mainly as negative regulators in the dark (Lorrain et al., 2009).

We also compared our *pif3*-D data to additional microarray analyses that have been published recently on the *pifq* (Shin et al., 2009) and *pif1* (Moon et al., 2008) mutants grown in the dark, and a more limited analysis of photosynthetic genes in the *pif1*, *pif3* and *pif1 pif3* mutants (Stephenson et al., 2009). Although these arrays were not as informative as the ones used for the comparisons shown in Supplemental Figure 4 because of their reduced number of genes, the results obtained in the comparisons have confirmed the above conclusions:

For *pif1*, only tetrapyrrole pathway genes were reported and three were SS1.5F (Moon et al., 2008). These three genes are not shared with *pif3* or *pif4 pif5*, whereas

two of them are common with *pifq*. For the other gene that did not make the *pifq* SS2F list in the dark, the scenario could be similar to the Class-P3 genes discussed above.

For the *pifq* array published by Shin and colleagues (2009), 19 (22.6%) of the genes that we identified as SS1.5F-HC in our *pif3* array overlap with those identified by Shin et al. (2009), in contrast to the 60% shared with the *pifq* array published by Leivar et al. (2009). Likewise, only 45 genes (39.8%) are shared between *pif4 pif5* and the *pifq* genes identified by Shin et al. (2009), compared to 75% shared with the *pifq* array published by Leivar et al. (2009). This could partly be due to the lower number of genes identified by Shin et al. (2009) (331 SSTF genes) compared to Leivar et al. (2009) (1028 SSTF genes). Reasons for the discrepancy in the number of genes identified by each group have been previously discussed in detail by Leivar et al. (2009).

A comparison with the work by Stephenson et al. (2009) did not reveal any overlap between our *pif3*-D gene list and their three photosynthetic genes. This was expected, given that the authors reported two-fold or greater enhancement of expression of these genes only in 2-d and/or 3-d dark-grown *pif3*, whereas they did not detect any differences in 4-d dark-grown seedlings.

#### **SUPPLEMENTAL ANALYSIS 4. Comparative analysis of the PIF3-regulated transcriptome in the dark with genes displaying SSTF alterations in the WT after 1 h and after 18 h of red light (Rc) treatment.**

We compared the genes displaying SS1.5F-HC alterations in *pif3* after 4 d in darkness (*pif3*-D) with genes displaying SSTF alterations in the WT after 1 h Rc (WT-R1) and after 18 h Rc (WT-R18) (Supplemental Figure 8). The three-way Venn diagram of this comparison is shown in Supplemental Figure 8A. Ten out of the 82 *pif3*-D genes (12.1%) are early light responsive genes, whereas 54 (65.8%) are late. Eight of these genes are both early and late. Thus, 56 (67%) of the *pif3*-D genes are light responsive genes, with 3.6% being only early, 83.6% only late, and 14.5% both early and late. These results indicate that *pif3*-D genes responding to light after 4 d of dark growth are mostly genes responding to the Rc treatment later than 1 h after the onset of illumination.

Supplemental Figure 8B shows the same comparison as 8A, but with *pif3*-D genes divided into repressed (Rep) or induced (Ind) based on the direction of their response

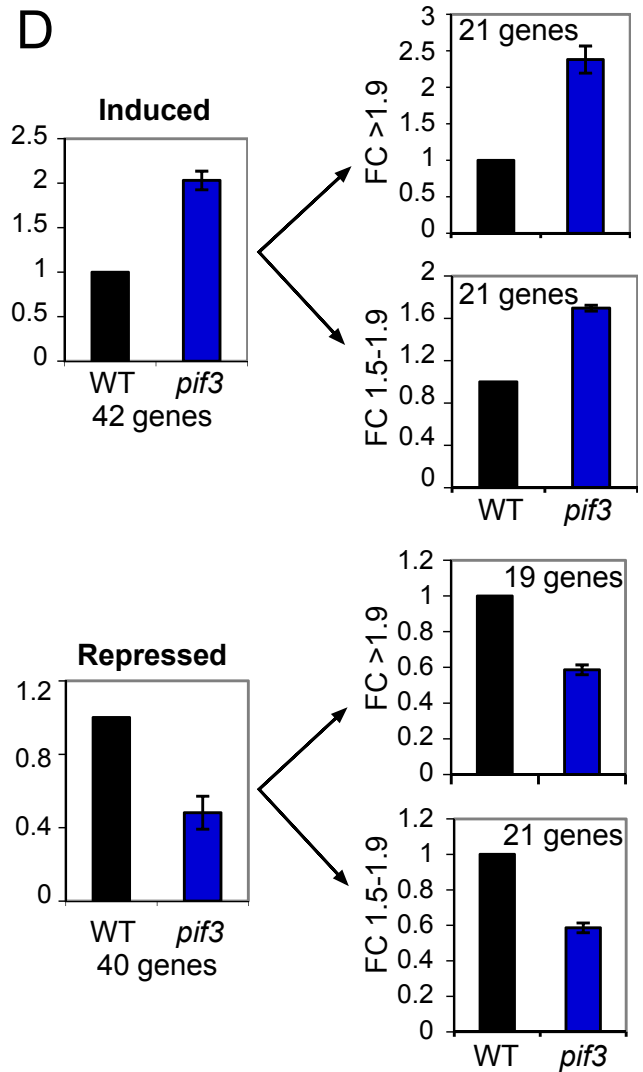
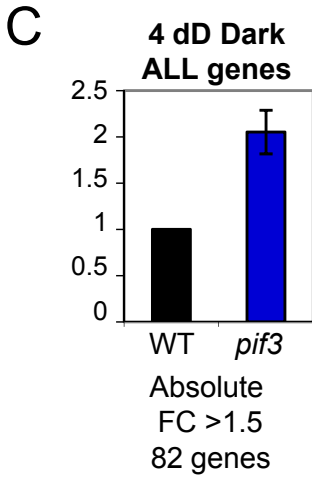
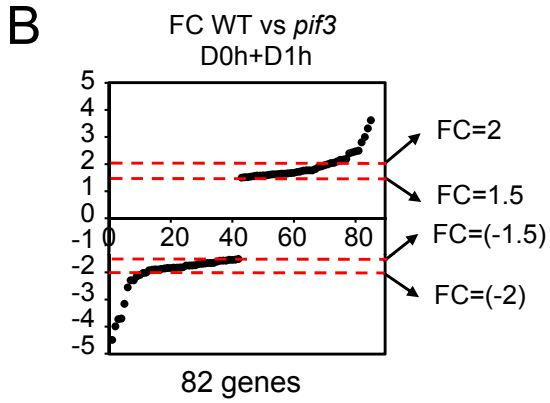
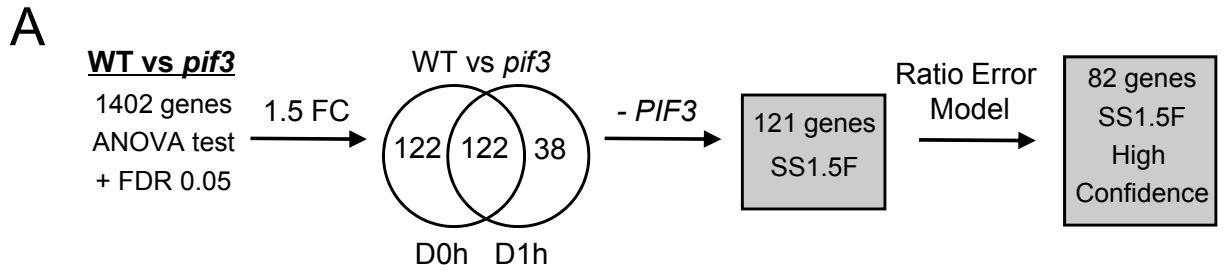
relative to WT\_Dark (WT-D). For convenience, genes in the induced and repressed Venn diagrams that are in the sectors relevant to this study (seven sectors displaying genes altered in *pif3-D*) are designated with Ind-Class 1 through 3 and Rep- Class 1 through 4 (no genes fall into Ind-Class 4 and thus this Class is not represented) (Supplemental Figure 8B). The bar graph data in Supplemental Figure 8C represent the mean FC in expression level relative to WT-D for all the genes in each class defined in Supplemental Figure 8B. Because the two genes in Rep-Class 4, and five out of 23 genes in Ind-Class 2 show ambiguity in their response to different treatments (they respond in different directions in *pif3-D*, WT-R1 and/or WT-R18), they were excluded from the bar graph data in Supplemental Figure 8C. See Supplemental Dataset 8 for the gene lists containing Ind Class and Rep Class genes.

The bar graphs show that the Rep-Class 1 are *pif3-D* genes that do not display responsiveness to 1 h or 18 h of Rc, indicating that they are PIF3-dependent genes with no indication of being light responsive at least in the two time points included (R1h and R18h). Although transient light responsiveness between darkness (D0h) and R1h and/or R1h and R18h cannot be excluded, the lack of light responsiveness might indicate long-term indirect regulation by PIF3. In contrast, Rep-Class 2 genes show repression in the absence of PIF3 in the dark and late light repression at R18h. And Rep-Class 3 shows response to all three treatments analyzed: they are repressed in *pif3-D*, and they show rapid R1h repression that is amplified after 18h of Rc.

The patterns of regulation of the induced genes are basically mirror images of what we observed for the corresponding repressed classes. Ind-Class 1 are *pif3-D* genes that do not display responsiveness to R1h or R18h, indicating that they are PIF3-dependent genes with no indication of being light responsive in the two time points included (R1h and R18h). As above for Rep-Class 1, this might indicate long-term indirect regulation by PIF3. Ind-Class 2 genes show induction in the absence of PIF3 in the dark and late light induction at R18h. And finally, genes in Ind-Class 3 show response to all three treatments analyzed: they are induced in *pif3-D*, and they show rapid R1h induction that is amplified after R18h of Rc. The *CAB* genes up-regulated in *pif3* in the dark fall into this class (four of the six Ind-Class 3 genes are *CAB* genes).

## SUPPLEMENTAL REFERENCES

- Gilmartin, P.M., Sarokin, L., Memelink, J. and Chua, N.H.** (1990). Molecular light switches for plant genes. *Plant Cell* **2**: 369–378.
- Leivar, P., Monte, E., Oka, Y., Liu, T., Carle, C., Castillon, A., Huq, E., and Quail, P.H.** (2008). Multiple phytochrome-interacting bHLH transcription factors repress premature seedling photomorphogenesis in darkness. *Curr. Biol.* **18**: 1815-1823.
- Leivar, P., Tepperman, J.M., Monte, E., Calderon, R.H., Liu, T.L., and Quail, P.H.** (2009). Definition of early transcriptional circuitry involved in light-induced reversal of PIF-imposed repression of photomorphogenesis in young *Arabidopsis* seedlings. *Plant Cell* **21**: 3535-3353.
- Lorrain, S., Trevisan, M., Pradervand, S., and Fankhauser, C.** (2009). Phytochrome interacting factors 4 and 5 redundantly limit seedling de-etiolation in continuous far-red light. *Plant J.* **60**: 449-461.
- Monte, E., Tepperman, J.M., Al-Sady, B., Kaczorowski, K.A., Alonso, J.M., Ecker, J.R., Li, X., Zhang, Y.L., and Quail, P.H.** (2004). The phytochrome-interacting transcription factor, PIF3, acts early, selectively, and positively in light-induced chloroplast development. *Proc. Natl. Acad. Sci. USA* **101**: 16091-16098.
- Moon, J., Zhu, L., Shen, H., and Huq, E.** (2008). PIF1 directly and indirectly regulates chlorophyll biosynthesis to optimize the greening process in *Arabidopsis*. *Proc. Natl. Acad. Sci. USA* **105**: 9433-9438.
- Shin, J., Kim, K., Kang, H., Zulfugarov, I.S., Bae, G., Lee, C.H., Lee, D., and Choi, G.** (2009). Phytochromes promote seedling light responses by inhibiting four negatively-acting phytochrome-interacting factors. *Proc. Natl. Acad. Sci. USA* **106**: 7660-7665.
- Stephenson, P.G., Fankhauser, C., and Terry, M.J.** (2009). PIF3 is a repressor of chloroplast development. *Proc. Natl. Acad. Sci. USA* **106**: 7654-7659.
- Weng, L., Dai, H., Zhan, Y., He, Y., Stepaniants, S.B., and Bassett, D.E.** (2006). Rosetta error model for gene expression analysis. *Bioinformatics* **22**: 1111-1121.



Supplemental Figure 1

### Supplemental Figure 1. PIF3 regulation of gene expression in the dark.

(A) Microarray expression profiling identified 82 high-confidence (HC) target genes that are statistically significantly deregulated in the absence of PIF3 in the dark and by a fold-change (FC) greater than 1.5 (SS1.5F-HC).

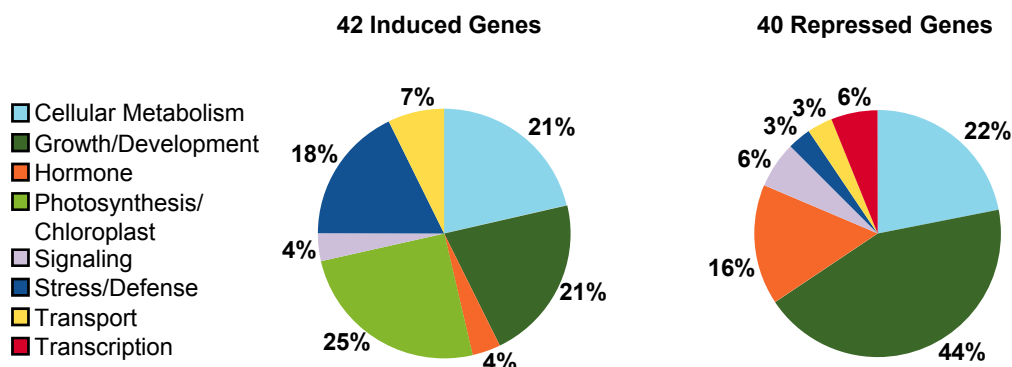
Flow chart of the analysis process to compare the expression profiles of WT and *pif3* seedlings in the dark. Statistical Anova test identified 1402 genes with a false discovery rate (FDR) set at 5%. The Venn diagram shows pairwise comparison between genes differentially expressed in WT seedlings compared to *pif3* at Dark 0 h (D0h) and Dark 1 h (D1h) time points with a FC greater than 1.5. The number of shared genes (SS1.5F gene list) is indicated in the intersection and contained *PIF3*, which was removed. The subsequent application of a ratio error model (Weng et al., 2006) yielded 82 high-confidence PIF3 target genes (SS1.5F-HC). Lists of each class of genes are in Supplemental Datasets 1 and 2.

(B) Scatter plot of FC values (*pif3*/WT) for the 82 genes showing altered SS1.5F-HC expression in *pif3* relative to WT.

(C) and (D). Sorting of PIF3 regulated gene expression in the dark according to FC difference. Mean FC for PIF3-regulated genes is expressed relative to the wild type dark value set at unity.

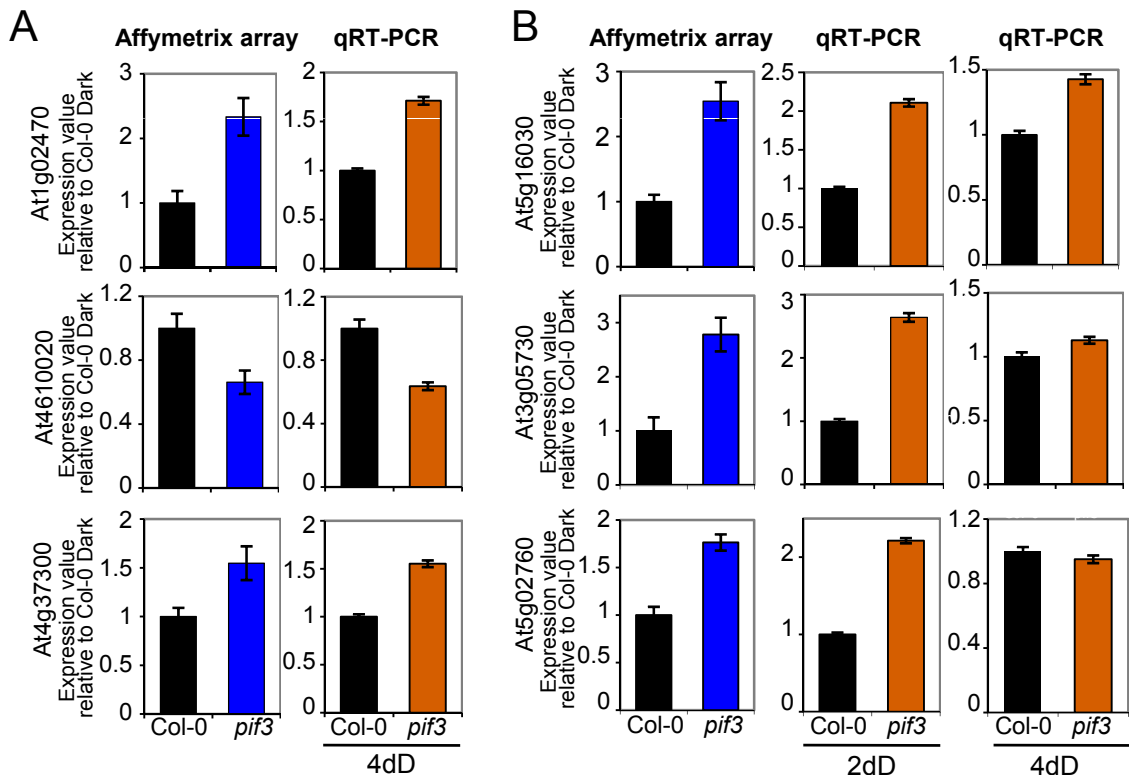
(C) Absolute mean FC for the 82 genes that are statistically significantly deregulated in the absence of PIF3 in the dark and by a FC greater than 1.5. Bars indicate SE for the genes averaged for each group.

(D) Mean FC for 42 up-regulated genes (induced) and the 40 down-regulated genes (repressed) in the *pif3-3* mutant in the dark. Induced and repressed genes were further classified according to their FC into two classes: FC >1.9 and FC 1.5-1.9. Bar graphs show the mean FC of each class of genes, and the number of genes falling into each category is specified. Bars indicate SE for the genes averaged for each group.



**Supplemental Figure 2. Distribution of PIF3-regulated genes among functional categories.**

Distribution of PIF3-regulated genes among functional categories, expressed as a percentage, for up- (left) and down- (right) regulated genes in the dark in the absence of PIF3. The assignment of functional categories was based on Gene Ontology annotations for biological and/or molecular function available at TAIR ([www.Arabidopsis.org](http://www.Arabidopsis.org)). Genes with unknown biological or molecular function (representing 34.8% of up-regulated and 19.5% of down-regulated genes) are not included.

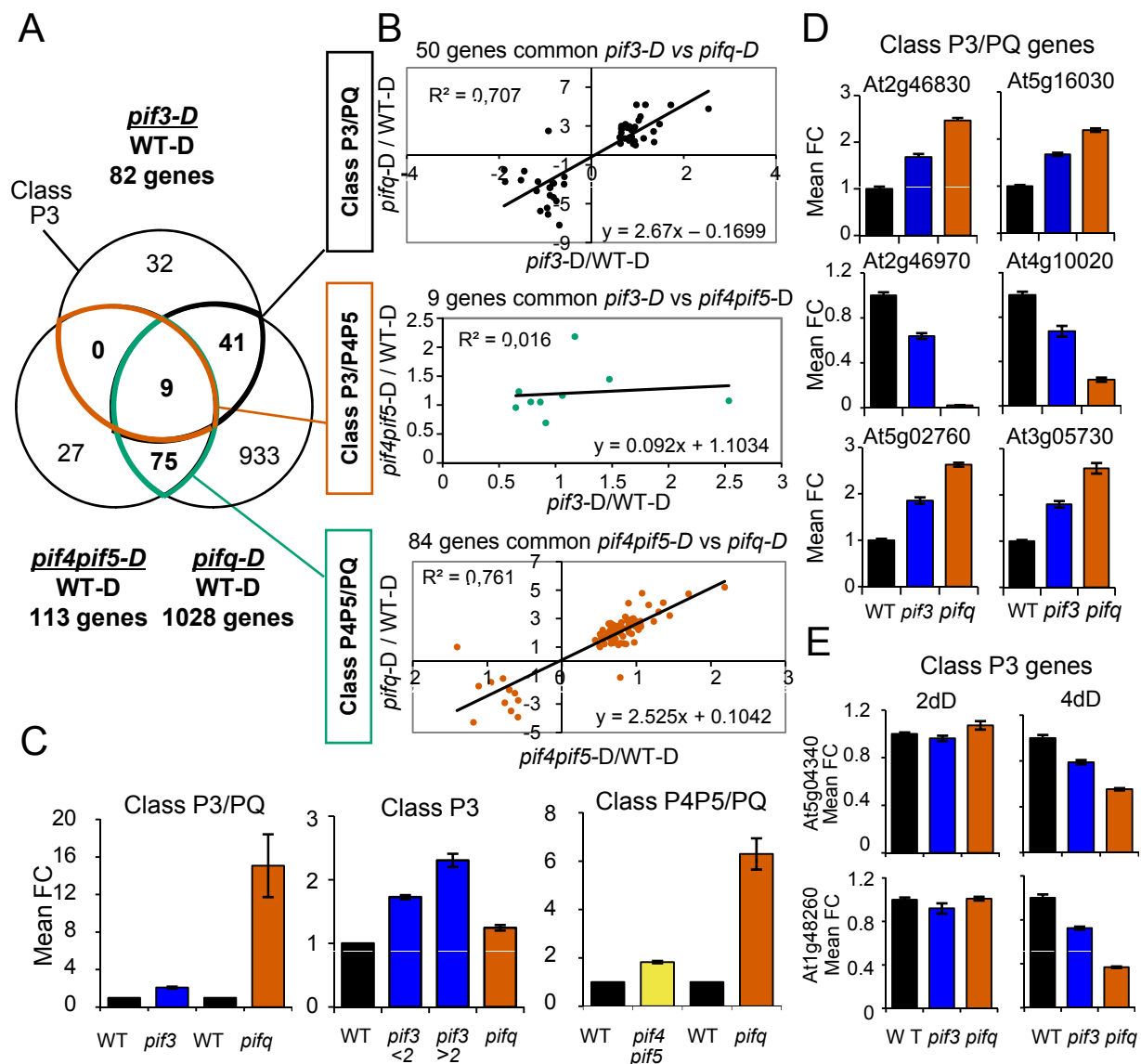


**Supplemental Figure 3. qRT-PCR validation of microarray data.**

(A) (B). Expression analysis of PIF3-dependent genes in WT Col-0 and *pif3-3* (*pif3*) mutant seedlings in the dark. For each gene, comparison of microarray and qRT-PCR data are shown. Microarray data displays the mean expression levels obtained by microarray analysis of three biological replicates relative to the Col-0 Dark value set at unity (bar graphs in blue). Validation of these results for each *MIDA* gene was performed by qRT-PCR analysis (bar graphs in vermillion). Levels were normalized to *PP2A* as described (Shin et al., 2007) and expressed relative to the Col-0 Dark value set at unity. Bars indicate SE of technical triplicates.

(A) Comparison of microarray data and qRT-PCR data performed on 4-d-old dark-grown seedlings (4dD).

(B) Comparison of microarray data and qRT-PCR data performed on 2-d-old dark-grown seedlings (2dD) and 4-d-old dark-grown seedlings (4dD).



**Supplemental Figure 4. Comparative expression analysis of PIF3 function with other PIF factors in the dark.**

Three-way comparison of genes responding to the *pif3* mutation (*pif3-D* versus *WT-D*), the *pif4 pif5* mutation (*pif4pif5-D* versus *WT-D*) (Lorrain et al., 2009), and the *pifq* mutation (*pifq-D* versus *WT-D*) (Leivar et al., 2009) in darkness.

(A) Venn diagram showing comparison of all genes in the three different sets of differentially PIF-regulated genes. This comparison between genes responding to *pif3-D*, *pif4pif5-D* and *pifq-D* resulted in the identification of four classes of genes responsive to: *pif3-D* and *pifq-D* (Class P3/PQ, 50 genes)(corresponding sections are indicated in black), *pif3-D* and *pif4pif5-D* (Class P3/P4P5, 9 genes)(indicated in vermillion), and *pif4pif5-D* and *pifq-D* (Class P4P5/PQ, 84 genes)(indicated in green), and to only *pif3-D* (Class P3, 32 genes). Lists for each class of genes are in Supplemental Dataset 4.

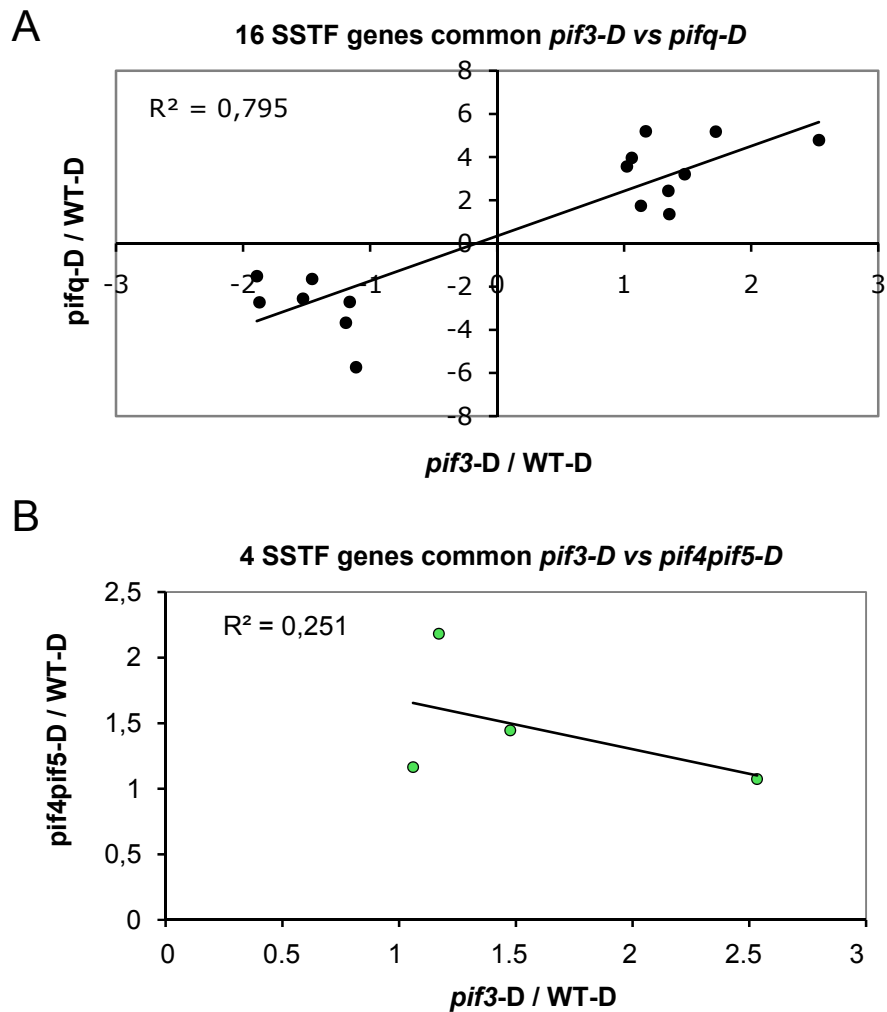
(B) Scatterplots of log<sub>2</sub> fold change values for the three classes of genes identified in (A). The top plot corresponds to Class P3/PQ, the middle plot to Class P3/P4P5, and the bottom plot to Class P4P5/PQ. Dots in each plot represent genes that are shared between both genotypes as shown in the Venn diagram in (A). Correlation coefficient for the genes, the trendline and the regression equation are indicated.

#### **Supplemental Figure 4 (Cont.)**

(C) Mean fold change (FC) in WT, *pif3* and *pifq* for the 50 Class P3/PQ genes (left), the 32 Class P3 genes (middle), and the 84 Class P4P5/PQ genes (right) relative to the WT dark value set at unity. Class P3 genes are divided between FC<2 (17 genes, *pif3*<2 in legend) and FC>2 (15 genes, *pif3*>2 in legend). Bars indicate SE for the genes averaged for each group.

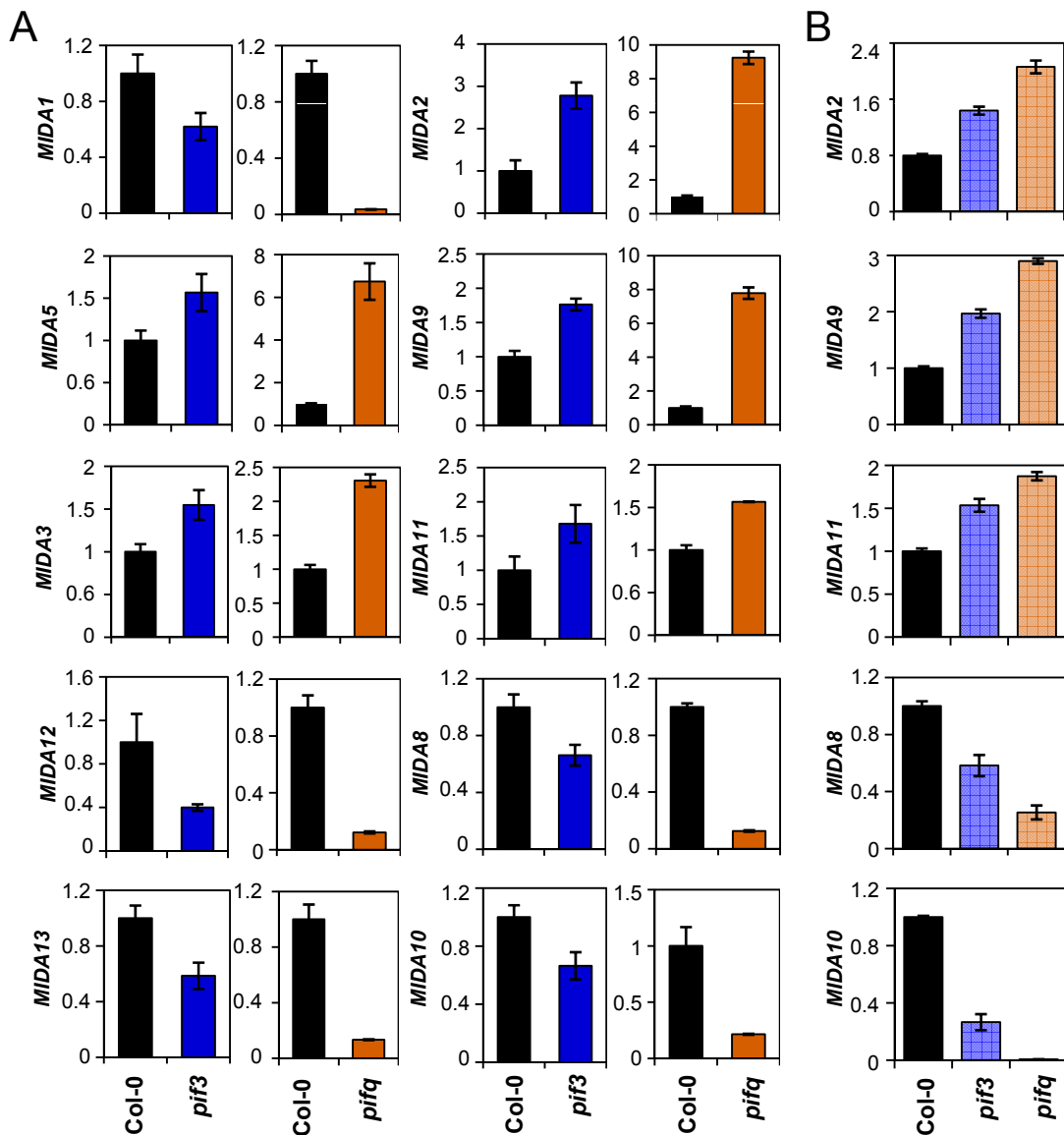
(D) Expression analysis by qRT-PCR of Class P3/PQ genes in 2-day-old dark-grown Col-0 wild-type (WT), *pif3-3* (*pif3*), and *pifq* mutant seedlings. *AT2G46830* and *AT2G46970* were selected as controls based on Leivar et al., 2009. Expression levels were normalized to *PP2A* as described (Shin et al., 2007) and expressed relative to the WT value set at unity. Error bars represent SE values of technical triplicates.

(E) Expression analysis by qRT-PCR of Class P3 genes *AT1G48260* and *AT5G04340*, in 2- (2dD) and 4-day-old (4dD) dark-grown Col-0 wild-type (WT), *pif3-3* (*pif3*), and *pifq* mutant seedlings. Expression levels were normalized to *PP2A* as described (Shin et al., 2007), and expressed relative to the 2dD WT value set at unity. Error bars correspond to SE values of technical triplicates.



**Supplemental Figure 5. Comparison of *pif3-D* SSTF-HC genes versus *pifq-D* and *pif4pif5-D*.**

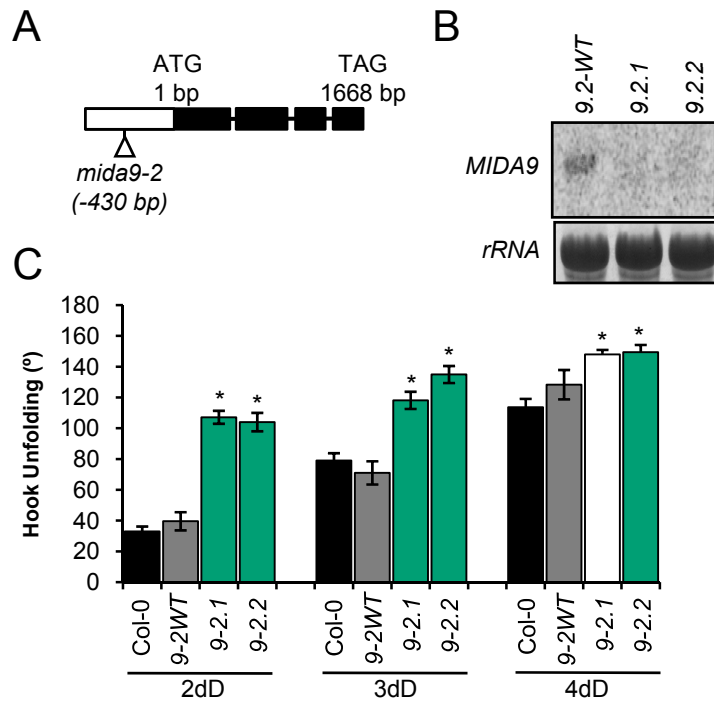
Scatterplots of log<sub>2</sub> fold change values for *pif3-D* SSTF-HC genes shared with *pifq-D* (A) and *pif4pif5-D* (B). Dots in each plot represent genes that are shared between both genotypes. Correlation coefficient for the genes and the trendline are indicated.



**Supplemental Figure 6. Expression of *MIDA* genes in *pif3* and *pifq*.**

(A) Microarray expression analysis of *MIDA* genes in WT Col-0, *pif3-3* (*pif3*) (in blue), and *pifq* (in vermillion) mutant seedlings in the dark. For each gene, comparison of *pif3* (this work) and *pifq* (Leivar et al., 2009) microarray data are shown displaying the mean expression levels obtained by microarray analysis of three biological replicates relative to the Col-0 Dark value set at unity. Bars indicate SE.

(B) qRT-PCR expression analysis of selected *MIDA* genes in wild-type Col-0, *pif3-3* (*pif3*) (in light blue), and *pifq* (in light vermillion) in 2-day-old dark-grown seedlings. Expression levels assayed by qRT-PCR were normalized to *PP2A* as described (Shin et al., 2007). Data correspond to technical triplicates and error bars indicate SE.

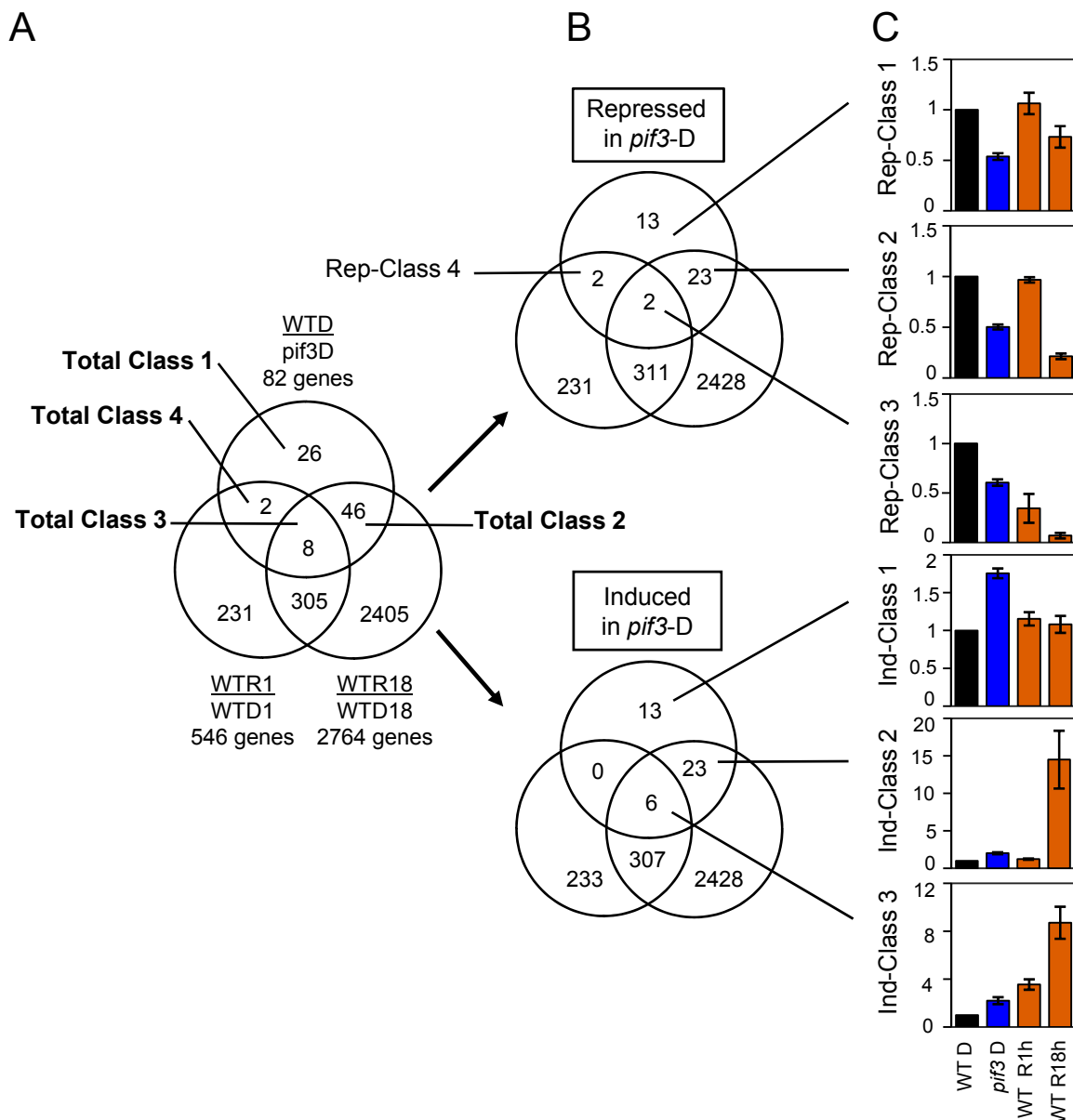


**Supplemental Figure 7. Characterization of *mida9-2*.**

(A) The mutation identified in Arabidopsis *MIDA9*. The T-DNA insert in *mida9-2* is indicated at position -430 bp relative to the ATG.

(B) RNA blot of 2-day-old, dark-grown wild-type and *mida9-2* mutant seedlings. No *MIDA9* transcript was detected in *mida9-2*, indicating that the line is likely a functional knock-out mutant.

(C) Quantification of hook angle in *mida9-2.1* and *mida9-2.2* compared to Col-0 and a WT sibling line after 2, 3 and 4 days of growth in the dark (dD) after germination. Bars correspond to SE of at least 30 seedlings and asterisks indicate statistically different mean values compared to their corresponding WT.



**Supplemental Figure 8. Light-responsiveness of PIF3-regulated genes in the dark.**

(A) (B) and (C). Three-way comparison of genes responding to the *pif3* mutation in darkness (SS1.5F-HC of WT-D versus *pif3-D*) (Supplemental Dataset 2), 1 h Rc in the WT (genes displaying statistically significant differences in gene expression by at least two fold (SSTF) of WT-R1 versus WT-D1) (Supplemental Dataset 6), and to 18 h Rc in the WT (SSTF of WT-R18 versus WT-D18) (Supplemental Dataset 7). Classification of genes as induced or repressed (B) is based on the direction of the response of *pif3-D* relative to the WT-D. This classification includes all genes shown in A except those that are not light responsive in *pif3* (Total Class 1), which are divided between induced or repressed accordingly.

(A) Venn diagram showing comparison of all genes in the three sets of differentially regulated genes. This comparison resulted in the identification of four classes of genes responsive to: only *pif3-D* (Total-Class 1, 26 genes), *pif3-D* and WT-R18h only (Total-Class 2, 46 genes), *pif3-D* and WT-R1h and R18h (Total-Class 3, eight genes), and *pif3-D* and WT-R1h only (Total-Class 4, two genes).

### Supplemental Figure 8. (Cont)

(B) (Top) Venn diagram showing comparison of repressed genes in PIF3-deficient seedlings in the dark with light responsive genes in the WT at R1h and R18h. This comparison resulted in the identification of four classes of repressed genes responsive to: only *pif3-D* (Rep-Class 1, 13 genes), *pif3-D* and WT-R18h only (Rep-Class 2, 23 genes), *pif3-D* and WT-R1h and R18h (Rep-Class 3, two genes), and *pif3-D* and WT-R1h only (Rep-Class 4, two genes).

(Bottom) Venn diagram showing comparison of induced genes in PIF3-deficient seedlings in the dark with light responsive genes in the WT at R1h and R18h. This comparison resulted in the identification of three classes of induced genes responsive to: only *pif3-D* (Ind-Class 1, 13 genes), *pif3-D* and WT-R18h only (Ind-Class 2, 23 genes), and *pif3-D* and WT-R1h and R18h (Ind-Class 3, six genes). Gene lists for each class of genes are presented in Supplemental Dataset 8.

(C) Bar graphs showing the mean fold change in expression relative to WT-D (set at unity) for all genes in each class as defined in (B). Error bars represent the mean SE for the genes averaged for each genotype and treatment combination defined in (B). Excluded from this analysis are a few ambiguous genes that respond in a different direction in *pif3-D*, WT-R1h and/or WT-R18h relative to WT-D: two genes in Repressed Class 4 and five genes in Induced Class 2 (Supplemental Dataset 8).

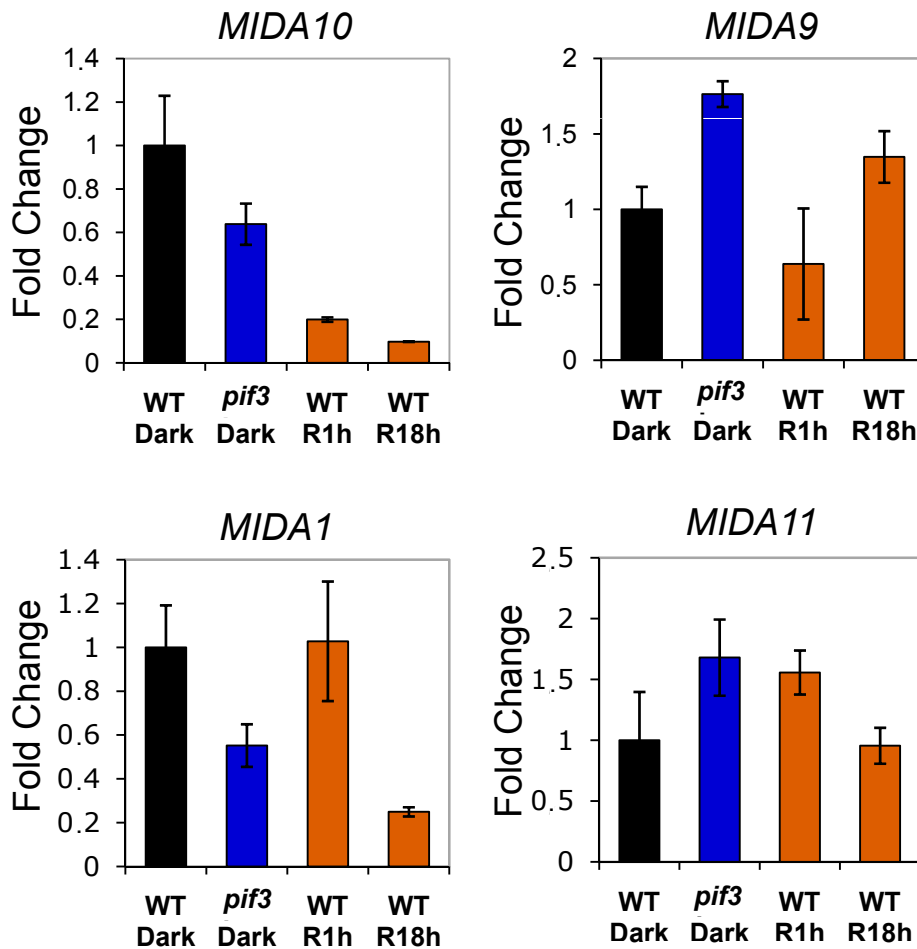
*pif3-D*, genes misexpressed in 4-day-old, dark-grown seedlings in the absence of PIF3 compared to the wild type.

WTD, wild type after 4 days in darkness

WTR1, wild type after 1 h of Rc relative to WTD

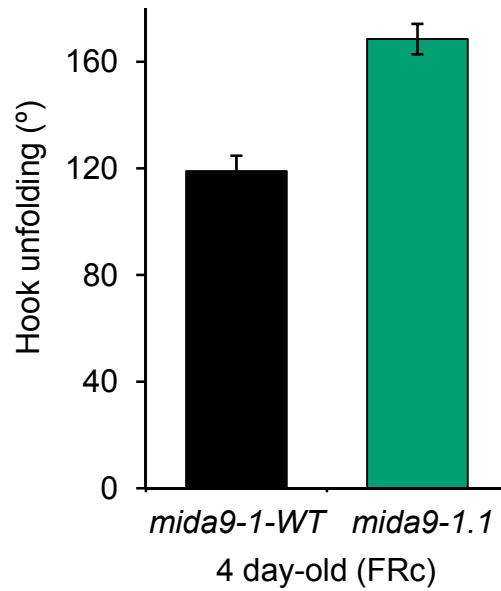
WTR18, wild type after 18 h of Rc relative to WTD

*pif3D*, *pif3* after 4 days in darkness

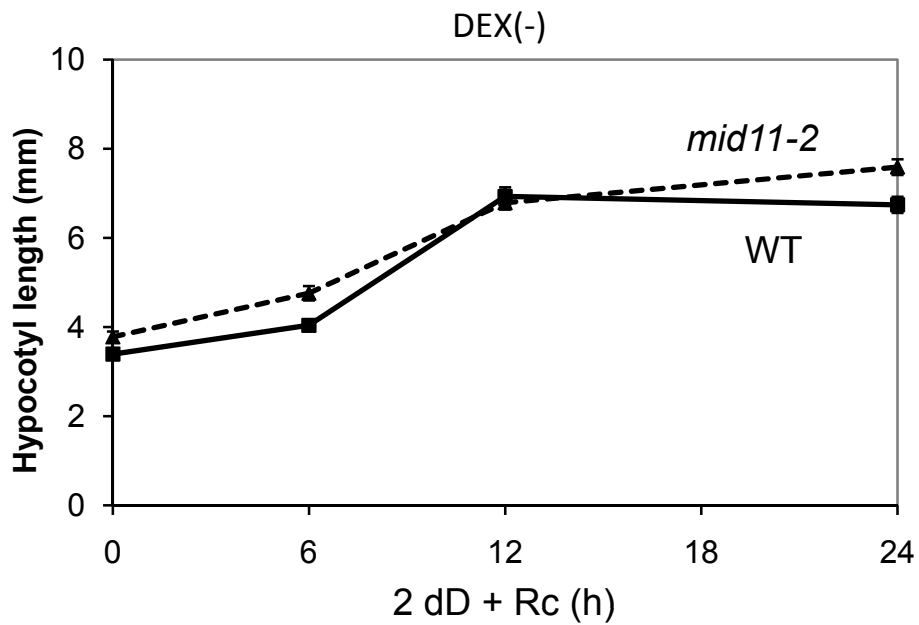


**Supplemental Figure 9. Microarray data displaying the mean expression level of *MIDA10*, *MIDA9*, *MIDA11* and *MIDA1* after 1 h and 18 h of Rc treatment.**

Microarray data displaying the mean expression level obtained for *MIDA10*, *MIDA9*, *MIDA11* and *MIDA1* replicates relative to the Col-0 Dark value set at unity after 1 h (WT R1h) or 18 h (WT R18h) of Rc (8  $\mu\text{mol}/\text{m}^2/\text{s}$ ). Dark levels in the *pif3* mutant are also shown for comparison (*pif3* Dark). Dark, WT level is set at unity (WT Dark). Error bars correspond to SE values of three biological replicates.

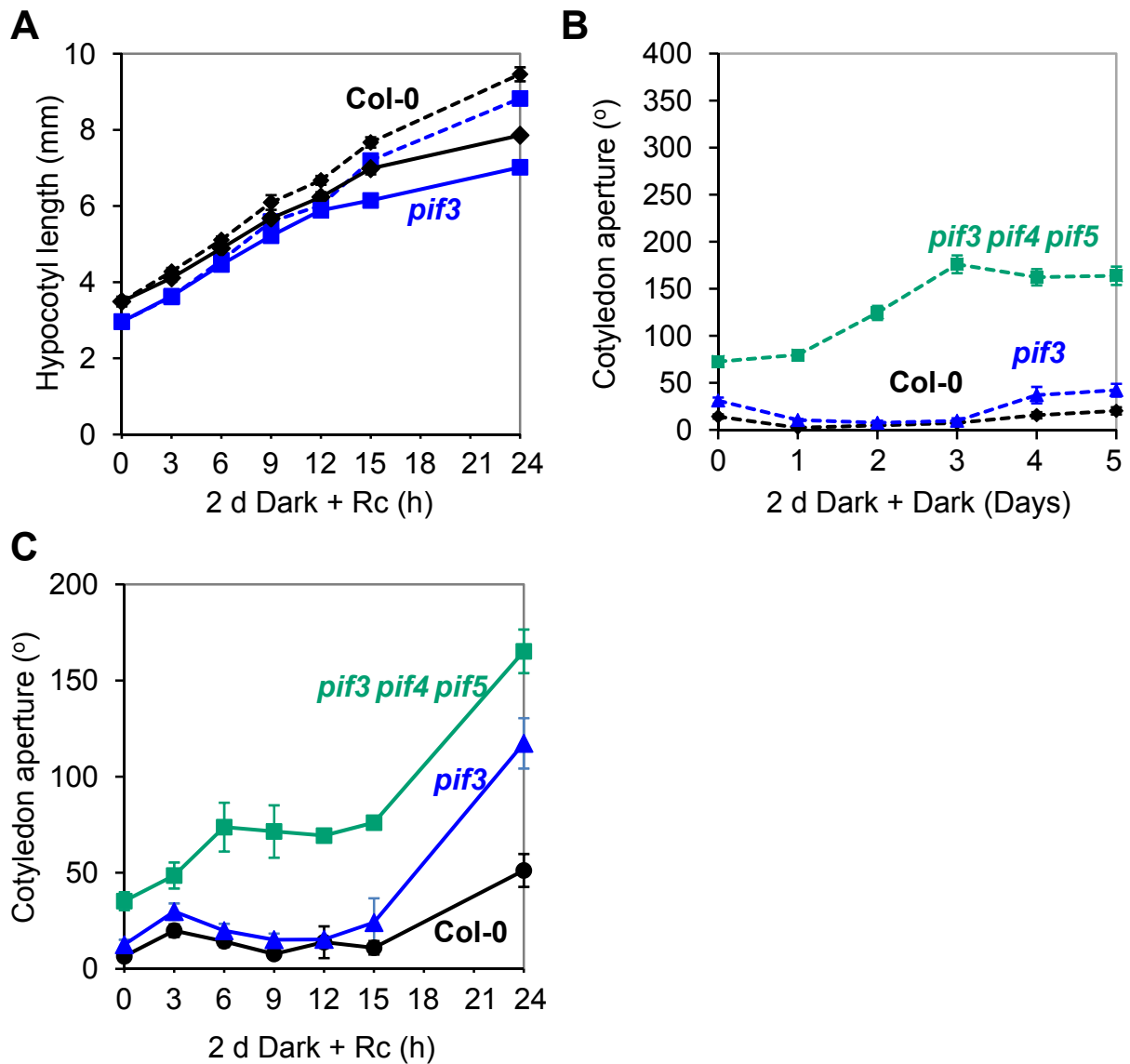


**Supplemental Figure 10. Hook angle phenotype displayed by *mida9-1* in FRc**  
Quantification of the hook angle exhibited by 4-day-old *mida9-1.1* mutant seedlings compared to WT control siblings *mida9-1-WT* after growth in continuous far-red light (FRc) (0.01  $\mu\text{mol}/\text{m}^2/\text{s}$ ). Bars indicate SE of at least 30 seedlings.



**Supplemental Figure 11. Quantification of hypocotyl length displayed by *mid11* in the dark-to-light transition in the absence of DEX.**

Time-course quantification of hypocotyl growth in the WT (solid line) and *mid11-2* (dashed line), of 2-day-old dark-grown seedlings during the dark-to-Rc transition (Rc = 8  $\mu\text{mol}/\text{m}^2/\text{s}$ ) in the absence of dexamethasone (DEX). Bars indicate SE of at least 30 seedlings.



**Supplemental Figure 12. Quantification of hypocotyl length in *pif3* and cotyledon separation angle in *pif3* and *pif3 pif4 pif5* after dark-to-light transition.**

(A) Time-course quantification of hypocotyl length of 2-day-old, dark-grown Col-0 and *pif3* seedlings kept in the dark (dashed lines) or during the dark-to-light transition (solid lines) for 24 h.

(B) Time-course quantification of cotyledon separation of 2-day-old, dark-grown Col-0, and *pif3* and *pif3 pif4 pif5* seedlings kept in the dark for 5 days.

(C) Time-course quantification of cotyledon separation of 2-day-old, dark-grown Col-0, *pif3* and *pif3 pif4 pif5* seedlings during the dark-to-light transition for 24 h.

(A) (B) (C). Bars indicate SE of at least 30 seedlings.

<i>MIDA</i>	Regulation by PIF3 in the Dark	Response in <i>pif3-D</i>	Response to Red Light	Dark K.O. phenotype	Dark OX phenotype	Role in Deetiolation
<i>MIDA9</i>	Repressed	Induced	Induced (Late)	Open hooks		Repressor
<i>MIDA10</i>	Induced	Repressed	Repressed (Early)	Open hooks		Repressor
<i>MIDA11</i>	Repressed	Induced	Induced (Late)	Short hypocotyl		Repressor
<i>MIDA1</i>	Induced	Repressed	Induced (Early) Repressed (Late)		Open Cotyledons	Inducer

**Supplemental Table 1. Summary of *MIDA9*, *MIDA10*, *MIDA11* and *MIDA1* gene regulation by PIF3 and by red light, as well as the phenotype of their respective *Arabidopsis* mutants.**

Newly identified MIDA factors *MIDA9*, *MIDA10*, *MIDA11* and *MIDA1* are novel regulators of photomorphogenesis in the dark. This table summarizes their gene regulation by PIF3 and by red light (8  $\mu\text{mol}/\text{m}^2/\text{s}$ ), as well as the phenotype of the respective *Arabidopsis mida* mutants and the inferred role of each MIDA factor as Inducer or Repressor in deetiolation. “Early” indicates a response within 1-3h, whereas “Late” indicates a response after 3h. K.O. and OX indicate loss-of-function and overexpressor mutants respectively.

Use	Reference			Sequence from 5' to 3'
	Gene	AGI number	Code	
Genotyping	<i>MIDA2</i>	<i>AT3G05730</i>	EMP33	TATCACAAATTAGCCTCAGCCG
			EMP34	ACCACCCACCCTTGTACTAC
	<i>MIDA3</i>	<i>AT4G37300</i>	EMP67	TTTGTCTAGAAGGTCTGCTGG
			EMP68	AAAGCTGTGGACAGAGACGAC
	<i>MIDA4</i>	<i>AT3G47250</i>	EMP27	TGGCAAGAACTTAAATTTGGAG
			EMP28	TGGCAACGAGAATGAGGTATC
	<i>MIDA5</i>	<i>AT1G02470</i>	EMP23	CTCCATAAACGGTTTCATTGC
			EMP24	CCAAATCGACTCACCGTTAAC
	<i>MIDA6</i>	<i>AT5G04340</i>	EMP314	TGCCCAATACAAATTTGTCAAC
			EMP315	AGTAAGCGAAAAGCTTTTCCG
	<i>MIDA7</i>	<i>AT1G48260</i>	EMP307	AAACATGCATCCATCTTGGAG
			EMP308b	CTTCTCGATGATTTTGATGG
	<i>MIDA8</i>	<i>AT4G10020</i>	EMP318	TGGGCTTGCGGTATAATGAGG
			EMP319	AATTCGATGCAGTGGATCATC
	<i>MIDA9</i>	<i>AT5G02760</i>	EMP69	AAGAATGGTGGGGTCATTAGG
		EMP70	GACAGAGAATCATCATCGAACAG	
<i>MIDA9</i>	<i>AT5G02760</i>	EMP223	AATGTGCCTTGAACGTGTCGG	
		EMP105	ACGAGAGACTGAGAAAAGGGC	
<i>MIDA10</i>	<i>AT4G10240</i>	EMP305	TATGATCCCACCACACATGTG	
		EMP306	TGGTCAAATCCAACAAGGTC	
<i>MIDA12</i>	<i>AT1G05510</i>	EMP9	ATTTCCGGATAAAGTTGTCCG	
		EMP10	GTCATAGTCCATGCAAATGCC	
<i>MIDA13</i>	<i>AT5G45690</i>	EMP7	CCCCTGAAATTACCAAAACATAAC	
		EMP8	CCTTCTCAAATCATCCACGTC	
qRT-PCR	<i>MIDA1</i>	<i>AT5G50600</i>	EMP378	GATTGAGTGGGGTTGTCCG
			EMP379	TACAGAGTACTACTACGTACACC
	<i>MIDA2</i>	<i>AT3G05730</i>	EMP346	CGAAGTCACAGTGATTACCC
			EMP347	AATGCTCTTCTCGTTGTCATG
	<i>MIDA3</i>	<i>AT4G37300</i>	EMP350	GAAGGAAGACAACGGTGAAG
			EMP351	CCGGATTGCTTCTGTA AAC
	<i>MIDA5</i>	<i>AT1G02470</i>	EMP340	TTCAGACCCGTTATGCAATGG
			EMP341	GCGTATAAATTGTAAGCCACG
	<i>MIDA6</i>	<i>AT5G04340</i>	EMP354	TTCGCTTACTCAATCTGCCG
			EMP355	ACGTGCGACTTCACACTTCC
	<i>MIDA7</i>	<i>AT1G48260</i>	EMP342	AATGAGCTGGGCTCATCATCAC
			EMP343	GAAAATGTCTCTAGCATCCCG
	<i>MIDA8</i>	<i>AT4G10020</i>	EMP348	CCACCTCGAGTTCCTGCAAG
			EMP349	GCTTGCAGGATACCGTGGTG
	<i>MIDA9</i>	<i>AT5G02760</i>	EMP352	TCATGTTGCTTGGCAGGAGTG
			EMP353	TAActGAAcAGCTCTcACTCC
	<i>MIDA10</i>	<i>AT4G10240</i>	EMP426	TCCAAAGACATCACCGAGTCG
			EMP427	GTACCCTTTTCTCTCCTGGCAG
	<i>MIDA11</i>	<i>AT2G46070</i>	EMP344	CCAGTGATCAATGCCGTTTCC
			EMP345	TCGAGTTAAGTAGCACGTTGC
<i>CCA1</i>	<i>AT2G46830</i>	EMP368	CCGCAACTTTGCCTCAT	
		EMP369	GCCAGATTCGGAGGTGAGTTC	
<i>PIL1</i>	<i>AT2G46970</i>	EMP370	AAATTGCTCTCAGCCATTCTGTGG	
		EMP371	TTCTAAGTTTGAGGCGGACGCAG	
<i>UNK</i>	<i>AT5G16030</i>	EMP356	CTCATGGGTGAGATCAAGAC	
		EMP357	AGATGAGGAACACAAATAGGG	
<i>PP2A</i>	<i>AT1G13320</i>	EMP338	TATCGGATGACGATTCTTCTGTGAG	
		EMP339	GCTTGGTGCAGTATCGGAATGAGAG	
Probes for RNA Blots	<i>MIDA9</i>	<i>AT5G02760</i>	EMP104	ACAACCAGCACTGCTACTAC
			EMP105	AATGTGCCTTGAACGTGTCGG
	<i>MIDA10</i>	<i>AT4G10240</i>	EMP326	GACATCACCGAGTCGCC
		EMP327	CTCCGGAACCATGATGTTG	

**Supplemental Table 2. Primer sequences used for PCR amplification.**

**Functional Profiling Identifies Genes Involved in Organ-Specific Branches of the PIF3 Regulatory Network in *Arabidopsis***

Maria Sentandreu, Guiomar Martín, Nahuel González-Schain, Pablo Leivar, Judit Soy, James M. Tepperman, Peter H. Quail and Elena Monte

*Plant Cell* 2011;23;3974-3991; originally published online November 22, 2011;  
DOI 10.1105/tpc.111.088161

This information is current as of August 6, 2012

- Supplemental Data**      <http://www.plantcell.org/content/suppl/2011/11/07/tpc.111.088161.DC1.html>
- References**              This article cites 61 articles, 33 of which can be accessed free at:  
<http://www.plantcell.org/content/23/11/3974.full.html#ref-list-1>
- Permissions**            [https://www.copyright.com/ccc/openurl.do?sid=pd\\_hw1532298X&issn=1532298X&WT.mc\\_id=pd\\_hw1532298X](https://www.copyright.com/ccc/openurl.do?sid=pd_hw1532298X&issn=1532298X&WT.mc_id=pd_hw1532298X)
- eTOCs**                    Sign up for eTOCs at:  
<http://www.plantcell.org/cgi/alerts/ctmain>
- CiteTrack Alerts**      Sign up for CiteTrack Alerts at:  
<http://www.plantcell.org/cgi/alerts/ctmain>
- Subscription Information**      Subscription Information for *The Plant Cell* and *Plant Physiology* is available at:  
<http://www.aspb.org/publications/subscriptions.cfm>

## **Resumen artículo 1:**

### **Functional profiling identifies genes involved in organ-specific branches of the PIF3 regulatory network in Arabidopsis.**

Maria Sentandreu, Guiomar Martín, Nahuel González-Schain, Pablo Leivar, Judit Soy, James M. Tepperman, Peter Quail and Elena Monte.

### **Identificación de genes involucrados en la ramificación específica de órgano de la red regulatoria de PIF3 en Arabidopsis mediante un estudio funcional.**

Los reguladores transcripcionales PIF, factores de interacción con fitocromos de tipo bHLH, aseguran de manera constitutiva el estado etiolado de las plántulas germinadas en oscuridad mediante la represión activa del proceso de desetiolación. Tras la exposición a luz, los fitocromos revierten rápidamente esta acción induciendo la degradación proteolítica de los PIFs. Un análisis reciente del transcriptoma de un cuádruple mutante deficiente en PIF1, PIF3, PIF4 y PIF5 demuestra que los PIFs, en condiciones de oscuridad, regulan transcripcionalmente un grupo de genes que coincide ampliamente con genes regulados por luz en las líneas salvajes. Tales resultados establecen que la inducción de la desetiolación mediada por los fitocromos, implica la reversión del perfil transcripcional mantenido por los PIFs en oscuridad. En este trabajo, elucidamos, como los PIFs implementan la desetiolación de la planta combinando una aproximación basada en el análisis de expresión génica con una estrategia de descripción funcional. Como resultado identificamos también cuatro genes regulados por PIF3 como nuevos reguladores del desarrollo en oscuridad, los genes MIDA de “MISREGULATED IN DARK” (DESREGULADOS EN OSCURIDAD) y proporcionamos evidencia de que cada uno de estos cuatro MIDA, regula un aspecto diferente de la etiolación (mantenimiento del gancho apical, cierre de los cotiledones o elongación del hipocotilo), sugiriendo así, una ramificación de la señal que PIF3 ejerce sobre estos genes. Además, tras los estudios con mutantes, combinamos la función inferida para los genes MIDA con sus perfiles de expresión en respuesta a la degradación por luz de PIF3 y evidenciamos consistentemente con un modelo,

que la acción de la red reguladora PIF3/MIDAS posibilita, tras la exposición a luz, una primera respuesta que induciría rápidamente el proceso de desetiología y una segunda que modularía los efectos de la primera optimizando el proceso de desetiología de la plántula en función de las condiciones ambientales que la rodean. Los datos presentados sugieren colectivamente que al menos parte del sistema phy/PIF actúa a través de estos cuatro MIDAs para iniciar y optimizar la desetiología de la plántula, y que éste mecanismo podría permitir la implementación de respuestas espaciales (específicas de órgano) y temporales durante el programa fotomorfogénico.

## **2<sup>nd</sup> Article**



# Branching of the PIF3 regulatory network in Arabidopsis

## Roles of PIF3-regulated MIDAs in seedling development in the dark and in response to light

Maria Sentandreu, Pablo Leivar, Guiomar Martín and Elena Monte\*

Departament de Genètica Molecular; Center for Research in Agricultural Genomics (CRAG) CSIC-IRTA-UAB-UB; Campus UAB; Bellaterra; Barcelona, Spain

**P**lants need to accurately adjust their development after germination in the underground darkness to ensure survival of the seedling, both in the dark and in the light upon reaching the soil surface. Recent studies have established that the photoreceptors phytochromes and the bHLH phytochrome interacting factors PIFs regulate seedling development to adjust it to the prevailing light environment during post-germinative growth. However, complete understanding of the downstream regulatory network implementing these developmental responses is still lacking. In a recent work, published in *The Plant Cell*, we report a subset of PIF3-regulated genes in dark-grown seedlings that we have named *MIDAs* (*MISREGULATED IN DARK*). Analysis of their functional relevance using mutants showed that four of them present phenotypic alterations in the dark, and that each affected a particular facet of seedling development, suggesting organ-specific branching in the signal that PIF3 relays downstream. Furthermore, our results also showed an altered response to light in seedlings with an impaired PIF3/MIDA regulatory network, indicating that these factors might also be essential to initiate and optimize the developmental adjustment of the seedling to the light environment.

characterized by closed apical hooks, appressed cotyledons and fast hypocotyl growth to quickly reach the sunlight at the soil surface. Upon exposure to light, etiolated seedlings undergo a developmental switch termed deetiolation that involves the coordinated inhibition of hypocotyl elongation, apical hook unfolding, separation and expansion of the cotyledons, and induction of chloroplast and pigment biosynthesis to start photosynthesis.<sup>1</sup> Deetiolation is mediated by photoactivated phytochrome (phy) photoreceptors,<sup>2,3</sup> which interact with the PIFs (PIF1, PIF3, PIF4, PIF5, PIF6 and PIF7 in Arabidopsis<sup>4</sup>) upon exposure of dark-grown seedlings to the light. This phy/PIF interaction induces the rapid degradation of at least four of these PIFs (PIF1, PIF3, PIF4 and PIF5) triggering the gene expression changes that orchestrate the initiation of the deetiolation response.<sup>4,5</sup> Although several genome-wide expression analyses have identified subsets of genes regulated by the PIFs in Arabidopsis,<sup>6–8</sup> the functional relevance of these genes to implement etiolation is still largely lacking. In a recent study, we report the identification and characterization of several PIF3-regulated genes in the dark that we have named *MIDAs* (*MISREGULATED IN DARK*).<sup>9</sup> We show that four of them are novel regulators of seedling deetiolation and that each regulates a specific facet of the seedling response to light, suggesting spatial branching of the PIF3 signal. Our data also suggest that the rapid initial response of seedlings to light is followed by a PIF/MIDA-mediated counteraction to prevent an overresponse to the illumination, effectively optimizing deetiolation to ensure seedling survival.

**Keywords:** Arabidopsis, bHLH transcription factors PIFs, phytochrome, seedling deetiolation, MIDAs, organ-specificity, branching of PIF3 signal, over response to light

Submitted: 01/11/12

Accepted: 01/12/12

<http://dx.doi.org/10.4161/psb.7.4.19339>

\*Correspondence to: Elena Monte;  
Email: elena.monte@cragenomics.es

### Introduction

When Arabidopsis seedlings germinate in the underground darkness, a group of bHLH transcription factors called PIFs (Phytochrome Interacting Factors) maintain an etiolated developmental program

Addendum to: Sentandreu M, Martín G, González-Schain N, Leivar P, Soy J, Tepperman JM, et al. Functional profiling identifies genes involved in organ-specific branches of the PIF3 regulatory network in Arabidopsis. *Plant Cell* 2011; 23:3974–91; PMID:22108407; <http://dx.doi.org/10.1105/tpc.111.088161>

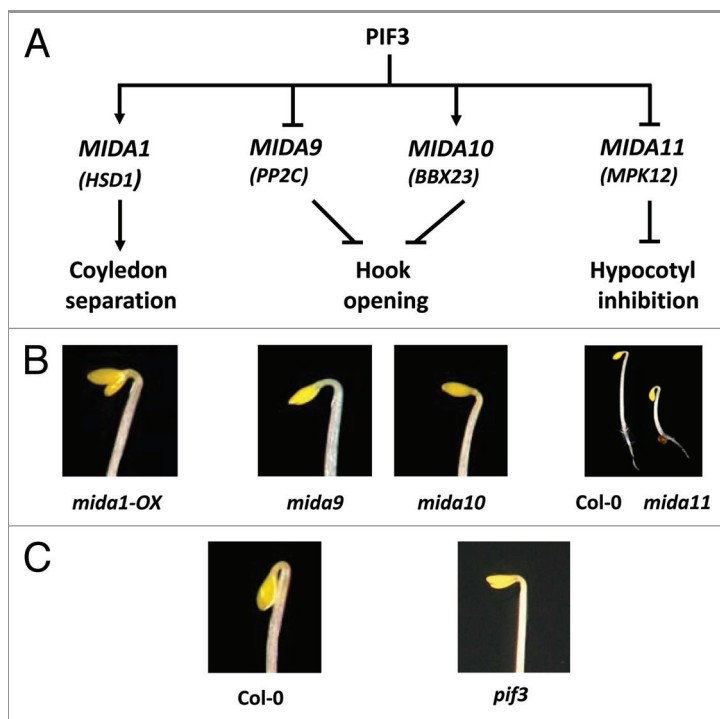


**Figure 1.** PIF-regulated transcriptional network in the dark. (A) Simplified schematic model depicting the branching in the signaling that PIF3 relays downstream to regulate specific aspects of deetiolation through the MIDAs. MIDA1 (HSD1, a hydroxysteroid dehydrogenase11) induces cotyledon separation, MIDA9 (a type 2C phosphatase) and MIDA10 (BBX23, a B-Box transcription factor 13) repress hook unfolding, and MIDA11 (MPK12, a MAP kinase 12) represses hypocotyl inhibition. (B) Visual phenotype of representative 2-d-old, dark-grown *mida* mutant seedlings. For *mida1-OX*, *mida9* and *mida10*, only a detail of their apical area is shown. For *mida11*, the mutant seedling is shown in comparison to the wild-type Col-0. (C) Visual phenotype of 2-d-old, dark-grown *pif3* and Col-0 wild-type seedlings for comparison with the seedlings shown in B. Detail of the apical area is shown. Experimental procedures are described in Sentandreu et al., 2011.

## MIDAs in the Dark

**Branching of PIF3 signaling to repress organ-specific facets of seedling deetiolation.** Comparison of PIF3-deficient mutants<sup>10</sup> to a wild-type control during post-germinative growth in the dark revealed that PIF3 has a role as repressor of deetiolation in dark-grown seedlings from 2 d onward. Our data showed that after 2 d, *pif3* mutants grown in the dark start displaying a partially deetiolated phenotype with more open hooks and cotyledons and marginal short hypocotyls. Definition of the PIF3-regulated transcriptome in these conditions allowed us to identify 82 high-confidence target genes. Mutant analysis of the function of 13 of them (that we named *MIDA*, for *MISREGULATED IN DARK*) enabled us to identify four novel genes that caused seedling phenotypes in the dark when mutated: *MIDA1*, *MIDA9*, *MIDA10* and

*MIDA11*. Based on their regulation by PIF3, the observed mutant phenotypes, and the available information on their annotation and/or function, our work concluded that: MIDA1 is a PIF3-induced hydroxysteroid dehydrogenase HSD1, proposed to participate in the biosynthesis of brassinosteroids,<sup>11</sup> with a role as inducer of cotyledon separation; MIDA11 is a PIF3-repressed MAP kinase MPK12, involved in auxin responses,<sup>12</sup> with a role as inducer of hypocotyl elongation; MIDA9 is a PIF3-repressed novel type 2C phosphatase that has a role as repressor of hook unfolding; and, finally, MIDA10 is a PIF3-induced B-box containing transcription factor BBX2313, with a role as repressor of hook unfolding (Fig. 1). Interestingly, our finding that each of these factors regulates a distinct facet of the seedling deetiolation response (hook unfolding, cotyledon separation or hypocotyl elongation) suggest branching of

the signal that PIF3 relays through the MIDAs to repress organ-specific aspects of the deetiolation response in the dark. Moreover, the proposed functions of these MIDA factors with a role in deetiolation support the current view<sup>4,5</sup> that hormone action, transcriptional regulation, and control of protein phosphorylation status play critical roles in the regulation of the deetiolation process.

## MIDAs in the Light

**Initiation of de-etiolation and prevention of seedling overresponses to the light stimulus.** In the dark, our data suggest that PIF3 action involves the induction of MIDA1 and MIDA10, a positive and negative regulator of deetiolation, respectively, and the repression of MIDA9 and MIDA11, both negative regulators of deetiolation in the dark. This complex regulatory network was further examined during exposure of dark-grown seedlings to light, when PIF3 is rapidly degraded by phy activity. Expression of *MIDA1* showed a rapid (within 1–2 h) and transient induction by red light, whereas *MIDA10* showed a rapid downregulation in response to illumination. These expression profiles agree with the current model of early deetiolation,<sup>7,14</sup> where deetiolation inducers like MIDA1 are rapidly light induced, whereas repressors like *MIDA10* are rapidly light repressed, to allow for a fast (in less than 3 h) deetiolation response upon light exposure of dark-grown seedlings. However, the deetiolation repressors *MIDA9* and *MIDA11* were found to be slowly induced by light (within 3 to 12 h). This finding made us hypothesize that a counter active action on the rapid deetiolation response might take place in the seedling under the regulation of the phy/PIF/MIDA network late after illumination (after 6–12 h), possibly to prevent an exaggerated response to the light stimulus. To test this possibility, we examined the light response of *mida*, *pif3*, and higher order *pif3pif4pif5*<sup>15</sup> dark-grown mutants. Our data showed defects in hypocotyl growth inhibition and cotyledon separation (Fig. 2) consistent with our hypothesis that the phy/PIF/MIDA network prevents an overresponse to light once deetiolation has been initially triggered.

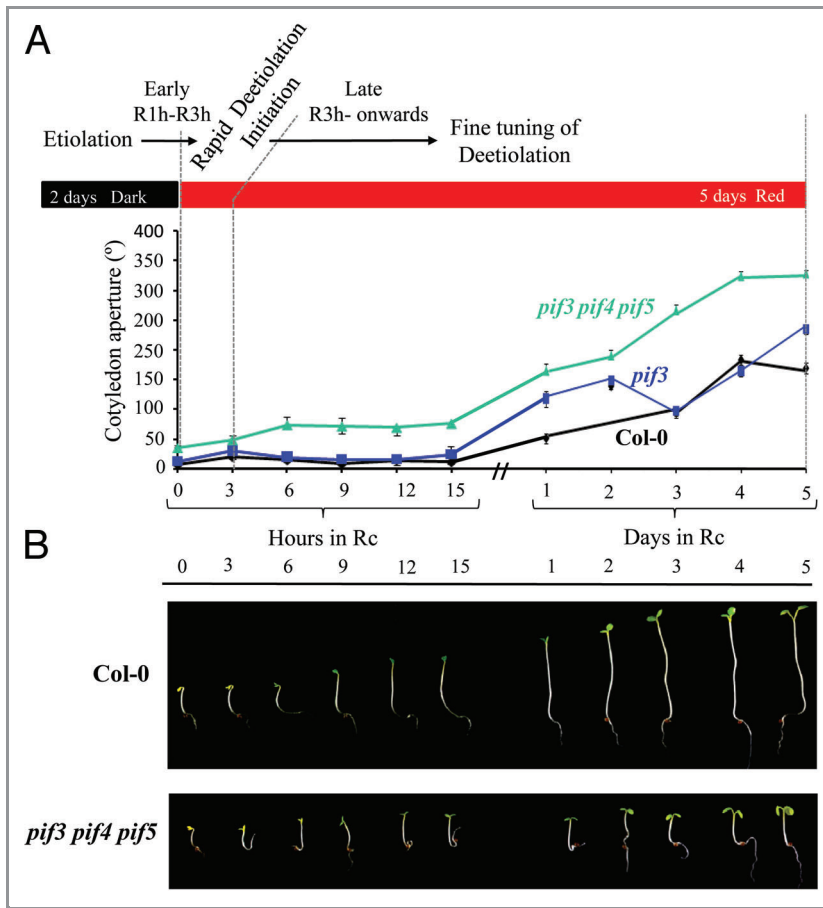


**Figure 2.** PIF-regulated initiation of deetiolation and prevention of seedling overresponses to light. (A, B) Dark-grown PIF-deficient seedlings exhibit an exaggerated response to Red Light (Rc = 8  $\mu\text{mol}/\text{m}^2/\text{s}$ ). (A) Time-course quantification of cotyledon separation of 2-d-old, dark-grown Col-0, *pif3* and *pif3 pif4 pif5* seedlings during the transition to Rc light for 5 d, showing the exaggerated cotyledon aperture in *pif3* and *pif3 pif4 pif5* seedlings compared with the wild-type Col-0. (B) Visual phenotype of 2-d-old, dark-grown *pif3 pif4 pif5* mutant seedlings, exposed to 0–5 d of Rc, showing the phenotypes displayed in comparison to the wild-type Col-0. Over response in cotyledon aperture and hypocotyl growth inhibition is shown. Experimental procedures are described in Sentandreu et al., 2011.

## Conclusions

Our results suggest that the etiolation program involves branching of the PIF3

## References

- Chen M, Chory J, Fankhauser C. Light signal transduction in higher plants. *Annu Rev Genet* 2004; 38:87-117; PMID:15568973; <http://dx.doi.org/10.1146/annurev.genet.38.072902.092259>
- Schäfer E, Nagy F. *Photomorphogenesis in Plants and Bacteria* 2006. Dordrecht, The Netherlands: Springer.
- Quail PH. Phytochromes. *Curr Biol* 2010; 20:R504-7; PMID:20620899; <http://dx.doi.org/10.1016/j.cub.2010.04.014>
- Leivar P, Quail PH. PIFs: pivotal components in a cellular signaling hub. *Trends Plant Sci* 2011; 16:19-28; PMID:20833098; <http://dx.doi.org/10.1016/j.tplants.2010.08.003>
- Bae G, Choi G. Decoding of light signals by plant phytochromes and their interacting proteins. *Annu Rev Plant Biol* 2008; 59:281-311; PMID:18257712; <http://dx.doi.org/10.1146/annurev.arplant.59.032607.092859>
- Moon J, Zhu L, Shen H, Huq E. PIF1 directly and indirectly regulates chlorophyll biosynthesis to optimize the greening process in Arabidopsis. *Proc Natl Acad Sci U S A* 2008; 105:9433-8; PMID:18591656; <http://dx.doi.org/10.1073/pnas.0803611105>
- Leivar P, Tepperman JM, Monte E, Calderon RH, Liu TL, Quail PH. Definition of early transcriptional circuitry involved in light-induced reversal of PIF-imposed repression of photomorphogenesis in young Arabidopsis seedlings. *Plant Cell* 2009; 21:3535-53; PMID:19920208; <http://dx.doi.org/10.1105/tpc.109.070672>
- Lorrain S, Trevisan M, Pradervand S, Fankhauser C. Phytochrome interacting factors 4 and 5 redundantly limit seedling de-etiolation in continuous far-red light. *Plant J* 2009; 60:449-61; PMID:19619162; <http://dx.doi.org/10.1111/j.1365-3113X.2009.03971.x>
- Sentandreu M, Martín G, González-Schain N, Leivar P, Soy J, Tepperman JM, et al. Functional profiling identifies genes involved in organ-specific branches of the PIF3 regulatory network in Arabidopsis. *Plant Cell* 2011; 23:3974-91; PMID:22108407; <http://dx.doi.org/10.1105/tpc.111.088161>

(Fig. 1). Branching of the signal that PIF3 exerts might be achieved through organ- or tissue-specific expression of these MIDA factors (Fig. 1). We propose that the action of the phy/PIF3/MIDA network extends beyond the maintenance of etiolation in the dark and the rapid initial deetiolation in response to light, and might be also critical to counteract the response to the light stimulus once deetiolation is underway (Fig. 2). We suggest that this counteractive regulation provides a fine-tuning mechanism to optimize the seedling response by allowing accurate adjustment and ensuring seedling fitness in the prevailing light environment.

## Acknowledgments

We thank Adrian J. Cutler for AOHSO seeds<sup>11</sup> (*mida1-OX*), and Brian E. Ellis for MPK12RNAi seeds<sup>12</sup> (*mida11*). SALK<sup>16</sup> and SAIL (Syngenta Arabidopsis Insertion Library) T-DNA lines (*mida9* and *mida10* respectively) were obtained from NASC. This work was supported by a Beatriu de Pinós fellowship from the “Comissionat per a Universitat i Recerca del Departament d’Innovació, Universitat i Empresa” and by Marie Curie IRG PIRG06-GA-2009-256420 grant to P.L., and by grants Marie Curie IRG-046568, Spanish “Ministerio de Ciencia e Innovación” BIO2006-09254 and BIO2009-07675, and Generalitat de Catalunya 2009-SGR-206 to E.M.

10. Monte E, Tepperman JM, Al-Sady B, Kaczorowski KA, Alonso JM, Ecker JR, et al. The phytochrome-interacting transcription factor, PIF3, acts early, selectively, and positively in light-induced chloroplast development. *Proc Natl Acad Sci U S A* 2004; 101:16091-8; PMID:15505214; <http://dx.doi.org/10.1073/pnas.0407107101>
11. Li F, Asami T, Wu X, Tsang EW, Cutler AJ. A putative hydroxysteroid dehydrogenase involved in regulating plant growth and development. *Plant Physiol* 2007; 145:87-97; PMID:17616511; <http://dx.doi.org/10.1104/pp.107.100560>
12. Lee JS, Wang S, Sritubtim S, Chen JG, Ellis BE. Arabidopsis mitogen-activated protein kinase MPK12 interacts with the MAPK phosphatase IBR5 and regulates auxin signaling. *Plant J* 2009; 57:975-85; PMID:19000167; <http://dx.doi.org/10.1111/j.1365-313X.2008.03741.x>
13. Khanna R, Kronmiller B, Maszle DR, Coupland G, Holm M, Mizuno T, et al. The Arabidopsis B-box zinc finger family. *Plant Cell* 2009; 21:3416-20; PMID:19920209; <http://dx.doi.org/10.1105/tpc.109.069088>
14. Shin J, Kim K, Kang H, Zulfugarov IS, Bae G, Lee CH, et al. Phytochromes promote seedling light responses by inhibiting four negatively-acting phytochrome-interacting factors. *Proc Natl Acad Sci U S A* 2009; 106:7660-5; PMID:19380720; <http://dx.doi.org/10.1073/pnas.0812219106>
15. Leivar P, Monte E, Oka Y, Liu T, Carle C, Castillon A, et al. Multiple phytochrome-interacting bHLH transcription factors repress premature seedling photomorphogenesis in darkness. *Curr Biol* 2008; 18:1815-23; PMID:19062289; <http://dx.doi.org/10.1016/j.cub.2008.10.058>
16. Alonso JM, Stepanova AN, Leisse TJ, Kim CJ, Chen H, Shinn P, et al. Genome-wide insertional mutagenesis of Arabidopsis thaliana. *Science* 2003; 301:653-7; PMID:12893945; <http://dx.doi.org/10.1126/science.1086391>

## Resumen Artículo 2:

### **Branching of the PIF3 regulatory network in Arabidopsis: Roles of PIF3-regulated MIDAs in seedling development in the dark and in response to light**

Maria Sentandreu, Pablo Leivar, Guiomar Martín, and Elena Monte.

### **Ramificación de la red de señalización de PIF3 en Arabidopsis: Función de los genes MIDA, regulados por PIF3, en el desarrollo de la plántula en oscuridad y durante la respuesta a luz.**

Tras germinar bajo tierra, las plantas necesitan ajustar cuidadosamente su desarrollo con tal de asegurar su supervivencia tanto en oscuridad, como en condiciones de luz, una vez alcanzada la superficie del suelo.

Estudios recientes demuestran que los foto-receptores de tipo fitocromo y los factores de interacción de fitocromos de tipo bHLH, los PIFs, regulan el desarrollo de la plántula ajustándolo a las condiciones lumínicas prevalecientes durante el estado post-germinativo. Aún así, todavía se desconoce con exactitud cuales son los mecanismos reguladores que implementan tales respuestas durante el desarrollo. En un estudio reciente publicado en la revista *The Plant Cell*, revelamos un grupo de genes regulados por el factor de transcripción PIF3 como potenciales reguladores del desarrollo de plántulas crecidas en oscuridad. Se trata de los genes MIDA, del inglés “MISREGULATED IN DARK” (DESREGULADOS EN OSCURIDAD). El análisis de la relevancia funcional de los MIDA mediante el uso de mutantes, demuestra que cuatro de ellos presentan alteraciones en el fenotipo durante la etiolación y además sugiere que la señal que PIF3 ejerce sobre estos genes se ramifica de manera específica de manera que cada mutante presenta defectos en el desarrollo de un órgano diferente. Además, nuestros resultados también indican una respuesta exagerada tras la exposición a luz en plántulas con una red de señalización PIF3/MIDA dañada o comprometida, lo que sugiere, que estos factores también son esenciales a la hora de iniciar y modular los ajustes necesarios que la plántula debe efectuar durante su desarrollo para adaptarse.



## **3<sup>rd</sup> Article**



# Phytochrome-imposed oscillations in PIF3 protein abundance regulate hypocotyl growth under diurnal light/dark conditions in Arabidopsis

Judit Soy<sup>1</sup>, Pablo Leivar<sup>1</sup>, Nahuel González-Schain<sup>1</sup>, Maria Sentandreu<sup>1</sup>, Salomé Prat<sup>2</sup>, Peter H. Quail<sup>3,4</sup> and Elena Monte<sup>1,\*</sup>

<sup>1</sup>Departament de Genètica Molecular, Center for Research in Agricultural Genomics (CRAG), CSIC-IRTA-UAB-UB, Campus Universitat Autònoma de Barcelona, Bellaterra, 08193 Barcelona, Spain,

<sup>2</sup>Departamento de Genética Molecular de Plantas, Centro Nacional de Biotecnología CSIC, Campus Universidad Autónoma de Madrid, Cantoblanco, 28049 Madrid, Spain,

<sup>3</sup>Department of Plant and Microbial Biology, University of California, Berkeley, CA 94720, USA, and

<sup>4</sup>United States Department of Agriculture, Plant Gene Expression Center, Albany, CA 94710, USA

Received 28 December 2011; revised 4 March 2012; accepted 8 March 2012; published online 11 June 2012.

\*For correspondence (e-mail elena.monte@cragenomics.es).

## SUMMARY

Arabidopsis seedlings display rhythmic growth when grown under diurnal conditions, with maximal elongation rates occurring at the end of the night under short-day photoperiods. Current evidence indicates that this behavior involves the action of the growth-promoting bHLH factors PHYTOCHROME-INTERACTING FACTOR 4 (PIF4) and PHYTOCHROME-INTERACTING FACTOR 5 (PIF5) at the end of the night, through a coincidence mechanism that combines their transcriptional regulation by the circadian clock with control of protein accumulation by light. To assess the possible role of PIF3 in this process, we have analyzed hypocotyl responses and marker gene expression in *pif* single- and higher-order mutants. The data show that PIF3 plays a prominent role as a promoter of seedling growth under diurnal light/dark conditions, in conjunction with PIF4 and PIF5. In addition, we provide evidence that PIF3 functions in this process through its intrinsic transcriptional regulatory activity, at least in part by directly targeting growth-related genes, and independently of its ability to regulate phytochrome B (phyB) levels. Furthermore, in sharp contrast to *PIF4* and *PIF5*, our data show that the *PIF3* gene is not subject to transcriptional regulation by the clock, but that PIF3 protein abundance oscillates under diurnal conditions as a result of a progressive decline in PIF3 protein degradation mediated by photoactivated phyB, and consequent accumulation of the bHLH factor during the dark period. Collectively, the data suggest that phyB-mediated, post-translational regulation allows PIF3 accumulation to peak just before dawn, at which time it accelerates hypocotyl growth, together with PIF4 and PIF5, by directly regulating the induction of growth-related genes.

**Keywords:** PIF3, hypocotyl elongation, short day, phytochrome-mediated degradation, transcriptional regulation, Arabidopsis.

## INTRODUCTION

Light is fundamental for plants as a source of energy as well as an indicator of their living environment. Plants perceive and respond to ambient light signals through informational photoreceptors that include the phytochrome family (phyA–phyE in Arabidopsis) (Rockwell *et al.*, 2006; Schafer and Nagy, 2006; Quail, 2010). The phytochromes perceive red (660 nm) and far red (720 nm) light of the solar spectrum, and monitor changes in light quality, quantity and duration

to control developmental and growth responses such as germination, seedling de-etiolation, shade avoidance and flowering time (Franklin and Quail, 2010; Strasser *et al.*, 2010). phyA is the only receptor for continuous far red light, but both phyA and phyB contribute to perception of continuous red light during early de-etiolation, with phyB being the dominant if not exclusive regulator of the hypocotyl-elongation response to continuous red light (Rockwell *et al.*,

2006; Schafer and Nagy, 2006; Tepperman *et al.*, 2006; Franklin and Quail, 2010). The phytochromes reversibly photoconvert between two conformers: the inactive red light-absorbing Pr form and the biologically active far red light-absorbing Pfr form. Pr to Pfr photoconversion takes place within seconds upon absorption of red light photons (Linschitz and Kasche, 1966), and reversion of Pfr to Pr occurs in far red light-enriched environments (Franklin, 2008), and also in the dark. In seedlings grown in the light, Pfr remains active upon initial transfer to the dark, but slowly reverts, at least partially, back to Pr with a half-life of approximately 60 min (Sweere *et al.*, 2001; Rausenberger *et al.*, 2010).

Phytochromes are synthesized in the cytoplasm in the inactive Pr form, and, upon photoactivation to Pfr, are translocated into the nucleus (Nagatani, 2004), where they associate with a subset of basic helix-loop-helix (bHLH) transcription factors called phytochrome-interacting factors (PIFs). The PIFs (PIF1, PIF3, PIF4, PIF5, PIF6 and PIF7 in *Arabidopsis*) accumulate in the dark and interact photoreversibly and conformation-specifically with the active Pfr phytochrome in the light (Leivar and Quail, 2011). This light-induced interaction between the Pfr phytochrome and PIF initiates a cascade of transcriptional changes that allows the seedling to adjust to the new light environment (Castillon *et al.*, 2007; Jiao *et al.*, 2007; Bae and Choi, 2008; Leivar and Quail, 2011). For a subset of these PIFs (PIF1, PIF3, PIF4 and PIF5), interaction with phyA and/or phyB triggers rapid phosphorylation and degradation of the PIF proteins within minutes (Bauer *et al.*, 2004; Park *et al.*, 2004; Shen *et al.*, 2005; Oh *et al.*, 2006; Nozue *et al.*, 2007; Shen *et al.*, 2007; Lorrain *et al.*, 2008; Shen *et al.*, 2008), establishing a new lower steady-state level of PIFs in continuous light (Monte *et al.*, 2004). Concomitantly, exposure to light induces rapid phyA degradation (with a half-life of <2 h), and a slower and more modest degradation of phyB (Hennig *et al.*, 1999; Khanna *et al.*, 2007; Al-Sady *et al.*, 2008), which remains relatively abundant in the light, together with phyC–phyE (Hirschfeld *et al.*, 1998). During prolonged growth in continuous light, the PIFs induce phyB proteolytic degradation through the proteasome system using COP1 as an E3 ligase (Khanna *et al.*, 2007; Al-Sady *et al.*, 2008; Leivar *et al.*, 2008a; Jang *et al.*, 2010), suggesting the existence of a mutually negative feedback loop between the phyB and PIF proteins (Leivar and Quail, 2011). This light-induced phyB degradation is expected to contribute to the progressive decline in Pfr levels during the dark period under diurnal conditions (light/dark cycles). In addition, the PIFs re-accumulate in light-grown seedlings upon exposure to darkness (such as under diurnal conditions) (Monte *et al.*, 2004; Shen *et al.*, 2005; Nozue *et al.*, 2007) or far red light-enriched environments (such as vegetational shade) (Lorrain *et al.*, 2008) through a process that depends on the activation state (or Pfr/Pr ratio) of the phytochromes.

Hypocotyl elongation is a well-established light-regulated response that is maximal in seedlings grown in continuous dark. In post-germinative darkness, the PIF proteins promote hypocotyl elongation through their intrinsic transcription factor capacity, regulating a transcriptional network that sustains etiolated growth (Leivar *et al.*, 2009; Shin *et al.*, 2009). This conclusion is supported by the observation that a quadruple mutant deficient in PIF1, 3, 4 and 5 (*pifq*) exhibits a partial constitutively photomorphogenic phenotype in the dark, characterized by a short-hypocotyl phenotype (Leivar *et al.*, 2008b). In continuous light, under which PIFs induce phyB degradation, PIF-deficient mutants display a hypersensitive short-hypocotyl phenotype that is interpreted to be, at least partially, the result of enhanced photosensitivity of the seedling due to elevated photoreceptor levels (Khanna *et al.*, 2007; Al-Sady *et al.*, 2008; Leivar *et al.*, 2008a).

Under diurnal conditions, with an alternating light/dark cycle, the extent of hypocotyl elongation depends on the duration of the dark period (Niwa *et al.*, 2009). During dark hours, the hypocotyl elongation rate is maximal at the end of the night in seedlings grown under short-day (SD) photoperiods (Nozue *et al.*, 2007). Studies have indicated that PIF4 and PIF5 are positive regulators of this response (Nozue *et al.*, 2007; Niwa *et al.*, 2009). The precise regulation of their time of action at the end of the dark period has been proposed to involve a coincidence mechanism that combines regulation of *PIF4* and *PIF5* transcript levels by the circadian clock, superimposed on the control of PIF protein accumulation by light (Nozue *et al.*, 2007; Nusinow *et al.*, 2011). In addition to PIF4 and PIF5, the current model predicts that additional, yet to be identified, factors are involved in the regulation of seedling growth under SD conditions.

In this study, we have used single and multiple *pif3*, *pif4* and *pif5* mutants, combined with analyses of PIF3 protein accumulation and target gene expression, to define the role of PIF3 in the regulation of hypocotyl elongation in seedlings grown under diurnal conditions, and have examined the relative contributions of PIF3, PIF4 and PIF5 to this response. Our results suggest that phytochromes generate an oscillation of PIF3 abundance under SD conditions such that it peaks just before dawn, at which time PIF3 plays a prominent role in promoting elongation growth, in conjunction with PIF4 and PIF5, at least in part by directly regulating the expression of growth-related genes.

## RESULTS

### The pattern of PIF3 accumulation under SD conditions is regulated by phyA and phyB and is independent of transcriptional regulation by the clock

To establish the pattern of *PIF3* expression under diurnal SD conditions [8 h white light + 16 h darkness], we analyzed *PIF3* transcript levels over 24 h during the third day of seedling growth under SD conditions (Figure 1a), and

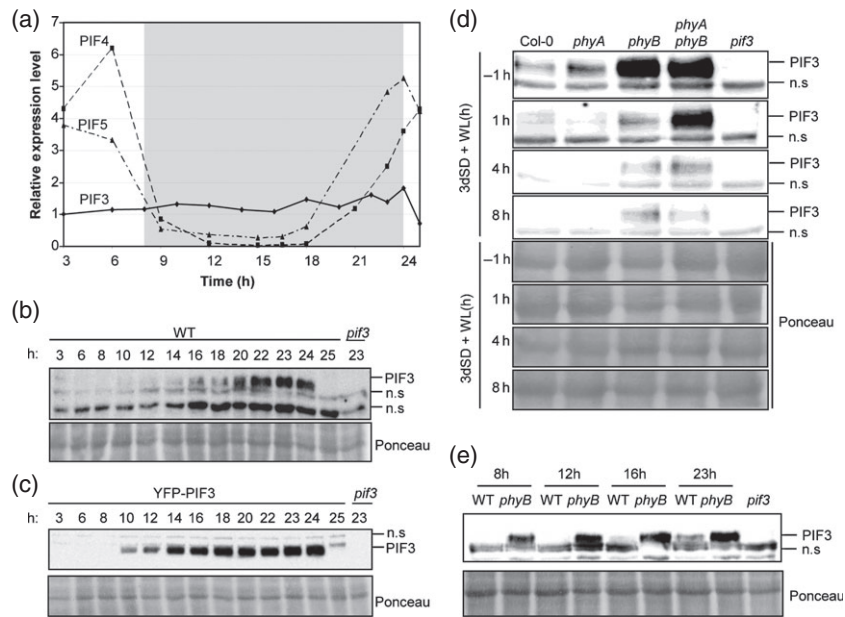


**Figure 1.** PIF3 protein accumulation under SD conditions.

Seedlings were grown under SD conditions for 2 days (a–c, e) or 3 days (d), and samples were taken during the following day at the specified time points.

(a) The expression of *PIF3*, *PIF4* and *PIF5* was analyzed by quantitative RT-PCR. Values were normalized to *PP2A*, and expression levels relative to *PIF3* at 3 h are shown. Values are means of technical triplicates.

(b) Immunoblot of protein extracts from WT seedlings.

(c) Immunoblot of protein extracts from seedlings over-expressing YFP-PIF3.

(d) Immunoblot of protein extracts from WT, *phyA-211*, *phyB-9* and *phyA phyB* seedlings.

(e) Immunoblot of protein extracts from WT and *phyB-9* seedlings.

For (b–e), a PIF3-specific polyclonal antibody was used as the probe (top). As an antibody specificity control, a protein extract from *pif3-3* harvested at time 23 h was included. Ponceau staining was used as a loading control (bottom). n.s., non-specific cross-reacting bands.

compared them to the expression pattern of *PIF4* and *PIF5*. *PIF3* transcript levels remained fairly constant over the 24 h photoperiod (Figure 1a). In sharp contrast, *PIF4* and *PIF5* transcript levels decreased during the day, stayed low during most of the dark period, and increased again to peak at the end of the night (Figure 1a), consistent with the previously reported circadian clock regulation of *PIF4* and *PIF5* transcript levels (Yamashino *et al.*, 2003; Nozue *et al.*, 2007; Niwa *et al.*, 2009). These results indicate that, in contrast to *PIF4* and *PIF5*, *PIF3* transcript levels do not oscillate under diurnal conditions, and suggest that the circadian clock does not regulate *PIF3* transcription under SD conditions.

We next examined the pattern of accumulation of the endogenous PIF3 protein under diurnal light/dark cycles. To do this, we grew seedlings under SD conditions and tested the levels of endogenous PIF3 protein every 1–3 h over a period of 24 h. PIF3 protein started to accumulate at the start of the dark period, as early as 2 h after the transition from light to dark (10 h time point, Figures 1b and S1), and kept accumulating progressively to reach a maximum at the end of the night, after 14–16 h of darkness (22, 23 and 24 h time points, Figure 1b). PIF3 protein levels then dropped to below the detection limit after exposure of seedlings to white light

for 1 h (25 h time point, Figure 1b). Transgenic plants over-expressing a YFP-PIF3 fusion (Al-Sady *et al.*, 2006) showed a similar pattern of YFP-PIF3 accumulation under SD conditions, with low levels during the light period and a progressive increase during the night and a peak at the end of the night (Figure 1c). A similar pattern was also observed in transgenic lines over-expressing PIF4:HA and PIF5:HA, although in these experiments the seedlings were grown under SD/3 conditions (i.e. 8 h light/dark cycles comprising 160 min light + 320 min dark) (Nozue *et al.*, 2007).

Together, the above experiments indicate that, under SD conditions, PIF3 protein levels are very low during the light period, but increase progressively during the night (Figure 1b) through post-transcriptional regulation (Figure 1a). In order to examine the role of phytochrome activity in regulation of this pattern of PIF3 accumulation, we measured PIF3 levels at the end of the night (-1 h) and after 1, 4 and 8 h of light exposure in *phyA* and *phyB* single and double mutants (Figure 1d). Wild-type (WT) seedlings accumulated PIF3 protein during the dark period, and light induced a rapid reduction in these levels within 1 h. Compared to WT, *phyA phyB* double mutants accumulated higher levels of PIF3 both at the end of the night and during the light period (Figure 1d), suggesting that *phyA* and/or

phyB act to reduce PIF3 levels under SD conditions. Detailed single *phyA* and *phyB* mutant analysis at various time points suggests that the two photoreceptors contribute differentially to this activity. First, *phyA* mutants showed similar levels of PIF3 at the end of the night compared to WT (Figure 1d), but the levels in *phyB* and *phyA phyB* mutants were much higher (Figure 1d). Second, in contrast to the rapid light-induced degradation of PIF3 observed in WT, *phyA* and *phyB* seedlings, PIF3 levels remained relatively constant in *phyA phyB* double mutants after 1 h of illumination (Figure 1d). Finally, PIF3 levels further decreased and remained below the detection limit in *phyA* mutants during the day (4 and 8 h time points), similar to the WT (Figure 1d). In *phyA phyB* mutants, PIF3 levels also decreased between 1 and 4 h of illumination but PIF3 was still detectable after 4 and 8 h of light. In contrast, PIF3 levels in the *phyB* mutant did not further decrease after 1 h of illumination, and its levels were similar during the rest of the light period. Together, these results suggest that *phyA* and *phyB* act redundantly to rapidly reduce PIF3 levels within 1 h of illumination, and that at least one other photoreceptor is involved in the decrease in PIF3 levels at later time points (between 1 and 4 h). This scenario is similar to that reported during seedling de-etiolation, where *phyD* was shown to act together with *phyA* and *phyB* to induce PIF3 degradation in etiolated seedlings transferred to light (Bauer *et al.*, 2004; Al-Sady *et al.*, 2006). In addition, *phyB* activity is required to induce complete PIF3 degradation during the light period, and to prevent re-accumulation of PIF3 during the dark hours, in a process that requires little or no participation of *phyA*.

To obtain further insight into the role of *phyB* in preventing re-accumulation of PIF3 during the night in SD-grown seedlings, we performed a more detailed comparison of PIF3 levels in WT and the *phyB* mutant during the dark period. Figure 1(e) shows that PIF3 levels at the start of the night (8 h time point) were higher in *phyB* compared to WT seedlings, and rapidly increased in *phyB* during the first 4 h of darkness (8–12 h time points), reaching a new steady-state level that remained relatively constant until the end of the night (23 h). In contrast, PIF3 re-accumulation in the WT was slower during the first hours of darkness, and much lower levels were observed at the end of the night (Figure 1e). Together, our results suggest that the induction of PIF3 degradation by photoactive *phyB* Pfr during the light period extends into the first hours of the subsequent dark period. This possibility is in accordance with previous data showing that a far red light pulse given at the start of a 12 h dark period (removing the Pfr phytochrome pool from the cell) induced faster re-accumulation of GUS activity in GUS:PIF3 over-expressing seedlings grown under day-neutral conditions (Monte *et al.*, 2004), and with the observation that the Pfr form of the photoreceptor continues to function in the dark to induce PIF3 degradation (Al-Sady *et al.*, 2006).

### PIF3 is necessary for hypocotyl growth under SD conditions

To examine the role of PIF3 during seedling growth under SD conditions, we measured hypocotyl elongation in seedlings lacking PIF3 (Monte *et al.*, 2004). Hypocotyls of 3-day-old SD-grown *pif3* mutants were approximately 40% shorter than the Col-0 control under these conditions (Figure 2a,b). In detailed time-course analyses, we found that WT hypocotyls elongated from 2 days onwards after germination under SD conditions, but the growth rate was severely reduced in the *pif3* mutants (Figure 2c). The impact of PIF3 deficiency on growth was already apparent 48 h after initial exposure to SD, the first time point at which it was possible to measure seedling length (Figure 2c). In comparison to SD conditions, WT seedlings were shorter when grown under continuous white light (Figure 2b,d), and *pif3* mutants grown under continuous white light were only slightly shorter than the WT (Figure 2d). These data indicate that the 16 h dark period in SD-grown seedlings accelerates hypocotyl elongation, consistent with previous reports (Niwa *et al.*, 2009). Together with the PIF3 protein accumulation pattern (Figure 1), our data suggest that PIF3 is an important component of the cellular machinery that induces growth during the night hours.

In contrast to the short phenotype of *pif3* (Figure 2b), *phyB* mutant seedlings had more elongated hypocotyls than WT under SD conditions (Michael *et al.*, 2008; Niwa *et al.*, 2009), indicating an antagonistic functional relationship between *phyB* and PIF3 in regulating this response. Characterization of *phyB* and *pif3* single and double mutants showed that *phyB* seedlings grown under SD conditions were approximately 1.5 mm taller than the corresponding WT (Figure 2b,e), and that genetic removal of PIF3 partially and significantly suppressed the *phyB* phenotype by 1 mm (Figure 2b, *phyB* versus *pif3 phyB*). These data suggest that the increased levels of PIF3 (Figure 1d) are at least partially responsible for the elongated hypocotyl phenotype of *phyB* mutant seedlings. In addition, compared to SD conditions, *phyB* mutant seedlings grown under continuous white light displayed a much reduced tall-hypocotyl phenotype (Figure 2d) and reduced suppression of this phenotype by the *pif3* mutation (Figure 2d, *phyB* versus *pif3 phyB*). These data suggest that the dark period is necessary for full expression of the *phyB* mutant phenotype, probably by allowing higher accumulation of PIF3 protein under SD conditions compared to continuous white light (Figure 1d,e). Correlation between PIF3 levels and hypocotyl elongation was further observed in *phyA phyB* mutants (Figure S2). Compared to *phyB*, the double *phyA phyB* mutant had slightly longer hypocotyls under SD conditions, in agreement with the higher PIF3 levels detected at the start of the day in *phyA phyB* compared to *phyB* (Figure 1d).

Previously, PIF3-deficient mutants were shown to have increased *phyB* levels under continuous red light,

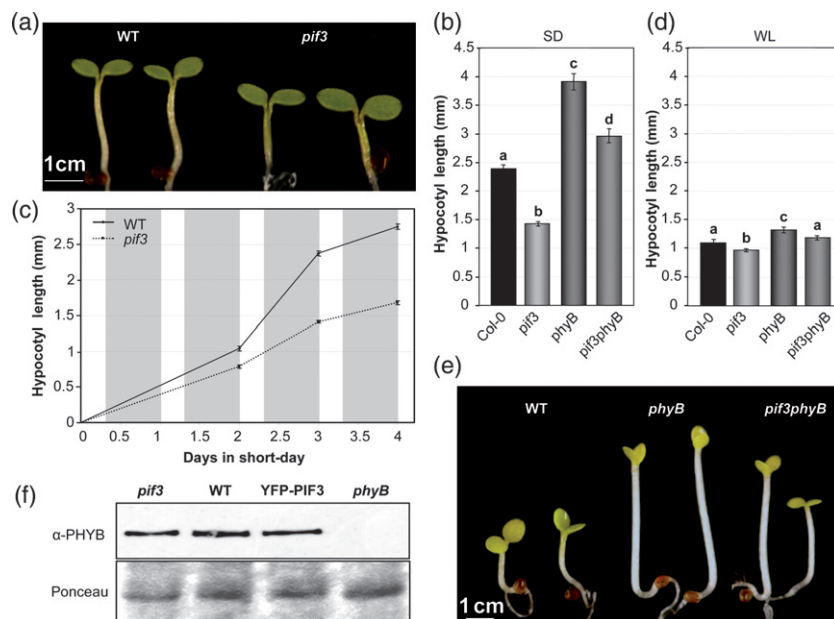


**Figure 2.** PIF3 promotes hypocotyl growth under SD conditions (8 h light/16 h dark).

(a) Visual phenotype of 3-day-old SD-grown WT and *pif3* mutant seedlings.

(b) Hypocotyl length in 3-day-old SD-grown WT and *pif3* seedlings.

(c) Growth curves for hypocotyl length in WT and *pif3* seedlings grown under SD for 4 days.

(d) Hypocotyl length in 3-day-old WT and *pif3* seedlings grown under continuous white light (WL).

(e) Visual phenotype of 3-day-old SD-grown WT, *pif3*, *phyB* and *pif3 phyB* mutant seedlings.

(f) Immunoblots of protein extracts from 3-day-old WT and *pif3* seedlings. Seedlings were grown under SD conditions for 2 days, and samples were harvested during the third day at the specified time points. Extracts were probed using *phyB*-specific monoclonal antibodies (top). Ponceau staining was used as a loading control (bottom).

For (b–d), data are means  $\pm$  SE of at least 30 seedlings. For (b, d), different letters indicate significant differences among means ( $P < 0.05$ ).

contributing to their hypersensitive hypocotyl phenotype (Monte *et al.*, 2004; Al-Sady *et al.*, 2008; Leivar *et al.*, 2008a). To examine whether the described negative feedback modulation of *phyB* photoreceptor levels by PIF3 under prolonged continuous red light and continuous white light conditions (Leivar *et al.*, 2012a) operates under SD conditions, we measured *phyB* levels in the *pif3* mutant and in YFP-PIF3 over-expressing lines at the end of the light period (8 h time point). Figure 2(f) shows that there were no significant differences in *phyB* levels between genotypes after 8 h of illumination, suggesting that PIF3-induced down-regulation of *phyB* requires more extended periods of light exposure. Together with our observation that PIF3 promotes growth under SD conditions in the absence of *phyB* (Figure 2b), these results indicate that PIF3 function under SD conditions is not exerted indirectly through regulation of *phyB* levels, and instead suggest that the PIF3 contribution to hypocotyl length under SD conditions is exerted through its intrinsic transcriptional activity, in accordance with previous data in etiolated seedlings (Al-Sady *et al.*, 2008; Leivar *et al.*, 2008b; Moon *et al.*, 2008; Leivar *et al.*, 2009; Shin *et al.*, 2009; Sentandreu *et al.*, 2011) and during shade avoidance (Hornitschek *et al.*, 2009).

### Expression of phytochrome-regulated, growth-related genes peaks at the end of the night under SD conditions and requires PIF3

To test whether PIF3 regulates growth-related genes under SD conditions, we measured the expression of *PIL1* (*PHYTOCHROME-INTERACTING FACTOR 3-LIKE 1*), *HFR1* (*LONG HYPOCOTYL IN FAR-RED 1*) and *XTR7* (*XYLOGLUCAN ENDOTRANSGLYCOSYLASE 7*) in WT and *pif3* seedlings. These genes are repressed by the phytochromes and are up-regulated under conditions in which hypocotyl elongation is induced (Salter *et al.*, 2003; Lorrain *et al.*, 2008; Hornitschek *et al.*, 2009; Leivar *et al.*, 2009; Nozue *et al.*, 2011), and have been proposed to be direct targets of transcriptional regulation by PIF4 in dark-adapted plants (de Lucas *et al.*, 2008) and/or by PIF5 during shade avoidance (Hornitschek *et al.*, 2009). *PIL1* and *HFR1* are PIF-related transcription factors (Leivar and Quail, 2011), and *XTR7* encodes a xyloglucan endotransglycosylase-related protein that is potentially involved in cell-wall growth (Sasidharan *et al.*, 2010).

Time-course expression analysis indicated that the expression levels of these three genes under SD conditions remain low during the light period in the WT, and start accumulating during the dark, peaking at the end of the night

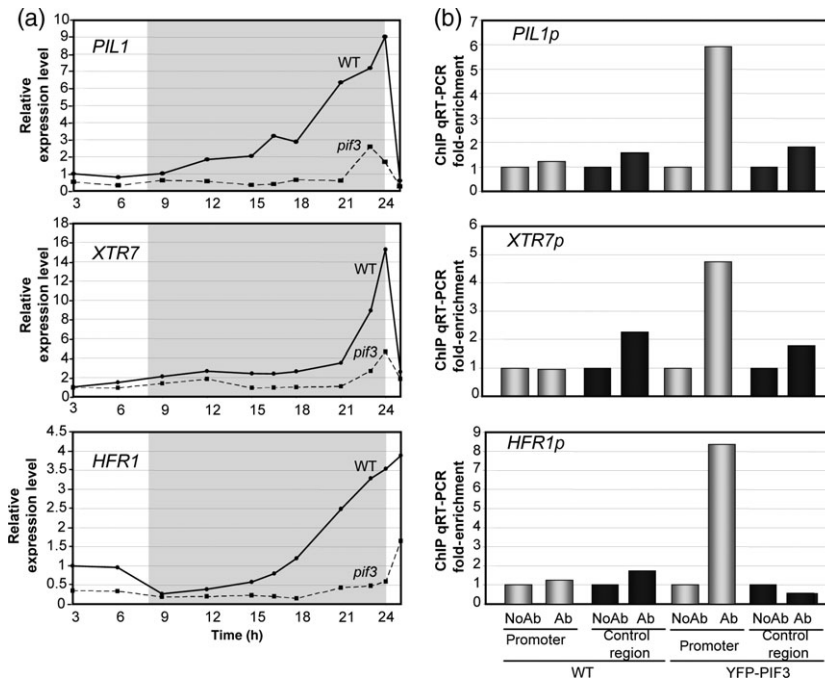


**Figure 3.** PIF3 regulates gene expression under SD conditions.

(a) Expression of *PIL1*, *XTR7* and *HFR1* was analyzed by quantitative RT-PCR in 2-day-old SD-grown seedlings. Samples were taken during the third day under SD conditions at the specified time points. Values were normalized to *PP2A*. Expression levels relative to WT at 3 h are shown. Data are the means of technical triplicates.

(b) Chromatin immunoprecipitation (ChIP) from 3-day-old SD-grown WT and YFP-PIF3 seedlings. Immunoprecipitated DNA was quantified by quantitative RT-PCR using primers in promoter regions containing G-boxes (promoter) or control regions without G-boxes (control region). Experiments include samples processed with anti-GFP antibody (Ab) and controls processed without antibody (NoAb). Data shown correspond to one representative ChIP experiment. The results of an additional ChIP experiment are shown in Figure S4. Data are the means of at least two technical replicates.

(Figure 3a). The expression levels at the end of the night were 4-, 10- and 16-fold greater than the levels during the light period for *HFR1*, *PIL1* and *XTR7*, respectively (Figure 3a). Interestingly, the pattern of expression of these genes parallels the accumulation pattern of PIF3 protein (Figure 1b,c), rendering them good candidate genes for regulation by PIF3. Expression analysis by quantitative RT-PCR showed that their transcript levels are clearly reduced in the *pif3* mutant, with the amplitude of the peak at the end of the night reduced by 80–90% for the three genes tested (Figure 3a). These data indicate that PIF3 induces expression of *PIL1*, *HFR1* and *XTR7* during the dark period under SD conditions, and suggest that PIF3 promotes growth under diurnal conditions by regulating expression of growth-related genes.

#### PIF3 directly binds to G-box-containing promoters of growth marker genes *in vivo*

*HFR1*, *PIL1* and *XTR7* genes harbor G-boxes in their promoters (Hornitschek *et al.*, 2009) (Figure S3), suggesting that they are possible direct targets of PIF3 (Martínez-García *et al.*, 2000; Shin *et al.*, 2007). We analyzed the binding of PIF3 to the promoters of *HFR1*, *PIL1* and *XTR7* by chromatin immunoprecipitation (ChIP) using plants expressing PIF3

tagged with YFP (YFP-PIF3). ChIP was performed using an anti-GFP antibody, and immunoprecipitated G-box-containing and control DNA fragments were quantified by quantitative RT-PCR. Control DNA regions included non-G-box-containing regions of tested or unrelated genes. As controls, we used YFP-PIF3 plants processed without anti-GFP antibody, and Col-0 plants subjected to the same process with and without antibody. We performed these experiments in seedlings grown under SD conditions for 3 days and harvested at the end of the night (time point 23 h), when the maximum levels of PIF3 (Figure 1b) and the peak of expression of these genes coincide (Figure 3a). We observed significant enrichment of binding of PIF3 to the regions of *HFR1*, *PIL1* and *XTR7* promoters containing the G-box (Figures 3b and S4). These data indicate that PIF3 directly binds to the promoter regions of *HFR1*, *PIL1* and *XTR7*, presumably through the G-box motif, and suggest that these genes are direct targets of transcriptional regulation by PIF3 under SD conditions.

#### PIF3 regulates hypocotyl growth and gene expression under SD conditions, together with PIF4 and PIF5

The observation that *pif3* seedlings exhibit a reduced but still significant growth response to SD conditions compared to

WT (Figure 2b,c) indicates that factors other than PIF3 are involved in the induction of hypocotyl elongation under SD conditions. Evidence obtained using *pif4* and *pif5* mutants indicates that these additional factors are probably PIF4 and PIF5 (Nozue *et al.*, 2007; Niwa *et al.*, 2009). To obtain insight into the contribution of PIF3 to the promotion of hypocotyl elongation under SD conditions relative to that of PIF4 and PIF5, we first analyzed the hypocotyl length of 3-day-old SD-grown *pif3*, *pif4*, *pif5*, *pif4 pif5* and *pif3 pif4 pif5* mutant seedlings. Under these conditions, *pif4* and *pif5* single mutants showed a quantitatively similar short-hypocotyl phenotype compared to the WT, an effect that was additive in the *pif4 pif5* mutant, in accordance with previous reports (Figure 4a) (Nozue *et al.*, 2007). In comparison, *pif3* seedlings had more prominent short-hypocotyl phenotype than either *pif4* or *pif5*, and this phenotype was similar in magnitude to that of the double *pif4 pif5* mutant (Figure 4a). Moreover, the triple *pif3 pif4 pif5* mutant had slightly shorter hypocotyls compared to *pif3* (Figure 4a), confirming that PIF4 and PIF5 promote at least part of the residual growth of *pif3* seedlings under SD conditions. We also compared the hypocotyl lengths of *pif3 phyB* and the *pif3 pif4 pif5 phyB* quadruple mutant. Our data indicate that removal of PIF4 and PIF5 in *pif3 pif4 pif5 phyB* had an additive effect over removal of PIF3 in *pif3 phyB*, and further suppressed the *phyB* tall phenotype (Figure 4b). Altogether, these results suggest that PIF3, PIF4 and PIF5 collectively function in the promotion of hypocotyl length under SD conditions, with the role of PIF3 probably being more prominent.

To examine the interactions between PIF3, PIF4 and PIF5 in regulating gene expression under SD conditions, we analyzed *PIL1* expression in various *pif3*, *pif4* and *pif5* mutant combinations at the end of the night when expression of this gene peaks in the WT (23 h time point) (Figure 3a). The data show that individual deficiencies in PIF4 or PIF5 marginally reduced the level of *PIL1* transcript (WT versus *pif4* and *pif5* single mutants), but a greater (and significant) reduction was observed in *pif3* seedlings (Figure 4c). In addition, double mutant combinations including *pif3 (pif3 pif4 and pif3 pif5)* showed a further dramatic reduction in *PIL1* expression (Figure 4c), indicating synergistic interactions between these factors for induction of *PIL1* expression under SD conditions. Similar to the phenotypic analysis (Figure 4a), the magnitude of the reduction in *PIL1* gene expression in *pif3* mutants was similar to that of the double *pif4 pif5* mutant (Figure 4c), and a further reduction in *PIL1* expression was observed in *pif3 pif4 pif5*. These results suggest that PIF3 dominates the induction of *PIL1* under SD conditions at the 23 h time point, and PIF4 and PIF5 are responsible for the residual *PIL1* expression observed in *pif3* single mutant seedlings at the end of the night (Figures 3a and 4c). Consistent with this observation, time-course analysis of *XTR7* expression over the night showed that the peak of expression detected in *pif3*

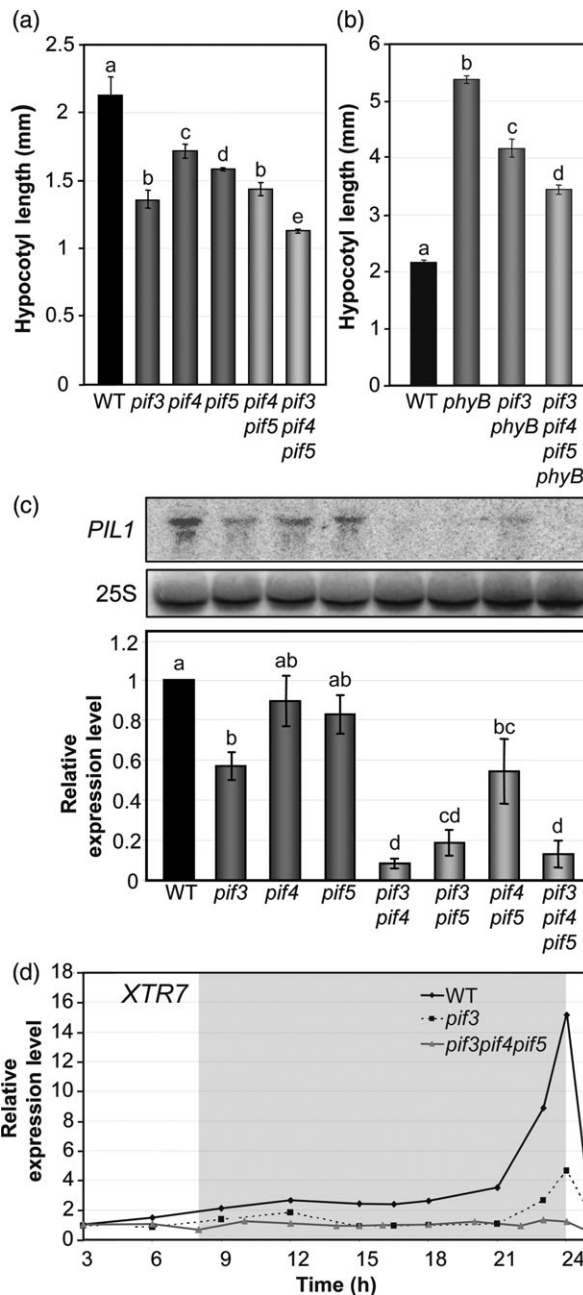


**Figure 4.** PIF3, PIF4 and PIF5 collectively regulate hypocotyl length and gene expression under SD conditions.

(a) Hypocotyl length in 3-day-old SD-grown WT, *pif3*, *pif4*, *pif5*, *pif4 pif5* and *pif3 pif4 pif5* seedlings.

(b) Hypocotyl length in 3-day-old SD-grown WT, *phyB*, *pif3 phyB* and *pif3 pif4 pif5 phyB* seedlings.

(c) The expression of *PIL1* was analyzed by RNA blots of 3-day-old SD-grown WT, *pif3*, *pif4*, *pif5*, *pif3 pif4*, *pif3 pif5*, *pif4 pif5* and *pif3 pif4 pif5* seedlings. A representative blot is shown (top). Quantitative data (bottom) are means of three biological replicates; bars represent SE. Values were normalized to 25S rRNA.

(d) Expression of *XTR7* was analyzed by quantitative RT-PCR in 2-day-old SD-grown WT, *pif3* and *pif3 pif4 pif5* seedlings during the third day of SD conditions. Values were normalized to *PP2A*. Expression levels relative to WT at 3 h are shown. Data are the means of technical triplicates.

For (a, b), data are means  $\pm$  SE of at least 30 seedlings. For (a–c), different letters indicate significant differences among means ( $P < 0.05$ ).

(Figures 3a and 4d) is essentially absent in *pif3 pif4 pif5* (Figure 4d), again suggesting that PIF4 and PIF5 are responsible for the residual *XTR7* expression observed in *pif3* single mutant seedlings at the end of the night. Together, the morphological (Figure 4a,b) and gene expression analyses (Figure 4c,d) suggest that PIF3, in conjunction with PIF4 and PIF5, plays a prominent role in induction of growth-related genes at the end of the night to promote growth under SD conditions.

#### PIF3 is required to promote growth at the end of the night under SD conditions

When grown under SD conditions, seedlings display rhythmic growth, with maximal elongation rates occurring at the end of the night (Nozue *et al.*, 2007). To test whether the *pif3* mutant shows an impaired growth pattern, we monitored seedling growth during a 24 h cycle, and calculated the growth rate of *pif3* seedlings compared to WT. Our data show that WT seedlings, in accordance with previously published results (Nozue *et al.*, 2007), maintain low growth rates during the day and the first half of the night, and the growth rate peaks at the end of the night (Figure 5a). In contrast, *pif3* seedlings show a strong reduction in this growth peak (Figure 5a). These results are in accordance with the progressive pattern of PIF3 protein accumulation in the dark (Figure 1b,c) and the occurrence of PIF3-induced gene expression at the end of the night (Figure 3a), and suggest that the short hypocotyls in the *pif3* mutant under SD conditions (Figure 2a,b) are mainly the result of a reduced growth rate at dawn. Together, these results indicate that PIF3 is required for hypocotyl elongation under diurnal conditions by promoting growth at the end of the night, as has been previously shown for PIF4 and PIF5 (Nozue *et al.*, 2007).

#### DISCUSSION

For *Arabidopsis* seedlings grown under SD conditions, the growth rate peaks at the end of the dark period. This rhythmic growth is implemented in part by the growth-promoting factors PIF4 and PIF5, and coincidence of both light and the circadian clock regulation determines their time of action just before dawn (Nozue *et al.*, 2007; Niwa *et al.*, 2009). The experiments presented here examine whether and through what mechanism PIF3 contributes to seedling growth under diurnal conditions. The data indicate that PIF3 protein accumulates progressively during the night under the control of phyB through a mechanism that does not involve transcriptional regulation by the clock, and provide evidence that PIF3, in conjunction with PIF4 and PIF5, is a major component of the cellular machinery that promotes hypocotyl elongation at dawn during growth under SD conditions, functioning at least in part through direct regulation of expression of growth-related genes (Figure 5b).

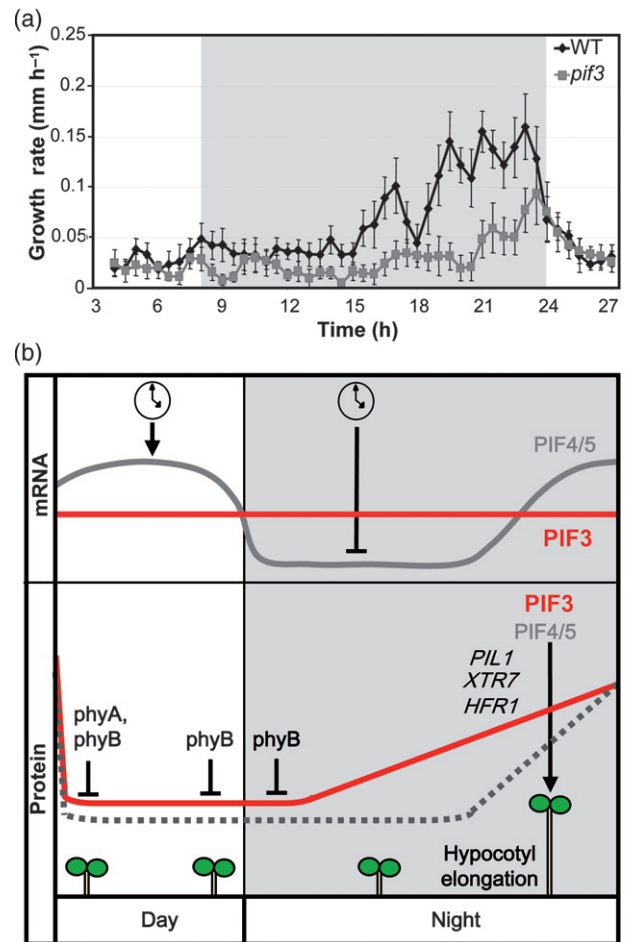


**Figure 5.** PIF3 is required to promote growth at the end of the night under SD conditions.

(a) Hypocotyl elongation rate under SD conditions. Infrared imaging was used to monitor seedling growth from 2 days onwards. The growth rate is plotted as a function of time. Values are means  $\pm$  SE of seven seedlings.

(b) Simplified model depicting PIF3- and PIF4/5-mediated hypocotyl growth under SD conditions. Top: the circadian clock regulates oscillation of *PIF4* and *PIF5* transcript abundance in SD-grown seedlings, whereas *PIF3* remains constant throughout the day. Bottom: phyA and phyB activities induce degradation of PIF3 during the day (probably with an additional contribution from phyD), and phyB is active during the first part of the night to keep PIF3 levels low. As the night proceeds, phyB activity decreases and PIF3 progressively accumulates, peaking at the end of the night. For PIF4 and PIF5, coincidence of the circadian clock and light regulation ensures that protein accumulation peaks at the end of the night (Nozue *et al.*, 2007). Endogenous PIF3 protein oscillation is indicated by a solid line, and the predicted endogenous PIF4/5 protein oscillation is indicated by a dashed line. PIF3 directly induces the expression of growth-related genes at the end of the night (exemplified by *PIL1*, *HFR1* and *XTR7*), in conjunction with PIF4 and PIF5, to induce hypocotyl growth before dawn.

Our phenotypic and marker gene expression analyses of *pif* single and higher-order mutants provide evidence that PIF3 is necessary for seedling growth under SD conditions in conjunction with PIF4 and PIF5, and suggest that the PIF3 contribution is comparable to that of PIF4 and PIF5 combined. Various lines of evidence support this conclusion.

First, the *pif3* mutant displays a more prominent short-hypocotyl phenotype than either *pif4* or *pif5* under SD conditions, and this phenotype is similar in magnitude to that of the *pif4 pif5* double mutant (Figure 4a). Second, the *PIL1* expression level in *pif3* shows a greater reduction with respect to WT than in either single *pif4* or *pif5* mutants, and a similar level of reduction to *pif4 pif5* (Figure 4c). Finally, the *pif3 pif4* and *pif3 pif5* mutants show even more reduced *PIL1* gene expression compared to *pif3* or *pif4 pif5*, and this is similar to the triple mutant *pif3 pif4 pif5* (Figure 4c). These data thus suggest that PIF3, PIF4 and PIF5 act together to promote hypocotyl elongation under diurnal conditions, and that PIF3 appears to play a more prominent role. Interestingly, the relative contributions of PIF3 and PIF4/PIF5 to the promotion of seedling growth under diurnal conditions appear to be different from the relative contribution of each PIF under other growth conditions. For example, the roles of PIF3, PIF4 or PIF5 in induction of hypocotyl growth in etiolated seedlings are mainly apparent in the absence of PIF1, the PIF with the strongest contribution to the hypocotyl response in post-germinative growth in the dark (Leivar *et al.*, 2012b). In contrast, although no individual PIF appears to dominate the growth response to a continuous low red/far red ratio (Leivar *et al.*, 2012b), PIF3 makes a greater contribution to afternoon shade events under diurnal conditions (Sellaro *et al.*, 2012), and PIF4 is the strongest contributor to high-temperature effects (Koini *et al.*, 2009; Stavang *et al.*, 2009; Franklin *et al.*, 2011). Together, these data suggest that the contribution of a given PIF to hypocotyl elongation varies between growth situations.

Previous results have shown that PIF3 demonstrates dual functioning during seedling de-etiolation: (i) as a transcriptional regulator during development in the dark and in the initial dark-to-light transition, and (ii) as a regulator of phyB homeostasis during sustained growth under prolonged light conditions. Evidence presented here suggests that, under SD conditions, a growth regime that alternates dark and light periods, PIF3 does not regulate phyB levels (Figure 2). Given the slow dynamics of PIF-induced phyB degradation in response to the initial light signal (Khanna *et al.*, 2007; Al-Sady *et al.*, 2008), it is likely that the short length of the light period (only 8 h) under SD conditions is not enough to promote a detectable effect. Instead, the role of PIF3 as promoter of hypocotyl growth appears to be mediated through its intrinsic transcriptional activity directly regulating the expression of growth-related genes (Figure 3). Our results show that, under SD conditions, PIF3 binds to the promoters and probably directly regulates expression of target genes that were previously reported to be growth-related during etiolation and shade avoidance, such as *PIL1*, *HFR1* and *XTR7* (Figure 3). These genes have been previously shown to be direct targets of PIF4 and/or PIF5 in dark-adapted plants (de Lucas *et al.*, 2008) and under shade conditions (Hornitschek *et al.*, 2009), respectively, and there-

fore it was not unexpected to find that PIF4 and PIF5 regulate their expression also under SD conditions (Figure 4), in accordance with recent data from Nozue *et al.* (2011) for *HFR1* and *XTR7*. However, as indicated by the results for *PIL1*, the contribution of each of these PIFs to full induction appears to vary between growth conditions: whereas PIF3 is the strongest contributor under SD conditions (Figure 4b), PIF5 dominates in shade (Lorrain *et al.*, 2008; Leivar *et al.*, 2012b). These results suggest different target affinity and/or different relative levels of each PIF depending on the growth conditions.

The results presented here indicate that phyA and phyB are redundant in the rapid phytochrome-mediated degradation of PIF3 within 1 h after transition from darkness to light under SD conditions (Figure 1d), mirroring the phytochrome-mediated degradation of PIF3 during early stages of illumination of etiolated seedlings (Bauer *et al.*, 2004; Al-Sady *et al.*, 2006). These data suggest that PIF3 degradation under SD conditions may also require direct interaction with the phytochrome photoreceptor, leading to rapid phosphorylation of the transcription factor and degradation via the ubiquitin–proteasome system, as described for etiolated seedlings (Bauer *et al.*, 2004; Al-Sady *et al.*, 2006). In addition, our results show that the absence of phyB in *phyB* and *phyA phyB* mutants results in over-accumulation of PIF3 during the dark period, and that these elevated levels are reduced to a certain extent in response to prolonged light conditions (after 4 h), indicating that another photoreceptor is also involved in regulation of PIF3 degradation during the day. These results again mirror those observed in de-etiolation experiments, suggesting that this additional photoreceptor may be phyD (Bauer *et al.*, 2004; Al-Sady *et al.*, 2006). However, adding to previous data for dark-grown seedlings exposed to light (Bauer *et al.*, 2004; Al-Sady *et al.*, 2006), our evidence that the pool of PIF3 protein is not degraded in the absence of phyB indicates that phyB is necessary to mediate complete degradation of PIF3 during the light period under diurnal conditions (Figure 1e). This result provides evidence that phyB regulates degradation of PIF3 under SD conditions during the last part of the day. In addition, the observed re-accumulation of PIF3 in the absence of phyB during the first part of the night (Figure 1e) provides evidence that phyB also targets PIF3 for degradation at the start of the dark period. The extent of phyB action during the night is presumably determined by its dark reversion rate, which has been estimated to have a half-life of 1 h (Sweere *et al.*, 2001; Rausenberger *et al.*, 2010), as well as potentially via selective degradation of the Pfr form.

Our observation that phytochrome regulation keeps PIF3 protein levels low during the day and the first part of the night, with subsequent progressive accumulation, provides evidence for a phytochrome-mediated mechanism of PIF3 oscillation under SD conditions. Although phytochrome-imposed regulation of PIF3 protein accumulation may be

sufficient to ensure timing of action of PIF3 at the end of the night, without additional transcriptional regulation by the circadian clock, a scenario in which the clock post-translationally regulates or fine-tunes PIF3 accumulation and/or activity indirectly cannot be completely discounted. DELLA proteins have been shown to interfere with PIF3 and PIF4 binding to DNA (de Lucas *et al.*, 2008; Feng *et al.*, 2008), and a recent report showed that DELLA proteins accumulate at the start of the night in seedlings grown under diurnal conditions (Arana *et al.*, 2011). Therefore, DELLA proteins could represent a mechanism to prevent PIF3 from binding and inducing its target genes when its levels start to increase during the first part of the night. Further investigation is required to address this possibility.

Taken together, the data presented here indicate that PIF3 has a prominent role as a promoter of hypocotyl elongation under SD conditions, at least in part by directly regulating the expression of growth-related genes. Our work also reveals that phyA, phyB and possibly phyD induce degradation of PIF3 during the dark-to-light transition and the light period of diurnally grown seedlings, and residual photoactivated phyB prevents re-accumulation of PIF3 during the first part of the night. Our findings imply that PIFs regulating growth under diurnal conditions do not necessarily have to be transcriptionally regulated by the clock as previously shown for PIF4 and PIF5, and that phytochrome-mediated regulation may be sufficient. However, the existence of other more indirect layers of regulation of PIF3 by the clock and/or factors such as DELLA proteins (or other unknown mechanisms) cannot be excluded, and these may fine-tune the timing of PIF3 action under SD conditions.

## EXPERIMENTAL PROCEDURES

### Seedling growth and hypocotyl measurements

Wild-type and mutant *Arabidopsis thaliana* seeds used in these studies were all in the Columbia (Col-0) ecotype and have been described elsewhere, including *pif3-3* (Monte *et al.*, 2004), *pif4-2* and *pif3 pif4* (Leivar *et al.*, 2008a), *pif5-3* (Khanna *et al.*, 2007), *pif3 pif5*, *pif4 pif5* and *pif3 pif4 pif5 phyB* (Leivar *et al.*, 2012a), *pif3 pif4 pif5* (Leivar *et al.*, 2008b), *phyB-9* (Reed *et al.*, 1993), *pif3 phyB* (Al-Sady *et al.*, 2008), *phyA-211* (Nagatani *et al.*, 1993), *phyA phyB* (Cerdan and Chory, 2003) and *pif3::YFP-PIF3* (Al-Sady *et al.*, 2006).

Seeds were sterilized and plated on germination medium (GM) (Valvekens *et al.*, 1988) without sucrose as previously described (Monte *et al.*, 2003). Seedlings were then stratified for 4 days at 4°C in darkness, and then placed under short-day (SD) conditions [8 h white light (85  $\mu\text{mol m}^{-2} \text{sec}^{-1}$ ) + 16 h dark] for the time indicated in each experiment. For hypocotyl measurements, seedlings were arranged horizontally on a plate, photographed using a digital camera (Nikon D80, <http://www.nikon.com/>) and measured as described previously (Monte *et al.*, 2003). At least 30 seedlings for each line were measured to calculate the mean and standard error. For time-lapse photography, seedlings were grown on vertical plates, and, after 2 days of growth, photographs were taken at 30 min intervals for 24 h. To acquire images in the dark, 5 sec illumination was provided by an infrared light-emitting diode, and

photographs were taken using an infrared-sensitive digital camera (Nikon D80). Hypocotyls of seven Col-0 and *pif3* seedlings were measured, and the growth rate was calculated for each individual seedling.

### Protein extraction and immunoblots

Protein extracts were prepared from 2- and 3-day-old seedlings grown under SD conditions as indicated. Tissue samples were collected and frozen in liquid nitrogen, and samples were manually ground under frozen conditions before resuspension in extraction buffer. The extraction buffer used and protein quantification were as previously described (Leivar *et al.*, 2008a). Total protein extracts were subjected to SDS-PAGE (7.5%) for immunodetection of phyB and YFP-PIF3 protein (80  $\mu\text{g}$ ) or endogenous PIF3 (200  $\mu\text{g}$ ). Proteins were transferred to Hybond C membrane (Amersham Biosciences), and the membrane was stained with Ponceau S as a loading control. Immunodetection of PIF3 and YFP-PIF3 was performed using a rabbit anti-PIF3 polyclonal antibody (Al-Sady *et al.*, 2006), incubated overnight with Hikari solution (Nacalai Tesque), and immunodetection of phyB was performed using mouse monoclonal anti-phyB (B1 and B7) antibodies (Somers *et al.*, 1991). Peroxidase-linked anti-rabbit secondary antibody (Amersham Biosciences) for PIF3 and anti-mouse secondary antibody for phyB (Amersham Biosciences) and a SuperSignal West Femto chemiluminescence kit (Pierce) were used for detection of luminescence using a LAS-4000 Image imaging system (Fujifilm).

### Gene expression analysis

For RNA blots, total RNA was extracted from 4-day-old SD-grown seedlings as described by Monte *et al.* (2003) (see Table S1 for primer sequences used to amplify the *PIL1* probe). Hybridization signal was quantified using a Storm 860 PhosphorImager (Molecular Dynamics) and normalized to 25S rRNA levels.

For quantitative RT-PCR analysis, RNA extraction, cDNA synthesis and quantitative RT-PCR were performed as described previously (Sentandreu *et al.*, 2011). Gene expression was measured in three technical replicates for each biological sample. *PP2A* (*AT1G13320*) was used as a normalization control as described previously (Shin *et al.*, 2007). Table S1 lists primer sequences.

### Chromatin immunoprecipitation (ChIP) assays

ChIP assays were performed using 3-day-old SD-grown *pif3::YFP-PIF3* and Col-0 seedlings as described previously (Gendrel *et al.*, 2002). After sonication, protein was quantified, and the inputs used in the subsequent immunoprecipitation step were equivalent for all samples. Antibody samples were immunoprecipitated by overnight incubation with GFP antibody-bound resin (GFP Agarose Beads, MBL). Mock ChIP reactions were performed without antibody to measure non-specific binding to target sequences. After immunoprecipitation, purified DNA was subjected to quantitative RT-PCR using promoter- and control-specific primers (Table S1) for each gene of interest. Quantitative RT-PCR results in the presence or absence of antibody for each genotype were first normalized to their input, and fold enrichment was then calculated for each antibody-containing sample relative to the corresponding sample lacking antibody.

### Statistics

Data were analyzed by one-way ANOVA, and the differences between means were evaluated using Duncan's *post-hoc* multiple comparison test (SPSS statistics software, IBM). Statistically significant differences were defined as those with a *P* value < 0.05.

## ACKNOWLEDGEMENTS

This work was supported by a JAE pre-doctoral fellowship (Jae-Pre\_08\_01049) and a JAE Estancia Breve grant (2010ESTCSIC-12125 for a short stay in S.P.'s laboratory) from CSIC to J.S., a 'Comissionat per a Universitats i Recerca del Departament d'Innovació, Universitats i Empresa' fellowship from the Generalitat de Catalunya (Beatriu de Pinós program) and Marie Curie International Reintegration Grant PIRG06-GA-2009-256420 to P.L., by National Institutes of Health Grant GM-47475, Department of Energy Grant DEFG03-87ER13742, and USDA Agricultural Research Service Current Research Information System Grant 5335-21000-027-00D to P.H.Q., and Marie Curie International Reintegration Grant 046568, grants from the Spanish Ministerio de Ciencia e Innovación (BIO2006-09254 and BIO2009-07675), and a grant from the Generalitat de Catalunya (2009-SGR-206) to E.M.

## SUPPORTING INFORMATION

Additional Supporting Information may be found in the online version of this article:

**Figure S1.** Accumulation of PIF3 in SD-grown seedlings.

**Figure S2.** Hypocotyl phenotype of *phyA*, *phyB* and *phyA phyB* seedlings under SD conditions.

**Figure S3.** Relative position of ChIP primers.

**Figure S4.** Additional biological replicate for the ChIP experiment shown in Figure 3(b).

**Table S1.** List of primer sequences.

Please note: As a service to our authors and readers, this journal provides supporting information supplied by the authors. Such materials are peer-reviewed and may be re-organized for online delivery, but are not copy-edited or typeset. Technical support issues arising from supporting information (other than missing files) should be addressed to the authors.

## REFERENCES

- Al-Sady, B., Ni, W., Kircher, S., Schafer, E. and Quail, P.H. (2006) Photoactivated phytochrome induces rapid PIF3 phosphorylation prior to proteasome-mediated degradation. *Mol. Cell*, **23**, 439–446.
- Al-Sady, B., Kikis, E.A., Monte, E. and Quail, P.H. (2008) Mechanistic duality of transcription factor function in phytochrome signaling. *Proc. Natl Acad. Sci. USA*, **105**, 2232–2237.
- Arana, M.V., Marin-de la Rosa, N., Maloof, J.N., Blazquez, M.A. and Alabadi, D. (2011) Circadian oscillation of gibberellin signaling in Arabidopsis. *Proc. Natl. Acad. Sci. USA*, **108**, 9292–9297.
- Bae, G. and Choi, G. (2008) Decoding of light signals by plant phytochromes and their interacting proteins. *Annu. Rev. Plant Biol.*, **59**, 281–311.
- Bauer, D., Viczian, A., Kircher, S. et al. (2004) Constitutive photomorphogenesis 1 and multiple photoreceptors control degradation of phytochrome interacting factor 3, a transcription factor required for light signaling in Arabidopsis. *Plant Cell*, **16**, 1433–1445.
- Castillon, A., Shen, H. and Huq, E. (2007) Phytochrome interacting factors: central players in phytochrome-mediated light signaling networks. *Trends Plant Sci.* **12**, 514–521.
- Cerdan, P.D. and Chory, J. (2003) Regulation of flowering time by light quality. *Nature*, **423**, 881–885.
- Feng, S., Martinez, C., Gusmaroli, G. et al. (2008) Coordinated regulation of *Arabidopsis thaliana* development by light and gibberellins. *Nature*, **451**, 475–479.
- Franklin, K.A. (2008) Shade avoidance. *New Phytol.* **179**, 930–944.
- Franklin, K.A. and Quail, P.H. (2010) Phytochrome functions in Arabidopsis development. *J. Exp. Bot.* **61**, 11–24.
- Franklin, K.A., Lee, S.H., Patel, D. et al. (2011) Phytochrome-interacting factor 4 (PIF4) regulates auxin biosynthesis at high temperature. *Proc. Natl Acad. Sci. USA*, **108**, 20231–20235.
- Gendrel, A.V., Lippman, Z., Yordan, C., Colot, V. and Martienssen, R.A. (2002) Dependence of heterochromatic histone H3 methylation patterns on the Arabidopsis gene *DDM1*. *Science*, **297**, 1871–1873.
- Hennig, L., Buche, C., Eichenberg, K. and Schafer, E. (1999) Dynamic properties of endogenous phytochrome A in Arabidopsis seedlings. *Plant Physiol.* **121**, 571–577.
- Hirschfeld, M., Tepperman, J.M., Clack, T., Quail, P.H. and Sharrock, R.A. (1998) Coordination of phytochrome levels in *phyB* mutants of Arabidopsis as revealed by apoprotein-specific monoclonal antibodies. *Genetics*, **149**, 523–535.
- Hornitschek, P., Lorrain, S., Zoete, V., Michielin, O. and Fankhauser, C. (2009) Inhibition of the shade avoidance response by formation of non-DNA binding bHLH heterodimers. *EMBO J.* **28**, 3893–3902.
- Jang, I.C., Henriques, R., Seo, H.S., Nagatani, A. and Chua, N.H. (2010) Arabidopsis Phytochrome interacting factor proteins promote phytochrome B polyubiquitination by COP1 E3 ligase in the nucleus. *Plant Cell*, **22**, 2370–2383.
- Jiao, Y., Lau, O.S. and Deng, X.W. (2007) Light-regulated transcriptional networks in higher plants. *Nat. Rev. Genet.* **8**, 217–230.
- Khanna, R., Shen, Y., Marion, C.M., Tsuchisaka, A., Theologis, A., Schafer, E. and Quail, P.H. (2007) The basic helix-loop-helix transcription factor PIF5 acts on ethylene biosynthesis and phytochrome signaling by distinct mechanisms. *Plant Cell*, **19**, 3915–3929.
- Koini, M.A., Alvey, L., Allen, T., Tilley, C.A., Harberd, N.P., Whitelam, G.C. and Franklin, K.A. (2009) High temperature-mediated adaptations in plant architecture require the bHLH transcription factor PIF4. *Curr. Biol.* **19**, 408–413.
- Leivar, P. and Quail, P.H. (2011) PIFs: pivotal components in a cellular signaling hub. *Trends Plant Sci.* **16**, 19–28.
- Leivar, P., Monte, E., Al-Sady, B., Carle, C., Storer, A., Alonso, J.M., Ecker, J.R. and Quail, P.H. (2008a) The Arabidopsis phytochrome-interacting factor PIF7, together with PIF3 and PIF4, regulates responses to prolonged red light by modulating *phyB* levels. *Plant Cell*, **20**, 337–352.
- Leivar, P., Monte, E., Oka, Y., Liu, T., Carle, C., Castillon, A., Huq, E. and Quail, P.H. (2008b) Multiple phytochrome-interacting bHLH transcription factors repress premature seedling photomorphogenesis in darkness. *Curr. Biol.* **18**, 1815–1823.
- Leivar, P., Tepperman, J.M., Monte, E., Calderon, R.H., Liu, T.L. and Quail, P.H. (2009) Definition of early transcriptional circuitry involved in light-induced reversal of PIF-imposed repression of photomorphogenesis in young Arabidopsis seedlings. *Plant Cell*, **21**, 3535–3553.
- Leivar, P., Monte, E., Cohn, M.M. and Quail, P.H. (2012a) Phytochrome signaling in green Arabidopsis seedlings: impact assessment of a mutually-negative *phyB*-PIF feedback loop. *Mol. Plant*, **5**, 208–223.
- Leivar, P., Tepperman, J.M., Cohn, M.M., Monte, E., Al-Sady, B., Erickson, E. and Quail, P.H. (2012b) Dynamic Antagonism Between Phytochromes and PIF-family bHLHs Induces Selective Reciprocal Responses to Light and Shade in a Rapidly Responsive Transcriptional Network in Arabidopsis. *Plant Cell*, **24**, 1398–1419.
- Linschitz, H. and Kasche, V. (1966) The kinetics of phytochrome conversion. *J. Biol. Chem.* **241**, 3395–3403.
- Lorrain, S., Allen, T., Duek, P.D., Whitelam, G.C. and Fankhauser, C. (2008) Phytochrome-mediated inhibition of shade avoidance involves degradation of growth-promoting bHLH transcription factors. *Plant J.* **53**, 312–323.
- de Lucas, M., Daviere, J.M., Rodriguez-Falcon, M., Pontin, M., Iglesias-Pedraz, J.M., Lorrain, S., Fankhauser, C., Blazquez, M.A., Titarenko, E. and Prat, S. (2008) A molecular framework for light and gibberellin control of cell elongation. *Nature*, **451**, 480–484.
- Martinez-Garcia, J.F., Huq, E. and Quail, P.H. (2000) Direct targeting of light signals to a promoter element-bound transcription factor. *Science*, **288**, 859–863.
- Michael, T.P., Breton, G., Hazen, S.P., Priest, H., Mockler, T.C., Kay, S.A. and Chory, J. (2008) A morning-specific phytohormone gene expression program underlying rhythmic plant growth. *PLoS Biol.* **6**, e225.
- Monte, E., Alonso, J.M., Ecker, J.R., Zhang, Y., Li, X., Young, J., Austin-Phillips, S. and Quail, P.H. (2003) Isolation and characterization of *phyC* mutants in Arabidopsis reveals complex crosstalk between phytochrome signaling pathways. *Plant Cell*, **15**, 1962–1980.
- Monte, E., Tepperman, J.M., Al-Sady, B., Kaczorowski, K.A., Alonso, J.M., Ecker, J.R., Li, X., Zhang, Y. and Quail, P.H. (2004) The phytochrome-interacting transcription factor, PIF3, acts early, selectively, and positively in light-induced chloroplast development. *Proc. Natl Acad. Sci. USA*, **101**, 16091–16098.

- Moon, J., Zhu, L., Shen, H. and Huq, E. (2008) PIF1 directly and indirectly regulates chlorophyll biosynthesis to optimize the greening process in *Arabidopsis*. *Proc. Natl Acad. Sci. USA*, **105**, 9433–9438.
- Nagatani, A. (2004) Light-regulated nuclear localization of phytochromes. *Curr. Opin. Plant Biol.* **7**, 708–711.
- Nagatani, A., Reed, J.W. and Chory, J. (1993) Isolation and initial characterization of *Arabidopsis* mutants that are deficient in phytochrome A. *Plant Physiol* **102**, 269–277.
- Niwa, Y., Yamashino, T. and Mizuno, T. (2009) The circadian clock regulates the photoperiodic response of hypocotyl elongation through a coincidence mechanism in *Arabidopsis thaliana*. *Plant Cell Physiol.* **50**, 838–854.
- Nozue, K., Covington, M.F., Duek, P.D., Lorrain, S., Fankhauser, C., Harmer, S.L. and Maloof, J.N. (2007) Rhythmic growth explained by coincidence between internal and external cues. *Nature*, **448**, 358–361.
- Nozue, K., Harmer, S.L. and Maloof, J.N. (2011) Genomic analysis of circadian clock-, light-, and growth-correlated genes reveals Phytochrome-Interacting Factor5 as a modulator of auxin signaling in *Arabidopsis*. *Plant Physiol.* **156**, 357–372.
- Nusinow, D.A., Helfer, A., Hamilton, E.E., King, J.J., Imaizumi, T., Schultz, T.F., Farre, E.M. and Kay, S.A. (2011) The ELF4-ELF3-LUX complex links the circadian clock to diurnal control of hypocotyl growth. *Nature*, **475**, 398–402.
- Oh, E., Yamaguchi, S., Kamiya, Y., Bae, G., Chung, W.I. and Choi, G. (2006) Light activates the degradation of PIL5 protein to promote seed germination through gibberellin in *Arabidopsis*. *Plant J.* **47**, 124–139.
- Park, E., Kim, J., Lee, Y., Shin, J., Oh, E., Chung, W.I., Liu, J.R. and Choi, G. (2004) Degradation of phytochrome interacting factor 3 in phytochrome-mediated light signaling. *Plant Cell Physiol.* **45**, 968–975.
- Quail, P.H. (2010) Phytochromes. *Curr. Biol.* **20**, R504–R507.
- Rausenberger, J., Hussong, A., Kircher, S., Kirchenbauer, D., Timmer, J., Nagy, F., Schafer, E. and Fleck, C. (2010) An integrative model for phytochrome B mediated photomorphogenesis: from protein dynamics to physiology. *PLoS One*, **5**, e10721.
- Reed, J.W., Nagpal, P., Poole, D.S., Furuya, M. and Chory, J. (1993) Mutations in the gene for the red/far-red light receptor phytochrome B alter cell elongation and physiological responses throughout *Arabidopsis* development. *Plant Cell*, **5**, 147–157.
- Rockwell, N.C., Su, Y.S. and Lagarias, J.C. (2006) Phytochrome structure and signaling mechanisms. *Annu. Rev. Plant Biol.* **57**, 837–858.
- Salter, M.G., Franklin, K.A. and Whitelam, G.C. (2003) Gating of the rapid shade-avoidance response by the circadian clock in plants. *Nature*, **426**, 680–683.
- Sasidharan, R., Chinnappa, C.C., Staal, M., Elzenga, J.T., Yokoyama, R., Nishitani, K., Voeselek, L.A. and Pierik, R. (2010) Light quality-mediated petiole elongation in *Arabidopsis* during shade avoidance involves cell wall modification by xyloglucan endotransglucosylase/hydrolases. *Plant Physiol.* **154**, 978–990.
- Schafer, E. and Nagy, F. (2006) *Photomorphogenesis in Plants and Bacteria*. Dordrecht, The Netherlands: Springer.
- Sellaro, R., Pacin, M. and Casal, J.J. (2012) Diurnal dependence of growth responses to shade in *Arabidopsis*: role of hormone, clock, and light signaling. *Mol. Plant*, **5**, 93–102.
- Sentandreu, M., Martin, G., Gonzalez-Schain, N., Leivar, P., Soy, J., Tepperman, J.M., Quail, P.H. and Monte, E. (2011) Functional profiling identifies genes involved in organ-specific branches of the PIF3 regulatory network in *Arabidopsis*. *Plant Cell*, **23**, 3974–3991.
- Shen, H., Moon, J. and Huq, E. (2005) PIF1 is regulated by light-mediated degradation through the ubiquitin-26S proteasome pathway to optimize photomorphogenesis of seedlings in *Arabidopsis*. *Plant J.* **44**, 1023–1035.
- Shen, Y., Khanna, R., Carle, C.M. and Quail, P.H. (2007) Phytochrome induces rapid PIF5 phosphorylation and degradation in response to red-light activation. *Plant Physiol.* **145**, 1043–1051.
- Shen, H., Zhu, L., Castillon, A., Majee, M., Downie, B. and Huq, E. (2008) Light-induced phosphorylation and degradation of the negative regulator Phytochrome-Interacting Factor1 from *Arabidopsis* depend upon its direct physical interactions with photoactivated phytochromes. *Plant Cell*, **20**, 1586–1602.
- Shin, J., Park, E. and Choi, G. (2007) PIF3 regulates anthocyanin biosynthesis in an HY5-dependent manner with both factors directly binding anthocyanin biosynthetic gene promoters in *Arabidopsis*. *Plant J.* **49**, 981–994.
- Shin, J., Kim, K., Kang, H., Zulfugarov, I.S., Bae, G., Lee, C.H., Lee, D. and Choi, G. (2009) Phytochromes promote seedling light responses by inhibiting four negatively-acting phytochrome-interacting factors. *Proc. Natl Acad. Sci. USA*, **106**, 7660–7665.
- Somers, D.E., Sharrock, R.A., Tepperman, J.M. and Quail, P.H. (1991) The *hy3* long hypocotyl mutant of *Arabidopsis* is deficient in phytochrome B. *Plant Cell*, **3**, 1263–1274.
- Stavang, J.A., Gallego-Bartolome, J., Gomez, M.D., Yoshida, S., Asami, T., Olsen, J.E., Garcia-Martinez, J.L., Alabadi, D. and Blazquez, M.A. (2009) Hormonal regulation of temperature-induced growth in *Arabidopsis*. *Plant J.* **60**, 589–601.
- Strasser, B., Sanchez-Lamas, M., Yanovsky, M.J., Casal, J.J. and Cerdan, P.D. (2010) *Arabidopsis thaliana* life without phytochromes. *Proc. Natl Acad. Sci. USA*, **107**, 4776–4781.
- Sweere, U., Eichenberg, K., Lohrmann, J., Mira-Rodado, V., Baurle, I., Kudla, J., Nagy, F., Schafer, E. and Harter, K. (2001) Interaction of the response regulator ARR4 with phytochrome B in modulating red light signaling. *Science*, **294**, 1108–1111.
- Tepperman, J.M., Hwang, Y.S. and Quail, P.H. (2006) *phyA* dominates in transduction of red-light signals to rapidly responding genes at the initiation of *Arabidopsis* seedling de-etiolation. *Plant J.* **48**, 728–742.
- Valvekens, D., Montagu, M.V. and Van Lijsebettens, M. (1988) *Agrobacterium tumefaciens*-mediated transformation of *Arabidopsis thaliana* root explants by using kanamycin selection. *Proc. Natl Acad. Sci. USA*, **85**, 5536–5540.
- Yamashino, T., Matsushika, A., Fujimori, T., Sato, S., Kato, T., Tabata, S. and Mizuno, T. (2003) A link between circadian-controlled bHLH factors and the APRR1/TOC1 quintet in *Arabidopsis thaliana*. *Plant Cell Physiol.* **44**, 619–629.

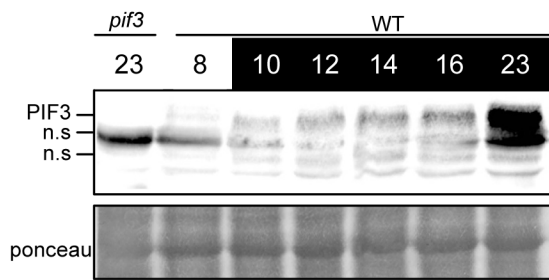


**Figure S1**

(a)



(b)

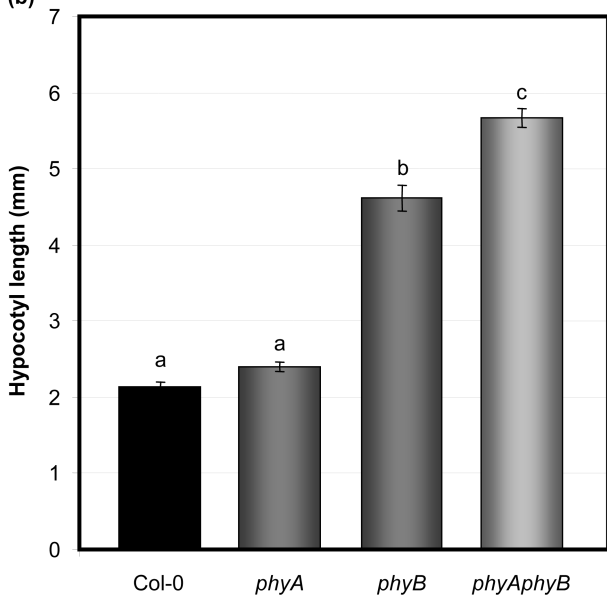


**Figure S2**

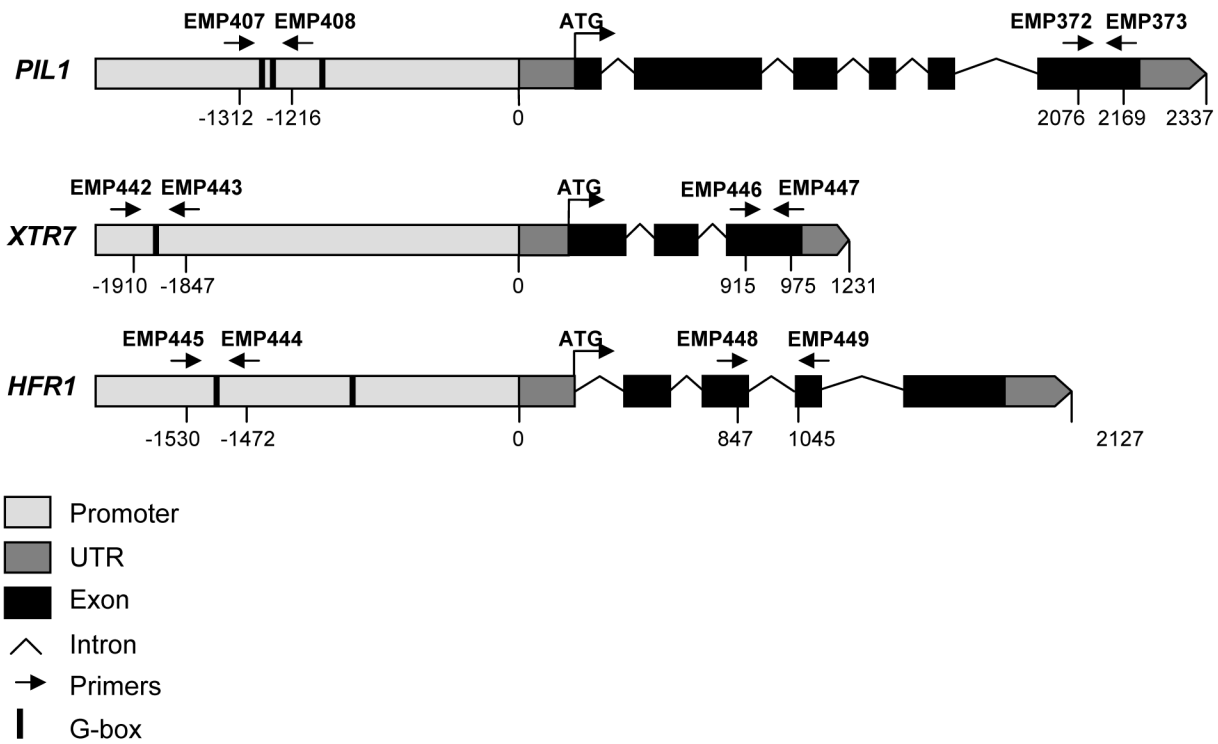


**Figure S3**

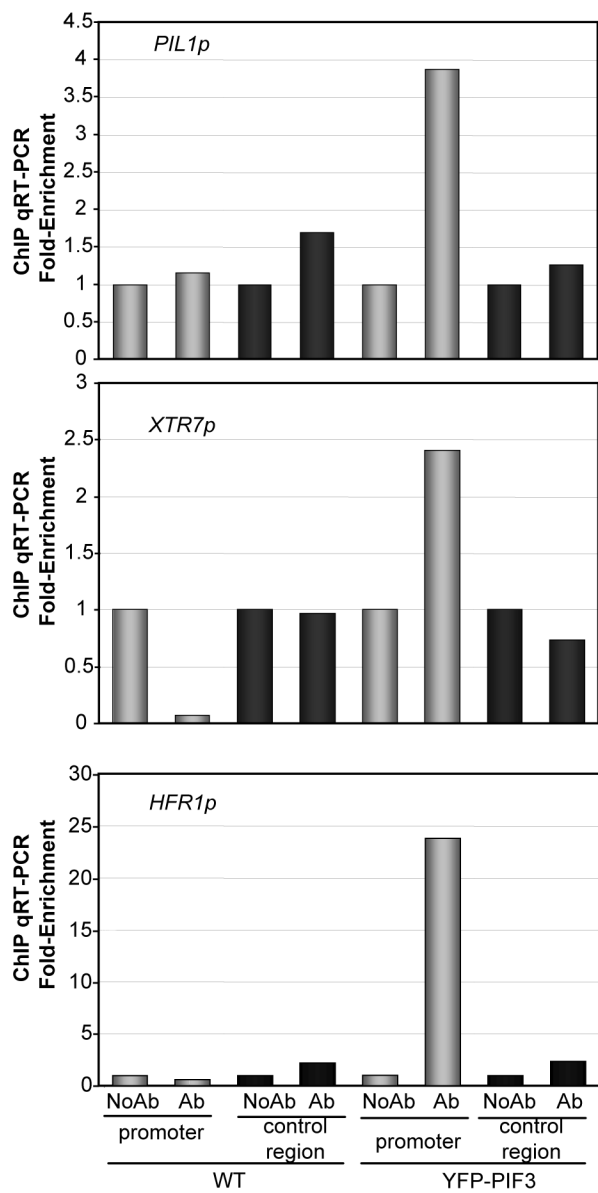


**Figure S4**

## Supplemental Legends

### Figure S1. Accumulation of PIF3 in short-day (SD) grown seedlings

Immunoblot of protein extracts from wild-type Col-0 seedlings. Seedlings were grown in SD for 2 days and samples were taken during the third day at the specified time points. A PIF3-specific polyclonal antibody was used as probe (top). As antibody specificity control, a protein extract from *pif3-3* harvested at time 21 h is included. Ponceau staining was used as a loading control (bottom). n.s., nonspecific, cross-reacting bands.

### Figure S2. Hypocotyl phenotype of *phyA*, *phyB*, and *phyAphyB* seedlings in SD conditions

(A) Visual phenotype of 3-day-old SD-grown WT, *phyA*, *phyB* and *phyAphyB* mutant seedlings.

(B) Hypocotyl length in 3-day-old SD-grown WT, *phyA*, *phyB* and *phyAphyB* seedlings. Data are means and s.e. of at least 30 seedlings. Different letters denote significant differences among means ( $P < 0.05$ ).

### Figure S3. Relative position of ChIP primers

Relative position of the primers used to amplify promoter and control regions in the ChIP experiments. G-boxes are indicated with vertical black lines.

### Figure S4. Additional biological replicate for the ChIP experiment shown in Figure 3b.

Chromatin immunoprecipitation (ChIP) from 3 day-old SD-grown wild-type and YFP-PIF3 seedlings. Immunoprecipitated DNA was quantified by qRT-PCR using primers in the promoter region containing G-boxes (promoter) or control regions without G-boxes (control region). Experiments include samples processed with anti-GFP antibody (Ab) and controls processed without antibody (NoAb). Data are average of at least two technical replicates.

### Table S1. List of primer sequences

Reference					Sequence (from 5' to 3')
Use	Gene	AGI number	Code	Original Code (*)	
RNA blots	<i>PIL1</i>	<i>AT2G46970</i>	EMP3		GATGAAGATTATATGGAGCTGGTG
			EMP4		CGAAGTTCCTCGAGAAAACCTTCG
qRT-PCR	<i>PIL1</i>	<i>AT2G46970</i> Promoter	EMP407		ACAAGAAAGAAGGGAGGGAGACA
			EMP408		TTCTCTTTAAATGGGACCCACAAT
		Coding region	EMP372		TGCCTTCGTGTGTTTCTCAG
			EMP373		AACTAAAACCGTTGCTTCCTC
	<i>XTR7</i>	<i>AT4G14130</i> Promoter	EMP442	pPH120	CGCATGCCGGCTGGAATAGATAG
			EMP443	pPH121	CGACGTGTCACTTCCCTCGTACC
		Coding region	EMP446	pPH130	CGGCTTGCACAGCCTCTT
			EMP447	pPH131	TCGGTTGCCACTTGCAATT
	<i>HFR1</i>	<i>AT1G02340</i> Promoter	EMP444	pPH112	ACGTGATGCCCTCGTGATGGAC
			EMP445	pPH113	GTCGCTCGCTAAGACACCAAC
		Coding region	EMP448	pPH126	GATGCGTAAGCTACAGCAACTCGT
			EMP449	pPH127	AGAACCGAAACCTTGCCGTCTTG
	<i>PIF3</i>	<i>AT1G09530</i>	EMP417		GGT ATG GGA ATG CCT TAT GCA
			EMP418		TGG AAC TGT GGT CCG TGG TTA
	<i>PIF4</i>	<i>AT2G43010</i>	EMP419		GCG GCT TCG GCT CCG ATG AT
			EMP420		AGT CGC GGC CTG CAT GTG TG
	<i>PIF5</i>	<i>AT3G59060</i>	EMP421		TCG GAG CAG CTC GCT AGG TA
			EMP422		TTG TTG CAC GGT CTG CAT CT
	<i>PP2A</i>	<i>AT1G13320</i>	EMP338		TATCGGATGACGATTCTTCGTGCAG
			EMP339		GCTTGGTCTGACTATCGGAATGAGAG

(\*) Hornitschek, P., Lorrain, S., Zoete, V., Michielin, O., Fankhauser, C. (2009). Inhibition of the shade avoidance response by formation of non-DNA binding bHLH heterodimers. *EMBO J.* **28**:3893-3902.

**Table S1**

### **Resumen artículo 3**

#### **Phytochrome-imposed oscillations in PIF3 protein abundance regulate hypocotyl growth under diurnal light/dark conditions in Arabidopsis**

Judit Soy, Pablo Leivar, Nahuel González-Schain, Maria Sentandreu, Salomé Prat, Peter H. Quail, and Elena Monte.

#### **Oscilaciones en la abundancia de la proteína PIF3 dirigidas por los fitocromos, regulan la elongación del Hipocotilo bajo condiciones diurnas de luz/oscuridad en Arabidopsis.**

Las plántulas de Arabidopsis crecidas en condiciones diurnas, presentan un crecimiento rítmico con una ratio de elongación máxima que tiene lugar al final de la noche en condiciones de día corto. Actualmente hay evidencias de que este comportamiento involucra la acción de factores promotores del crecimiento de tipo bHLH, el factor de interacción de fitocromo (PHYTOCHROME-INTERACTING FACTORS) 4 (PIF4) y el factor de interacción de fitocromo 5 (PIF5) al final de la noche, mediante un mecanismo de coincidencia que combina su regulación transcripcional por el reloj circadiano con el control de la acumulación de la proteína regulada por luz. Para elucidar el posible rol de PIF3 en este proceso, hemos analizado las respuestas de hipocotilo y la expresión génica de genes marcadores en mutantes simples y múltiples de las proteínas PIF. Los resultados muestran que PIF3 juega un papel prominente como promotor de la elongación bajo condiciones de luz/oscuridad, conjuntamente con PIF4 y PIF5. Además, proporcionamos evidencias de que PIF3 funciona en este proceso regulando actividad transcripcional, en parte mediante la unión directa a genes relacionados con el crecimiento y de manera independiente a través de su habilidad para regular los niveles de fitocromo B (phy B).

Asimismo, en contra de lo observado para PIF4 y PIF5, nuestros resultados demuestran que PIF3 no está sujeto a la regulación transcripcional por parte del reloj, sino que los niveles de proteína PIF3 en condiciones

diurnas, disminuyen progresivamente debido a la degradación inducida por el fitocromo B, y se acumulan subsiguientemente durante el periodo de oscuridad. Conjuntamente, los datos sugieren que la regulación post-transcripcional de PIF3 mediada por phyB permite la acumulación de ésta en un pico máximo antes de decaer el cual permite una aceleración del crecimiento del hipocotilo conjuntamente con la acción de PIF4 y PIF5 mediante una regulación directa de la inducción de genes relacionados con el crecimiento.

## **Appendix**

**Supplemental Dataset 1**

**Expression Data and statistical analysis for the SS1.5F genes at D0h and D1h Reported in Figure 1 and Supplemental Figure 1.**

Genes were defined as SS1.5F if:

- (a) the differences in expression values between WT and *pif3* were statistically significant using a two-way ANOVA approach with a false discovery rate (FDR) set at 5%
- (b) the expression values in the Dark varied by >1.5-fold between the WT and *pif3* genotypes at D0h and D1h

A	ATH1 Probe set
B	AGI Locus
C	TAIR Annotation
D	Fold change <i>pif3</i> /WT at D0h
E	Ratio <i>pif3</i> /WT at D0h
F	Fold change <i>pif3</i> /WT at D1h
G	Ratio <i>pif3</i> /WT at D1h
H	ANOVA P-value
I	Ratio D0h P-value
J	Ratio D1h P-value

Ratio refers to *pif3*/WT values, and Fold Change (FC) refers to  $-1/\text{Ratio}$  if Ratio is  $<1$ .

Ratio P-value refers to the p-value obtained when applying the Rosetta Ratio Error Model (Weng et al., 2006) as in contrast to the ANOVA P-value.

Weng, L., Dai, H., Zhan, Y., He, Y., Stepaniants, S.B., and Bassett, D.E. (2006). Rosetta error model for gene expression analysis. *Bioinformatics* 22: 1111-1121.

Sequence Code	Accession #	Sequence Description	Fold Change D0h	Ratio D0h	Fold Change D1h	Ratio D1h	ANOVA P-value	Ratio D0h P-value	Ratio D1h P-value
260933_at	At1g02470	hypothetical protein contains non-consensus	2,33482	2,33482	2,4910	2,49104	3,83832E-09	0,00007	0,00033
265095_at	At1g03880	putative cruciferin 12S seed storage protei	-2,2344	0,44755	-2,5441	0,39306	1,23497E-08	0,06613	0,03672
265094_at	At1g03890	putative cruciferin 12S seed storage protei	-2,41692	0,41375	-2,1803	0,45866	0,017	0,09596	0,13023
261175_at	At1g04800	unknown protein	1,56322	1,56322	1,7181	1,7181	0,00002	0,00941	0,00033
263175_at	At1g05510	hypothetical protein similar to unknown pro	-2,50351	0,39944	-3,0426	0,32867	0,00046	0,07646	0,05351
260950_s_at	At1g06120	delta 9 desaturase, putative similar to delta	1,62681	1,62681	1,6812	1,68116	0,04653	0,0413	0,05546
261814_at	At1g08310	unknown protein	-1,80184	0,55499	-1,5665	0,63836	0,00746	0,00935	0,03294
261815_at	At1g08325	leucine zipper protein, putative similar to b	-1,80585	0,55376	-1,5346	0,65166	0,00001	0,00014	0,01419
261474_at	At1g14540	anionic peroxidase, putative similar to anio	-15,91476	0,06283	2,8245	2,82448	0,00795	0,02236	0,63347
262857_at	At1g14930	major latex homologue type2 identical to m	-2,53269	0,39484	-1,8772	0,53272	0,03371	0,05129	0,12465
264899_at	At1g23130	unknown protein similar to ripening-induce	2,19183	2,19183	2,4372	2,43724	0,00113	0,01392	0,00655
263034_at	At1g24020	pollen allergen-like protein similar to major	1,88416	1,88416	1,7276	1,72761	0,02818	0,07874	0,03265
259789_at	At1g29395	Expressed protein ; supported by full-length	2,15497	2,15497	2,1609	2,1609	3,05143E-06	1,26E-06	0,00089
255997_s_at	At1g29910	photosystem II type I chlorophyll a /b bindi	1,66461	1,66461	1,9542	1,95419	2,53242E-13	7,74E-11	2,72E-18
245771_at	At1g30250	hypothetical protein predicted by genemark	2,12897	2,12897	1,7095	1,70954	0,00144	0,00311	0,01619
262427_s_at	At1g47600	thioglycosidase, putative similar to thioglu	2,11185	2,11185	1,8227	1,82271	0,00869	0,00365	0,02446
259615_at	At1g47980	desiccation-related protein, putative simila	-1,64112	0,60934	-1,7365	0,57587	0,00269	0,02007	0,0211
262244_at	At1g48260	serine threonine kinase, putative similar to	-1,76389	0,56693	-1,8909	0,52884	2,75844E-07	0,00019	3,37E-07
256352_at	At1g54970	proline-rich protein, putative similar to proli	1,64588	1,64588	1,7133	1,71334	0,0474	0,10647	0,01971
259653_at	At1g55240	unknown protein	-1,5537	0,64363	-1,9043	0,52512	0,00884	0,06137	0,00694
265108_s_at	At1g62620	similar to flavin-binding monooxygenase (Z	-1,52694	0,65491	-1,5290	0,65402	0,00328	0,01475	0,0225
260004_at	At1g67860	unknown protein ;supported by full-length c	1,9431	1,9431	1,5716	1,57158	0,03109	0,01095	0,09521
260385_at	At1g74090	putative flavonol sulfotransferase similar to	-1,58685	0,63018	-1,8349	0,54498	0,00057	0,00378	0,00015
262679_at	At1g75830	unknown protein ; supported by cDNA: gj_1	-1,7976	0,5563	-1,6485	0,6066	2,65183E-06	0,01745	0,03077
262185_at	At1g77950	MADS box transcription factor, putative sin	-1,70327	0,58711	-3,0442	0,32849	0,04912	0,35505	0,01698
264124_at	At1g79360	hypothetical protein predicted by genemark	2,00011	2,00011	1,7671	1,76713	2,53242E-13	9,96E-17	1,84E-09
266141_at	At2g02120	protease inhibitor II contains a gamma-thio	-2,51613	0,39744	-1,8165	0,55051	0,00002	0,00928	0,0734
263345_s_at	At2g05070	putative chlorophyll a/b binding protein ; su	1,96166	1,96166	2,0310	2,03098	9,85533E-11	0,00001	2,99E-12
263376_at	At2g20520	putative surface protein ; supported by cDN	1,78918	1,78918	1,5732	1,57324	0,01255	0,03055	0,02551
257396_at	At2g20875	predicted protein	1,73716	1,73716	1,5549	1,55494	0,01455	0,01736	0,12159
245070_at	At2g23240	metallothionein-like protein identical to an E	-1,86602	0,5359	-1,6017	0,62434	0,00234	0,00384	0,01996
267607_s_at	At2g26740	epoxide hydrolase (ATsEH) identical to GB:	1,95664	1,95664	1,7542	1,7542	2,53242E-13	7,39E-14	1,17E-15
265279_at	At2g28460	hypothetical protein predicted by genscan	-1,5274	0,65471	-1,5086	0,66287	0,00608	0,02216	0,01697
264079_at	At2g28490	putative seed storage protein (vicilin-like)	-1,7602	0,56812	-1,8725	0,53403	0,00011	0,01962	0,00586
266222_at	At2g28780	hypothetical protein predicted by genscan	-2,02149	0,49468	-1,6814	0,59474	0,00701	0,00549	0,01495
266279_at	At2g29290	putative tropinone reductase	1,92231	1,92231	1,6521	1,65206	0,00009	0,00368	0,00134
266674_at	At2g29620	hypothetical protein predicted by genscan	-1,83841	0,54395	-2,4889	0,40178	0,0091	0,05699	0,00097
267115_s_at	At2g32540	putative cellulose synthase	2,55949	2,55949	2,1489	2,14887	2,75844E-07	1,08E-06	0,00085
267457_at	At2g33790	putative proline-rich protein	1,818	1,818	2,4079	2,40789	0,03044	0,16448	0,00346
267002_s_at	At2g34430	putative photosystem II type I chlorophyll a	3,29775	3,29775	3,6153	3,61532	2,53242E-13	2,89E-30	0
266899_at	At2g34620	hypothetical protein predicted by genefinde	1,8754	1,8754	2,3630	2,36301	0,02635	0,08813	0,00145
263385_at	At2g40170	ABA-regulated gene (ATEM6) ; supported	-1,76911	0,56526	-1,8362	0,54459	0,00045	0,0228	0,00239
266393_at	At2g41260	late embryogenesis abundant M17 protein i	-1,94718	0,51356	-1,9038	0,52526	9,94318E-07	0,00113	0,00076
266392_at	At2g41280	late embryogenesis abundant M10 protein i	-1,85677	0,53857	-1,8251	0,54791	0,03506	0,01635	0,03233
267635_at	At2g42220	rhodanese-like family protein ;supported by	1,82061	1,82061	1,5027	1,50268	0,01217	0,01309	0,01569
260546_at	At2g43520	putative trypsin inhibitor ;supported by full-	1,53422	1,53422	1,5524	1,55236	0,00218	0,00405	0,00975
260560_at	At2g43590	putative endochitinase	-1,56381	0,63947	-1,6526	0,60511	0,00089	0,02794	0,02345
266600_at	At2g46070	putative mitogen-activated protein kinase	1,67983	1,67983	1,9883	1,9883	0,01994	0,06184	0,03195
266319_s_at	At2g46720	putative beta-ketoacyl-CoA synthase	1,57571	1,57571	1,6826	1,68256	0,04657	0,06933	0,02899

259161_at	At3g01500	carbonic anhydrase, chloroplast precursor	1,59641	1,59641	1,5841	1,58411	6,22399E-09	0,00002	2,56E-07
258972_at	At3g01920	hypothetical protein predicted by genscan+	2,00762	2,00762	1,9154	1,91535	1,257E-07	0,00007	0,00003
259314_at	At3g05260	putative glucose and ribitol dehydrogenase	-1,70776	0,58556	-2,5593	0,39073	0,00075	0,08844	0,00718
259297_at	At3g05360	putative disease resistance protein similar t	-1,9247	0,51956	-1,6659	0,60026	0,03546	0,02916	0,08219
258897_at	At3g05730	unknown protein	2,78217	2,78217	3,3132	3,31315	9,98071E-12	0,00004	1,80E-12
258746_at	At3g05950	germin-like protein similar to germin precu:	-2,28585	0,43747	-1,6729	0,59778	0,00117	0,00034	0,00491
257697_at	At3g12700	hypothetical protein predicted by genemark	-1,88937	0,52928	-1,8542	0,53931	2,42881E-07	0,00005	0,00019
257853_at	At3g12960	hypothetical protein predicted by genefindr	-2,29203	0,43629	-2,3655	0,42274	0,00125	0,0486	0,06747
256647_at	At3g13610	unknown protein contains similarity to DNA	-7,00385	0,14278	2,7278	2,72781	0,00004	0,00319	0,34197
257008_at	At3g14210	myrosinase-associated protein, putative sii	1,54685	1,54685	1,5543	1,55426	0,01085	0,0079	0,05299
256548_at	At3g14770	hypothetical protein contains similarity to M	-1,90623	0,5246	-1,6565	0,6037	0,00095	0,00492	0,00433
258418_at	At3g16660	unknown protein	1,8744	1,8744	1,9922	1,9922	0,02497	0,03951	0,00391
257128_at	At3g20080	cytochrome P450, putative contains Pfam	-3,03906	0,32905	-3,7266	0,26834	0,00499	0,00265	0,00412
256815_at	At3g21380	unknown protein contains Pfam profile: PFC	-2,39438	0,41764	-2,2935	0,43601	5,23575E-06	0,01075	0,01062
256938_at	At3g22500	LEA protein, putative similar to LEA protein	-2,06654	0,4839	-2,7665	0,36146	0,00344	0,11744	0,03168
258327_at	At3g22640	unknown protein contains similarity to majo	-1,695	0,58997	-1,8060	0,5537	5,68009E-06	0,00282	4,04E-06
258240_at	At3g27660	oleosin isoform identical to oleosin isoform	-3,65881	0,27331	-3,9947	0,25033	9,12589E-08	0,0095	0,00921
256601_s_at	At3g28290	At14a-1 protein identical to At14a protein C	-2,31944	0,43114	-3,1607	0,31638	2,53242E-13	3,34E-19	2,16E-36
252511_at	At3g46280	putative protein serine/threonine-specific p	-5,33387	0,18748	1,6742	1,67416	0,0348	0,01854	0,43
252462_at	At3g47250	putative protein various predicted genes, A	-1,56817	1,56817	1,6028	1,6028	0,00641	0,01627	0,01285
252317_at	At3g48720	putative protein hypersensitivity-related hsi	1,88291	1,88291	1,8882	1,88818	0,00147	0,00042	0,00433
252222_at	At3g49840	putative protein various predicted proteins,	-3,53514	0,28287	-2,1522	0,46465	0,01455	0,00436	0,02696
246299_at	At3g51810	embryonic abundant protein AtEm1	-1,5238	0,65625	-1,5736	0,63548	0,00456	0,07066	0,00775
251814_at	At3g54890	chlorophyll a/b-binding protein ; supported	2,08494	2,08494	2,0456	2,04556	2,53242E-13	1,75E-08	8,94E-14
251785_at	At3g55130	ABC transporter - like protein breast cance	1,93621	1,93621	1,5789	1,57887	0,00016	4,96E-06	0,00399
251181_at	At3g62820	putative protein pectinesterase homolog - l	1,91198	1,91198	1,7659	1,76592	0,00003	0,00007	0,0134
255516_at	At4g02270	hypothetical protein similar to extensin-like	1,55697	1,55697	1,7783	1,77832	0,00493	0,09723	0,00081
255248_at	At4g05180	Oxygen-evolving enhancer protein 3 precu	1,56708	1,56708	1,6429	1,64291	1,64927E-08	0,00004	7,94E-09
255048_at	At4g09600	gibberellin-regulated protein GASA3 precu	-2,28278	0,43806	-2,0884	0,47883	0,0001	0,00547	0,00525
255049_at	At4g09610	gibberellin-regulated protein GASA2 precu	-2,88459	0,34667	-2,5495	0,39223	0,00169	0,0494	0,04511
255007_at	At4g10020	putative oxidoreductase 11beta-hydroxyste	-1,50981	0,66233	-1,7441	0,57338	0,00005	0,0036	0,0001
255805_at	At4g10240	zinc-finger - like protein zinc-finger protein	-1,50432	0,66475	-1,5673	0,63803	0,00005	0,00986	0,00014
254761_at	At4g13195	Expressed protein ; supported by full-length	-1,76083	0,56792	-1,5334	0,65217	0,00159	0,00178	0,03367
245306_at	At4g14690	Expressed protein ; supported by full-length	-1,61409	0,61954	-2,2893	0,43682	0,00181	0,05876	0,00055
245505_at	At4g15690	glutaredoxin	1,82037	1,82037	1,6373	1,63729	0,01283	0,02281	0,05366
254396_at	At4g21680	peptide transporter - like protein peptide tra	-2,07792	0,48125	-1,5281	0,65441	0,02038	0,00096	0,09999
254095_at	At4g25140	oleosin, 18.5K	-1,87575	0,53312	-1,9244	0,51965	2,05845E-06	0,02473	0,01702
253930_at	At4g26740	embryo-specific protein 1 (ATS1)	-2,74475	0,36433	-4,4872	0,22286	1,27406E-06	0,0351	0,01219
253904_at	At4g27140	NWMU1 - 2S albumin 1 precursor ; suppor	-2,36899	0,42212	-2,2919	0,43631	2,37715E-06	0,00994	0,02579
253894_at	At4g27150	NWMU2 - 2S albumin 2 precursor	-2,23567	0,44729	-2,0248	0,49389	0,00004	0,01615	0,03716
253895_at	At4g27160	NWMU3 - 2S albumin 3 precursor	-3,70924	0,2696	-3,7068	0,26977	2,22853E-10	0,01589	0,01465
253902_at	At4g27170	NWMU4 - 2S albumin 4 precursor ; suppor	-2,53359	0,3947	-2,5324	0,39489	0,00005	0,11591	0,15306
253767_at	At4g28520	12S cruciferin seed storage protein	-1,92259	0,52013	-1,8887	0,52946	3,89603E-12	0,0015	0,00175
253494_at	At4g31830	putative protein	-2,43156	0,41126	-1,7447	0,57317	0,00937	0,02159	0,11804
253331_at	At4g33490	nucellin -like protein nucellin - Hordeum vu	1,85478	1,85478	1,6643	1,66427	2,88802E-06	3,46E-06	0,00044
253049_at	At4g37300	putative protein ; supported by cDNA: gj_14	1,54716	1,54716	1,5116	1,51158	0,00009	0,00246	0,00062
253040_at	At4g37800	endo-xyloglucan transferase - like protein c	5,7886	5,7886	3,0036	3,00358	2,16117E-09	1,48E-11	0,00003
251017_at	At5g02760	protein phosphatase - like protein protein p	1,76423	1,76423	1,6397	1,63966	1,1511E-12	3,77E-09	1,53E-11
245711_at	At5g04340	putative c2h2 zinc finger transcription factor	-2,04231	0,48964	-1,7482	0,57203	0,00011	0,00037	0,00782
245713_at	At5g04370	S-adenosyl-L-methionine:salicylic acid carb	2,0613	2,0613	1,5698	1,56982	3,16868E-06	1,91E-07	0,0017

250492_at	At5g09790	putative protein Requiem protein, Xenopus	-1,87265	0,534	-2,2652	0,44147	0,0385	0,08821	0,03367
250351_at	At5g12030	heat shock protein 17.6A	-2,04848	0,48817	-2,3676	0,42238	0,02909	0,07819	0,06442
246490_at	At5g15950	S-adenosylmethionine decarboxylase (adol	2,03442	2,03442	1,6014	1,60141	0,00578	0,00065	0,11818
246487_at	At5g16030	putative protein with poly glutamic acid stre	2,54473	2,54473	2,1856	2,18559	2,53242E-13	4,32E-09	1,11E-08
250043_at	At5g18430	putative protein proline-rich protein APG, A	1,81315	1,81315	2,4721	2,47209	0,00304	0,01952	0,00287
249894_at	At5g22580	unknown protein ; supported by cDNA: gi_	1,5006	1,5006	1,8496	1,84955	0,00035	0,07038	0,00023
246860_at	At5g25840	putative protein various predicted proteins,	1,82915	1,82915	2,0919	2,0919	0,00075	0,00699	0,00922
249474_s_at	At5g39190	germin-like protein (GLP2a) copy2 ; suppo	1,60289	1,60289	1,6404	1,64044	0,00233	0,00252	0,01806
249082_at	At5g44120	legumin-like protein	-1,6226	0,6163	-1,7488	0,57181	1,78301E-10	0,00007	2,71E-06
249010_at	At5g44580	unknown protein ; supported by cDNA: gi_	1,75623	1,75623	1,6186	1,61856	9,24928E-06	0,00155	0,00023
248915_at	At5g45690	putative protein strong similarity to unknowi	-1,70526	0,58642	-1,7670	0,56592	0,00315	0,1276	0,11545
248931_at	At5g46040	peptide transporter	-2,09927	0,47636	-1,5736	0,63548	0,00066	0,00017	0,04479
248784_at	At5g47380	putative protein similar to unknown protein	2,73735	2,73735	1,5622	1,56216	0,00156	0,00005	0,08731
248759_at	At5g47610	putative protein similar to unknown protein	1,57416	1,57416	1,6203	1,62028	0,00313	0,00309	0,0053
248684_at	At5g48485	Expressed protein ; supported by full-lengt	1,53585	1,53585	1,6808	1,68078	1,05227E-07	0,00025	0,00014
248683_at	At5g48490	putative protein similar to unknown protein	2,25094	2,25094	2,8011	2,80105	1,89117E-10	0,00077	9,52E-10
248520_at	At5g50600	11-beta-hydroxysteroid dehydrogenase-like	-1,61226	0,62025	-1,8113	0,55209	6,18449E-07	0,01985	0,00473
248151_at	At5g54270	Lhcb3 chlorophyll a/b binding protein (gb)A	1,71711	1,71711	1,7645	1,76454	0,00003	0,00372	0,00001
248125_at	At5g54740	2S storage protein-like	-2,15966	0,46304	-2,0067	0,49832	1,78301E-10	0,00111	0,00349
248128_at	At5g54770	thiazole biosynthetic enzyme precursor (AF	1,6465	1,6465	1,5216	1,52159	2,53242E-13	4,25E-21	1,92E-14
247914_at	At5g57540	xyloglucan endotransglycosylase	1,58866	1,58866	1,9006	1,90056	0,02947	0,13281	0,01132
247162_at	At5g65730	xyloglucan endo-transglycosylase-like prote	2,02949	2,02949	1,5387	1,53872	0,0024	0,00995	0,04589

**Supplemental Dataset 2**

**Expression Data and statistical analysis for the SS1.5F-HC genes at D0h and D1h Reported in Figure 1 and Supplemental Figure 1.**

Genes were defined as SS1.5F-HC if:

- (a) the differences in expression values between WT and *pif3* were statistically significant using a two-way ANOVA approach with a FDR set at 5%
- (b) the expression values in the Dark varied by >1.5-fold between the WT and *pif3* genotypes at D0h and D1h
- (c) their Ratio P-value was <0.05

A	ATH1 Probe set
B	AGI Locus
C	TAIR Annotation
D	Fold change <i>pif3</i> /WT at D0h
E	Ratio <i>pif3</i> /WT at D0h
F	Fold change <i>pif3</i> /WT at D1h
G	Ratio <i>pif3</i> /WT at D1h
H	ANOVA P-value
I	Ratio P-value at D0h
J	Ratio P-value at D1h
K	Functional Designation used in Figure 2

Ratio refers to *pif3*/WT values, and Fold Change (FC) refers to  $-1/\text{Ratio}$  if Ratio is <1.

Ratio P-value refers to the p-value obtained when applying the Rosetta Ratio Error Model (Weng et al., 2006) as in contrast to the ANOVA P-value.

Weng, L., Dai, H., Zhan, Y., He, Y., Stepaniants, S.B., and Bassett, D.E. (2006). Rosetta error model for gene expression analysis. *Bioinformatics* 22: 1111-1121.

Probe Set	Accession #	Sequence Description	Fold Change D0h	Ratio D0h	Fold Change D1h	Ratio D1h	ANOVA P-value	Ratio D0h P-value	Ratio D1h P-value	Functional Classification
260933_at	At1g02470	hypothetical protein contains non-con	2,33482	2,33482	2,4910	2,49104	3,83832E-09	0,00007	0,00033	UNK
261175_at	At1g04800	unknown protein	1,56322	1,56322	1,7181	1,7181	0,00002	0,00941	0,00033	UNK
261814_at	At1g08310	unknown protein	-1,80184	0,55499	-1,5665	0,63836	0,00746	0,00935	0,03294	UNK
261815_at	At1g08325	leucine zipper protein, putative simila	-1,80585	0,55376	-1,5346	0,65166	0,00001	0,00014	0,01419	UNK
264899_at	At1g23130	unknown protein similar to ripening-i	2,19183	2,19183	2,4372	2,43724	0,00113	0,01392	0,00655	S/D
259789_at	At1g29395	Expressed protein ; supported by full-	2,15497	2,15497	2,1609	2,1609	3,05143E-06	1,26E-06	0,00089	S/D
255997_s_at	At1g29910	photosystem II type I chlorophyll a /	1,66461	1,66461	1,9542	1,95419	2,53242E-13	7,74E-11	2,72E-18	P/C
245771_at	At1g30250	hypothetical protein predicted by gene	2,12897	2,12897	1,7095	1,70954	0,00144	0,00311	0,01619	UNK
262427_s_at	At1g47600	thioglycosidase, putative similar to th	2,11185	2,11185	1,8227	1,82271	0,00869	0,00365	0,02446	CM
259615_at	At1g47980	desiccation-related protein, putative :	-1,64112	0,60934	-1,7365	0,57587	0,00269	0,02007	0,0211	UNK
262244_at	At1g48260	serine threonine kinase, putative sim	-1,76389	0,56693	-1,8909	0,52884	2,75844E-07	0,00019	3,37E-07	S
265108_s_at	At1g62620	similar to flavin-binding monooxygen	-1,52694	0,65491	-1,5290	0,65402	0,00328	0,01475	0,0225	UNK
260385_at	At1g74090	putative flavonol sulfotransferase simi	-1,58685	0,63018	-1,8349	0,54498	0,00057	0,00378	0,00015	CM
262679_at	At1g75830	unknown protein ; supported by cDNA	-1,7976	0,5563	-1,6485	0,6066	2,65183E-06	0,01745	0,03077	S/D
264124_at	At1g79360	hypothetical protein predicted by gene	2,00011	2,00011	1,7671	1,76713	2,53242E-13	9,96E-17	1,84E-09	TR
263345_s_at	At2g05070	putative chlorophyll a/b binding prote	1,96166	1,96166	2,0310	2,03098	9,85533E-11	0,00001	2,99E-12	P/C
263376_at	At2g20520	putative surface protein ; supported l	1,78918	1,78918	1,5732	1,57324	0,01255	0,03055	0,02551	UNK
245070_at	At2g23240	metallothionein-like protein identical t	-1,86602	0,5359	-1,6017	0,62434	0,00234	0,00384	0,01996	CM
267607_s_at	At2g26740	epoxide hydrolase (ATEH) identical to	1,95664	1,95664	1,7542	1,7542	2,53242E-13	7,39E-14	1,17E-15	H
265279_at	At2g28460	hypothetical protein predicted by gene	-1,5274	0,65471	-1,5086	0,66287	0,00608	0,02216	0,01697	CM
264079_at	At2g28490	putative seed storage protein (vicilin-l	-1,7602	0,56812	-1,8725	0,53403	0,00011	0,01962	0,00586	G/D
266222_at	At2g28780	hypothetical protein predicted by gene	-2,02149	0,49468	-1,6814	0,59474	0,00701	0,00549	0,01495	UNK
266279_at	At2g29290	putative tropinone reductase	1,92231	1,92231	1,6521	1,65206	0,00009	0,00368	0,00134	CM
267115_s_at	At2g32540	putative cellulose synthase	2,55949	2,55949	2,1489	2,14887	2,75844E-07	1,08E-06	0,00085	G/D
267002_s_at	At2g34430	putative photosystem II type I chloro	3,29775	3,29775	3,6153	3,61532	2,53242E-13	2,89E-30	0	P/C
263385_at	At2g40170	ABA-regulated gene (ATEM6) ; suppo	-1,76911	0,56526	-1,8362	0,54459	0,00045	0,0228	0,00239	H
266393_at	At2g41260	late embryogenesis abundant M17 prc	-1,94718	0,51356	-1,9038	0,52526	9,94318E-07	0,00113	0,00076	G/D
266392_at	At2g41280	late embryogenesis abundant M10 prc	-1,85677	0,53857	-1,8251	0,54791	0,03506	0,01635	0,03233	G/D
267635_at	At2g42220	rhodanese-like family protein ;suppor	1,82061	1,82061	1,5027	1,50268	0,01217	0,01309	0,01569	UNK
260546_at	At2g43520	putative trypsin inhibitor ;supported l	1,53422	1,53422	1,5524	1,55236	0,00218	0,00405	0,00975	S/D
260560_at	At2g43590	putative endochitinase	-1,56381	0,63947	-1,6526	0,60511	0,00089	0,02794	0,02345	G/D
259161_at	At3g01500	carbonic anhydrase, chloroplast prec	1,59641	1,59641	1,5841	1,58411	6,22399E-09	0,00002	2,56E-07	P/C
258972_at	At3g01920	hypothetical protein predicted by gene	2,00762	2,00762	1,9154	1,91535	1,257E-07	0,00007	0,00003	UNK
258897_at	At3g05730	unknown protein	2,78217	2,78217	3,3132	3,31315	9,98071E-12	0,00004	1,80E-12	S/D
258746_at	At3g05950	germin-like protein similar to germin l	-2,28585	0,43747	-1,6729	0,59778	0,00117	0,00034	0,00491	CM
257697_at	At3g12700	hypothetical protein predicted by gene	-1,88937	0,52928	-1,8542	0,53931	2,42881E-07	0,00005	0,00019	CM
256548_at	At3g14770	hypothetical protein contains similarit	-1,90623	0,5246	-1,6565	0,6037	0,00095	0,00492	0,00433	UNK
258418_at	At3g16660	unknown protein	1,8744	1,8744	1,9922	1,9922	0,02497	0,03951	0,00391	UNK
257128_at	At3g20080	cytochrome P450, putative contains f	-3,03906	0,32905	-3,7266	0,26834	0,00499	0,00265	0,00412	CM
256815_at	At3g21380	unknown protein contains Pfam profil	-2,39438	0,41764	-2,2935	0,43601	5,23575E-06	0,01075	0,01062	UNK
258327_at	At3g22640	unknown protein contains similarity to	-1,695	0,58997	-1,8060	0,5537	5,68009E-06	0,00282	4,04E-06	UNK
258240_at	At3g27660	oleosin isoform identical to oleosin iso	-3,65881	0,27331	-3,9947	0,25033	9,12589E-08	0,0095	0,00921	G/D
256601_s_at	At3g28290	At14a-1 protein identical to At14a pr	-2,31944	0,43114	-3,1607	0,31638	2,53242E-13	3,34E-19	2,16E-36	G/D
252462_at	At3g47250	putative protein various predicted ge	1,56817	1,56817	1,6028	1,6028	0,00641	0,01627	0,01285	UNK
252317_at	At3g48720	putative protein hypersensitivity-rela	1,88291	1,88291	1,8882	1,88818	0,00147	0,00042	0,00433	CM
252222_at	At3g49840	putative protein various predicted prc	-3,53514	0,28287	-2,1522	0,46465	0,01455	0,00436	0,02696	UNK
251814_at	At3g54890	chlorophyll a/b-binding protein ; sup	2,08494	2,08494	2,0456	2,04556	2,53242E-13	1,75E-08	8,94E-14	P/C
251785_at	At3g55130	ABC transporter - like protein breast	1,93621	1,93621	1,5789	1,57887	0,00016	4,96E-06	0,00399	TR
251181_at	At3g62820	putative protein pectinesterase homo	1,91198	1,91198	1,7659	1,76592	0,00003	0,00007	0,0134	UNK
255248_at	At4g05180	Oxygen-evolving enhancer protein 3	1,56708	1,56708	1,6429	1,64291	1,64927E-08	0,00004	7,94E-09	P/C
255048_at	At4g09600	gibberellin-regulated protein GASA3 p	-2,28278	0,43806	-2,0884	0,47883	0,0001	0,00547	0,00525	H
255049_at	At4g09610	gibberellin-regulated protein GASA2 p	-2,88459	0,34667	-2,5495	0,39223	0,00169	0,0494	0,04511	H
255007_at	At4g10020	putative oxidoreductase 11beta-hydr	-1,50981	0,66233	-1,7441	0,57338	0,00005	0,0036	0,0001	H
255805_at	At4g10240	zinc-finger - like protein zinc-finger p	-1,50432	0,66475	-1,5673	0,63803	0,00005	0,00986	0,00014	TX
254761_at	At4g13195	Expressed protein ; supported by full-	-1,76083	0,56792	-1,5334	0,65217	0,00159	0,00178	0,03367	S
254095_at	At4g25140	oleosin, 18.5K	-1,87575	0,53312	-1,9244	0,51965	2,05845E-06	0,02473	0,01702	G/D
253930_at	At4g26740	embryo-specific protein 1 (ATS1)	-2,74475	0,36433	-4,4872	0,22286	1,27406E-06	0,0351	0,01219	G/D
253904_at	At4g27140	NWMU1 - 2S albumin 1 precursor ; si	-2,36899	0,42212	-2,2919	0,43631	2,37715E-06	0,00994	0,02579	G/D
253894_at	At4g27150	NWMU2 - 2S albumin 2 precursor	-2,23567	0,44729	-2,0248	0,49389	0,00004	0,01615	0,03716	G/D
253895_at	At4g27160	NWMU3 - 2S albumin 3 precursor	-3,70924	0,2696	-3,7068	0,26977	2,22853E-10	0,01589	0,01465	G/D
253767_at	At4g28520	12S cruciferin seed storage protein	-1,92259	0,52013	-1,8887	0,52946	3,89603E-12	0,0015	0,00175	G/D

253331_at	At4g33490	nucellin-like protein nucellin - Horde	1,85478	1,85478	1,6643	1,66427	2,88802E-06	3,46E-06	0,00044	CM
253049_at	At4g37300	putative protein ; supported by cDNA:	1,54716	1,54716	1,5116	1,51158	0,00009	0,00246	0,00062	G/D
253040_at	At4g37800	endo-xyloglucan transferase - like pr	5,7886	5,7886	3,0036	3,00358	2,16117E-09	1,48E-11	0,00003	G/D
251017_at	At5g02760	protein phosphatase - like protein prc	1,76423	1,76423	1,6397	1,63966	1,1511E-12	3,77E-09	1,53E-11	S
245711_at	At5g04340	putative c2h2 zinc finger transcription	-2,04231	0,48964	-1,7482	0,57203	0,00011	0,00037	0,00782	TX
245713_at	At5g04370	S-adenosyl-L-methionine:salicylic acid	2,0613	2,0613	1,5698	1,56982	3,16868E-06	1,91E-07	0,0017	UNK
246487_at	At5g16030	putative protein with poly glutamic ac	2,54473	2,54473	2,1856	2,18559	2,53242E-13	4,32E-09	1,11E-08	UNK
250043_at	At5g18430	putative protein proline-rich protein /	1,81315	1,81315	2,4721	2,47209	0,00304	0,01952	0,00287	CM
246860_at	At5g25840	putative protein various predicted prc	1,82915	1,82915	2,0919	2,0919	0,00075	0,00699	0,00922	UNK
249474_s_at	At5g39190	germin-like protein (GLP2a) copy2 ; †	1,60289	1,60289	1,6404	1,64044	0,00233	0,00252	0,01806	G/D
249082_at	At5g44120	legumin-like protein	-1,6226	0,6163	-1,7488	0,57181	1,78301E-10	0,00007	2,71E-06	G/D
249010_at	At5g44580	unknown protein ; supported by cDN.	1,75623	1,75623	1,6186	1,61856	9,24928E-06	0,00155	0,00023	UNK
248931_at	At5g46040	peptide transporter	-2,09927	0,47636	-1,5736	0,63548	0,00066	0,00017	0,04479	TR
248759_at	At5g47610	putative protein similar to unknown pi	1,57416	1,57416	1,6203	1,62028	0,00313	0,00309	0,0053	UNK
248684_at	At5g48485	Expressed protein ; supported by full-	1,53585	1,53585	1,6808	1,68078	1,05227E-07	0,00025	0,00014	S/D
248683_at	At5g48490	putative protein similar to unknown pi	2,25094	2,25094	2,8011	2,80105	1,89117E-10	0,00077	9,52E-10	G/D
248520_at	At5g50600	11-beta-hydroxysteroid dehydrogenas	-1,61226	0,62025	-1,8113	0,55209	6,18449E-07	0,01985	0,00473	H
248151_at	At5g54270	Lhcb3 chlorophyll a/b binding protein	1,71711	1,71711	1,7645	1,76454	0,00003	0,00372	0,00001	P/C
248125_at	At5g54740	2S storage protein-like	-2,15966	0,46304	-2,0067	0,49832	1,78301E-10	0,00111	0,00349	G/D
248128_at	At5g54770	thiazole biosynthetic enzyme precursc	1,6465	1,6465	1,5216	1,52159	2,53242E-13	4,25E-21	1,92E-14	CM
247162_at	At5g65730	xyloglucan endo-transglycosylase-like	2,02949	2,02949	1,5387	1,53872	0,0024	0,00995	0,04589	G/D

Supplemental Data. Sentandreu et al. (2011). Plant Cell 10.1105/tpc.111.088161

**Supplemental Dataset 3**

**List of SS1.5F genes that do not meet the requirements to be designated as SS1.5F-HC genes as Reported in Figure 1 and Supplemental Figure 1.**

Genes included in these list are SS1.5F that do not meet the requirements to be included in SS1.5F-HC gene list

A	ATH1 Probe set
B	AGI Locus
C	TAIR Annotation
D	Fold change <i>pif3</i> /WT at D0h
E	Ratio <i>pif3</i> /WT at D0h
F	Fold change <i>pif3</i> /WT at D1h
G	Ratio <i>pif3</i> /WT at D1h
H	ANOVA P-value
I	Ratio P-value at D0h
F	Ratio P-value at D1h

Ratio refers to *pif3*/WT values, and Fold Change (FC) refers to  $-1/\text{Ratio}$  if Ratio is  $<1$ .

Ratio P-value refers to the p-value obtained when applying the Rosetta Ratio Error Model (Weng et al., 2006) as in contrast to the ANOVA P-value.

Weng, L., Dai, H., Zhan, Y., He, Y., Stepaniants, S.B., and Bassett, D.E. (2006). Rosetta error model for gene expression analysis. *Bioinformatics* 22: 1111-1121.



**Supplemental Dataset 4**

**List of class P3, P3/PQ, P3/P4P5 and P4P5/PQ genes reported in Supplemental Figure 4.**

Class P3/P4P5 (9 genes)

Class P3/PQ (50 genes)

Class P3 (32 genes)

A	ATH1 Probe set
B	AGI Locus
C	TAIR Annotation
D	Fold change <i>pif3</i> /WT at D0h
E	Ratio <i>pif3</i> /WT at D0h
F	Fold change <i>pif3</i> /WT at D1h
G	Ratio <i>pif3</i> /WT at D1h
H	ANOVA P-value
I	Ratio P-value at D0h
F	Ratio P-value at D1h
G	Functional Designation used in Figure 2

Class P4P5/PQ (84 genes)

A	AGI Locus
---	-----------

Ratio refers to *pif3*/WT values, and Fold Change (FC) refers to  $-1/\text{Ratio}$  if Ratio is  $<1$ .

Ratio P-value refers to the p-value obtained when applying the Rosetta Ratio Error Model (Weng et al., 2006) as in contrast to the ANOVA P-value.

Weng, L., Dai, H., Zhan, Y., He, Y., Stepaniants, S.B., and Bassett, D.E. (2006). Rosetta error model for gene expression analysis. *Bioinformatics* 22: 1111-1121.

Probe Set	Accession #	Sequence Description	ANOVA P-value	Fold Change D0h	Ratio D0h	Fold Change D1h	Ratio D1h	ANOVA P-value	Ratio D0h P-value	Ratio D1h P-value	Functional Classification
261175_at	At1g04800	unknown protein	0,00002	1,56322	1,56322	1,7181	1,7181	0,00002	0,00941	0,00033	UNK
264899_at	At1g23130	unknown protein similar to ripening-i	0,00113	2,19183	2,19183	2,4372	2,43724	0,00113	0,01392	0,00655	S/D
255997_s_at	At1g29910	photosystem II type I chlorophyll a /	2,53242E-13	1,66461	1,66461	1,9542	1,95419	2,53E-08	7,74E-11	2,72E-18	P/C
262679_at	At1g75830	unknown protein ; supported by cDNA	2,65183E-06	-1,7976	0,5563	-1,6485	0,6066	2,65E-01	0,01745	0,03077	S/D
263345_s_at	At2g05070	putative chlorophyll a/b binding protei	9,85533E-11	1,96166	1,96166	2,0310	2,03098	9,86E-06	0,00001	2,99E-12	P/C
245070_at	At2g23240	metallothionein-like protein identical t	0,00234	-1,86602	0,5359	-1,6017	0,62434	0,00234	0,00384	0,01996	CM
264079_at	At2g28490	putative seed storage protein (vicilin-l	0,00011	-1,7602	0,56812	-1,8725	0,53403	0,00011	0,01962	0,00586	G/D
266279_at	At2g29290	putative tropinone reductase	0,00009	1,92231	1,92231	1,6521	1,65206	0,00009	0,00368	0,00134	CM
267115_s_at	At2g32540	putative cellulose synthase	2,75844E-07	2,55949	2,55949	2,1489	2,14887	2,76E-02	1,08E-06	0,00085	G/D
267002_s_at	At2g34430	putative photosystem II type I chloro	2,53242E-13	3,29775	3,29775	3,6153	3,61532	2,53E-08	2,89E-30	0	P/C
263385_at	At2g40170	ABA-regulated gene (ATEM6) ; suppo	0,00045	-1,76911	0,56526	-1,8362	0,54459	0,00045	0,0228	0,00239	H
266393_at	At2g41260	late embryogenesis abundant M17 prc	9,94318E-07	-1,94718	0,51356	-1,9038	0,52526	9,94E-02	0,00113	0,00076	G/D
266392_at	At2g41280	late embryogenesis abundant M10 prc	0,03506	-1,85677	0,53857	-1,8251	0,54791	0,03506	0,01635	0,03233	G/D
267635_at	At2g42220	rhodanese-like family protein ;suppor	0,01217	1,82061	1,82061	1,5027	1,50268	0,01217	0,01309	0,01569	UNK
260546_at	At2g43520	putative trypsin inhibitor ;supported	0,00218	1,53422	1,53422	1,5524	1,55236	0,00218	0,00405	0,00975	S/D
259161_at	At3g01500	carbonic anhydrase, chloroplast prec	6,22399E-09	1,59641	1,59641	1,5841	1,58411	6,22E-04	0,00002	2,56E-07	P/C
258897_at	At3g05730	unknown protein	9,98071E-12	2,78217	2,78217	3,3132	3,31315	9,98E-07	0,00004	1,80E-12	S/D
256548_at	At3g14770	hypothetical protein contains similarit	0,00095	-1,90623	0,5246	-1,6565	0,6037	0,00095	0,00492	0,00433	UNK
258418_at	At3g16660	unknown protein	0,02497	1,8744	1,8744	1,9922	1,9922	0,02497	0,03951	0,00391	UNK
258327_at	At3g22640	unknown protein contains similarity tc	5,68009E-06	-1,695	0,58997	-1,8060	0,5537	5,68E-01	0,00282	4,04E-06	UNK
258240_at	At3g27660	oleosin isoform identical to oleosin iso	9,12589E-08	-3,65881	0,27331	-3,9947	0,25033	9,13E-03	0,0095	0,00921	G/D
252462_at	At3g47250	putative protein various predicted ge	0,00641	1,56817	1,56817	1,6028	1,6028	0,00641	0,01627	0,01285	UNK
252317_at	At3g48720	putative protein hypersensitivity-relai	0,00147	1,88291	1,88291	1,8882	1,88818	0,00147	0,00042	0,00433	CM
251814_at	At3g54890	chlorophyll a/b-binding protein ; sup	2,53242E-13	2,08494	2,08494	2,0456	2,04556	2,53E-08	1,75E-08	8,94E-14	P/C
251785_at	At3g55130	ABC transporter - like protein breast	0,00016	1,93621	1,93621	1,5789	1,57887	0,00016	4,96E-06	0,00399	TR
251181_at	At3g62820	putative protein pectinesterase homo	0,00003	1,91198	1,91198	1,7659	1,76592	0,00003	0,00007	0,0134	UNK
255248_at	At4g05180	Oxygen-evolving enhancer protein 3	1,64927E-08	1,56708	1,56708	1,6429	1,64291	1,65E-03	0,00004	7,94E-09	P/C
255048_at	At4g09600	gibberellin-regulated protein GASA3 p	0,00011	-2,28278	0,43806	-2,0884	0,47883	0,00011	0,00547	0,00525	H
255049_at	At4g09610	gibberellin-regulated protein GASA2 p	0,00169	-2,88459	0,34667	-2,5495	0,39223	0,00169	0,0494	0,04511	H
255007_at	At4g10020	putative oxidoreductase 11beta-hydr	0,00005	-1,50981	0,66233	-1,7441	0,57338	0,00005	0,0036	0,00011	H
255805_at	At4g10240	zinc-finger - like protein zinc-finger p	0,00005	-1,50432	0,66475	-1,5673	0,63803	0,00005	0,00986	0,00014	TX
254095_at	At4g25140	oleosin, 18.5K	2,05845E-06	-1,87575	0,53312	-1,9244	0,51965	2,06E-01	0,02473	0,01702	G/D
253930_at	At4g26740	embryo-specific protein 1 (ATS1)	1,27406E-06	-2,74475	0,36433	-4,4872	0,22286	1,27E-01	0,0351	0,01219	G/D
253894_at	At4g27150	NWMU2 - 2S albumin 2 precursor	0,00004	-2,23567	0,44729	-2,0248	0,49389	0,00004	0,01615	0,03716	G/D
253895_at	At4g27160	NWMU3 - 2S albumin 3 precursor	2,22853E-10	-3,70924	0,2696	-3,7068	0,26977	2,23E-05	0,01589	0,01465	G/D
253767_at	At4g28520	12S cruciferin seed storage protein	3,89603E-12	-1,92259	0,52013	-1,8887	0,52946	3,90E-07	0,0015	0,00175	G/D
253049_at	At4g37300	putative protein ; supported by cDNA:	0,00009	1,54716	1,54716	1,5116	1,51158	0,00009	0,00246	0,00062	G/D
253040_at	At4g37800	endo-xyloglucan transferase - like pr	2,16117E-09	5,7886	5,7886	3,0036	3,00358	2,16E-04	1,48E-11	0,00003	G/D
251017_at	At5g02760	protein phosphatase - like protein prc	1,1511E-12	1,76423	1,76423	1,6397	1,63966	1,15E-07	3,77E-09	1,53E-11	S
246487_at	At5g16030	putative protein with poly glutamic ac	2,53242E-13	2,54473	2,54473	2,1856	2,18559	2,53E-08	4,32E-09	1,11E-08	UNK
246860_at	At5g25840	putative protein various predicted prc	0,00075	1,82915	1,82915	2,0919	2,0919	0,00075	0,00699	0,00922	UNK
249082_at	At5g44120	legumin-like protein	1,78301E-10	-1,6226	0,6163	-1,7488	0,57181	1,78E-05	0,00007	2,71E-06	G/D
249010_at	At5g44580	unknown protein ; supported by cDN.	9,24928E-06	1,75623	1,75623	1,6186	1,61856	9,25E-01	0,00155	0,00023	UNK
248759_at	At5g47610	putative protein similar to unknown pi	0,00313	1,57416	1,57416	1,6203	1,62028	0,00313	0,00309	0,0053	UNK
248684_at	At5g48485	Expressed protein ; supported by full-	1,05227E-07	1,53585	1,53585	1,6808	1,68078	1,05E-02	0,00025	0,00014	S/D
248683_at	At5g48490	putative protein similar to unknown pi	1,89117E-10	2,25094	2,25094	2,8011	2,80105	1,89E-05	0,00077	9,52E-10	G/D
248151_at	At5g54270	Lhcb3 chlorophyll a/b binding protein	0,00003	1,71711	1,71711	1,7645	1,76454	0,00003	0,00372	0,00001	P/C
248125_at	At5g54740	2S storage protein-like	1,78301E-10	-2,15966	0,46304	-2,0067	0,49832	1,78E-05	0,00111	0,00349	G/D
248128_at	At5g54770	thiazole biosynthetic enzyme precursc	2,53242E-13	1,6465	1,6465	1,5216	1,52159	2,53E-08	4,25E-21	1,92E-14	CM
247162_at	At5g65730	xyloglucan endo-transglycosylase-like	0,0024	2,02949	2,02949	1,5387	1,53872	0,0024	0,00995	0,04589	G/D

Probe Set	Accession #	Sequence Description	ANOVA P-value	Fold Change D0h	Ratio D0h	Fold Change D1h	Ratio D1h	Ratio D0h P-value	Ratio D1h P-value	Functional Classification
260933_at	At1g02470	hypothetical protein contains non-con	3,83832E-09	2,33482	2,33482	2,4910	2,49104	0,00007	0,00033	UNK
261814_at	At1g08310	unknown protein	0,00746	-1,80184	0,55499	-1,5665	0,63836	0,00935	0,03294	UNK
261815_at	At1g08325	leucine zipper protein, putative simila	0,00001	-1,80585	0,55376	-1,5346	0,65166	0,00014	0,01419	UNK
259789_at	At1g29395	Expressed protein ; supported by full-	3,05143E-06	2,15497	2,15497	2,1609	2,1609	1,26E-06	0,00089	S/D
245771_at	At1g30250	hypothetical protein predicted by gene	0,00144	2,12897	2,12897	1,7095	1,70954	0,00311	0,01619	UNK
262427_s_at	At1g47600	thioglucohydrolase, putative similar to th	0,00869	2,11185	2,11185	1,8227	1,82271	0,00365	0,02446	CM
259615_at	At1g47980	desiccation-related protein, putative :	0,00269	-1,64112	0,60934	-1,7365	0,57587	0,02007	0,0211	UNK
262244_at	At1g48260	serine threonine kinase, putative sim	2,75844E-07	-1,76389	0,56693	-1,8909	0,52884	0,00019	3,37E-07	S
265108_s_at	At1g62620	similar to flavin-binding monooxygen	0,00328	-1,52694	0,65491	-1,5290	0,65402	0,01475	0,0225	UNK
260385_at	At1g74090	putative flavonol sulfotransferase simi	0,00057	-1,58685	0,63018	-1,8349	0,54498	0,00378	0,00015	CM
264124_at	At1g79360	hypothetical protein predicted by gene	2,53242E-13	2,00011	2,00011	1,7671	1,76713	9,96E-17	1,84E-09	TR
263376_at	At2g20520	putative surface protein ; supported l	0,01255	1,78918	1,78918	1,5732	1,57324	0,03055	0,02551	UNK
267607_s_at	At2g26740	epoxide hydrolase (ATsEH) identical to	2,53242E-13	1,95664	1,95664	1,7542	1,7542	7,39E-14	1,17E-15	H
265279_at	At2g28460	hypothetical protein predicted by gene	0,00608	-1,5274	0,65471	-1,5086	0,66287	0,02216	0,01697	CM
266222_at	At2g28780	hypothetical protein predicted by gene	0,00701	-2,02149	0,49468	-1,6814	0,59474	0,00549	0,01495	UNK
260560_at	At2g43590	putative endochitinase	0,00089	-1,56381	0,63947	-1,6526	0,60511	0,02794	0,02345	G/D
258972_at	At3g01920	hypothetical protein predicted by gene	1,257E-07	2,00762	2,00762	1,9154	1,91535	0,00007	0,00003	UNK
258746_at	At3g05950	germin-like protein similar to germin l	0,00117	-2,28585	0,43747	-1,6729	0,59778	0,00034	0,00491	CM
257697_at	At3g12700	hypothetical protein predicted by gene	2,42881E-07	-1,88937	0,52928	-1,8542	0,53931	0,00005	0,00019	CM
257128_at	At3g20080	cytochrome P450, putative contains f	0,00499	-3,03906	0,32905	-3,7266	0,26834	0,00265	0,00412	CM
256815_at	At3g21380	unknown protein contains Pfam profilin	5,23575E-06	-2,39438	0,41764	-2,2935	0,43601	0,01075	0,01062	UNK
256601_s_at	At3g28290	At14a-1 protein identical to At14a pr	2,53242E-13	-2,31944	0,43114	-3,1607	0,31638	3,34E-19	2,16E-36	G/D
252222_at	At3g49840	putative protein various predicted pr	0,01455	-3,53514	0,28287	-2,1522	0,46465	0,00436	0,02696	UNK
254761_at	At4g13195	Expressed protein ; supported by full-	0,00159	-1,76083	0,56792	-1,5334	0,65217	0,00178	0,03367	S
253904_at	At4g27140	NWMU1 - 2S albumin 1 precursor ; si	2,37715E-06	-2,36899	0,42212	-2,2919	0,43631	0,00994	0,02579	G/D
253331_at	At4g33490	nucellin -like protein nucellin - Horde	2,88802E-06	1,85478	1,85478	1,6643	1,66427	3,46E-06	0,00044	CM
245711_at	At5g04340	putative c2h2 zinc finger transcription	0,00011	-2,04231	0,48964	-1,7482	0,57203	0,00037	0,00782	TX
245713_at	At5g04370	S-adenosyl-L-methionine:salicylic acid	3,16868E-06	2,0613	2,0613	1,5698	1,56982	1,91E-07	0,0017	UNK
250043_at	At5g18430	putative protein proline-rich protein f	0,00304	1,81315	1,81315	2,4721	2,47209	0,01952	0,00287	CM
249474_s_at	At5g39190	germin-like protein (GLP2a) copy2 ; t	0,00233	1,60289	1,60289	1,6404	1,64044	0,00252	0,01806	G/D
248931_at	At5g46040	peptide transporter	0,00066	-2,09927	0,47636	-1,5736	0,63548	0,00017	0,04479	TR
248520_at	At5g50600	11-beta-hydroxysteroid dehydrogenas	6,18449E-07	-1,61226	0,62025	-1,8113	0,55209	0,01985	0,00473	H

Probe Set	Accession #	Sequence Description	ANOVA P-value	Fold Change D	Ratio D0h	Fold Change D	Ratio D1h	ANOVA P*-val	Ratio D0h	P-v	Ratio D1h	P-v	Functional Classification
267635_at	At2g42220	rhodanese-like family p	0,01217	1,82061	1,82061	1,5027	1,50268	0,01217	0,01309	0,01569	UNK		
259161_at	At3g01500	carbonic anhydrase, cl	6,22399E-09	1,59641	1,59641	1,5841	1,58411	6,22E-04	0,00002	2,56E-07	P/C		
258897_at	At3g05730	unknown protein	9,98071E-12	2,78217	2,78217	3,3132	3,31315	9,98E-07	0,00004	1,80E-12	S/D		
252317_at	At3g48720	putative protein hyper	0,00147	1,88291	1,88291	1,8882	1,88818	0,00147	0,00042	0,00433	CM		
251814_at	At3g54890	chlorophyll a/b-binding	2,53242E-13	2,08494	2,08494	2,0456	2,04556	2,53E-08	1,75E-08	8,94E-14	P/C		
255248_at	At4g05180	Oxygen-evolving enha	1,64927E-08	1,56708	1,56708	1,6429	1,64291	1,65E-03	0,00004	7,94E-09	P/C		
253040_at	At4g37800	endo-xyloglucan trans	2,16117E-09	5,7886	5,7886	3,0036	3,00358	2,16E-04	1,48E-11	0,00003	G/D		
248683_at	At5g48490	putative protein simila	1,89117E-10	2,25094	2,25094	2,8011	2,80105	1,89E-05	0,00077	9,52E-10	G/D		
248151_at	At5g54270	Lhcb3 chlorophyll a/b t	0,00003	1,71711	1,71711	1,7645	1,76454	0,00003	0,00372	0,00001	P/C		

### Supplemental Dataset 5

#### Primary data and statistical analysis for *mida* mutant phenotypic characterization shown in Figure 2.

Phenotypes were defined as bona-fide if:

- (a) the differences in mean values between WT sibling and *mida* mutant were statistically significant (pvalue<0.05)
- (b) the mean value varied by at least 20% between the WT sibling and the *mida* mutant for hypocotyl, by at least 40% for hook, and by at least 80% for cotyledon.
- (c) the previous criteria were met for at least two of the three days assayed (2dD, 3dD and 4dD).

Hypocotyl, hook and cotyledon primary data are shown for *mida* seedlings grown for 2 days (2dD), 3 days (3dD), and 4 days (4dD) in the dark.

- A *mida* mutant designation
- B Mean Value for the WT sibling for each *mida* line and for *pif3* as reference. Also includes the average of all WT siblings.
- C Standard error (SE) of values shown in B.
- D Mean Value for each *mida* line and for *pif3* as reference.
- E Standard error (SE) of values shown in D
- F P-value of the comparison between the Mean values of WT sibling vs *mida*.
- G Mean fold change (FC) *mida*/WT sibling
- H SE of FC shown in G.

Hypocotyl values are expressed in mm, whereas Hook and Cotyledon values are expressed in degrees of unfolding or separation respectively.

Significant p values are shown in Red.

FC greater than the cutoff are shown in Blue.

*mida* lines showing bona-fide phenotypes are highlighted in color.

Average values for all the WT siblings (shown in Figure 2) are indicated in green.

<i>Hypocotyl</i>	2dD						
	Mean wt	SE wt	Mean mutant	SE mutant	pvalue	FC mut/wt	SE FC mut/wt
<i>pij3</i>	4,771	0,074	4,484	0,075	0,008	0,940	0,016
<i>mida1-OX</i>	3,380	0,047	3,282	0,065	0,213	0,971	0,019
<i>mida2</i>	2,534	0,063	2,894	0,069	2,868E-04	1,142	0,027
<i>mida3</i>	2,126	0,119	1,971	0,117	0,375	0,927	0,055
<i>mida4</i>	3,842	0,074	3,831	0,072	0,914	0,997	0,019
<i>mida5</i>	4,965	0,245	5,646	0,194	0,034	1,137	0,039
<i>mida7</i>	5,107	0,126	4,979	0,106	0,437	0,975	0,021
<i>mida8</i>	3,223	0,065	3,947	0,077	1,364E-09	1,225	0,024
<i>mida9</i>	5,072	0,250	5,433	0,124	0,230	1,071	0,024
<i>mida10</i>	4,596	0,125	4,933	0,129	0,067	1,073	0,028
<i>mida11</i>	4,606	0,143	2,993	0,126	2,069E-11	0,650	0,027
<i>mida12</i>	5,285	0,127	4,596	0,123	2,798E-04	0,870	0,023
<i>mida13</i>	2,722	0,183	3,759	0,122	3,769E-06	1,381	0,045
Average wt siblings	4,018						

<i>Hypocotyl</i>	3dD						
	Mean wt	SE wt	Mean mutant	SE mutant	pvalue	FC mut/wt	SE FC mut/wt
<i>pij3</i>	10,280	0,103	9,811	0,102	0,002	0,954	0,010
<i>mida1-OX</i>	9,064	0,100	9,225	0,129	0,334	1,018	0,014
<i>mida2</i>	9,152	0,185	8,795	0,152	0,143	0,961	0,017
<i>mida3</i>	5,390	0,237	7,544	0,219	2,702E-08	1,400	0,041
<i>mida4</i>	10,473	0,113	9,817	0,185	0,004	0,937	0,018
<i>mida5</i>	9,112	0,853	7,032	0,312	7,684E-03	0,772	0,034
<i>mida7</i>	10,555	0,151	9,992	0,173	0,018	0,947	0,016
<i>mida8</i>	9,741	0,199	10,647	0,194	2,511E-04	1,093	0,020
<i>mida9</i>	10,442	0,248	10,939	0,157	0,089	1,048	0,015
<i>mida10</i>	10,103	0,245	10,445	0,218	0,287	1,034	0,022
<i>mida11</i>	9,514	0,165	7,5050	0,3242	3,096E-07	0,789	0,034
<i>mida12</i>	10,789	0,150	9,800	0,211	2,239E-04	0,908	0,020
<i>mida13</i>	8,811	0,162	9,453	0,167	0,007	1,073	0,019
Average wt siblings	9,494						

<i>Hypocotyl</i>	4dD						
	Mean wt	SE wt	Mean mutant	SE mutant	pvalue	FC mut/wt	SE FC mut/wt
<i>pij3</i>	13,519	0,141	12,866	0,129	0,001	0,952	0,010
<i>mida1-OX</i>	13,418	0,113	13,797	0,183	0,069	1,028	0,014
<i>mida2</i>	13,798	0,241	13,564	0,160	0,419	0,983	0,012
<i>mida3</i>	10,449	0,425	11,556	0,313	0,037	1,106	0,030
<i>mida4</i>	13,598	0,181	13,893	0,192	0,266	1,022	0,014
<i>mida5</i>	13,200	0,583	12,590	0,517	0,439	0,954	0,039
<i>mida7</i>	13,508	0,235	13,857	0,207	0,278	1,026	0,015
<i>mida8</i>	14,817	0,034	15,520	0,319	0,092	1,047	0,022
<i>mida9</i>	11,746	0,274	12,471	0,281	0,071	1,062	0,024
<i>mida10</i>	14,573	0,284	14,076	0,255	0,198	0,966	0,017
<i>mida11</i>	12,037	0,346	10,574	0,325	2,822E-03	0,878	0,027
<i>mida12</i>	13,707	0,401	14,085	0,315	0,457	1,028	0,023
<i>mida13</i>	11,771	0,283	11,709	0,226	0,862	0,995	0,019
Average wt siblings	13,088						

<i>Hook</i>	<b>2dD</b>							
	Mean wt	SE wt	Mean mutant	SE mutant		pvalue	FC mut/wt	SE FC mut/wt
<i>pif3</i>	18,634	2,879	51,894	6,009		8,242E-07	2,785	0,32
<i>mida1-OX</i>	42,744	5,869	54,237	4,624		0,124	1,269	0,108
<i>mida2</i>	21,954	5,488	19,263	2,948		0,670	0,877	0,134
<i>mida3</i>	11,155	4,367	8,515	1,792		0,507	0,763	0,161
<i>mida4</i>	16,311	2,529	20,808	2,755		0,235	1,276	0,169
<i>mida5</i>	41,490	6,736	46,911	6,020		0,509	1,131	0,145
<i>mida7</i>	12,233	2,643	18,325	3,473		0,172	1,498	0,284
<i>mida8</i>	28,227	3,079	34,540	3,314		0,171	1,224	0,117
<i>mida9</i>	27,537	3,226	69,787	3,712		1,409E-11	2,534	0,135
<i>mida10</i>	29,957	4,944	43,199	4,269		0,050	1,442	0,143
<i>mida11</i>	16,475	4,294	10,593	2,654		0,236	0,643	0,161
<i>mida12</i>	19,285	4,365	17,113	3,885		0,729	0,887	0,201
<i>mida13</i>	41,039	3,633457694	41,285	3,727		0,963	1,006	0,091
Average wt siblings	25,157							

<i>Hook</i>	<b>3dD</b>							
	Mean wt	SE wt	Mean mutant	SE mutant		pvalue	FC mut/wt	SE FC mut/wt
<i>pif3</i>	35,915	2,964	90,341	6,142		2,784E-12	2,515	0,171
<i>mida1-OX</i>	83,147	5,297	74,195	3,964		0,177	0,892	0,048
<i>mida2</i>	28,058	3,915	39,678	4,035		0,043	1,414	0,144
<i>mida3</i>	22,786	3,650	26,963	4,440		0,476	1,183	0,195
<i>mida4</i>	59,948	5,820	51,133	4,977		0,258	0,853	0,083
<i>mida5</i>	71,540	9,137	78,891	7,961		0,553	1,103	0,111
<i>mida7</i>	23,404	4,604	25,595	6,850		0,795	1,094	0,293
<i>mida8</i>	53,004	4,727	53,598	5,612		0,935	1,011	0,106
<i>mida9</i>	37,194	2,607	103,3521538	5,097		6,047E-14	2,779	0,137
<i>mida10</i>	53,165	4,328	80,224	4,085		1,405E-05	1,509	0,077
<i>mida11</i>	61,577	4,924	26,258	5,285		6,194E-06	0,426	0,086
<i>mida12</i>	47,682	3,532	39,061	3,373		0,084	0,819	0,071
<i>mida13</i>	51,656	4,350	47,971	4,343		0,127	0,929	0,084
Average wt siblings	48,390							

<i>Hook</i>	<b>4dD</b>							
	Mean wt	SE wt	Mean mutant	SE mutant		pvalue	FC mut/wt	SE FC mut/wt
<i>pif3</i>	91,14	4,007	118,378	5,479		1,256E-04	1,299	0,060
<i>mida1-OX</i>	118,338	4,306	96,927	3,246		1,465E-04	0,819	0,027
<i>mida2</i>	43,588	4,229	53,171	4,280		0,117	1,220	0,098
<i>mida3</i>	52,77	4,858	47,762	4,239		0,442	0,905	0,080
<i>mida4</i>	99,860	5,613	97,924	4,815		0,795	0,981	0,048
<i>mida5</i>	113,509	8,351	110,217	7,792		0,779	0,971	0,069
<i>mida7</i>	112,973	4,193	122,446	4,783		0,144	1,084	0,042
<i>mida8</i>	84,934	4,549	106,323	4,492		0,002	1,252	0,053
<i>mida9</i>	143,797	5,994	159,901	3,534		0,022	1,112	0,025
<i>mida10</i>	119,615	3,417	132,271	4,750		0,047	1,106	0,040
<i>mida11</i>	109,439	4,606	75,621	5,557		1,899E-05	0,691	0,051
<i>mida12</i>	96,867	5,325	64,451	5,018		5,378E-05	0,665	0,052
<i>mida13</i>	101,647	5,657	129,1	3,809		3,333E-04	1,270	0,037
Average wt siblings	99,114							

<i>Cotyledon</i>	2dD		Mean mutant	SE mutant	pvalue	FC mut/wt	SE FC mut/wt
	Mean wt	SE wt					
<i>pif3</i>	6,141	1,340	28,62	2,735	2,315E-10	4,660	0,445
<i>mida1-OX</i>	6,501	1,140	22,220	2,733	2,040E-07	3,419	0,420
<i>mida2</i>	7,074	2,037	6,337	1,450	0,769	0,896	0,205
<i>mida3</i>	3,975	2,241	2,357	1,528	0,607	0,593	0,384
<i>mida4</i>	11,677	2,122	7,820	2,172	0,210	0,670	0,186
<i>mida5</i>	4,399	1,458	3,752	1,385	0,765	0,853	0,315
<i>mida7</i>	5,962	1,565	4,059	1,262	0,344	0,681	0,212
<i>mida8</i>	5,556	1,280	5,185	1,327	0,841	0,933	0,239
<i>mida9</i>	7,708	1,750	4,667	1,523	0,215	0,606	0,198
<i>mida10</i>	4,538	1,534	8,013	2,168	0,215	1,766	0,478
<i>mida11</i>	8,075	2,633	3,765	1,964	0,187	0,466	0,243
<i>mida12</i>	13,035	2,617	10,547	2,444	0,490	0,809	0,187
<i>mida13</i>	5,715	1,883	5,337	1,859	0,890	0,934	0,325
Average wt siblings	6,950						

<i>Cotyledon</i>	3dD		Mean mutant	SE mutant	pvalue	FC mut/wt	SE FC mut/wt
	Mean wt	SE wt					
<i>pif3</i>	6,74	1,496	12,258	2,191	0,039	1,818	0,325
<i>mida1-OX</i>	7,669253521	1,102	15,021	1,638	4,188E-04	1,959	0,214
<i>mida2</i>	3,999	1,390	4,018	1,612	0,986	1,005	0,403
<i>mida3</i>	10,802	2,3614	11,518	2,462	0,835	1,066	0,228
<i>mida4</i>	7,442	1,690	6,186	1,715	0,604	0,831	0,230
<i>mida5</i>	6,605157895	2,287	2,353	1,265	0,089	0,356	0,191
<i>mida7</i>	0,735	0,232	0,338	0,057	0,097	0,460	0,078
<i>mida8</i>	0,746	0,224	2,127	1,090	0,238	2,852	1,462
<i>mida9</i>	3,209	1,157	3,605	1,322	0,857	1,123	0,412
<i>mida10</i>	4,84	1,245	6,445	1,710	0,461	1,332	0,353
<i>mida11</i>	8,180231426	1,804	1,278	0,573	0,004	0,156	0,070
<i>mida12</i>	3,422	1,135	2,98784	1,490	0,815	0,873	0,435
<i>mida13</i>	3,614	0,930	3,236	1,049	0,789	0,895	0,290
Average wt siblings	5,231						

<i>Cotyledon</i>	4dD		Mean mutant	SE mutant	pvalue	FC mut/wt	SE FC mut/wt
	Mean wt	SE wt					
<i>pif3</i>	3,438	1,403	10,989	2,482	0,006	3,196	0,722
<i>mida1-OX</i>	3,589	0,707	10,423	0,945	4,140E-08	2,904	0,263
<i>mida2</i>	2,752	1,208	2,709	0,894	0,976	0,984	0,325
<i>mida3</i>	6,706	1,681	3,783	0,976	0,141	0,564	0,146
<i>mida4</i>	5,019	1,024	4,668	0,934	0,837	0,930	0,186
<i>mida5</i>	5,557	1,582	12,376	2,811	0,056	2,227	0,506
<i>mida7</i>	2,989	0,994	6,493	1,930	0,105	2,172	0,646
<i>mida8</i>	4,694	1,300	6,639	2,054	0,426	1,414	0,438
<i>mida9</i>	18,918	5,046	16,972	5,321	0,788	0,897	0,281
<i>mida10</i>	3,552	2,035	10,347	3,321	0,084	2,913	0,935
<i>mida11</i>	7,772	2,950	6,759	1,733	0,761	0,870	0,223
<i>mida12</i>	12,016	3,979	4,53	1,614	0,083	0,377	0,134
<i>mida13</i>	8,91	2,166	9,119	2,444	0,950	1,023	0,274
Average wt siblings	6,609						

Due to the large extension of the documents here listed:

- Monte\_DataSet\_6\_final-1
- Monte\_DataSet\_7\_final-1
- Monte\_DataSet\_8\_final-1

, we refer the lector to the attached web link indicated below.

<http://www.plantcell.org/content/23/11/3974/suppl/DC1>







